

Program and Abstracts



BONE QUALITY:

What Is It and
Can We Measure It?

May 2-3, 2005 | Bethesda, MD, USA

Sponsored by:



National Institute of Health

National Institute of Arthritis and
Musculoskeletal and Skin Diseases



The American Society for
Bone and Mineral Research

Co-Sponsored by:

Inserm

Institut national
de la santé et de la recherche médicale



Bone Quality: What Is It and Can We Measure It?

**May 2-3, 2005
Bethesda, Maryland, USA**

A Scientific Meeting

**Sponsored by:
National Institute of Arthritis and Musculoskeletal and Skin Diseases
(NIAMS)**

**National Institutes of Health
U.S. Department of Health and Human Services
and**

**American Society for Bone and Mineral Research
(ASBMR)**

**Co-Sponsored by:
The French National Institute of Medical Research
(INSERM)
and
National Institute of Biomedical Imaging and Bioengineering
(NIBIB)**

Supported by:
This meeting was supported by educational grants from the following companies:

**Platinum Level
Ei Lilly and Company
NPS Pharmaceuticals**

**Gold Level
Alliance for Better Bone Health
(Procter & Gamble Pharmaceuticals and Aventis,
a member of the sanofi-aventis Group)
Merck & Co., Inc.**

**Silver Level
Novartis Pharmaceuticals Corporation**

**Friend Level
Amgen, Inc.
Wyeth Pharmaceuticals**

Welcome!

On behalf of the organizers of this NIAMS-ASBMR sponsored meeting, **Bone Quality: What Is It and Can We Measure It?**, we welcome you and thank you for your participation.

The debate regarding bone quantity versus quality was initiated more than ten years ago at the NIH-sponsored "Workshop on Aging and Bone Quality." Since that time, there has been progress in the diagnosis and treatment of patients with osteoporosis, including approval of several therapies proven to reduce fracture risk. In addition, research studies have increased our knowledge regarding the biomechanical, genetic and molecular mechanisms that contribute to skeletal fragility. Yet, fractures are still common, too common.

Worldwide, one in three women and one in eight men over the age of 50 will suffer an osteoporotic fracture during their remaining lifetimes. As highlighted in the recent Surgeon General's Report on Bone Health and Osteoporosis (www.surgeongeneral.gov), each year over 1.5 million Americans suffer an osteoporosis-related fracture, and as a result many experience an increased risk of future fractures, long-term disability and even premature death. As our population ages, it is predicted that the number and cost of osteoporotic fractures will double in the next 50 years. Therefore, reducing the number of osteoporotic fractures is a vital public health concern and identifying those at highest risk in the population is critical.

A better understanding of the factors that influence bone strength is key to developing improved diagnostic techniques and more effective treatments. The term bone quality has been used ambiguously to describe the various factors that influence bone strength, yet the precise definition and practical implications of measurements of bone quality remain obscure.

The purpose of this meeting is to shed light on this important and interesting area, from basic science and clinical perspectives. Our goals are to bring together both young investigators and senior scientists, including engineers, physicists, biologists and clinicians, to share cutting-edge research, debate current paradigms, and foster innovative collaborations. We invite each of you to participate as we discuss the effect of osteoporosis therapies on the architecture of bone, the mechanics of fracture, the factors related to why bone breaks, the novel techniques used to assess skeletal fragility, the best methods for conducting clinical trials in osteoporosis, and the techniques that are most promising for widespread clinical evaluation.

We want to thank many individuals for the support and partnership that enabled the Organizing Committee to plan this meeting, beginning with the National Institute of Arthritis and Musculoskeletal and Skin Diseases (NIAMS) Director Dr. Stephen Katz, ASBMR President Dr. Sylvia Christakos, ASBMR Executive Director Joan Goldberg, and National Institute of Biomedical Imaging and Bioengineering (NIBIB) Director Roderic Pettigrew. We are also thankful for the input of Dr. John Haller, the Acting Director of the Division of Applied Science and Technology at NIBIB, and Dr. William Sharrock, Bone Biology Program Director at NIAMS, and to Dr. Marc Drezner, ASBMR's Secretary-Treasurer who helped to plan this meeting in its initial phases. We are also grateful for the co-sponsorship of the NIBIB and the French National Institute of Health and Medical Research (INSERM). And special thanks to our colleagues (too many to name) for ideas, recommendations and guidance along the way. We also want to thank the commercial sponsors who have helped to support this meeting. Finally, we wish to thank the ASBMR staff who provided continuous organizational support and guidance, particularly Karen Hasson for her leadership.

Sincerely,

Organizing Committee

Gayle E. Lester, Ph.D., *Chair*

Mary L. Bouxsein, Ph.D.

Pierre Delmas, M.D., Ph.D.

Steven A. Goldstein, Ph.D.

Theresa Kehoe, M.D.

Joan McGowan, Ph.D.

Robert R. Recker, M.D.

CONTENTS

Schedule/Program	i
General Information	x
Abstracts	1
Author Index	54



**The ASBMR endorses the U.S. Bone and Joint Decade (USBJD)
and is a founding member of the USBJD organization.**



Bone Quality: What Is It and Can It Be Measured?

ORGANIZING COMMITTEE

Gayle Lester, Ph.D., *Organizing Committee Chair*,

Musculoskeletal Diseases Branch, National Institute of Arthritis and Musculoskeletal and Skin Diseases (NIAMS),
National Institutes of Health, U.S. Department of Health and Human Services, Bethesda, Maryland, USA

Mary Bouxsein, Ph.D., Department of Orthopedic Surgery,
Beth Israel Deaconess Medical Center, Boston, Massachusetts, USA

Pierre Delmas, M.D., Ph.D., INSERM, Lyon, France

Steven Goldstein, Ph.D., Department of Orthopedic Surgery,
University of Michigan Orthopedic Research Labs, Ann Arbor, Michigan, USA

Theresa Kehoe, M.D., Division of Metabolic and Endocrine Drug Products,
CDER, Food and Drug Administration, Rockville, Maryland, USA

Joan McGowan, Ph.D., Musculoskeletal Diseases Branch,
National Institute of Arthritis and Musculoskeletal and Skin Diseases (NIAMS), National Institutes of Health,
U.S. Department of Health and Human Services, Bethesda, Maryland, USA Bethesda, Maryland, USA

Robert R. Recker, M.D., Creighton University,
Osteoporosis Research Center, Omaha, Nebraska, USA

ASBMR STAFF

Joan R. Goldberg, *Executive Director*

Karen R. Hasson, *Deputy Executive Director*

D. Douglas Fesler, *Project Manager*

Gretchen Bretsch, *Project Manager*

Yvette Dalka, *Program Manager*

Earline Marshall, *Executive Assistant*

Kimberly Seyran, *Project Coordinator*

Amy Werner, *Senior Program Assistant*

Anna Camele, *Senior Membership/Marketing Assistant*

Rebecca Boulos, *Association Assistant*

Kiley Thornton, *Association Assistant*

William Gaskill, *Accountant*

Melissa Huston, *Convention Manager*

Brooke Hirsch, *Convention Assistant*

Cliff Pratt, *Registration Coordinator*

Kelly Marks, *Exhibits Coordinator*

Melissa Haynes, *Public Relations Manager*

Adrienne Lea, *Director of Publications*

Heather Price, *Publications Project Manager*

Amber Williams, *Managing Editor*

David Allen, *Publications Specialist*

NIAMS STAFF ASSISTING

Kelli Carrington, *Writer-Health Educator*

Richard Clark, *Writer/Editor*

ASBMR BUSINESS OFFICE

2025 M Street, NW, Suite 800

Washington, DC 20036-3309, USA

Tel: (202) 367-1161, Fax: (202) 367-2161,

E-mail: ASBMR@smithbucklin.com, Internet: www.asbmr.org

YOUNG INVESTIGATOR AWARD RECIPIENTS

Co-supported by an educational grant from Amgen, Inc.

Ozan Akkus, Ph.D.
Maria Benito, M.D.
Stéphanie Boutroy
Hayden-William Courtland, M.S.
Eve Donnelly, M.S.
Dan Faibish, D.M.D.
Gloria López Franco, D.D.S, M.S.
Glenn A. Ladinsky, M.D., Ph.D.
Diana J. Leeming, M.Sc
Guiyang Li, Ph.D.
Ravi K. Nalla, M.S., Ph.D.
Glen L. Niebur, Ph.D.
Christopher Price
Hui Shen, Ph.D.
Steven M. Tommasini, M.S.

The ASBMR Job Placement Service Is Accessible Year-round On-line

Access the most up-to-date job and candidate listings using the ASBMR On-line Job Placement Service at www.asbmr.org.

The ASBMR On-line Job Placement Service offers the following:

Job Candidates

- Year-round access to the ASBMR on-line job placement database
- Selection of job openings in academia, industry, government, and private practice
- Opportunity to showcase your skills and expertise
- Free candidate enrollment

Employers

- Opportunity to post unlimited on-line job announcements for one year
- Ability to review candidates' CVs online
- Access to a pool of qualified applicants
- Year-round access to the ASBMR on-line job placement database and updates as new candidates register with the service
- Enrollment includes posting of job announcements at the 27th ASBMR Annual Meeting in Nashville, Tennessee, USA

ASBMR Job Placement Service

2025 M Street, NW, Suite 800, Washington, DC 20036-3309, USA
Tel: (202) 367-1161, Fax: (202) 367-2161
E-mail: ASBMR@smithbucklin.com, Internet: www.asbmr.org

Bone Quality: What Is It and Can We Measure It? May 2-3, 2005 # Bethesda, Maryland, USA			
Time	Topic	Moderators and Speakers	Abstract Number
Note: Speaker/Moderator disclosures are included below, except for those individuals who submitted abstracts. For abstract submitters, disclosures are included at the end of each abstract.			
Monday, May 2, 2005			
7:00 am	Breakfast		
8:00 am	Welcome and Announcements		
8:00 am	Welcome on Behalf of NIAMS	Stephen I. Katz, M.D., Ph.D. Director, National Institute of Arthritis and Musculoskeletal and Skin Diseases, National Institutes of Health, U.S. Department of Health and Human Services, Bethesda, Maryland, USA <i>Disclosures: None.</i>	
8:05 am	Welcome on Behalf of ASBMR	Sylvia Christakos, Ph.D. President, American Society for Bone and Mineral Research Department of Biochemistry and Molecular Biology, UMDNJ, New Jersey Medical School, Newark, New Jersey, USA <i>Disclosures: None.</i>	
8:10 am	Welcome on Behalf of INSERM	Pierre Delmas, M.D., Ph.D. Representative, The French National Institute of Medical Research (INSERM) Department of Rheumatology, INSERM, Hopital Edouard Herriot, Lyon, FRANCE	
8:15 am	Introductory Session: The Bone Quality Paradigm	Moderator: Robert R. Recker, M.D. Creighton University Osteoporosis Research Center, Omaha, Nebraska, USA	
8:20 am	Bone Quality: Definition, History, Current Overview	A. Michael Parfitt, M.D. Department of Internal Medicine, Division of Endocrinology, University of Arkansas for Medical Sciences, Little Rock, Arkansas, USA	1
8:45 am	Bone Quality: A Biomechanical Perspective	Steven A. Goldstein, Ph.D. Department of Orthopaedic Surgery, University of Michigan Orthopedic Research Laboratories, Ann Arbor, Michigan, USA	2
9:10 am	Bone Quality: A Clinical Perspective	Juliet E. Compston, F.R.C. Path., F.R.C.P., F. Med. Sci. Department of Medicine, University of Cambridge School of Clinical Medicine, Cambridge, UNITED KINGDOM	3
9:35 am	Panel Discussion	Speakers and Moderator	
9:50 am	Break		

10:05 am	Macrostructure and Microstructure	Moderator: Marjolein C. van der Meulen, Ph.D. Department of Mechanical and Aerospace Engineering, Cornell University, Ithaca, New York, USA <i>Disclosures: None.</i>	
10:10 am	Bone Geometry and Skeletal Fragility	Mary L. Bouxsein, Ph.D. Orthopedic Biomechanics Laboratory, Beth Israel Deaconess Medical Center, Boston, Massachusetts, USA	4
10:30 am	Effect of Microarchitecture on Bone Strength	Harrie Weinans, Ph.D. Department of Orthopedics, Erasmus University, Rotterdam, THE NETHERLANDS	5
10:50 am	Effect of Osteoporosis Therapies on Microarchitecture	David W. Dempster, Ph.D. College of Physicians and Surgeons, Columbia University, West Haverstraw, New York, USA	6
11:10 am	Trabecular Bone Failure at the Microstructural Level	Ralph Mueller, Ph.D. Institute for Biomedical Engineering, ETH and University of Zurich, Zurich, SWITZERLAND	7
11:30 am	Panel Discussion	Speakers and Moderator	
11:50 am	Lunch - Box lunches will be available.		
12:35 pm	Ultrastructure and Material Properties	Moderator: Mary L. Bouxsein, Ph.D. Orthopedic Biomechanics Laboratory, Beth Israel Deaconess Medical Center, Boston, Massachusetts, USA	
12:40 pm	Characteristics of the Collagen-Mineral Nano-Composite and Skeletal Fragility	Paul Roschger, Ph.D. Ludwig Boltzmann-Institute of Osteology at the Hanusch Hospital of WGKK and AUVA Trauma Centre Meidling, Vienna, AUSTRIA	8
1:00 pm	Collagen Composition, Cross-links and Skeletal Fragility	Deepak Vashishth, B.E. (HONS), M.S.M.E., Ph.D. Department of Biomedical Engineering, Rensselaer Polytechnic Institute, Troy, New York, USA	9
1:20 pm	Mineral Matrix Interactions	William Landis, Ph.D. Department of Microbiology, Immunology, and Biochemistry, Northeastern Ohio Universities College of Medicine, Rootstown, Ohio, USA	10
1:40 pm	How Does Bone Break? Fracture Mechanics and Crack Propagation	Robert O. Ritchie, Ph.D., Sc.D. Department of Materials Science and Engineering, University of California, Berkeley, California, USA	11
2:00 pm	Bone Failure at the Ultrastructural Level	David P. Fyhrie, Ph.D. Orthopaedic Research Laboratories, UC Davis School of Medicine, Sacramento, California, USA	12
2:20 pm	Panel Discussion	Speakers and Moderator	

2:40 pm	What Can Skeletal Diseases Teach Us About Bone Quality?	Moderator: Steven Goldstein, Ph.D. Department of Orthopaedic Surgery, University of Michigan Orthopedic Research, Ann Arbor, Michigan, USA	
2:45 pm	Skeletal Variations in Humans	Michael P. Whyte, M.D. Department of Medicine, Washington University School of Medicine, St. Louis, Missouri, USA	13
3:05 pm	Using Mice to Understand Structure-Function Relationships in the Skeleton	Karl J. Jepsen, Ph.D. Department of Orthopaedics, Mount Sinai School of Medicine, New York, New York, USA	14
3:25 pm	Panel Discussion	Speakers and Moderator	
3:40 pm	Break		
3:55 pm	Young Investigator Oral Session I	Moderator: Clifford J. Rosen, M.D. Maine Center for Osteoporosis Research, St. Joseph Hospital, Bangor, Maine, USA <i>Disclosures: Eli Lilly, Merck, Aventis, NPS, Wyeth, Novartis 2.</i>	
3:55 pm	Mapping Quantitative Trait Loci for Bone Quality: A Study of Cross-Sectional Geometry of Femoral Neck	H. Shen¹, D. Xiong¹, J. Long¹, Y. Zhang¹, Y. Liu¹, P. Xiao¹, L. Zhao¹, Y. Liu¹, V. Dvornyk¹, S. Rocha-Sanchez¹, P. Liu¹, T. Conway¹, K. Davies¹, R. R. Recker¹, H. Deng^{1,2}. ¹ Creighton University, Omaha, NE, USA, ² HuNan Normal University, ChangSha, China	15
4:10 pm	Effect of Aging on the Fracture Toughness of Human Cortical Bone: A Hierarchical Approach	R. K. Nalla¹, J. S. Stölken², J. H. Kinney², R. O. Ritchie¹. ¹ Lawrence Berkeley National Laboratory, Berkeley, CA, USA, ² Lawrence Livermore National Laboratory, Livermore, CA, USA	16
4:25 pm	In Vivo Assessment of Trabecular Microarchitecture by High-Resolution Peripheral Computed Tomography	S. Boutroy¹, M. L. Bouxsein², F. Munoz¹, P. D. Delmas¹. ¹ INSERM Research Unit 403 and Claude Bernard University of Lyon, Lyon, France, ² Forsyth Institute and Harvard Medical School, Boston, MA, USA	17
4:40 pm	Bone Remodeling, Microdamage Accumulation and Skeletal Fragility	Moderator: Ego Seeman, B.Sc., M.B.B.S., F.R.A.C.P., M.D. Department of Endocrinology, Austin Hospital, University of Melbourne, Heidelberg, Melbourne, AUSTRALIA <i>Disclosures: MSD, Aventis, Eli Lilly, Novartis 5.</i>	
4:45 pm	Effects of Microdamage on Bone Strength	David Burr, Ph.D. Department of Anatomy and Cell Biology, Indiana University School of Medicine, Indianapolis, Indiana, USA	18
5:05 pm	Clinical Relevance of Microdamage Accumulation and Excess Remodeling Suppression	Robert R. Recker, M.D. Creighton University Osteoporosis Research Center, Omaha, Nebraska, USA	19
5:25 pm	Role of the Osteocyte in Mechanotransduction and Skeletal Fragility	Mitchell B. Schaffler, Ph.D. Department of Orthopaedics, Mount Sinai School of Medicine, New York, New York, USA	20

5:45 pm	What Is the Evidence for Sustained Anti-Fracture Efficacy Following Long-Term Bisphosphonate Use?	René E. Rizzoli, M.D. Department of Rehabilitation and Geriatrics, University Hospital, Geneva, SWITZERLAND	21
6:05 pm	Panel Discussion	Speakers and Moderator and A. Michael Parfitt, M.D.	
6:30 pm	Poster Session & Reception		
7:45 pm	Adjourn		
Tuesday, May 3, 2005			
7:00 am	Breakfast		
8:00 am	Non-Invasive Assessments	Moderator: Harry K. Genant, M.D. Department of Radiology, Osteoporosis and Arthritis Research Group, University of California at San Francisco, San Francisco, California, USA <i>Disclosures: GE Lunar, Hologic 2,5,8; Scanco 2,8; Synarc 1, 5.</i>	
8:05 am	Promises and Perils of the Widespread Use of DXA for Assessment of Fracture Risk	Robert P. Heaney, M.D. Creighton University, Omaha, Nebraska, USA	22
8:25 am	Current Methods and Clinical Utility of Macroarchitecture Measurements	Thomas M. Link, M.D. Department of Radiology, University of California at San Francisco, San Francisco, California, USA	23
8:45 am	Current Methods and Clinical Utility of Microarchitecture Measurements	Sharmila Majumdar, Ph.D. Magnetic Resonance Science Center, Department of Radiology University of California at San Francisco, San Francisco, California, USA	24
9:05 am	Remodeling and Skeletal Integrity: What Can Bone Turnover Markers (Existing or New) Tell Us About Fracture Risk and Treatment Efficacy?	Pierre Delmas, M.D., Ph.D. Department of Rheumatology, The French National Institute of Medical Research (INSERM), Hopital Edouard Herriot, Lyon, FRANCE	25
9:25 am	Combining In Vivo Assessments of Density and Geometry for Fracture Risk Assessment In Vivo	Tony M. Keaveny, Ph.D. Department of Mechanical Engineering and Bioengineering, University of California at Berkeley, Berkeley, California, USA	26
9:45 am	Panel Discussion	Speakers and Moderator	
10:05 am	Break		

10:25 am	Young Investigator Oral Session II	Moderator: Ego Seeman, M.D., FRACP Department of Endocrinology, University of Melbourne, Melbourne, VIC, AUSTRALIA <i>Disclosures: MSD, Aventis, Eli Lilly, Novartis 5.</i>	
10:25 am	Preliminary Correlations Between Fracture Risk and IR Imaging	D. Faibish¹ , E. R. Myers¹ , R. R. Recker² , A. L. Boskey¹ . ¹ Hospital for Special Surgery, New York, NY, USA, ² Creighton University, Omaha, NE, USA	27
10:40 am	Testosterone Improves Trabecular Architecture in Hypogonadal Men	M. Benito¹ , B. Vasilic² , F. W. Wehrli² , B. Bunker² , M. Wald² , B. Gomberg² , A. C. Wright² , B. Zemel³ , A. Cucchiara⁴ , P. J. Snyder¹ . ¹ Endocrinology, University of Pennsylvania, Philadelphia, PA, USA, ² Radiology, University of Pennsylvania, Philadelphia, PA, USA, ³ Children's Hospital of Philadelphia, Philadelphia, PA, USA, ⁴ GCRC, University of Pennsylvania, Philadelphia, PA, USA	28
10:55 am	Potential for Diagnosis of Bone Quality by Near IR (NIR) Spectroscopy	G. Li , A. Huang , N. P. Camacho . Hospital for Special Surgery, New York, NY, USA	29
11:10 am	Novel Assessments of the Skeleton	Moderator: Pierre Delmas, M.D., Ph.D. Department of Rheumatology, The French National Institute of Medical Research (INSERM), Hopital Edouard Herriot, Lyon, FRANCE	
11:15 am	Non-Destructive Assessment of Microdamage	Daniel P. Nicolella, Ph.D. Department of Mechanical and Materials Engineering, Southwest Research Institute, San Antonio, Texas, USA	30
11:35 am	Raman Assessment of Matrix and Mineral	Barbara R. McCreadie, Ph.D. Department of Orthopaedic Surgery, University of Michigan, Ann Arbor, Michigan, USA	31
11:55 am	FTIR and Backscatter EM Assessment of Matrix and Mineral	Adele L. Boskey, Ph.D. Mineralized Tissue Laboratory, Hospital for Special Surgery, New York, New York, USA	32
12:15 pm	Using Atomic Force Microscopy and Nanoindentation to Assess Bone Material Properties	Matthew J. Silva, Ph.D. Department of Orthopaedic Surgery, Washington University School of Medicine, St. Louis, Missouri, USA	33
12:35 pm	In Vivo Imaging Techniques for Assessment of Bone Fragility	Felix W. Wehrli, Ph.D. Department of Radiology, University of Pennsylvania, Philadelphia, Pennsylvania, USA	34
12:55 pm	Panel Discussion	Speakers and Moderator	
1:15 pm	Lunch Break - Box lunches will be available.		

2:00 pm	Surrogate Endpoints for Clinical Trials	Moderator: Clifford J. Rosen, M.D. Maine Center for Osteoporosis Research, St. Joseph Hospital, Bangor, Maine, USA <i>Disclosures: Eli Lilly, Merck, Aventis, NPS, Wyeth, Novartis 2.</i>	
2:10 pm	Surrogate Endpoints for Clinical Trials: FDA Perspective	Theresa Kehoe, M.D. Division of Metabolic and Endocrine Drug Products, Center for Drug Evaluation and Research, U.S. Food and Drug Administration, Rockville, Maryland, USA	35
2:30 pm	Incorporation of New Surrogates into Clinical Trials	Henry Bone, M.D., F.A.C.P. Michigan Bone and Mineral Clinic, Detroit, Michigan, USA	36
2:50 pm	Validating New Surrogate Markers for Fracture	Steven R. Cummings, M.D. Department of Medicine and Epidemiology, California Pacific Medical Center Research Institute, San Francisco, California, USA	37
3:10 pm	New Opportunities for Collaborations and Funding	Gayle E. Lester, Ph.D. Musculoskeletal Diseases Branch, National Institute of Arthritis and Musculoskeletal and Skin Diseases, National Institutes of Health, U.S. Department of Health and Human Services, Bethesda, Maryland, USA Joan A. McGowan, Ph.D. Musculoskeletal Diseases Branch, National Institute of Arthritis and Musculoskeletal and Skin Diseases, National Institutes of Health, U.S. Department of Health and Human Services, Bethesda, Maryland, USA	38
3:30 pm	Panel Discussion	Speakers and Moderators and Harry K. Genant, M.D., and Pierre Delmas, M.D., Ph.D.	
4:00 pm	Adjourn		

General Information

VENUE

This meeting will take place in the Crystal Ballroom of the Hyatt Regency Bethesda located at One Bethesda Metro Center (corner of Wisconsin Ave. and Old Georgetown Rd.), Bethesda, Maryland, USA.

REGISTRATION

All registration services will take place in the Foyer of the Crystal Ballroom at the Hyatt Regency Bethesda.

Registration Hours

Sunday, May 1, 2005	4:00 pm – 7:00 pm
Monday, May 2, 2005	7:00 am – 8:00 am
Tuesday, May 3, 2005	7:00 am – 8:00 am

SPEAKER READY ROOM

All speakers must check in at the Speaker Ready Room a minimum of one hour prior to their presentation, but preferably the day before their presentation, if possible. At that time, speakers may review their slides. The Speaker Ready Room is located in the Chairman's Boardroom on the Conference Level of the Hyatt Regency Bethesda. We encourage speakers to review their slides in the Speaker Ready Room to ensure all Greek characters and graphs transferred successfully. The Speaker Ready Room will be open during the following times:

Speaker Ready Room Hours

Sunday, May 1, 2005	4:30 pm – 9:00 pm
Monday, May 2, 2005	7:00 am – 8:00 pm
Tuesday, May 3, 2005	7:00 am – 3:30 pm

WELCOME RECEPTION/POSTER SESSION

Supported by Novartis Pharmaceuticals Corporation

A Welcome Reception for the Bone Quality Meeting will be held in the Cabinet-Judiciary Suite, Old Georgetown and Congressional Rooms on the Conference Level of the Hyatt Regency Bethesda. The reception is scheduled for Monday, May 2nd, from 6:30 pm to 7:45 pm, and will be held in conjunction with the Poster Session. See below for more information.

POSTER INFORMATION

Poster presentation time is scheduled from 7:00 pm to 7:45 pm. Presenters must be at their posters during this time period on Monday evening, May 2nd, and available to answer questions.

POSTER SCHEDULE		
	Monday, May 2, 2005	Tuesday, May 3, 2005
Poster Set-Up	7:00 am – 8:00 am	
Welcome Reception/ Poster Session	6:30 pm – 7:45 pm	
Presentation Time	7:00 pm – 7:45 pm	
Poster Dismantle		4:30 pm – 5:00 pm
Poster Viewing Schedule		
Morning Break	9:50 am – 10:05 am	10:05 am – 10:25 am
Lunch Break	11:50 pm – 12:35 pm	1:15 pm – 2:00 pm
Afternoon Break	3:40 pm – 3:55 pm	
Evening Hours	6:30 pm – 7:45 pm	4:00 pm – 4:30 pm

CONFERENCE MEALS

Your registration for the conference includes a continental breakfast and boxed lunch on Monday and Tuesday, May 2nd and 3rd, 2005. The meals will be served in the Foyer of the Crystal Ballroom at the Hyatt Regency Bethesda.

EXPECTATIONS OF PRESENTERS

NIAMS and ASBMR wish to promote excellence in bone and mineral research. To that end, NIAMS and ASBMR expect that all presenters participating in the Bone Quality Meeting will provide informative and fully accurate scientific and other information. Furthermore, NIAMS and ASBMR expect that all presentations at this meeting will reflect the highest level of scientific rigor and integrity.

The content of speaker presentations, slides, and reference materials must remain the ultimate responsibility of the faculty. The planning, content and execution of speaker presentations, slides, abstracts and reference materials should be free from corporate influence or control. Industry-sponsored presenters should provide full disclosure of their relationship with the respective company(ies).

DISCLOSURE/CONFLICT OF INTEREST

NIAMS and ASBMR are committed to ensuring balance, independence, objectivity and scientific rigor in all educational activities. NIAMS and ASBMR require that their presenters inform the audience of the presenters' (speakers', faculties', authors', and contributors') academic and professional affiliations, and disclose the existence of any financial interest or other relationships a presenter has with the manufacturer(s) of any commercial product(s) discussed in an educational presentation.

For full-time employees of industry or government, the affiliation listed in the program will constitute full disclosure.

Disclosure should include any relationship that may bias one's presentation or which could give the perception of bias. These situations may include, but are not limited to:

1. stock options or bond holdings in a for-profit corporation or self-directed pension plan
2. research grants
3. employment (full- or part-time)
4. ownership or partnership
5. consulting fees or other remuneration (payment)
6. non-remunerative positions of influence such as officer, board member, trustee, or public spokesperson
7. receipt of royalties
8. speakers bureau

DISCLAIMER

All authored abstracts, findings, conclusions, recommendations, or oral presentations are those of the author(s) and/or speaker(s) and do not reflect the views of NIAMS or ASBMR or imply any endorsement. No responsibility is assumed, and responsibility is hereby disclaimed, by NIAMS and the ASBMR for any injury and/or damage to persons or property as a matter of product liability, negligence or otherwise, or from any use or operation of methods, products, instructions or ideas presented in the abstracts or at the Bone Quality Meeting. Independent verification of diagnosis and drug dosages should be made. Discussions, views and recommendations regarding medical procedures, choice of drugs, and drug dosages are the responsibility of the authors and presenters.

AUDIO- AND VIDEOTAPING

NIAMS and ASBMR expect that attendees will respect each presenter's willingness to provide free exchange of scientific information without the abridgement of his or her rights or privacy and without the unauthorized copying and use of the scientific data shared during his or her presentation. Cameras and recording devices will not be permitted in the Oral Scientific Sessions or the Poster Session, **without the prior written permission of the ASBMR Convention Management.**

The use of cameras, audiotaping devices, and videotaping equipment is strictly prohibited within all Oral Scientific Sessions and the Poster Session without the express written permission of the ASBMR Convention Management.

Unauthorized use of this taping equipment may result in the confiscation of the equipment or the individual may be asked to leave the Scientific Session. These rules will be strictly enforced.

MEETING WEBCAST

Supported by an educational grant from Eli Lilly and Company

A webcast of many of the presentations from the Bone Quality Meeting will be available via the ASBMR website at **www.asbmr.org/bonequality.cfm** about a month after the meeting. We are pleased to be able to provide this added benefit and educational opportunity.

PRESS ROOM

A Press Room will be in operation to facilitate media-related activities during the Bone Quality Meeting. The Press Room will be located in the Tiffany Salon of the Hyatt Regency Bethesda.

Press Room Hours

Monday, May 2, 2005	8:00 am – 6:30 pm
Tuesday, May 3, 2005	8:00 am – 4:00 pm

ASBMR MEMBERSHIP

The ASBMR Membership Booth will be located in the Foyer of the Crystal Ballroom. Come by and meet the ASBMR staff, pick up information about the Society, the high-ranking *Journal of Bone and Mineral Research (JBMR)*, and the upcoming 27th ASBMR Annual Meeting in Nashville, Tennessee, USA, September 23-27, 2005.

MEETING EVALUATION

An evaluation form for the NIAMS-ASBMR Scientific Meeting, Bone Quality: What Is It and Can We Measure It? will be available online via the Bone Quality Website, **www.asbmr.org/bonequality.cfm**, following the meeting. Your participation in the evaluation is extremely important to us. Please take a moment to complete the evaluation of this meeting to aid in planning future meetings. Thank you in advance for your feedback.

USE OF NIAMS AND ASBMR NAMES AND LOGOS

NIAMS and ASBMR reserve the right to approve use of their names in all material disseminated to the media, public and professionals. NIAMS' and ASBMR's name, meeting name, logo(s), and meeting logo may not be used without permission. Use of the ASBMR logo is prohibited without the express written permission of the ASBMR Executive Director Joan Goldberg. Use of the NIAMS logo is prohibited without the express written permission of the NIAMS Office of Communications. All corporate supporters should share their media outreach plans with the ASBMR Executive Director and the NIAMS Office of Communications before any release.

No abstract presented at the NIAMS-ASBMR Scientific Meeting, Bone Quality: What Is It and Can We Measure It?, may be released to the press before its official presentation date and time. Press releases must be embargoed until one hour after the presentation.

FUTURE ASBMR ANNUAL MEETING DATES

ASBMR 27th Annual Meeting

September 23-27, 2005

Gaylord Opryland Resort and Convention Center
Nashville, Tennessee, USA

ASBMR 29th Annual Meeting

September 16-20, 2007

Hawaii Convention Center
Honolulu, Hawaii, USA

ASBMR 28th Annual Meeting

September 15-19, 2006

Philadelphia Convention Center
Philadelphia, Pennsylvania, USA

ASBMR 30th Annual Meeting

September 12-16, 2008

Palais Des Congres
Montreal, Quebec, Canada

ABSTRACT KEY		
Posters		P
Denotes non-ASBMR membership		* (asterisk)
Session	Type of Presentation	Abstracts
Introductory Session: The Bone Quality Paradigm	Invited Speaker Oral Session	1-3
Macrostructure and Microstructure	Invited Speaker Oral Session	4-7
Ultrastructure and Material Properties	Invited Speaker Oral Session	8-12
What Can Skeletal Diseases Teach Us About Bone Quality?	Invited Speaker Oral Session	13-14
Young Investigator Oral Session I	Young Investigator Oral Session	15-17
Bone Remodeling, Microdamage Accumulation and Skeletal Fragility	Invited Speaker Oral Session	18-21
Non-Invasive Assessments	Invited Speaker Oral Session	22-26
Young Investigator Oral Session II	Young Investigator Oral Session	27-29
Novel Assessments of the Skeleton	Invited Speaker Oral Session	30-34
Surrogate Endpoints for Clinical Trials	Invited Speaker Oral Session	35-38
Novel Assessments of Bone Quality: Non-Invasive	Posters	P1-P10
Novel Assessments of Bone Quality: Invasive	Posters	P11-P20
Fracture Risk Assessment in the Clinical Setting	Posters	P21-P29
Effects of Treatment on Bone Quality: Clinical Studies	Posters	P30-P36
Effects of Treatment of Bone Quality: Pre-Clinical Studies	Posters	P37-P47
Genetic Determinants of Bone Quality	Posters	P48-P55
Effects of Bone Morphology/Geometry on Bone Quality	Posters	P56-P69
Effects of Bone Mineral and Matrix on Bone Quality	Posters	P70-P80

1

Bone Quality: Definition, History, Current Overview. A. Parfitt. University of Arkansas for Medical Sciences, Little Rock, AR, USA.

Bone quality, like color, is an elusive abstract concept, but bone *qualities*, like *colors*, can be precisely described and defined. Accordingly, the term bone quality is most useful as a collective name for all attributes of bone, other than its mass or density, that contribute to strength and resistance to fracture (1). Like so much else in the field, the idea of bone quality began with Harold Frost, who demonstrated the presence of microscopic fatigue damage in human bone, sufficient to reduce its strength (2). My personal interest in qualitative aspects of bone strength was stimulated by the discovery that cancellous bone microarchitecture was an independent determinant of vertebral fracture risk (3). In 1987 I organized the first session on bone quality at an international scientific meeting (4), and a few years later remarked that, at least from the standpoint of NIH, the notion that bone quality contributed to bone strength had traveled from heresy to dogma without encountering much new evidence; if a property of bone that contributes to strength declines with age in parallel with bone mass, it may be captured by bone densitometry (5). Since then interest in bone quality has strengthened because prevalent fracture is a predictor of incident fracture independent of bone density (6), and because for some treatments the reduction in fracture risk appears to be out of proportion to the increase in bone density (7).

The production, detection and repair of fatigue damage are now understood in greater detail (8). The histologic study of microarchitecture has become more sophisticated (9) and much effort has been devoted to non-invasive methods of detection (10). All bone in the extremities, and interstitial cancellous bone in the central skeleton, has both low turnover and correspondingly increased age (11), which can lead to changes in collagen structure (12) and to an undesirable increase in density (13). More recently discovered contributory factors include small bone size (14) and an unnecessarily high bone turnover (15), which can be determined by noninvasive studies, and osteocyte deficiency, whether due to defective formation (16) or to premature death (17), which at present can be determined only by bone biopsy. The multiplicity and collective importance of these factors calls in question the exclusive reliance on bone densitometry for definition and "diagnosis", and the usefulness of the term osteoporosis as the name of a disease (15,18).

References

1. Heaney RP. In: Christiansen C, Johansen C, Riis BJ, eds. Osteoporosis 1987. Osteopress ApS, Copenhagen, pp. 281-287.
2. Frost HM. Clin Ortho & Rel Res. 1985; 200:198-225.
3. Kleerekoper M, Villanueva AR, Stanciu J, Rao DS, Parfitt AM. Calcif Tissue Int 1985;37:594-597.
4. Parfitt AM, Johnston CC. In: Christiansen C, Johansen C, Riis BJ, eds. Osteoporosis 1987. Osteopress ApS, Copenhagen, pp. 279-320.
5. Parfitt AM. Calcif Tissue Int 1993; 53 (Suppl 1):S2.
6. Klotzbuecher CM, Ross PD, Landsman PB, Abbott TA, Berger M. J Bone Min Res. 2000; 15:721-739.
7. Cummings SR, Karpf DB, Harris F, Genant HK, Ensrud K, LaCroix AZ, Black DM. Amer. J Med. 2002; 112:281-289.
8. Verborgt O, Tatton NA, Majeska RJ, Schaffler MB. J Bone Min Res. 2002; 17:907-914.
9. Dalle Carbonare L, Giannini S. J Endocrin Invest. 2004; 27:99-105.
10. Modlesky CM, Majumdar S, Narasimhan A, Dudley GA. J Bone Min Res. 2004; 19:48-55.
11. Parfitt AM. In: Kleerekoper M, Krane S, eds. Clinical Disorders of Bone and Mineral Metabolism. Mary Ann Liebert Publishers, Inc, New York, 1989:7-14.
12. Bailey AJ, Knott L. Experimental Gerontology. 1999; 34:337-351.
13. Ciarelli TE, Fyhr DP, Parfitt AM. Bone. 2003; 32:311-315.
14. Seeman E, Duan Y, Fong C, Edmonds J. J Bone Min Res. 2001; 16:120-127.
15. Heaney RP. Bone. 2003; 33:457-465.
16. Qiu S, Rao DS, Palnitkar S, Parfitt A. J Bone Miner Res. 2003; 18:1657-1663.

17. O'Brien CA, Jia D, Plotkin LI, Bellido T, Powers CC, Steward SA, Manolagas SC, Weinstein RS. Endocrinology. 2004 145:1835-1841.
18. Parfitt AM. Bone. 2004; 35:1-3.

Disclosures: A. Parfitt, None.

2

Bone Quality: A Biomechanical Perspective. S. Goldstein. University of Michigan, Ann Arbor, MI, USA.

At first glance, the term bone quality appears to be a simple term selected to effectively capture those elements of the physical properties of bone that express its resistance to failure in the face of functional demand. Unfortunately, bone is an extraordinarily complex composite material that demonstrates inhomogeneous, anisotropic, non-linear viscoelastic behavior with the ability to alter its properties in response to damaging as well as non-damaging loads. These properties endow bone with the capacity to achieve two competing objectives; the provision of mechanical integrity for locomotion and protection, and participation in mineral homeostasis through localized remodeling activity. Advancing age and a variety of diseases and disorders compromise one or more of bone constituent properties resulting substantial increases in fragility. As a result, the clinical demand for a direct or surrogate measure of bone's ability to resist fracture is great. This paper presents a biomechanical perspective outlining those features of bone that may influence its ability to withstand loads without damage.

The most striking feature of bone is the hierarchical organization of its architecture. At each level of hierarchy, structural heterogeneity is present as well as the potential for material heterogeneity. Furthermore, any changes in the composition or organization of bone at one hierarchical level, will influence the properties at other levels. Correspondingly, a hierarchical paradigm becomes an effective reference frame for considering the impact or contributions of specific features of bone on resistance to failure.

Two distinct, interrelated classes of bone properties can influence its mechanical integrity; factors most closely associated with classical material science characterizations involving measures of structural and material constitutive properties, and variables associated with the biodynamic behavior of bone that may be influenced by genetic or environmental factors and regulate bone constitutive properties at multiple hierarchical levels. From a clinical/functional perspective, structural properties are the most important in that they incorporate the combined effect of geometry, shape and inherent material properties. Size does matter; bigger, thicker, wider structures impart greater resistance to failure. More importantly, the shape of the bone or more specifically how the mass is distributed relative to the direction of typical functional loads is a critical variable (quantified as a moment of inertia).

From a statistical perspective, in a bone dominantly composed of trabecular tissue, the greatest amount of variance in mechanical properties can be explained by the combination of bone mass and macroscopic architectural organization. Accurate measures of bone mass and 3D orientation have been demonstrated to explain 80 to 90% of the variance in the mechanical behavior of trabecular bone volumes. While this degree of explained variance may seem to make the prediction of fracture risk solvable, clinical and experimental experience suggests that the unexplained proportion of variance may be a key determinant in separating high and low risk patients. For example, measures of trabecular thickness and connectivity add more fidelity to the estimates but explain little variance. On the other hand, it is possible that specific disease states may exacerbate their effect. Stepping down in the hierarchy, the material properties of the extracellular matrix (tissue) explains additional variance, followed next by the combination of extracellular matrix organization and chemical constituency of both the organic and inorganic phases of bone. Importantly, at highly magnified levels, micro-anatomical features such as osteocyte lacunae, compositional transitions such as those that occur at the interface between mineralized and non-mineralized elements create mechanical stress risers that can lead to the initiation of localized damage.

The biodynamic factors that contribute to bone integrity may be better understood by conceptualizing their hierarchical affect working in the other direction. Beginning at the level of the extracellular matrix or

below, the chemical constituency and extracellular matrix organization, is reflective of remodeling behavior and genetic determination. Similarly, at higher levels, hierarchical structure is influenced by both biochemical and mechanical regulation of remodeling as well as genetically regulated patterning. Finally, at the extreme macroscopic hierarchy, geometric features are influenced by combinations of genetic and epigenetic factors.

References

1. Goldstein SA, Hollister SJ, Kuhn JL, Kikuchi N: The Mechanical and Remodeling Properties of Trabecular Bone. In *Biomechanics of Diarthrodial Joints - Vol. II* pg. 61-81, Ed. V.C. Mow, A. Ratcliffe, S.L. Woo, 1990.
2. Goulet, RW, Goldstein, SA, Ciarelli, MJ, Kuhn, JL, Brown, MB and Feldkamp, LA: The Relationship Between the Structural and Orthogonal Compressive Properties of Trabecular Bone. *Journal of Biomechanics* 27(4): 375-389, 1994.
3. McCreadie BR, Goldstein SA: Perspective: Biomechanics of Fracture: Is Bone Mineral Density Sufficient to Assess Risk. *J Bone Miner Res* 15(12): 2305-2308, 2000.
3. Ciarelli TE, Fyhrie DP, Schaffler MB, Goldstein SA: Variations in Three-Dimensional Cancellous Bone Architecture of the Proximal Femur in Women with Hip Fractures and in Controls. *Journal of Bone and Mineral Research*, 15(1):32-40, 2000.
4. Hoffer CE, McCreadie BR, Smith EA, Goldstein SA: A Hierarchical Approach to Exploring Bone Mechanical Properties. In *Mechanical Testing of Bone and the Bone-Implant Interface*, Y.H. An, R.A. Draughn (Eds.), CRC Press, Boca Raton, FL, Chapter 8, 133-149, 2000.

Disclosures: S. Goldstein, None.

3

Bone Quality: A Clinical Perspective. J. E. Compston. University of Cambridge School of Clinical Medicine, Cambridge, United Kingdom.

Bone strength is determined by a number of inter-related variables which include bone mineral density, bone geometry and bone quality. The latter consists of bone turnover, bone microarchitecture, the degree of mineralisation of bone, microdamage and its repair, and the composition of bone mineral and matrix. Of these, bone turnover is the most important and is a major determinant of the other components of bone quality. Whilst bone mineral density (BMD) is a strong predictor of bone strength and hence fracture risk in the untreated state, therapeutically induced changes in BMD explain only a small proportion of the associated reduction in fracture, indicating that changes in bone quality may be more important in this context.

The importance of the components of bone quality is evident from disease states in man, some of which are associated with increased fracture risk despite increased bone mineral density and even bone size. Thus increased bone fragility is seen at both extremes of mineralization, in the conditions of osteomalacia and osteopetrosis respectively. However, whereas osteomalacic bones are soft and bend easily, osteopetrotic bones are stiff and brittle and can thus absorb little energy before breaking. In bone exposed to supra-therapeutic doses of sodium fluoride, mineralisation of osteoid may be defective and the composition of hydroxyapatite is altered due to substitution of fluoride for the hydroxyl group; these changes are associated with reduced biomechanical strength of bone and increased fracture risk at appendicular skeletal sites. Multiple abnormalities of bone quality are seen in Paget's disease, including an abnormal bone matrix with a mosaic of lamellar and woven bone, abnormal mineralisation and alterations of bone microarchitecture. Osteogenesis imperfecta provides an example of a condition in which the primary defect is a relatively subtle alteration in type I collagen synthesis, with secondary changes in mineralisation. Finally, several lines of evidence support the contention that high bone turnover is an independent determinant of bone strength and fracture risk. However, whether the converse is true, i.e. that low bone turnover per se is associated with changes in bone fragility remains to be established.

Assessment of bone quality in clinical practice is currently limited to measurement of biochemical markers of bone turnover. Whilst these

have utility in clinical trials, their value in individual patients is limited by the high biovariability of markers and their measurement variance. Moreover, biochemical markers of resorption and formation reflect whole body bone turnover and may not be sensitive to regional changes, particularly where these predominantly affect cancellous bone. In many diseases the changes in bone quality may be so marked that pathognomonic changes are evident on plain radiography, for example Paget's disease, osteopetrosis, and severe cases of osteogenesis imperfecta. However, detection of more subtle alterations in bone quality may require bone biopsy, for example osteomalacia and low bone turnover states. For diagnostic purposes, qualitative assessment is adequate but quantitative assessment of the components of bone quality is becoming an important research tool that provides unique information about the pathophysiology of untreated and treated bone disease states.

A number of non-invasive techniques are emerging that may lead to improvements in the assessment of bone quality in clinical studies. These include high resolution peripheral quantitative computed tomography (pQCT) and high-resolution magnetic resonance imaging (MRI); in addition, assessment of regional osteoblastic activity using ^{18}F -fluoride positron emission tomography provides a potential means by which regional bone turnover could be assessed in both the axial and appendicular skeleton. Currently, however, bone biopsy remains the most powerful tool for studying bone quality in clinical studies and its use should be more actively encouraged, particularly in the context of the effects of pharmacological interventions on bone.

References

1. Frost ML, Cook GJR, Blake GM, Marsden PK, Benata NA, Fogelman I. A prospective study of risedronate on regional bone metabolism and blood flow at the lumbar spine measured by ^{18}F -Fluoride positron emission tomography. *Journal of Bone and Mineral Research* 2003;18:2215-2222.
2. Turner CH. Biomechanics of bone: determinants of skeletal fragility and bone quality. *Osteoporosis International* 2002;13:97-104.
3. Meunier PJ, Boivin G. Bone mineral density reflects bone mass but also the degree of mineralisation of bone: therapeutic implications. *Bone* 1997;21:373-377.

Disclosures: J.E. Compston, None.

4

Bone Geometry and Skeletal Fragility. M. L. Bouxsein. Beth Israel Deaconess Medical Center / Harvard Medical School, Boston, MA, USA.

In adolescence, boys suffer more fractures than girls. Yet, at later ages, fracture incidence is two to four-fold higher in women than in men. In addition, fracture incidence varies markedly by ethnicity and race. Understanding the mechanisms that underlie this marked sex- and ethnic/racial difference in fracture incidence will lead to improved strategies for fracture prevention. A bone fractures when the load applied to the bone generates an internal stress that exceeds the strength of the underlying tissue. Thus, for any given loading condition, the ability of a bone to resist fracture is determined by 1) the amount of bone tissue (size), 2) the spatial arrangement of the tissue (shape, microarchitecture), and 3) the intrinsic material properties of the tissue. Whereas there are few data indicating that bone material properties vary by sex- and race, age-, race- and sex-related differences in the size and shape of bones are well established. Direct measurements of bone geometry from modern and archeological skeletal specimens consistently show a consistent pattern of periosteal apposition and endosteal resorption with increasing age, and suggest that periosteal expansion is greater in men than women. This pattern of geometric adaptation would tend to preserve whole bone strength better in men than women. These trends have been further studied in population-based investigations that have used non-invasive assessment of bone geometry by 2-D radiographs, 2D dual-energy-X-ray absorptiometry (e.g. "hip strength analysis"), and more recently 3D quantitative computed tomography. Results of these investigations have been mixed, with some data corroborating the presence of sex-specific periosteal adaptation and other results challenging this long-held tenet. Fur-

thermore, there is increasing evidence that bone size and shape differ between individuals who suffer fractures and age- and sex-matched controls who do not. Thus, it is evident that an individual's bone size and shape, which are determined by genetic factors and by age-related changes are both key determinants of skeletal fragility. New methods to assess bone geometry are likely to improve the prediction of fracture risk.

Suggested Reading:

- 1) Ahlborg HG et al (2003) Bone Loss and Bone Size after the Menopause. *N Engl J Med*, 349: 327-334.
- 2) Beck TJ, et al (2000) Structural Trends in the Aging Femoral Neck and Proximal Shaft: Analysis of the Third National Health and Nutrition Examination Survey Dual-Energy X-ray Absorptiometry Data. *J Bone Min Res*, 15: 2297-2304.
- 3) Bouxsein ML, et al (1994) Age-Related Differences in Cross-Sectional Geometry of Forearm Bones in Healthy Women. *Calcif Tissue Int*, 54:113-118.
- 4) Duan Y, et al (2003) Structural and Biomechanical Basis of Sexual Dimorphism in Femoral Neck Fragility has its Origins in Growth and Aging. *J Bone Min Res*, 18: 1766-1774.
- 5) Faulkner K, et al (1993) Simple Measurement of Femoral Geometry Predicts Hip Fracture: the Study of Osteoporotic Fractures. *J Bone Min Res*, 8: 1211-1217.
- 6) Garn SM (1972) The Course of Bone Gain and the Phases of Bone Loss. *Orthop Clin North Am*, 3:503-520.
- 7) Gilsanz V, et al (1995) Vertebral Size in Elderly Women with Osteoporosis. Mechanical Implications and Relationship to Fracture. *J Clin Invest*, 95: 2232-2237.
- 8) Glüer C-C, et al (1994) Prediction of Hip Fracture from Pelvic Radiographs: the Study of Osteoporotic Fractures. *J Bone Min Res*, 9: 671-677.
- 9) Kaptoge S, et al (2003) Effects of Gender, Anthropometric Variables, and Again on the Evolution of Hip Strength in Men and Women Aged Over 65. *Bone*, 32: 561-70.
- 10) Mayhew P, et al (2004) Discrimination Between Cases of Hip Fracture and Controls is Improved by Hip Structural Analysis compared to Areal Bone Mineral Density. An ex vivo study of the femoral neck. 34: 352-61.
- 11) Peacock M, et al (1995) Better Discrimination of Hip Fracture using Bone Density, Geometry and Architecture. *Osteop Int*, 5:167-173.
- 12) Riggs BL, et al (2004) Population-based Study of Age and Sex Differences in Bone Volumetric Density, Size, Geometry and Structure at Different Skeletal Sites. *J Bone Min Res*, 19: 1945-1954.
- 13) Ruff CB and Hayes WC (1982) Subperiosteal Expansion and Cortical Remodeling of the Human Femur and Tibia with Aging. *Science*, 217: 945-948.
- 14) Russo CR, et al (2003) Aging Bone in Men and Women: Beyond Changes in Bone Mineral Density. *Osteop Int*, 14: 531-538.
- 15) Skaggs DL et al (2001) Increased Body Weight and Decreased Radial Cross-Sectional Dimensions in Girls with Forearm Fractures. *J Bone Min Res*, 16: 1337-1342.
- 16) Smith RW and Walker RR (1964) Femoral expansion in aging women: implications for osteoporosis and fractures. *Science*, 145: 156-157.
- 17) Yoshikawa T, et al (1994) Geometric Structure of the Femoral Neck Measured Using Dual-Energy X-ray Absorptiometry. *J Bone Min Res*, 9: 1053-1064.

Disclosures: **M.L. Bouxsein**, None.

5

Effect of Microarchitecture on Bone Strength. **H. Weinans**.

Erasmus MC, Rotterdam, The Netherlands.

The microarchitecture of cancellous bone refers to the size, shape and orientation of the trabeculae. It is obvious that this architecture has a direct relation to the amount of bone or bone mineral density, however it is widely assumed that architecture contributes independently to bone strength as well. Quantification of microarchitecture is not trivial and many parameters have been introduced that could be calcu-

lated in a reproducible and standardized manner with respect to both 2D histological slices and fully 3D reconstructions. The data so far on architectural parameters that contribute independently from BMD to bone strength is confusing. Most parameters concern scalars that do not reflect the intrinsic anisotropy (orientation) of the cancellous structure. Detailed biomechanical studies have shown that BMD in combination with parameters that include the orientation can almost fully predict the mechanical stiffness of cancellous bone in all directions [1]. Furthermore it was found that the trabecular orientation or anisotropy and its corresponding *mechanical* anisotropy correlates with fracture risk independent from BMD [2]. This indicates that the search for clinically relevant morphometric parameters should concentrate on measures of anisotropy.

Thus, the microarchitecture provided by volume fraction and its anisotropic parameters can reflect the strength at a specific moment in time in cross-sectional studies. However, it is well known now, e.g. from many bisphosphonate studies, that small changes in BMD and likely also small changes in trabecular orientation can have significant effects on fracture risk. The general idea being that turnover, that is reduced in anti-resorptive treatments, is an independent contributor of bone strength. Normally turnover rate is not included in microarchitecture. In 2D sections microarchitecture can be determined with a fairly high resolution, however it is hard to get an idea of the amount and size of the resorption pits generated by the osteoclasts. In 3D studies using microCT one could in theory parameterize the resorption pits, but in most 3D reconstructions the resolution is too low. In computer simulation studies it was shown how important the effects of the number and size of resorption pits are. With only 10 percent bone loss by an increased number of resorption pits the bone structure can loose as much as 35% of its stiffness. Even more important, the stress distribution through the trabecular network becomes much less uniform with increasing number of resorption pits, which further deteriorates the structure and reduces the strength in a strong nonlinear fashion [3,4]. The size and number of the resorption pits should be considered as part of the microarchitecture. So far this aspect of micro-architecture was not much studied, likely because of its technical difficulties and therefore the topic was severely undervalued.

New anabolic drugs can lead to higher increase of BMD and may be additional improvements in microarchitecture. However, such compounds likely not lead to reductions in size and number of resorption pits. Their mechanical improvement should therefore come entirely from the BMD increase and subsequent change in architecture. To which extent microarchitecture can be altered with such drugs is not known yet. If anabolic compounds only add tissue at existing surfaces, their microarchitectural improvement might be limited. With improved resolution in micro-CT and refined techniques for in-vivo micro-CT enabling longitudinal animal experiments, these important aspects will soon be addressed in animal experiments.

References

- [1] Rietbergen et al. Relationships between bone morphology and bone elastic properties can be accurately quantified using high-resolution computer reconstructions. *J Orthop Res*. 16:23-8, 1998.
- [2] Homminga et al. Cancellous bone mechanical properties from normals and patients with hip fractures differ on the structure level, not on the bone hard tissue level. *Bone*. 30:759-64, 2002.
- [3] Van der Linden et al. Mechanical consequences of bone loss in cancellous bone. *J Bone Miner Res*. 16:457-65, 2001.
- [4] Van der Linden et al. A three-dimensional simulation of age-related remodeling in trabecular bone. *J Bone Miner Res*. 16:688-96, 2001.
- [5] Day et al. Bisphosphonate treatment affects trabecular bone apparent modulus through micro-architecture rather than matrix properties. *J Orthop Res*. 22:465-71, 2004.

Disclosures: **H. Weinans**, None.

6

Effect of Osteoporosis Therapies on Microarchitecture. **D. W. Dempster**. Helen Hayes Hospital, West Haverstraw, NY, USA.

Deterioration of cancellous and cortical bone microarchitecture is a hallmark of osteoporosis. There are two distinct cellular mechanisms

(1). One involves osteoblast insufficiency, such that, with age, the osteoblasts become less and able to refill the resorption cavities created by the osteoclasts. The result is a decrease in the wall thickness of cortical and cancellous osteons, which in turn causes an increase in cortical porosity and a decrease in trabecular thickness. This is the primary mechanism underlying age-related bone loss. The second mechanism is responsible for postmenopausal bone loss. Here, the osteoclast teams become too aggressive and penetrate through the entire trabeculae causing perforations. These perforations gradually expand, converting what was once a sturdy plate-like structure into one composed of thin rods. During the final stages of bone loss by this mechanism, the trabecular rods are eroded through and the remaining trabeculae become progressively disconnected. Resorption depth is also increased on the endocortical surface, resulting in thinning and trabecularization of the cortex. This osteoclast-mediated bone loss has a more deleterious effect on bone strength than the osteoblast-mediated loss described above. These changes in bone microarchitecture are the consequences of aging and estrogen deficiency and are exaggerated in patients with osteoporosis. When matched for bone mass, patients who fracture have significantly poorer bone microarchitecture than non-fractured, control subjects (2-6).

Drugs that have been shown to lower fracture risk in humans have also been shown to have beneficial effects on cancellous and cortical bone microarchitecture. These drugs now fall into two classes: antiresorptive agents, which are perhaps better termed anticatabolic agents, and anabolic agents. Anticatabolic agents initially reduce fracture risk by lowering bone turnover. Biopsy studies have demonstrated preservation of key microarchitectural variables, such as cancellous bone volume, and trabecular number and thickness when post-treatment biopsies are compared to pre-treatment samples from the same individuals and the same variables in post-treatment biopsies from patients on active drug are improved when compared to those from patients on placebo (7-10). These agents also decrease cortical porosity.

In sharp contrast to anticatabolic agents, anabolic agents increase bone turnover with net bone formation exceeding net bone resorption. The result is an improvement in bone microarchitecture when biopsies taken after treatment are compared to those taken before treatment in the same patients. For example, significant improvements in connectivity density and cortical thickness have been demonstrated for teriparatide (11, 12).

We now have two classes of antifracture drugs, one of which improves bone microarchitecture while the other preserves it, lending support to the concept of sequential therapy in severely affected patients.

References

1. Dempster DW. The pathophysiology of bone loss. *Clin Geriatr Med* 19:259-270, 2003
2. Kleerekoper M, Villanueva AR, Stanciu J, Rao DS, Parfitt AM. The role of three-dimensional trabecular microstructure in the pathogenesis of vertebral compression fractures. *Calcif Tissue Int* 1985;37:594-7.
3. Legrand E, Chappard D, Pascaretti C, Duquenne M, Krebs S, Rohmer V, Basle MF, Audran M. Trabecular bone microarchitecture, bone mineral density, and vertebral fractures in male osteoporosis. *J Bone Miner Res* 2000;15:13-9.
4. Aaron JE, Shore PA, Shore RC, Beneton M, Kanis JA. Trabecular architecture in women and men of similar bone mass with and without vertebral fracture: II. Three-dimensional histology. *Bone* 2000;27:277-82.
5. Oleksik A, Ott SM, Vedi S, Bravenboer N, Compston J, Lips P. Bone structure in patients with low bone mineral density with or without vertebral fractures. *J Bone Miner Res* 2000 15:1368-75.
6. Ciarelli TE, Fyhrie DP, Schaffler MB, Goldstein SA. Variations in three-dimensional cancellous bone architecture of the proximal femur in female hip fractures and controls. *J Bone Miner Res* 2000;15:32-40.
7. Prestwood K.M. et al. A comparison of the effects of Raloxefine and Estrogen on bone in postmenopausal women *The Journal of Clinical Endocrinology & Metabolism*, 2000;85:2197-202.
8. Borah B, Dufresne TE, Chmielewski PA, Johnson TD, Chines A, Manhart MD. Risedronate preserves bone architecture in postmenopausal women with osteoporosis as measured by three-dimensional microcomputed tomography. *Bone*. 2004;34:736-46.

9. Dufresne TE, Chmielewski PA, Manhart MD, Johnson TD, Borah B.

Risedronate preserves bone architecture in early postmenopausal women in 1 year as measured by three-dimensional microcomputed tomography.

Calcif Tissue Int. 2003;73:423-32.

10. Recker R et al. Trabecular bone microarchitecture after alendronate treatment of osteoporotic women, *Current Medical Research and Opinion*, 2005;21:185-94.

11. Dempster DW, Cosman F, Kurland ES, Zhou H, Nieves J, Woelfert L, Shane E, Plavetic K, Müller R, Bilezikian JP, Lindsay R. Effects of daily treatment with parathyroid hormone on bone microarchitecture and turnover in patients with osteoporosis: a paired biopsy study. *J Bone Miner Res* 16:1846-1853, 2001.

12. Jiang Y, Zhao JJ, Mitlak BH, Wang O, Genant HK, Eriksen EF. Recombinant human parathyroid hormone (1-34) [teriparatide] improves both cortical and cancellous bone structure. *J Bone Miner Res*. 2003;18:1932-41.

Disclosures: D.W. Dempster, Eli Lilly, Merck, Procter & Gamble, Sanofi-Aventis, SKB-Roche, NPS 5, 8; Novartis 8.

7

Trabecular Bone Failure at the Microstructural Level. R. Müller.

Institute for Biomedical Engineering, Swiss Federal Institute of Technology (ETH) and University of Zürich, Zürich, Switzerland.

With recent advances in genetics and molecular medicine there is a strong need for quantitative imaging of three-dimensional (3D) biological structures. A number of new microstructural imaging modalities have been put forward recently allowing phenotypic quantification with high precision and accuracy in humans and animals (1-3). Although biomedical imaging technology is now readily available, few attempts have been made to expand the capabilities of these systems by adding not only quantitative but also functional analysis tools combining micro- and nano-scale imaging with time-lapsed mechanical testing (4,5). The approaches that are used for such quantification employ hierarchical bioimaging and visualization of biomaterials as well as biomechanical testing and simulation techniques. Today, these methods are successfully employed for the quantitative assessment of structure function relationships in tissue healing, growth and adaptation and are now also often used for precise phenotypic characterization of tissue response in mammalian genetics, gene therapy and molecular biology.

An area of special interest is functional imaging of bone to assess the relative importance of bone architecture and other parameters of bone quality in the assessment of the mechanical competence of bone. Towards that end, one needs to mention that many bones within the axial and appendicular skeleton are subjected to repetitive, cyclic loading during the course of ordinary daily activities. If this repetitive loading is of sufficient magnitude or duration, fatigue failure of the bone tissue may result which is often preceded by buckling and bending of microstructural elements.

Here we were investigating failure mechanisms of 3D trabecular bone using micro- and nano-computed tomography (μ CT/nCT) through dynamic, time-lapsed measurements of failure initiation and propagation, as well as damage accumulation. For this reason, we have developed an image-guided technique that utilizes micro-compression and allows, for the first time, the direct three-dimensional visualization and quantification of failure progression on the microscopic level and therefore also allows looking beyond the elastic range to gain new insight in the plasticity of microstructural bone failure (6). Functional bone imaging results in image sequences nicely illustrating the plastic behavior of the material. Based on these images, a computational method was developed and validated (7) to quantify individual trabecular strains during failure, which was characterized by an initial buckling and bending of structural elements followed by a collapse of the overloaded trabeculae. For a 1% global strain, the localized strains between nodes were as high as eight times and six times the global compressive and tensile strains, respectively, providing further evidence for a band-like, local failure behavior of trabecular bone. These strains were mostly found in rod-like elements that were aligned with the main strain axis.

In conclusion, the technique of micro-compression in combination with 3D μ CT allows visualization and quantification of failure initiation and propagation, and will improve our understanding of the relative importance of densitometric, morphological, and loading factors in the etiology of spontaneous fractures of the hip and the spine.

References

1. S. Majumdar. Magnetic resonance imaging of trabecular bone structure. *Top Magn Reson Imaging*, 13(5):323-334, 2002.
2. F. W. Wehrli, P. K. Saha, B. R. Gomberg, H. K. Song, P. J. Snyder, M. Benito, A. Wright, R. Weening. Role of magnetic resonance for assessing structure and function of trabecular bone. *Top Magn Reson Imaging*, 13(5):335-355, 2002.
3. R. Müller. Bone microarchitecture assessment - current and future trends. *Osteoporosis Int.*, 14(S5):89-99, 2003.
4. B. K. Bay. Texture correlation: a method for the measurement of detailed strain distributions within trabecular bone. *J. Orthop. Res.*, 13:258-267, 1995.
5. R. Müller, S. C. Gerber and W. C. Hayes. Micro-compression: A novel technique for the nondestructive assessment of local bone failure. *Technology and Health Care*, 6:433-444, 1998.
6. A. Nazarian and R. Müller. Time-lapsed microstructural imaging of bone failure behavior. *J. Biomech.*, 37:55-65, 2004.
7. R. Müller, T. Bösch, D. Jarak, M. Stauber, A. Nazarian, M. Tantiello and S. Boyd. Micro-mechanical evaluation of bone microstructures under load. In U. Bonse, editor, *Developments in X-Ray Tomography III*, SPIE Vol. 4503, pp. 189-200, 2002.

Disclosures: R. Müller, None.

8

Characteristics of the Collagen-Mineral Nano-Composite and Skeletal Fragility. P. Roschger¹, E. P. Paschalis¹, K. Klaushofer¹, P. Fratzl². ¹Ludwig Boltzmann Institute of Osteology at the Hanusch Hospital of the WGKK and at the AUVA Trauma Centre Meidling, 4th Med. Dept., Hanusch Hospital, Vienna, Austria, ²Max Planck Institute of Colloids and Interfaces, Dept. Biomaterials, Potsdam, Germany.

Bone has a highly complex hierarchical structure and achieves therewith a remarkable stiffness, strength and toughness. This structure can be altered by metabolic or genetic diseases, medical treatments or environmental influences. Since all hierarchical levels of bone structure from the macro- to the nano-scale contribute to its mechanical performance, modifications occurring on any level may compromise the integrity of the tissue. As a consequence, it is important to understand disease-related alterations on each structural level. In-vivo measurements of bone mass (BMD) give information at the organ level and only partially characterize the fracture risk. Factors of bone quality have to be taken into account in order to achieve a more accurate estimate.

Bone quality may be defined as the sum of all factors mediating bone mechanical competence at constant bone mass. Since there may be a number of contributing factors, it is useful to differentiate between architectural and material quality. The first one encompasses geometrical factors such as bone diameter (at constant mass) or trabecular architecture in cancellous bone. For example, it is well known that - for given amount of material - a hollow tube (as a rough approximation of a long bone) is stiffer in bending if it has a larger diameter and a correspondingly thinner cortex. The bone material quality considers all possible modifications at the material level, including lamellar versus woven bone structure, status (e.g. cross-linking) of the collagen-rich matrix, quantity, size and orientation of mineral particles, particle-collagen interactions, etc.

Bone material corresponds to a composite made of collagen fibrils and mineral (carbonated hydroxyapatite) nano-particles. It combines an organic phase with low E-modulus (~0.1 GPa) and high toughness (~10 kJ/m²) and a mineral phase with high E-modulus (~100 GPa) but low toughness (~0.01 kJ/m²). The composite material is both stiff and tough (E-modulus ~20 GPa, toughness ~4 kJ/m²). The mineralized collagen fibril represents the basic building block of bone and can be assembled in various ways into lamellae, osteons and other structural units. Focus-

ing on the lowest level, the composite can be approximated by a simple model of staggered mineral platelets embedded in an organic matrix. The mechanical properties calculated for such a model predict a non-linear dependence of the elastic modulus on the mineral content. In addition to the volume fraction of mineral, the particle shape (aspect ratio) and the shear modulus of the collagen matrix are the crucial parameters. Since the maximum deformation is much larger for bone (about 2% strain) than for the mineral (about 0.1%), it is clear that most of the deformation must take place in the organic matrix. The model shows that the mineral particles carry mainly the tensile stress, whereas the collagenous matrix transfers the load between the particles via shear. To ensure integrity and optimized strength of the mineralized fibril, the mineral platelets must be able to sustain large tensile stress without fracture, whereas the protein layer and protein/mineral interface must sustain shear strains without failure. It has been proposed that the nanometer size (~3.5 nm thick) increases the strength of the mineral platelets well beyond the value of macroscopic hydroxyapatite. According to other studies, sacrificial bonds within and between collagen molecules could permit large shears without failure. From this analysis it becomes clear that size and arrangement of mineral particles, the status of the collagen matrix (e.g. cross-linking), as well as the arrangement of mineralized collagen fibrils into lamellar or other structures will determine the material quality of bone. Hence, these parameters (and their changes with disease and treatment) will be essential in understanding bone strength or fragility.

A number of techniques allow the investigation of the status of the collagen-mineral composite and, hence, the bone material quality. They include:

- i) polarized light microscopy to assess lamellar architecture,
- ii) quantitative back-scattered electron imaging (qBEI) or microradiography to determine the distribution of mineral in the tissue,
- iii) transmission electron microscopy, small-angle x-ray scattering (SAXS) and (scanning) x-ray diffraction to estimate size, shape and orientation of mineral particles
- iv) infrared (FTIR) or Raman spectroscopic imaging to estimate the status of the organic matrix as well as the mineral
- v) nanoindentation to determine the local hardness and E-modulus.

All these techniques have specific advantages and drawbacks which will be discussed.

In some cases, the relation between skeletal fragility and bone material quality has been clearly demonstrated. A typical example is sodium fluoride treatment of osteoporosis, where the tremendous increase of bone mass failed to reduce the fracture incidence. However, SAXS and qBEI revealed, that the nano-composite structure was strongly altered by changes in mineral particle size and shape, as well as mineral local volume fraction. A classical case of high skeletal fragility is osteogenesis imperfecta. In this disease all hierarchical levels are involved. The bone mass is strongly reduced, the cortical and trabecular architecture is deteriorated, the bone material exhibits extreme brittleness. Again the nano-composite structure is altered by a false collagen synthesis and assembly to fibrils, and a reduction in crystal size and an increase of mineral volume fraction. In the cases of post menopausal and idiopathic osteoporosis there is rising evidence based on qBEI, nanoindentation and FTIR, that at material level the volume fraction of mineral and the collagen cross-linking is altered too, thus contributing to the bone fragility.

In conclusion, the integrity of the nano-composite structure of bone material is an important factor in defining the overall mechanical competence of the skeleton. An appropriate knowledge of the composite parameters in an individual patient is essential for a proper therapeutic targeting of the material quality.

Reviews:

J.D. Currey, *Bones: Structure and Mechanics*, Princeton University Press (2002).

P. Fratzl, H.S. Gupta, E.P. Paschalis and P. Roschger (2004) Structure and mechanical quality of the collagen-mineral nano-composite in bone. *J. Mater. Chem.* 14: 2115-2123.

S. Weiner, H.D. Wagner (1998) The material bone: structure mechanical function relations. *Annu. Rev. Mater. Sci.* 28:271-298.

SAXS:

S. Rinnerthaler, P. Roschger, H.F. Jakob, A. Nader, K. Klaushofer, P. Fratzl (1999) Scanning Small Angle X-ray Scattering Analysis of Human Bone Sections. *Calcif. Tiss. Int.* 64:422-429

qBEI:

P. Roschger, P. Fratzl, J. Eschberger, K. Klaushofer (1998) Validation of Quantitative Backscattered Electron Imaging (qBEI) for the Measurement of Mineral Density Distribution on Human Bone Biopsies. *Bone* 23:319-326

FTIR:

P.E. Paschalis, K. Verdelis, R. Mendelson, A. Boskey, M. Yamauchi (2001) Spectroscopic characterization of collagen cross-links in bone. *J. Bone Miner. Res.* 16:1821-1828.

TEM:

M.A. Rubin, I. Jasiuk, J. Taylor, J. Rubin, T. Ganey, and R.P. Apkarian (2003) TEM analysis of the nanostructure of normal and osteoporotic human trabecular bone. *Bone* 33:270-282.

Disclosures: **P. Roschger**, None.

9

Collagen Composition, Cross-links and Skeletal Fragility. D. Vashishth*. Rensselaer Polytechnic Institute, Troy, NY, USA.

Non-enzymatic glycation (NEG) products, resulting from the reduction of collagen with sugar, accumulate with age (Catanese et al., 1999; Wang et al., 2002) and may increase bone's propensity to fracture. Our group has developed a novel technique to induce NEG in vitro and investigate how NEG may affect bone fracture properties and contribute to age-related bone fragility (Vashishth et al., 2001). To this end, a series of multicyclic creep tests on control and glycated specimens of mineralized and demineralized cortical bone specimens were conducted in conjunction with fracture mechanics based initiation and propagation tests (human, age range 34-97) to identify the effects of NEG on bone toughening mechanisms including collagen deformation and fracture, and microcracking. It was found that the physiological levels of NEG increased stiffness (26%) and reduced the creep rate (70%) and maximum strain to failure (47%) of bone collagen. This modification in the deformation and fracture behavior of bone collagen eventually manifested itself in reduced fracture properties associated with propagation and not initiation of damage processes in mineralized bone. More significantly, the observed changes in bone toughness and toughening mechanisms due to NEG show a close correspondence to the age-related toughness changes measured by testing of human cadaveric bone specimens.

References

1. Catanese, J., Bank, R. A., Tekoppele, J. M. and Keaveny, T. M. "Increased cross-linking by non-enzymatic glycation reduces the ductility of bone and bone collagen". Proceedings of the ASME 1999 Bioengineering Conference. BED-Vol. 42, 267-268, 1999.
2. Wang X, Shen X, Li X, Agrawal CM. Age-related changes in the collagen network and toughness of bone. *Bone*. 2002 Jul;31(1):1-7.
3. Vashishth, D., Gibson, G.J., Khoury, J.I., Schaffler, M.B., Kimura, J., and Fyhrie, D.P. "Influence of nonenzymatic glycation on biomechanical properties of cortical bone". *Bone* 28: 1-7, 2001.

Disclosures: **D. Vashishth**, None.

10

Matrix Mineral Interactions. W. J. Landis. Northeastern Ohio Universities College of Medicine, Rootstown, OH, USA.

The deposition of inorganic crystals and mineral in bone or other calcifying vertebrate tissues is orchestrated by a variety of organic matrix components that regulate, direct and control inorganic ions, principally calcium and phosphorus, in the nucleation, growth and development of calcium phosphate (apatite) crystals. Organic constituents of bone involved in these events of matrix: mineral interaction include type I collagen, bone sialoprotein, osteopontin, osteocalcin, and several other molecules with type I collagen being considered of major importance. The recognition of the significance of type I collagen in this regard may be ascribed to its structural association with mineral that has been well documented by classical electron microscopy and subsequent physicochemical investigation [1-3].

More recently, the relationship between type I collagen and mineral in bone and calcifying tendon has been examined by novel methods of high voltage electron microscopy and three-dimensional (3D) tomography and atomic force microscopy [4-6], in which several details of very early events in mineral formation have been revealed. This work has shown that (a) crystals exist in the form of very small platelets that nucleate in channels or gaps created by type I collagen periodic (~67 nm) hole and overlap zones; (b) crystal platelets grow preferentially in length along their crystallographic c-axes and in width through the collagen channel or gap spaces; (c) growing crystals maintain a coplanar alignment within collagen such that their c-axes and (100) crystal faces are generally parallel for all crystals; (d) crystals grow in an oriented fashion such that their c-axes are generally parallel to the long axis of collagen with which they associate; (e) crystals within the same channel or gap fuse into larger and thicker plates that maintain their periodic deposition and parallel nature; and (f) through varying changes in length, width and thickness the crystals form a series of parallel plate aggregates that ultimately become lamellar in shape and constitute a portion of bone at its anatomical level of structural hierarchy. In addition to these features, mineral crystals may also nucleate and grow on the surfaces of type I fibrils, possibly adjacent to or near the putative surface origins of the channels or gaps [7]. Crystals growing on collagen surfaces appear in stellate and other forms with a random surface distribution. Thus there is both highly ordered intrafibrillar (within type I collagen in association with its hole and overlap zones) and relatively more disordered interfibrillar (between neighboring collagen fibrils) mineral deposition in bone. Both intrafibrillar and interfibrillar deposits associated with collagen eventually lead to complete mineralization of the extracellular spaces of bone tissue.

Current investigation of matrix: mineral interaction has concerned an analysis of type I collagen primary, secondary and tertiary structure and whether the stereochemistry of the protein dictates the normal characteristic size, shape, alignment, orientation, location and distribution of apatite crystals associated with collagen intrafibrillar or surface mineral deposition. In this context, computer modeling of the hole zone region of type I collagen suggests several potential sites of ion binding and calcium and phosphate localization [8]. Conceptually, the apparent close interatomic distances determined in this manner between calcium and phosphate ions may allow apatite crystal nucleation. Continuing studies are extrapolating these results to define possible relationships of putative apatite nucleation and growth sites to crystal alignment and orientation in association with type I collagen hole and overlap zones. Work also is in progress to determine potential apatite nucleation and growth sites on collagen surfaces as well to identify and localize bone sialoprotein, osteopontin, osteocalcin and other organic molecules that may be acting independently or in concert with type I collagen to mediate mineral formation in bone. The present analysis of type I collagen stereochemistry and identification of potential calcium and phosphate binding sites in the hole zones of the protein support the concepts that collagen provides a unique template for mineral nucleation, growth and development and serves as a critical underlying component of matrix: mineral interaction in bone and other calcifying vertebrate tissues except enamel.

References

1. Robinson RA (1952) *J Bone Joint Surg* 34:389-434.
2. Glimcher MJ, Krane SM (1968) In: Ramachandran GN, Gould BS (Eds) *Biology of collagen: A treatise on collagen*, Vol IIB, Academic Press, New York, pp 68-251.
3. Weiner S, Price PA (1986) *Calcif Tissue Int* 39:365-375.
4. Landis WJ, Song MJ, Leith A, McEwen L, McEwen B (1993) *J. Struct Biol* 110:39-54.
5. Landis WJ, Hodgins KJ, Arena J, Song MJ, McEwen BF (1996) *Microsc Res Technol* 33:192-202.
6. Landis WJ, Hodgins KJ, Song MJ, Arena J, Kiyonaga S, Marko M, Owen C, McEwen BF (1996) *J Struct Biol* 117:24-35.
7. Siperko LM, Landis WJ (2001) *J Struct Biol* 135:313-320.
8. Landis WJ, Silver FH (2002) *Compar Biochem Physiol -- Part A* 133:1135-1157.

Disclosures: **W.J. Landis**, None.

11

How Does Bone Break? Fracture Mechanics and Crack**Propagation.** R. O. Ritchie^{*1}, R. K. Nalla^{*2}, J. J. Kruzic^{*2}, J. H. Kinney^{*3}.¹University of California, Berkeley, Berkeley, CA, USA,²Lawrence Berkeley National Laboratory, Berkeley, CA, USA,³Lawrence Livermore National Laboratory, Livermore, CA, USA.

Biological materials comprising mineralized tissues, such as bone (and dentin), have hierarchical structures with characteristic length scales ranging from nanometers to millimeters. In this presentation, *in vitro* fracture toughness and fatigue-crack propagation properties of human cortical bone are examined from a perspective of discerning how these properties depend upon such microstructural hierarchies. The motivation for this is that although there is substantial clinical interest in the fracture resistance of bone, there is relatively little mechanistic information available on how bone derives its resistance to cracking and how this is affected by cyclic loads. In this presentation, *in vitro* experiments are described that establish that the initiation of fracture is locally strain-controlled [1] and that subsequent crack growth (characterized by resistance-curve behavior) is associated with a variety of extrinsic toughening (crack-tip shielding) mechanisms [2], most importantly crack bridging (from individual collagen fibrils and especially “uncracked ligaments”), macroscopic crack deflection and to a lesser extent diffuse microcracking [3]. Quantitative estimates for the relative contributions of these mechanisms to the overall toughness are derived from simple micromechanical models [4]. In a manner not unlike ceramic materials, it is shown that such extrinsic mechanisms act to toughen bone by lessening the magnitude of stresses experienced at the tip of any cracks. Although macroscopic crack deflection along cement lines provides a principal source of toughening in the transverse orientation, we show that crack bridging by intact regions in the crack wake (so-called uncracked ligaments) is the primary toughening mechanism in longitudinal orientations; such bridges act to sustain load that would otherwise be used to propagate the crack. We then describe *in vitro* fatigue experiments that seek to examine time- or cycle-dependent crack-growth behavior, which pertain to stress fractures in bone [5]. Finally, we show that the role of biological aging, which causes a marked deterioration in the fracture toughness of bone, can be attributed to an age-related deterioration in the potency of crack bridging [6], a phenomenon that we believe is associated with the role of excessive remodeling in increasing the density of secondary osteon structures. We attempt to discriminate between possible age-related changes in the constitutive properties of the hard tissue and age-related changes in its microstructure.

*Supported by National Institutes of Health (Grant 5R01 DE015633)

References

- [1] R. K. Nalla, J. H. Kinney, and R. O. Ritchie, “Mechanistic Fracture Criteria for the Failure of Human Cortical Bone”, *Nature Materials*, vol. 2, 2003, pp. 164-68.
- [2] R. K. Nalla, J. J. Kruzic, J. H. Kinney, and R. O. Ritchie, “Mechanistic Aspects of Fracture and R-Curve Behavior in Human Cortical Bone”, *Biomaterials*, vol. 26, 2005, pp. 217-31.
- [3] R. K. Nalla, J. J. Kruzic, and R. O. Ritchie, “On the Origin of Toughness of Mineralized Tissue: Microcracking or Uncracked-Ligament Bridging”, *Bone*, vol. 34, 2004, pp. 790-98.
- [4] R. K. Nalla, J. S. Stölken, J. H. Kinney, and R. O. Ritchie, “Fracture in Human Cortical Bone: Local Fracture Criteria and Toughening Mechanisms”, *Journal of Biomechanics*, doi:10.1016. 2004.07.010.
- [5] R. K. Nalla, J. J. Kruzic, J. H. Kinney, and R. O. Ritchie, “Aspects of *In Vitro* Fatigue-Crack Growth in Human Cortical Bone: Time- and Cycle-Dependent Crack Growth”, *Biomaterials*, vol. 26, 2005, pp. 2183-95.
- [6] R. K. Nalla, J. J. Kruzic, J. H. Kinney, and R. O. Ritchie, “Effect of Aging on the Toughness of Human Cortical Bone: Evaluation by R-Curves”, *Bone*, vol. 35, 2004, pp. 1240-46.

Disclosures: **R.O. Ritchie**, None.

12

Bone Failure at the Ultrastructural Level. D. Fyhrie^{*}. University of California, Davis, Sacramento, CA, USA.

Synthesis of the literature and examination of failed tissue suggests that a key factor in bone strength and toughness at the ultrastructural

level is cracking of the mineral (K. Hasegawa *et al.*, *Spine* **18**, 2314-20 (Nov, 1993), D. H. Kohn, *Crit Rev Biomed Eng* **23**, 221-306 (1995)) followed by failure of the collagen (D. Vashishth, J. C. Behiri, W. Bonfield, *J Biomech* **30**, 763-9 (Aug, 1997), R. K. Nalla, J. H. Kinney, R. O. Ritchie, *Nat Mater* **2**, 164-8 (Mar, 2003)). This interpretation is supported by studies where collagen denaturation or crosslinking are examined for effects on bone mechanical properties and by the ability of a microcrack bridging model to predict apparent bone strength (Y. N. Yeni, D. P. Fyhrie, *J Biomech* **36**, 1343-53 (Sep, 2003)). Collagen failure in bone is likely similar to the processes in tendon (J. Kastelic, E. Baer, *Symp Soc Exp Biol* **34**, 397-435 (1980)) which are known to be strongly dependent on crosslinking (H. S. Gupta *et al.*, *Phys Rev Lett* **93**, 158101 (Oct 8, 2004), R. Puxkandl *et al.*, *Philos Trans R Soc Lond B Biol Sci* **357**, 191-7 (Feb 28, 2002)). Other active processes in ultrastructural failure include modification of the mineral structure (A. Carden, R. M. Rajachar, M. D. Morris, D. H. Kohn, *Calcif Tissue Int* **72**, 166-75 (Feb, 2003)) and dissipation of energy by reversible bond breaking (J. B. Thompson *et al.*, *Nature* **414**, 773-6 (Dec 13, 2001)). “Quality” bones will maintain strength and not break before our lives are over. However, bone mechanical properties evolved through their effect on reproductive fitness rather than lifespan. Therefore, “quality” bones that last for a modern lifetime are a subset of the bone phenotypes that evolved prior to development of human culture.

As an example of an evolved material, it is reasonable to expect that bone tissue has a constellation of correlated mechanical properties appropriate to the demands of the environment. Such correlations exist between the strength and stiffness properties of bone tissue (Y. N. Yeni, X. N. Dong, D. P. Fyhrie, C. M. Les, *Biomed Mater Eng* **14**, 303-10 (2004).) and they may arise from the molecular level. If the evolved correlations of bone properties to each other and to the environment are lost, “bone quality” is lost and atraumatic bone fractures can occur. At the ultrastructural level, defects of collagen in osteogenesis imperfecta and mineralization defects in Vitamin D resistant rickets change the relationship between bone stiffness and strength and can cause disease. There are many other examples, such as fluorosis, lathyrism and age effects on crosslinking, where molecular changes affect the relationship between mechanical properties and are associated with disease. At the ultrastructural level, maintaining youthful normal correlations between strength, stiffness and other material properties is a key to bone quality.

Disclosures: **D. Fyhrie**, None.

13

Skeletal Variations in Humans. M. P. Whyte^{*}. Shriners Hospitals for Children-St Louis; Washington University in St. Louis, St. Louis, MO, USA.

Several heritable disorders reveal that humans can manifest a wide-ranging spectrum of bone mass and quality. These conditions may feature suppression or acceleration of bone turnover and/or alteration in osseous tissue itself. Cessation of osteoclast-mediated bone resorption causes osteopetrosis (OPT) (1). Most OPT patients carry a deactivating mutation in a gene that mediates pericellular acidification by osteoclasts including carbonic anhydrase II, a proton pump subunit, or chloride channel 7. Consequently, bone growth can be compromised and bone modeling and remodeling stopped. In OPT, bones are dense yet brittle not only due to the presence in metaphyses of unresorbed primary spongiosa (calcified cartilage) remaining from endochondral bone formation, but also because of failure of osteon interconnection and hyper-mineralization of osseous tissue (1). Now, anti-resorptive treatment can be so potent that it can recapitulate OPT in growing children (2) or cause a somewhat different osteopathy in adults featuring high bone mass and poor skeletal quality (see abstract # 129). Conversely, good-quality dense bone is formed excessively in the heritable disorders sclerosteosis and van Buchem disease involving deactivation or diminished expression of the SOST gene (1). The LRP5 gene mutations associated with a high bone mass phenotype are increasingly recognized to cause disease (3). Activating and deactivating mutations in LRP5 lead to high and low bone mass disorders, respectively, where bone quality seems good with LRP5 activation (3). In the acquired disorder hepatitis C-associated

osteosclerosis, bones are painful despite containing good quality, dense osseous tissue (4). Osteogenesis imperfecta (OI) is the classic disorder of bone matrix featuring quantitative and often qualitative defects in type I collagen biosynthesis where secondary matrix abnormalities are increasingly appreciated. Disorders of the RANKL/OPG/RANK/NF κ B signaling pathway include RANK activation causing familial expansile osteolysis (FEO) and OPG deficiency causing juvenile Paget's disease (JPD) (5) which feature accelerated bone turnover that can also lead to remarkable focal bone defects from aggressive osteoclast-mediated osteolysis resembling classic Paget bone disease (PBD) (6). PBD involves sequestosome gene deactivation and the ubiquitin pathway in many familial cases (4).

References

1. Whyte MP. Osteopetrosis. In, "Connective tissue and its heritable disorders: molecular, genetic, and medical aspects" 2nd Ed. Royce PM, Steinmann B, eds; Wiley-Liss, New York, pp 789-807, 2002
2. Whyte MP, Wenkert D, Clements KL, McAlister WH, Mumm S. Bisphosphonate-induced osteopetrosis. *N Engl J Med* 349:455-461, 2003.
3. Rickels MR, Zhang X, Mumm S, Whyte MP. Skeletal disease accompanying high bone mass and novel LRP5 mutation. *J Bone Miner Res* (in press)
4. Khosla S, Hassoun AAK, Baker BK, Liu F, Zien NN, Whyte MP, Reasner CA, Nippoldt TB, Tiegs RD, Hintz RL, Conover CA. Insulin-like growth factor system abnormalities in Hepatitis C-associated osteosclerosis: a means to increase bone mass in adults? *J Clin Invest* 101:2165-2173, 1998.
5. Whyte MP, Obrecht SE, Finnegan PM, Jones JL, Podgornik MN, McAlister WH, Mumm S. Osteoprotegrin deficiency and juvenile Paget's disease. *N Engl J Med*, 347:174-184, 2002.
6. Whyte MP, Mumm S. Heritable disorders of the RANKL/OPG/RANK signaling pathway. *J Musculoskelet Neuronal Interact.* 4:254-267, 2004

Disclosures: M.P. Whyte, None.

14

Using Mice to Understand Structure-Function Relationships in the Skeleton. K. J. Jepsen. Mount Sinai School of Medicine, New York, NY, USA.

A major challenge in studying biological traits is understanding how genes work together to provide for organismal structures and function (1). Conventional reductionist approaches that relate one gene or one set of genes to a single complex property like bone mineral density, strength, or work-to-failure may not capture the complexity of the interrelationships among intermediary traits that are important for whole bone mechanical function (2). Single perturbations, such as genetic mutations or pharmacological treatments, can be used to establish causality, but the results can be confounded due to associated strong biological effects. For example, *Mov13* transgenic mice, which have a regulatory mutation affecting type I collagen synthesis, exhibit decreased material properties and significant whole bone fragility, but also exhibit an age-related adaptive response, apparently to compensate for the poor bone quality (3).

The issue of genetic complexity and the interrelationship among component traits is not unique to bone. Recently, a novel and powerful approach for dealing with complex trait-function interactions has been described for cardiovascular genetics and function (1). This approach, which uses genetically randomized inbred mouse strains, tests multiple genetic perturbations that occur in a natural, non-pathological manner. Recombinant Inbred (RI) strains have a unique pattern of genetic randomization that can be used to measure the tendency of different traits to cosegregate. This genetic randomization can be used to define reference networks that describe the structure and function of normal bone, based on subtle, naturally occurring, and non-pathological variation. Using this novel approach, we tested whether the network analysis would correctly identify previously determined structure-function relationships for bone (4). Femurs from 20 adult AXB/BXA RI mouse strains were phenotyped for whole bone mechanical properties, morphology, and mineral content. Genetic randomization was associated with significant variation in all traits and properties among the RI

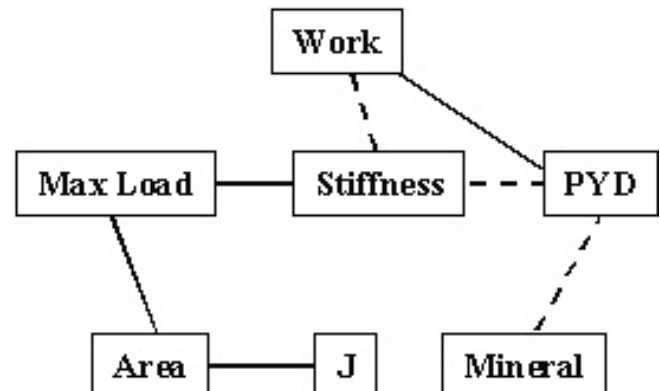
panel. Using the mean values for each RI strain, a correlation matrix was established by relating each trait and each property across the RI panel. Correlations that exceeded a statistical threshold value of 0.66 were considered significant ($p < 0.05$). The correlation matrix identified the traits and properties that cosegregated (i.e., remained functionally related) after randomization of AJ and B6 genes in the RI panel. A network of functional interactions was constructed in the appropriate hierarchical manner with traits arranged below properties. The structure-function relations were entirely consistent with those determined previously. In both studies, area correlated positively with stiffness and maximum load, mineral content correlated negatively with post-yield deflection, and post-yield deflection correlated positively with work-to-failure. This analysis revealed relationships that were not observed previously (e.g., the negative correlation between stiffness and post-yield deflection and between stiffness and work-to-failure). These latter relationships are consistent with prior work (5) indicating that matrix traits (mineral) that contribute to bone stiffness also tend to make the bone less ductile (more brittle).

Networks derived from RI mouse strains are ideally applicable to the study of bone, which possesses higher-level biological controls. RI strains, because they are inbred and genetically defined populations, can be rigorously characterized by repeated assays and data can be obtained for different age groups; both factors are critically important for identifying the biological processes operating during development that lead to variation in adult bone morphology and quality. This novel approach has the dual benefits of revealing the homeostatic functionality of complex biological systems as well as providing a conceptual and evidentiary framework for characterizing the diverse biological and clinical correlates of related diseases.

References

- (1) Nadeau et al, *Genome Res* 13(9):2082-91.
- (2) Sumner et al, *Bone* 19(2):121-6.
- (3) Bonadio et al, *J Clin Invest* 92(4):1697-705.
- (4) Jepsen et al, *Mamm Genome* 14(2):97-104.
- (5) Currey et al, *Philos Trans R Soc Lond B Biol Sci* 304(1121):509-18.

Fig 1. Reference network defining structure-function relations for mouse femurs. Solid and dashed lines indicate significant positive and negative correlations, respectively. PYD=post-yield deflection, J = moment of inertia.



Disclosures: K.J. Jepsen, None.

15

YOUNG INVESTIGATOR AWARD RECIPIENT

Mapping Quantitative Trait Loci for Bone Quality: A Study of Cross-Sectional Geometry of Femoral Neck. H. Shen^{*1}, D. Xiong^{*1}, J. Long^{*1}, Y. Zhang^{*1}, Y. Liu^{*1}, P. Xiao^{*1}, L. Zhao^{*1}, Y. Liu^{*1}, V. Dvornyk^{*1}, S. Rocha-Sanchez^{*1}, P. Liu^{*1}, T. Conway^{*1}, K. Davies^{*1}, R. R. Recker¹, H. Deng^{1,2}. ¹Creighton University, Omaha, NE, USA, ²HuNan Normal University, ChangSha, China.

Bone geometry is a critical determinant of bone quality and strength, which is the ultimate intrinsic determinant of fracture risk. Though bone geometry is highly heritable, little effort has been spent on searching for the underlying genes. In this study, we performed a genome-wide linkage scan for femoral neck bone geometry for the first time. In 1,816 subjects from 79 multi-generation pedigrees, we genotyped 451 microsatellite markers (~8.1 cM apart) across the human genome and performed variance component linkage analyses for five bone geometry parameters at the femoral neck, namely, cross-sectional area (CSA), cortical thickness (CT), endocortical diameter (ED), sectional modulus (Z), and buckling ratio (BR). The highest LOD score was achieved on chromosome 10q26 (LOD = 3.29) near marker D10S212 for BR. Interestingly, a relatively broad region on chromosome 20p12-q11 showed suggestive linkage evidence for CSA (LOD = 2.29), CT (LOD = 2.00), and BR (LOD = 1.95). One prominent candidate gene located in this region is the bone morphogenetic protein 2 (BMP2) gene, which is known to regulate bone growth and has recently been identified as a genetic determinant of osteoporosis risk.

Because the genome-wide linkage scan generally has limited statistical power and estrogen is known to have important effects on bone mass and bone remodeling in both women and men, we also tested the association between the estrogen receptor α (ER- α) gene and femoral neck bone geometry. By using the program QTDT, we tested seven single nucleotide polymorphisms (SNPs) and their haplotypes of the ER- α gene in relation to the five bone geometry parameters in a sample of 1,873 subjects from 405 Caucasian nuclear families. Significant association was detected between SNP4 (*rs1801132*) in exon 4 and ED in both single locus analyses ($P = 0.005$) and haplotype analyses ($P = 0.031$). Subjects carrying allele G at SNP 4 had 2.70% smaller ED than non-carriers. In addition, SNP5 (*rs932477*) in intron 4 is associated with both CT and BR (single locus analyses: $P = 0.035$ and 0.041 , respectively; haplotype analyses: $P = 0.010$ and 0.004 , respectively).

In summary, we identified several genomic regions that may contain quantitative trait loci underlying variation in bone geometry at the femoral neck and suggest that the ER- α gene may have modest genetic effects on variation in femoral neck geometry. This study represents an important step toward identifying genes underlying bone geometry (and thus bone quality) and ultimately the risk of osteoporotic fracture.

Disclosures: **H. Shen**, None.

16

YOUNG INVESTIGATOR AWARD RECIPIENT

Effect of Aging on the Fracture Toughness of Human Cortical Bone: A Hierarchical Approach. R. K. Nalla^{*1}, J. S. Stölken^{*2}, J. H. Kinney^{*2}, R. O. Ritchie^{*1}. ¹Lawrence Berkeley National Laboratory, Berkeley, CA, USA, ²Lawrence Livermore National Laboratory, Livermore, CA, USA.

There is increasing evidence that factors other than bone mineral density need to be considered to understand fracture risk. It has long been recognized that the relevant mechanical properties of bone—toughness, strength and elastic properties—change with age. Assessing such changes is complicated by the fact that the tissue remodels with age. Here we consider cortical bone, where the fracture toughness is believed to mediate failure. Understanding fracture toughness requires that the mechanical properties be understood over multiple structural/length scales, as the stress fields surrounding a crack probe its inherently complex, hierarchical microstructure. Thus, studies must

distinguish between the separate effects of changes in tissue “quality” from changes in tissue organization (microstructure), which act in concert to affect fracture toughness.

This study addresses the evolution of the fracture toughness of cortical bone with crack extension (Resistance-curve behaviour) in the context of the role of the microstructure. Fracture mechanics-based measurements were performed on compact-tension specimens using bone from mid-diaphyses of 34-99 year-old human humeri. Crack-initiation toughness decreased ~40% and more importantly, growth toughness was eliminated over this age range. Evidence from x-ray tomography showed that degradation of crack bridging, a potent toughening mechanism involving uncracked material in the crack wake that reduces the stresses experienced at the crack tip, was responsible for the reduction in crack-growth toughness. The reduction in bridging is related to microstructural changes associated with remodeling that lead to a higher density of crack initiation sites with age, and consequently smaller bridges.

These changes were also correlated with changes at the sub-microstructural level using Atomic Force Microscope-based nanoindentation and Deep-Ultraviolet Raman Spectroscopy performed on material from the fracture specimens to evaluate the collagen that forms crack bridges. Nanoindentation revealed deterioration in the elastic properties at the collagen level and spectroscopy revealed changes in collagen cross-linking chemistry with age. Such changes support the more macroscopic observations of poorer bridge formation in older bone. Fracture mechanics thus provides a useful framework for studying the evolution of the macroscopic fracture behavior with aging, but it is necessary to evaluate the mechanical properties at various length scales to develop a more complete mechanistic understanding of the fracture resistance of cortical bone.

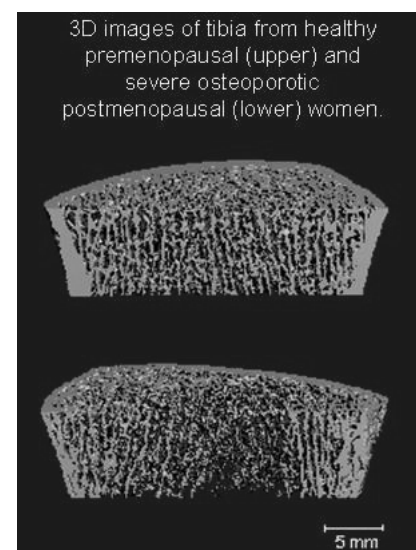
Disclosures: **R.K. Nalla**, None.

17

YOUNG INVESTIGATOR AWARD RECIPIENT

In Vivo Assessment of Trabecular Microarchitecture by High-Resolution Peripheral Computed Tomography. S. Boutry^{*1}, M. L. Bouxsein², F. Munoz^{*1}, P. D. Delmas¹. ¹INSERM Research Unit 403 and Claude Bernard University of Lyon, Lyon, France, ²Forsyth Institute and Harvard Medical School, Boston, MA, USA.

Although bone mineral density (BMD) is the gold standard for diagnosis of osteoporosis, recent clinical observations demonstrate limitations of areal BMD measurements. A newly developed high-resolution 3D-pQCT system permits in vivo assessment of trabecular architecture and volumetric BMD (vBMD) at the distal radius and tibia with an isotropic voxel size of 82 μm (XtremeCT, Scanco Medical AG). The aim of our study was to evaluate the clinical performance of this 3D-pQCT system.



We determined the short-term reproducibility of density and architecture parameters by measuring 8 healthy volunteers 3 times each within one month. We also compared 3D-pQCT measurements in healthy premenopausal ($n = 35$, age 19 - 45) and postmenopausal women, classified by femoral neck or spine BMD as osteopenic ($-1 < \text{T-score} < -2.5$, $n = 113$ women, age 52 - 88 yrs) or osteoporotic ($\text{T-score} \leq -2.5$, $n = 29$ women, age 61 - 84 yrs). We found that the reproducibility of 3D-pQCT parameters was

similar at the distal radius and tibia, with a coefficient of variation of 0.5 to 1.3% for total, trabecular and cortical vBMD, and 2.3 to 3.1% for trabecular architecture measurements. At both sites, vBMD ($r = -0.36$ to -0.70), trabecular thickness ($r = -0.22$ to -0.26), number ($r = -0.30$ to -0.45) and separation ($r = 0.31$ to 0.45) were correlated with age.

At both the radius and tibia, all density and structural parameters differed significantly between premenopausal and postmenopausal women. Trabecular and cortical density were 21 to 33% and 11 to 17% lower, respectively, in postmenopausal women ($p < 0.001$ for all). Postmenopausal women had lower trabecular number (-13 to -23% , $p < 0.001$) and thickness (-8 to -15% , $p < 0.001$), and increased trabecular separation (24 to 41%, $p < 0.001$) compared to premenopausal women. Cortical thickness was also 28 to 42% lower in postmenopausal than premenopausal women ($p < 0.001$). Compared to osteopenic, osteoporotic women had lower vBMD (-4 to -15% , $p < 0.027$), increased trabecular separation (6 to 14%, $p < 0.043$) and decreased cortical thickness (-16% , $p < 0.012$).

In conclusion, 3D-pQCT appears promising as a technique to assess trabecular microarchitecture, both in terms of reproducibility and ability to detect age- and disease-related changes.

Disclosures: **S. Boutroy**, None.

18

Effects of Microdamage on Bone Strength. D. B. Burr. Indiana University School of Medicine, Indianapolis, IN, USA.

Bone fragility increases with age, independent from declines in bone mineral density that also occur with aging [1]. This may be partly a consequence of the age-associated exponential increase in microdamage accumulation [2], which is known to reduce strength [3], stiffness [4] and toughness [5]. This may be the biological basis for the observation that the bone tissue of older women is inherently more fragile than that from younger women [6].

Both the stress required for the initiation of a crack, and the stress required for its growth, are reduced significantly with age [7]. This may be a function of reduced crack bridging, which operates in the wake of a crack and governs the energy required for crack growth. Typically, very tough materials, of which bone is one, are those in which cracks may initiate, but do not grow to critical size. The collagen-mineral composite in bone is generally very effective at preventing crack growth, but as matrix properties degrade with age, the composite becomes less effective at stopping crack growth. This could be a consequence of the increased mean tissue age (MTA), which allows bone tissue to become more mineralized. Increased MTA also increases the homogeneity of the bone tissue, so that there are fewer "stiffness discontinuities" that otherwise would slow or arrest a growing crack. This is consistent with the observation that crack bridging is less common in older bone.

Consequently, one would expect that any condition in which the repair of microdamage is suppressed - such as the artificial suppression of bone turnover by therapeutic agents used for osteoporosis - would allow for increased tissue mineralization, decreased heterogeneity of tissue properties, and increased damage accumulation. This is not necessarily critical if the degradation of tissue properties is compensated by increased bone mass. This in fact seems to occur. Suppression of bone turnover in animals for one year using high doses of bisphosphonates increased damage accumulation in the vertebrae by 3-4 fold [5,8], possibly as a consequence of increased tissue mineralization [9]. Even at clinical doses of two different bisphosphonates, there is a 2-3 fold increase in damage accumulation which is associated with a 5-20% decrease in toughness. But there is no significant relationship between damage and toughness in these studies ($r^2 = 0.02$, $p = \text{NS}$), and whether damage contributes to the decreased toughness, or whether increased mineralization and reduced stiffness heterogeneity in the tissue is more important to the degradation of toughness, is unresolved. Moreover, there appears to be a compensation for the increased microdamage that accumulates with anti-resorptive treatments through increased bone volume that prevents the loss of extrinsic stiffness and strength of the whole bone one would predict from the increased min-

eralization and damage [5, 10]. The result is that it is still unclear what role microdamage may play in fracture risk. Although microdamage is predicted to cause a degradation of material properties, as it does in other non-biological composite materials, it has been difficult to separate its effects on these properties from the effects of changes in the other components of the tissue matrix.

References

1. Kanis J et al. *Osteoporos Int* (2001) 12:989-995.
2. Zioupos P *J Microscopy*, (2001) 201:270-278
3. Burr DB et al *J Bone Miner Res* (1997) 12:6-15.
4. Burr DB et al *J Biomech* (1998) 31:337-345.
5. Mashiba T et al *Bone* (2001) 28:524-531.
6. Courtney AC et al *J Biomech* (1996) 29:1463-1471.
7. Nalla RK et al *Bone* (2004) 35:1240-1246.
8. Komatsubara S *J Bone Miner Res* (2003) 18:512-520.
9. Burr DB et al *Bone* (2003) 33:960-969.
10. Day JS et al *J Orthop Res* (2004) 22:465-471.

Disclosures: **D.B. Burr**, Eli Lilly and Co., Procter and Gamble Pharmaceuticals 2, 5, 8; Amgen 2, 5; Merck, MTA.

19

Clinical Relevance of Microdamage Accumulation and Excess Remodeling Suppression. R. Recker. Creighton University School of Medicine, Omaha, NE, USA.

For many clinicians, osteoporosis is a disease of decreased BMD. Bone mass, chiefly areal BMD, has been the basis of the osteoporosis paradigm since the introduction of accurate and precise methods for its measurement. However, it is increasingly clear that the paradigm is flawed. For example, the risk of fracture ranges two-fold from the 10th to the 90th percentile in BMD, but ranges ten-fold at a given BMD from age 50 to 80 {1}. Thus, risk of fracture increases with age independent of BMD. More recent data show discordance between BMD and propensity to fracture. The striking reduction in fracture risk with anti-resorptive treatment in osteoporosis is accompanied by a very modest increase in bone mass, the latter accounting for less than half of the reduction in fractures {2}. These anomalies in the BMD paradigm are focusing attention on elements of bone quality other than bone mass, as important in sustaining the load-bearing capacity of the skeleton. Indeed, this symposium is a product of that focus. This presentation will examine the role of bone remodeling in sustaining (or degrading) bone quality and load-bearing capacity of the skeleton. The principal homeostatic function of bone remodeling in adult humans and higher vertebrates is to maintain intrinsic material properties of bone by removing micro-damaged tissue, replacing it with new intact bone tissue {3}. Thus restorative bone remodeling is driven by the mechanical needs of the skeleton. In support of this hypothesis, animal data have shown that remodeling is targeted to sites of micro-damage {4}. Surely, mechanically driven bone remodeling weakens bone transiently. But it is more than compensated for by the gain in strength resulting from removal of micro-damage. However, the need for skeletal renewal is not the only signal governing the rate of bone remodeling {3}, and any bone remodeling in excess of that required for maintaining bone quality can only weaken bone. This is important in light of the (underappreciated) fact that bone remodeling rates in fracturing osteoporosis patients can be 3-fold and more above the level required for timely removal of micro-damage {5}. Thus, suppression of bone remodeling by as much as 60-70% accounts for more than half of the anti-fracture effect of treatment with bisphosphonates {2}. Proposed mechanisms for this improvement in bone quality are: 1) elimination or reduction in trabecular penetration and trabecular loss which preserves connectivity; 2) reduction in trabecular and cortical thinning; and 3) reduction in the fraction of newly formed, under-mineralized osteoid. Primary mineralization of osteoid at a remodeling site is completed by the end of the functional osteoblast lifespan, and is about 50-60% of the maximum attained {6-8}. In the period (months?) between primary and completion of secondary mineralization of new osteoid, new bone does not bear its full share of loads. Indeed, for some portion of this time, new bone is shielded from load bearing by the nearby older, stiffer bone tissue, and may not bear load at all. Thus when destructive bone remodeling accounts for a 60-70% excess in remodeling rates,

the large fraction of under-mineralized new bone tissue degrades bone quality significantly. Treatment effects of bisphosphonates are mediated through improvement in what we understand as bone quality much more prominently than increase in bone mass. Further, an average 60-70% reduction in remodeling rates in osteoporosis patients results in rates comparable to healthy, non-fracturing pre-menopausal women {5}. The question of over-suppression of bone remodeling has been raised. Work with animal models using doses of bisphosphonate well above those used in humans has shown that over-suppression of remodeling does result in spontaneous fractures. But it is unlikely that all osteoporosis patients fracture because of excessive remodeling. A few have pre-treatment remodeling rates below those in healthy pre-menopausal women, and their fracture risk may increase with treatment that suppresses remodeling {5}. So far, we do not have a practical method to identify such individuals. Several inferences can be made from experience described above: 1. Excessive, non-mechanically driven bone remodeling reduces bone quality, decreases load-bearing capacity, and is an important element in the cause of low-trauma fractures, and 2. Other elements of bone quality intrinsic to the skeleton may be involved in the cause of inappropriate low-trauma fractures. It seems clear that we need more comprehensive study of all aspects of bone quality in order to understand bone fragility, and to invent more effective treatments and preventive measures.

References

- (1) Hui SL, Slemenda CW, Johnston Jr CC. Age and bone mass as predictors of fracture in a prospective study. *J Clin Invest.* 1988;81:1804-9.
- (2) Cummings SR, Karpf DB, Harris F, Genant HK, Ensrud K, LaCroix AZ et al. Improvement in spine bone density and reduction in risk of vertebral fractures during treatment with antiresorptive drugs. *Am J Med.* 2002;112:281-89.
- (3) Burr DB. Targeted and nontargeted remodeling. *Bone.* 2002;30:2-4.
- (4) Mori S, Burr DB. Increased intracortical remodeling following fatigue damage. *Bone.* 1993;14:103-9.
- (5) Recker R, Lappe J, Davies KM, Heaney R. Bone remodeling increases substantially in the years after menopause and remains increased in older osteoporosis patients. *J Bone Miner Res.* 2004;19:1628-33.
- (6) Meunier PJ, Boivin G. Bone mineral density reflects bone mass but also the degree of mineralization of bone: therapeutic implications. *Bone.* 1997;21:373-77.
- (7) Boivin G, Meunier PJ. Methodological considerations in measurement of bone mineral content. *Osteoporos Int.* 2003;14:22-28.
- (8) Boivin G, Meunier PJ. Bone remodeling changes influence the mean degree of mineralization of bone. *Connective Tissue Res.* 2002;43:535-37.

Disclosures: **R. Recker**, Merck, Lilly, Roche, GSK, Wyeth, P&G, Pfizer, Amgen, Aventis, Novartis 2, 5.

20

Role of the Osteocyte in Mechanotransduction and Skeletal Fragility. M. B. Schaffler, R. J. Majeska. Mount Sinai School of Medicine, New York, NY, USA.

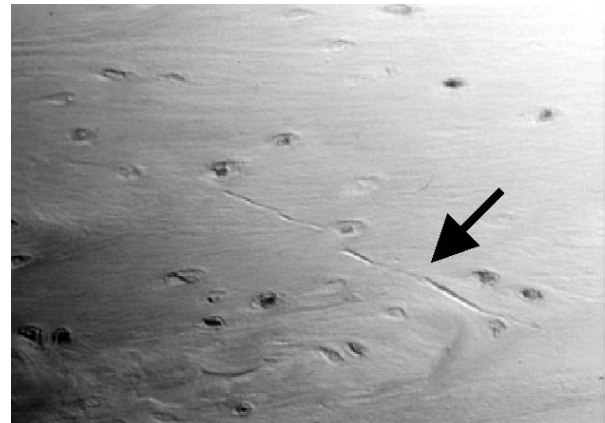
Among the central issues in bone research are how osteocytes may regulate bone adaptation, remodeling and maintenance of bone quality. There is strong experimental evidence that osteocytes respond to mechanical loading and are involved in regulating the modeling of growing bones. However, the role of osteocytes in regulating bone remodeling and their direct or indirect influence on bone quality, are less well understood. In this context, we will consider how osteocytes contribute "directly" (i.e., by altering bone matrix structure/composition) and "indirectly" (i.e., by controlling bone turnover) to maintaining bone quality.

Osteocytes and direct control of bone fragility- Osteocytes are well situated to modulate their surrounding bone matrix; they are extensively distributed throughout the matrix and their canalicular processes completely infiltrate the bone. However, evidence for a direct osteocyte role in maintaining bone quality is scant. Mature osteocytes in fully mineralized bone express high levels of osteocalcin, DMP-1 and MEPE, key proteins implicated in modulating bone mineralization, though their role in mature bone remains uncertain. Indirect evidence also suggests that osteocytes help maintain bone matrix. Where osteo-

cytes are absent from bone (e.g., radiation-induced death of osteocytes, allograft bone), fatigue and fragility fractures will occur. Osteocyte loss in microscopic regions of bone is associated with focal mineralization increases (micropetrosis) and local damage. However, it is not known whether changes in existing bone matrix composition result from absence of osteocyte activity, or if the increases in local mineral volume result from infilling of empty lacunae and canaliculi with mineralized debris. Thus osteocytes may directly modulate bone matrix quality, but data specifically testing this hypothesis are lacking. **Osteocytes and indirect control of bone fragility-** In contrast, our recent studies support a key role for osteocytes in regulating bone remodeling, a process that, while indirect, is essential for maintaining bone quality. Parfitt (1) proposed that bone remodeling is either "stochastic" or "targeted." In stochastic remodeling, systemic or regional stimulation of osteoclasts results in bone resorption without an identifiable tissue focus. Usually cited examples of stochastic remodeling are bone loss after estrogen depletion or immobilization. Alternatively, resorption in targeted remodeling is directed at removing microscopic foci of bone that have reached the end of their functional life mechanically (e.g., microcracking) or biologically (e.g., osteocyte aging, accrual of excessive mineral).

Our research has focused on the roles of osteocytes in controlling targeted remodeling of bone. In particular, we have studied how osteocytes respond to bone microdamage, and how that response may activate or target new BMUs to remodel those damaged areas. We found that osteocytes undergo apoptosis in bone areas surrounding induced bone microdamage (Fig 1).2,3

Fig 1: Top panel: Apoptotic osteocytes (caspase-3 stain) surrounding microcrack (arrow) in fatigue loaded rat ulna. Bottom panel: non-fatigued bone.

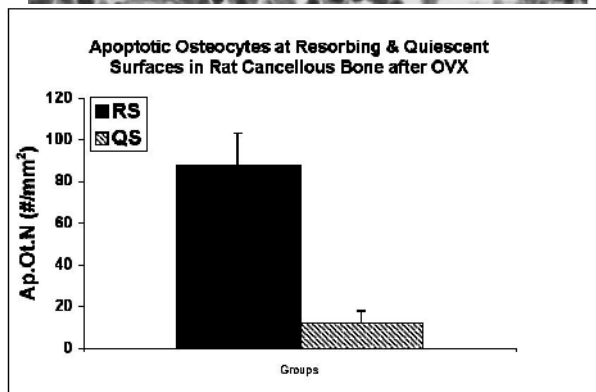
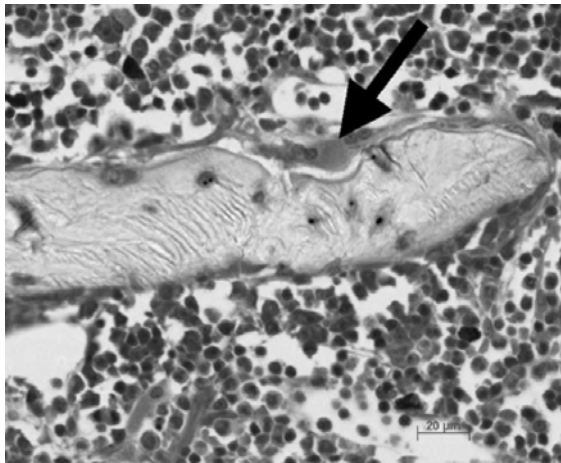


Moreover, areas of osteocyte apoptosis around microcracks corresponded to areas that undergo later resorption by osteoclasts. This led us to hypothesize that osteocyte loss is an essential element of the signaling process that osteoclasts use to target focal areas of bone for resorption.

We recently examined whether osteocyte apoptosis also occurs with other challenges known to activate bone remodeling. Estrogen withdrawal in rats (ovariectomy) led to a 50 percent increase in osteocyte apoptosis in

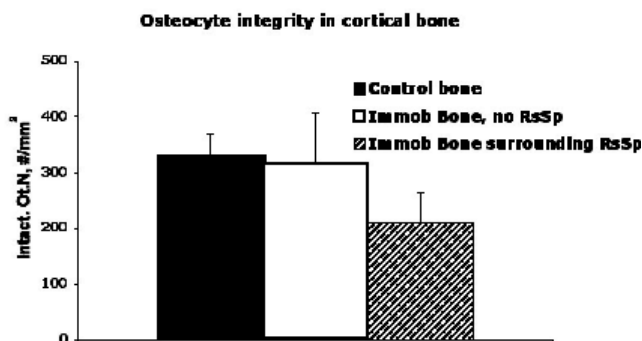
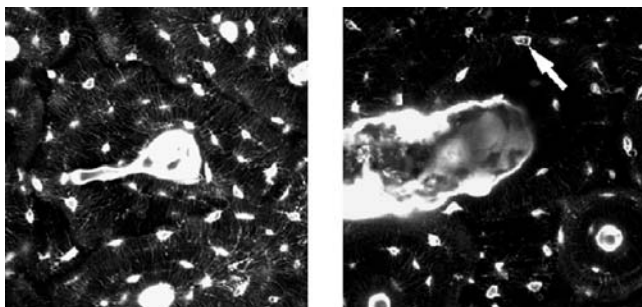
cancellous bone. Furthermore, as with microdamage, osteoclastic activity was concentrated in areas of osteocyte apoptosis (Fig 2) (4).

Fig 2: Apoptotic osteocytes (caspase-3 staining) localized beneath an osteoclast in rat cancellous bone after OVX.



A similar situation was seen in canine bones subjected to 3-6 weeks of immobilization. Osteocyte viability was dramatically impaired in focal regions where osteoclastic resorption occurred (Fig 3).

Fig 3: Top panel: Control bone with normal osteocyte, lacunae and canicular structure. Middle panel: Immobilized bone showing loss of osteocyte viability in bone surrounding a resorption space (RsSp).



Together, these studies argue that osteocytes play a central role in the control of bone remodeling, and by extension the maintenance of bone quality. Moreover, these studies suggest that osteocyte apoptosis may

be a final common pathway used to target sites in bone for osteoclastic resorption, regardless of the activating stimulus. Thus from an osteocyte perspective, all resorption is targeted.

References

1. Parfitt AM, Mundy GR, Roodman GD, Hughes DE, Boyce BF A new model for the regulation of bone resorption with particular reference to the effect of bisphosphonates. *J. Bone Miner Res.* 11: 1501-59, 1996.
2. Verborgt O, GJ Gibson and MB Schaffler Loss of osteocyte integrity in association with microdamage and bone remodeling after fatigue in vivo. *J Bone Miner Res* 15: 60, 2000.
3. Verborgt O, NA Tatton, RJ Majeska and MB Schaffler. Differential expression of Bax and Bcl-2 in osteocytes after bone fatigue: Complementary roles in bone remodeling regulation? *J Bone Miner Res* 17: 907, 2002.
4. Hernandez, CJ, CY Li, DM Laudier, H T Wolde-Semait, NA Tatton and MB Schaffler. Osteocyte apoptosis is strongly associated with resorption surfaces in cancellous bone. *Trans. Orthop Res. Soc* 28:52, 2003.

Disclosures: **M.B. Schaffler**, None.

21

What Is the Evidence for Sustained Anti-Fracture Efficacy Following Long-Term Bisphosphonate Use? R. E. Rizzoli. [World Health Organization Collaborating Center for Osteoporosis Prevention], University Hospital, Geneva, Switzerland.

The treatment of patients with osteoporosis aims at reducing fracture risk, by restoring a normal bone strength, and reducing thereby the rate of low trauma fracture to a level similar to that observed in young healthy people. Bisphosphonates normalize bone turnover within weeks and usually no further suppression is seen during long term use up to 10 years of continuous administration, indicating that the bisphosphonates retained in bone does not augment or contribute to pharmacological activity. Thus long term effects are unlikely to be different from short term treatment. The amount of bisphosphonates retained in bone after 10 years of treatment represents a small fraction, which is unevenly distributed between cancellous and cortical bone. The reduction in bone turnover is associated with increased BMD, through a more homogeneous tissue mineralization, and reduced fracture risk in multiple studies. Randomized placebo-controlled trials conducted in postmenopausal women with osteoporosis lasted between 3 and 4.3 years (up to 5 years for one study extension). In these studies, alendronate (3 studies), risedronate (2 studies), clodronate (1 study) and ibandronate (1 study) showed significant reduction in the risk of new vertebral fracture. Regarding hip fracture, alendronate and risedronate caused a significant reduction in fracture risk. Follow-up uncontrolled studies with continuous treatment lasting up to 10 years are available. Fracture risk between year 6 and 10 was comparable to that seen during the first 3 years. During the second half of a 10-year therapy, vertebral fracture risk was similar in the patients with continuous administration and in those who discontinued after 5 years of treatment. Thus, in the absence of further reduction in bone turnover, ie of oversuppression of bone remodeling, the aim of the latter being to remove microdamaged old tissue, there is no evidence that long-term bisphosphonates are harmful for the skeleton. At the present time, taken together, the known mechanism of action of bisphosphonates and the experience accumulated from treating a large number of patients over a long period of time, have not identified significant deleterious bisphosphonates effects on bone. However, a careful attention should be paid that a possible oversuppression of bone turnover and long-term bisphosphonates accumulation, will not be associated with microdamage spreading within bone tissue, and hence increased fragility.

References

1. Rodan G, Reszka A, Golub E, Rizzoli R. Bone safety of long-term bisphosphonate treatment. *Curr Med Res Opin.* 2004 Aug;20(8):1291-300.
2. Ott SM. Long-term safety of bisphosphonates. *J Clin Endocrinol*

Metab. 2005 Mar;90(3):1897-9.

3. Bone HG, Hosking D, Devogelaer JP, Tucci JR, Emkey RD, Tonino RP, Rodriguez-Portales JA, Downs RW, Gupta J, Santora AC, Liberman UA; Alendronate Phase III Osteoporosis Treatment Study Group. Ten years' experience with alendronate for osteoporosis in postmenopausal women. *N Engl J Med*. 2004 Mar 18;350(12):1189-99.

4. Mellstrom DD, Sorensen OH, Goemaere S, Roux C, Johnson TD, Chines AA. Seven years of treatment with risedronate in women with postmenopausal osteoporosis. *Calcif Tissue Int*. 2004 Dec;75(6):462-8.

Disclosures: **R.E. Rizzoli**, Merck, Servier, Amgen, Novartis, Nycomed, Wyeth, Roche, 8, 5; **Eli Lilly**, Procter & Gamble, Aventis 8.

22

Promises and Perils of the Widespread Use of DXA for Assessment of Fracture Risk. **R. P. Heaney**. Creighton University, Omaha, NE, USA.

A part of the reason for interest in bone quality is not just for completeness' sake, but because BMD, the mainstay of diagnosis, is neither a very sensitive nor a very specific measure of fracture risk. Hence the search for something more or better. In the NORA study⁽¹⁾ roughly 80% of osteoporotic fractures were found in individuals with BMD values above the cut-off value for a diagnosis of osteoporosis. An explanation often overlooked for these and similar shortcomings is not so much that DXA fails to measure important qualitative factors (such as microarchitecture and remodeling rate), as that BMD fails to exploit even the full value of the data actually provided by DXA.⁽²⁾

When BMD is used to estimate fracture risk, it is taken implicitly as a measure of bone strength. But that is substantially incorrect. Operationally, BMD is bone mineral mass divided by bone area. Accordingly, a rise in mass means a higher BMD, and to that extent BMD does reflect strength. But a rise in area (bone size) also increases strength. Unfortunately, because size is in the denominator of BMD, bigger bones will often have lower BMD, thus erroneously counting a strength factor as a weakness. This feature of BMD must inevitably degrade its utility as a predictor of fragility.

Ignoring microarchitectural features, the principal measurable strength determinants are bone mass and bone size, not density (not even true volumetric density). DXA actually provides information on both. In addition to BMD (and its T- and Z-scores), the DXA printout provides a straightforward measure of mass, i.e., BMC, and indirectly of bone size. To exploit this additional information, we analyzed 1,166 baseline spine scans from a population-based prospective study of fracture prevention in postmenopausal women. We first developed and applied a T-score algorithm to the lumbar spine BMC data, and compared the two sets of standardized values (BMD-T and BMC-T). The two T-scores departed significantly from the identity relationship when plotted one on the other, particularly at the clinically relevant low end of their ranges. For example, 162 women had BMD T-score values below -2.5, but only 60 of these (37%) had BMC T-score values below -2.5. The concordant set all had smaller bones and less bone mass, while those with BMD T-scores above the -2.5 cut-off had bigger, heavier (but not denser) bones - a fact not captured by measurement of BMD. In fact, the BMC T-scores for those with BMD T-scores below -2.5 ranged up to as high as -1.0. Conversely there was a correspondingly wide range of BMD values for any given BMC T-score. Both discordances reflect the well recognized fact that a given mass of bony material may be distributed in a larger or smaller volume producing, respectively, lower and higher BMD values.

Structural analysis of a set of vertebral bodies with BMD T-scores of ~ -2.5 (but varying BMC T-scores) revealed a broad range of compressive strengths for the same BMD value.

In brief, bone size is important, as Gilsanz showed 10 years ago.⁽³⁾ Standard DXA reports already include most of the information needed, and minor changes in the reporting software could supply the rest. The predictive utility of DXA would improve if we routinely used all the information it provided.

References

1. Siris ES, Miller PD, Barrett-Connor E, Faulkner KG, Wehren LE, Abbott TA, Berger ML, Santora AC, Sherwood LM 2001 Identification and fracture outcomes of undiagnosed low bone mineral density in postmenopausal women. *JAMA* 286:2815-2822.
2. Heaney RP 2005 BMD: The problem. *Osteoporos Int* (in press).
3. Gilsanz V, Loro LM, Roe TF, Sayre J, Gilsanz R, Schulz EE 1995 Vertebral size in elderly women with osteoporosis. *J Clin Invest* 95:2332-2337.

Disclosures: **R.P. Heaney**, None.

23

Current Methods and Clinical Utility of Macroarchitecture

Measurements. **T. M. Link**. University of California, San Francisco, San Francisco, CA, USA.

While imaging to assess microarchitecture is challenging, measures of macroarchitecture may be obtained without much difficulty from standard bone densitometry, cross-sectional and conventional imaging techniques. Macroarchitecture parameters have been determined in (i) dual x-ray absorptiometry (DXA) images, (ii) quantitative computed tomography (QCT) studies, (iii) conventional radiographs as well as in (iv) dedicated CT and (v) MR examinations. However, most of these measures are currently not applied in clinical routine and their use is limited to research studies.

(i) *DXA*: Given its projectional quality DXA has limitations in depicting the true bone macroarchitecture, yet the good reproducibility of the technique and the improving image quality allowed its use to derive geometrical measurements, in particular in DXA images of the proximal femur. One of the earliest geometrical measures used in DXA images to assess bone macroarchitecture was hip axis length; a direct correlation between this measure and the increase in hip fracture risk was demonstrated (1). It was also shown that cortical thickness, cross-sectional area and section modulus at the femur neck derived from DXA images were related to sex steroids, gender and aging (2). In addition race associated differences in geometrical parameters were found (3).

(ii) *QCT*: Compared to DXA the advantage of QCT is the visualization of the cross-sectional anatomy, which allows for a better assessment of geometrical properties. New 3D, volumetric techniques acquire datasets with which analysis of bone macroarchitecture may be further optimized. In contrast to biomechanical considerations suggesting that a higher cross-sectional vertebral area may be related to greater bone strength, it was shown that postmenopausal females with osteoporotic fractures of the spine had a larger cross sectional area than females without fractures (4). Geometric parameters determined in volumetric QCT studies of the proximal femur contributed to bone strength in an in vitro model, but were less well suited than BMD in predicting bone strength (5).

(iii) *Conventional radiographs*: Plain radiography is an inexpensive widely available technique, which was one of the earliest techniques to be used for the assessment of macroarchitecture in the diagnosis of osteoporosis. Some of these methods are still advocated though they their limitations have to be considered. One of these is the metacarpal index, the combined cortical thickness of the metacarpal bones as determined on standard hand radiographs. In radiographs of the proximal femur the Singh index and geometric parameters were found to be of limited use in differentiating patients with and without fractures of the proximal femur (6).

(iv) *CT*: With emerging CT methodologies such as Multislice CT and improved post-processing techniques, larger volumes of bone can be imaged with thinner slice thickness and 3D bone macrostructure may be better visualized. Multislice CT images obtained from distal radius human cadaver specimens were used to calculate geometric properties of the cortex before mechanically testing these specimens and it was shown that these properties improved prediction of mechanical failure strength marginally (7).

(v) *MRI*: The non-ionizing quality of MRI makes it particularly useful technique for the assessment of bone architecture. MRI has been used to study the geometrical qualities of the femur shaft during prepuberty and young adulthood; age and sex related changes could be demon-

strated (8), in addition it was found that DXA measures, compared to MR derived measures, were inaccurate in the determination of mid-femoral bone volume.

In summary these studies have shown that measures of macroarchitecture have a role in predicting bone strength, may predict osteoporotic fracture status independently of BMD and may give additional information to BMD and bone microstructure in diagnosing osteoporosis. Up to now, however, they are additive parameters, which are mostly used in research studies. At present it is not expected that they may in the future be able to substitute standard measures of BMD in the assessment of osteoporosis.

References

1. Faulkner KG, McClung M, Cummings SR (1994) Automated evaluation of hip axis length for predicting hip fracture. *J Bone Miner Res* 9:1065-1070.
2. Duan Y, Beck TJ, Wang XF, Seeman E (2003) Structural and biomechanical basis of sexual dimorphism in femoral neck fragility has its origins in growth and aging. *J Bone Miner Res* 18:1766-1774.
3. Nelson DA, Barondess DA, Hendrix SL, Beck TJ (2000) Cross-sectional geometry, bone strength, and bone mass in the proximal femur in black and white postmenopausal women. *J Bone Miner Res* 15:1992-1997.
4. Link T, Doren M, Lewing G, Meier N, Heinecke A, Rummeny E (2000) Cross-sectional area of lumbar vertebrae in peri- and postmenopausal patients with and without osteoporosis. *Osteoporos Int* 11:304-309.
5. Lang TF, Keyak JH, Heitz MW, Augat P, Lu Y, Mathur A, Genant HK (1997) Volumetric quantitative computed tomography of the proximal femur: precision and relation to bone strength. *Bone* 21:101-108.
6. Karlsson KM, Sernbo I, Obrant KJ, Redlund-Johnell I, Johnell O (1996) Femoral neck geometry and radiographic signs of osteoporosis as predictors of hip fracture. *Bone* 18:327-330.
7. Bonel HM, Lochmuller EM, Well H, Kuhn V, Hudelmaier M, Reiser M, Eckstein F (2004) Multislice computed tomography of the distal radius metaphysis: relationship of cortical bone structure with gender, age, osteoporotic status, and mechanical competence. *J Clin Densitom* 7:169-182.
8. Hogler W, Blimkie CJ, Cowell CT, Kemp AF, Briody J, Wiebe P, Farpour-Lambert N, Duncan CS, Woodhead HJ (2003) A comparison of bone geometry and cortical density at the mid-femur between prepuberty and young adulthood using magnetic resonance imaging. *Bone* 33:771-778.

Disclosures: T.M. Link, None.

24

Current Methods and Clinical Utility of Microarchitecture

Measurements. S. Majumdar. University of California San Francisco, San Francisco, CA, USA.

Trabecular bone quality can potentially be defined by several factors, for example trabecular micro-architecture, matrix composition of trabeculae and trabecular bone damage-repair. Considerable effort is being expended in developing techniques to assess trabecular bone micro-architecture non-invasively. The heterogeneity in the micro-architecture of trabecular bone is primarily governed by physiological function and mechanical loading on the skeleton. This results in trabecular bone micro-architecture being dependent on the anatomic site, as well as having a directional anisotropy of the mechanical properties and architecture. Thus, site-specific bone structure information would significantly contribute to understanding the results of different therapeutic interventions, and potentially assist in optimizing the course of treatment. Three dimensional techniques that reveal trabecular bone structure are emerging as important contenders for defining bone quality, at least partially.

Techniques such as micro-computed tomography have recently been developed and provide high resolution images of the trabecular architecture. A more recent development in the assessment of trabecular bone structure is the use of magnetic resonance imaging techniques that make it possible to obtain non-invasive bone biopsies at multiple anatomic sites. Cortical and trabecular bone have a low water content

and short T_2 and are not detectable using routine MR imaging methods. However, the marrow surrounding the trabecular bone network, if imaged at high resolution, reveals the trabecular network.

Using such images, multiple different image processing and image analysis algorithms have been developed. The goal of all of these is to quantify the trabecular bone structure in 2 or 3 dimensions. The measures that have been derived so far are many, some of them synonymous with the histomorphometric measures such as trabecular bone volume fraction (BV/TV), trabecular thickness (TbTh), trabecular spacing (TbSp), trabecular number (TbN), others include connectivity or Euler number, fractal dimension, tubularity, maximal entropy, etc.

A number of calibration and validation studies (in vitro and in vivo) have been undertaken in which MR-derived measures of structure are compared with measures derived from other modalities, such as histology, micro-CT, BMD, and with biomechanics. With recent advances in phased array coils and higher strength magnets, the potential of MR imaging of bone structure is ever increasing. At the present time, the skeletal sites most commonly imaged are the radius and calcaneus. The distal radius is a site with a large quantity of trabecular bone, and a common site for osteoporotic fractures. It is easily accessible with localized detection coils and subjects are able to comfortably tolerate immobilization for the period required for high resolution imaging. Calcaneus, although not a typical site for osteoporotic fractures, has been used with success to predict fracture at other sites, and this skeletal site is well adapted to high resolution MR imaging. Much of the work to date, has been focused at 1.5 Tesla as they were relatively widely available for *in vivo* human studies. However, recently 3 Tesla scanners have been approved for clinical use and many sites are now upgrading to this field in order to take advantage of the higher signal-to-noise capability at higher field strengths. The higher field strength of 3T thus would be a tremendous advantage and potentially would improve the resolution of MR images, reduce the imaging time for the current resolutions and also permit imaging sites such as the proximal femur. However, the role of femur images in fracture discrimination and therapy monitoring has not been established.

In establishing these methodologies as a clinical tool, for research or for routine evaluation has several challenges. Given the skeletal heterogeneity of trabecular bone, accurate region matching is a crucial issue. The relevance of these methodologies across multiple platforms is a second consideration, and standardization and high quality acquisitions are also key. Studies currently underway are exploring the possibility of obtaining micro-architectural features of trabecular bone and the understanding whether bone turnover and micro-architecture are related, and the underlying relationship between turnover, bone mineral density and architecture, is the first step towards unraveling the therapeutic efficacy of different treatment regimes.

References

1. Hipp JA, Jansujwicz A, Simmons CA, Snyder B. Trabecular bone morphology using micro-magnetic resonance imaging. *J Bone Miner Res* 1996;11(2): 286-297.
2. Kothari M, Keaveny TM, Lin JC, Newitt DC, Genant HK, Majumdar S. Impact of spatial resolution on the prediction of trabecular architecture parameters. *Bone* 1998;22(5): 437-443.
3. Laib A, Beuf O, Issever A, Newitt DC, Majumdar S. Direct Measures of Trabecular Bone Architecture From MR Images. In: *Noninvasive Assessment of Trabecular Bone Architecture and The Competence of Bone*, Majumdar S, Bay B (eds), vol 496. Kluwer Academic/Plenum Publishers: New York, 2001; 37-46.
4. Link TM, Majumdar S, Lin JC, Newitt D, Augat P, Ouyang X, Mathur A, Genant HK. A comparative study of trabecular bone properties in the spine and femur using high resolution MRI and CT. *J Bone Miner Res* 1998;13(1): 122-132.
5. Link TM, Vieth V, Langenberg R, Meier N, Lotter A, Newitt D, Majumdar S. Structure analysis of high resolution magnetic resonance imaging of the proximal femur: in vitro correlation with biomechanical strength and BMD. *Calcif Tissue Int* 2003;72(2): 156-165.
6. Link TM, Vieth V, Stehling C, Lotter A, Beer A, Newitt D, Majumdar S. High-resolution MRI vs multislice spiral CT: which technique depicts the trabecular bone structure best? *Eur Radiol* 2003;13(4): 663-671.
7. Majumdar S, Newitt D, Mathur A, Osman D, Gies A, Chiu E, Lotz J, Kinney J, Genant H. Magnetic resonance imaging of trabecular bone

structure in the distal radius: relationship with X-ray tomographic microscopy and biomechanics. *Osteoporos Int* 1996;**6**(5): 376-385.

8. Majumdar S, Link TM, Augat P, Lin JC, Newitt D, Lane NE, Genant HK. Trabecular bone architecture in the distal radius using magnetic resonance imaging in subjects with fractures of the proximal femur. *Osteoporos Int* 1999;**10**(3): 231-239.

9. Ouyang X, Selby K, Lang P, Engelke K, Klifa C, Fan B, Zucconi F, Hottya G, Chen M, Majumdar S, Genant HK. High resolution magnetic resonance imaging of the calcaneus: age-related changes in trabecular structure and comparison with dual X-ray absorptiometry measurements. *Calcif Tissue Int* 1997;**60**(2): 139-147.

10. Lin JC, Amling M, Newitt DC, Selby K, Srivastav SK, Delling G, Genant HK, Majumdar S. Heterogeneity of trabecular bone structure in the calcaneus using magnetic resonance imaging. *Osteoporos Int* 1998;**8**(1): 16-24.

11. Link TM, Majumdar S, Augat P, Lin JC, Newitt D, Lu Y, Lane NE, Genant HK. In vivo high resolution MRI of the calcaneus: differences in trabecular structure in osteoporosis patients. *J Bone Miner Res* 1998;**13**(7): 1175-1182.

12. Wehrli FW, Hopkins JA, Hwang SN, Song HK, Snyder PJ, Haddad JG. Cross-sectional study of osteopenia with quantitative MR imaging and bone densitometry. *Radiology* 2000;**217**(2): 527-538.

13. Wehrli FW, Gomberg BR, Saha PK, Song HK, Hwang SN, Snyder PJ. Digital topological analysis of in vivo magnetic resonance micro-images of trabecular bone reveals structural implications of osteoporosis. *J Bone Miner Res* 2001;**16**(8): 1520-1531.

14. Sell CA, Masi JN, Burghardt A, Newitt D, Link TM, Majumdar S. Quantification of Trabecular Bone Structure using Magnetic Resonance Imaging at 3 Tesla Calibration Studies Using Micro- computed Tomography as a Standard Of Reference. *Calc Tis Int* 2004; **accepted**.

15. Krug R, Han ET, Banerjee S, Newitt DC, Majumdar S. In vivo measurement of trabecular bone microarchitecture in the proximal femur with MRI at 1.5T and 3T. In: International Society For Magnetic Resonance in Medicine; 2004; Kyoto, Japan; 2004.

Disclosures: **S. Majumdar**, Aventis, Pfizer 2; Merck, 8.

25

Remodeling and Skeletal Integrity: What Can Bone Turnover Markers (Existing or New) Tell Us About Fracture Risk and Treatment Efficacy? **P. D. Delmas**, Professor of Medicine, University Claude Bernard and INSERM Unit 403, Lyon, France.

The assay features of biochemical markers of bone turnover (BTM) have markedly improved in the past few years. The most sensitive and specific markers of bone formation include serum bone alkaline phosphatase, total osteocalcin (including the intact molecule and the large N-Mid fragment) and the N extension peptide of type I collagen (PINP). Among the various markers of bone resorption, measurements of the urinary excretion of the (deoxy) pyridinoline crosslinks and of N- and C- related telopeptides (NTX and CTX respectively) as well as of serum CTX are the most sensitive and specific ones. Bone markers can be used to predict the rate of bone loss in postmenopausal women. Three independent studies have shown that high bone turnover is associated with increased bone loss over 4 to 15 years in women 50 to 70 years of age. In addition, we have shown in elderly women that increased bone resorption, i.e. above the premenopausal range, is associated with a twofold increase in the risk of hip fractures and that those with both a low BMD (T score below -2.5) and increased bone resorption have a 4 to 5 fold increase in hip fracture risk. We have recently confirmed that increased bone turnover predicts the risk of fragility fractures in a younger cohort of postmenopausal women followed for an average of 5 years. Bone markers can be used to monitor the efficacy of antiresorptive therapy such as hormone replacement therapy, raloxifene and bisphosphonates. We and others have shown that the short-term (3 to 6 months) decrease of bone turnover is significantly correlated with the long-term (2 years) increase in BMD of the spine. In addition, the short-term decrease of BTM is associated with the 2 to 3-year risk of vertebral and non-vertebral fractures in osteoporotic women treated with raloxifene, alendronate and risedronate. Thus,

with adequate cut-offs, individual patients can be monitored with bone markers earlier than with DXA. Finally, the IMPACT study indicates that monitoring bisphosphonate therapy with bone markers measurements at baseline, 3 and 6 months can improve the compliance to therapy by 20% at one year. Other studies should be performed to confirm whether or not monitoring with BTM can improve compliance to therapy in osteoporosis, that has been shown to be low. Taken together, these data indicate that BTM reflect an important component of bone quality that is not captured by BMD measurement, supporting histological evidence for a role of bone turnover in bone architecture and therefore strength.

Currently, attempts are made to develop new markers that would reflect the quality of bone matrix. Several in vitro studies suggest that the post translational modifications of type I collagen influence the mechanical properties of bone. One such non enzymatic modification, the beta-isomerization of aspartic residus in the CTX, can be measured with antibodies specific for the beta and alpha (non isomerized) CTX of type I Collagen. We have shown in vivo that the alpha / beta ratio in the urine of postmenopausal women is associated with the risk of fracture independently of BTM, and in vitro that this ratio is associated with bone toughness. Thus, the development of markers of bone quality is an exciting prospect for the future.

Disclosures: **P.D. Delmas**, None.

26

Combining In Vivo Assessments of Density and Geometry for Fracture Risk Assessment In Vivo. **T. M. Keaveny**, University of California, Berkeley, CA, USA.

It is now widely accepted for both fracture risk prediction and drug treatment assessment that DXA is limited due by its two-dimensional nature and its inability to differentiate material and geometric features and cortical vs. trabecular compartments. QCT-based finite element models are biomechanical models generated directly from clinical QCT scans that provide an output measure of actual bone strength [1,2]. Since these models integrate all the information in QCT scans in a biomechanically meaningful manner and account for the forces that act on bones *in vivo*, they promise to overcome all limitations associated with the 2D DXA and even surpass the 3D QCT. We call this technique the Biomechanical CT (BCT) scan. Its use on cadaver bones has demonstrated its superiority over both DXA and QCT alone in non-invasive bone strength assessment [3,4], and it is now in clinical trials to extend these comparisons to prediction of fractures and assessment of drug treatments.

BCT represents a new paradigm in functional imaging for bone, in which state-of-the-art technologies in radiological imaging and biomechanical analysis are combined to produce non-invasive measures of actual bone strength. After motivating the need for a more mechanistic approach to clinical bone strength assessment, this presentation will describe the BCT technology for non-invasive bone strength assessment, its strengths and limitations, and its application to clinical fracture risk prediction. The use of BCT for detailed assessment of drug treatments will also be discussed, focusing on such issues as quantification of the contribution of the peripheral bone to whole bone strength, the role of intra-vertebral density distribution, and the independent role of bone geometry. Illustrating the potential clinical importance of such new measures, application of BCT to ongoing clinical studies have shown that just the peripheral 2 mm of bone in the vertebral body accounts for up to 40% of vertebral strength [5]. Other analyses have shown that some individuals have normal strength characteristics for compressive loading but have relatively weak vertebrae when subjected to AP bending loads [6], suggesting that such individuals may be particularly susceptible to wedge fractures despite having normal strength characteristics for non-bending activities. These new types of strength considerations -- assessment of the biomechanical role of the peripheral bone, response to compressive vs. AP bending loads -- are expected to provide substantial new insight into macro-scale bone quality issues when applied to drug assessment trials. The possible role of sub-millimeter factors affecting bone quality will also be discussed, how such micro-scale effects should be manifested into

the macro-scale density-strength relation, and how these relations can be incorporated into the BCT scan. In this way, BCT can integrate multi-scale effects of bone quality into a true functional imaging assay that should greatly improve clinical assessment of bone strength, fracture risk, and interventional therapies.

References

1. Faulkner et al, Radiology 179:669-74, 1991.
2. Keyak et al, J Biomechanics 31:125-33, 1998.
3. Cody et al, J Biomechanics 32:1013-20, 1999.
4. Crawford et al, Bone 33:744-50, 2003.
5. Crawford et al, Trans Orthop Res Soc, p. 32, 2005.
6. Crawford and Keaveny, Spine 29:2248-55, 2004.

Disclosures: **T.M. Keaveny**, ON Diagnostics 4; Procter & Gamble 2; Eli Lilly and Amgen 5.

27

YOUNG INVESTIGATOR AWARD RECIPIENT

Preliminary Correlations Between Fracture Risk and IR Imaging Parameters. **D. Faibish**^{*1}, **E. R. Myers**^{*1}, **R. R. Recker**², **A. L. Boskey**¹. ¹Hospital for Special Surgery, New York, NY, USA,

²Creighton University, Omaha, NE, USA.

The aim of our study was to compare infrared spectroscopic parameters in iliac crest biopsies from fracture patients versus control subjects in a case-control design.

Biopsies from 22 patients with known spine bone mineral density (BMD) were analyzed by Fourier Transform InfraRed Spectroscopy (FTIR). Twelve of the patients had fractures of the hip and/or spine and 10 did not. IR images from 400 X 400 fields were collected from six locations in each section (3 cortical, 3 trabecular), using an FTIR spectrophotometer (Stingray). Each image corresponded to 64 X 64 pixels, with a ~6 μ spatial resolution. Each pixel has a corresponding spectrum, with 16cm⁻¹ spectral resolution, summing up to 4096 spectra from each image. Spectra were linearly baselined, and the embedding media contribution was spectrally subtracted. Mineral crystal size and perfection (crystallinity) was assessed by the 1030/1020 cm⁻¹ ratio. Mineral content, related to mineral ash weight, was calculated as the phosphate $\nu_1 \nu_3$ /amide I band area ratio. In previous studies, the increase in the non-reducible pyridinoline collagen cross-links was found to be related to an increase in the 1660/1690 cm⁻¹ ratio (XLR) of the IR spectrum.

A forward stepwise logistic regression analysis was performed with fracture as the dependent variable (fracture = 1, no fracture = 0) using Systat. The independent variables were BMD, mineral crystallinity, XLR and the mineral/matrix ratio. We examined cortical and trabecular spectroscopic properties separately. For cortical bone, only XLR entered the model, with a coefficient of 4.2 (1.7 SE), p=0.014.

Biopsies from patients with fractures had higher XLR than controls (Table 1).

Table 1: Mean values (SD) of infrared spectroscopic parameters

Variable	Fracture patients	Controls
Spine BMD (g/cm ³)	0.695 (0.089)	0.942 (0.177)
Mineral crystallinity	1.34 (0.05)	1.37 (0.05)
XLR	3.7 (0.3)	2.9 (0.5)
Mineral/matrix	4.1 (0.4)	3.9 (0.6)

The results suggest that XLR contributes to the risk of fracture. Our study strengthens the hypothesis that bone matrix properties are a contributing factor to tissue mechanical properties such as strength and for the ability of the tissue to resist fracture. We previously found higher ratios of non-reducible collagen cross-links in osteoporotic patients relative to controls. Mineral to matrix ratios, which can be correlated with the BMD values, were similar for fracture and non-fracture cases, and now, in an ongoing study, XLR was found to be related to fracture risk.

Supported by NIH grant AR041325

Disclosures: **D. Faibish**, None.

28

YOUNG INVESTIGATOR AWARD RECIPIENT

Testosterone Improves Trabecular Architecture in Hypogonadal Men. **M. Benito**^{*1}, **B. Vasilic**^{*2}, **F. W. Wehrli**², **B. Bunker**^{*2}, **M. Wald**^{*2}, **B. Gombert**^{*2}, **A. C. Wright**^{*2}, **B. Zemel**^{*3}, **A. Cucchiara**^{*4}, **P. J. Snyder**¹. ¹Endocrinology, U of PA, Phila, PA, USA, ²Radiology, U of PA, Phila, PA, USA, ³Children's Hospital of Philadelphia, Phila, PA, USA, ⁴GCRC, U of PA, Phila, PA, USA.

Hypogonadal men have decreased bone density and deteriorated trabecular architecture compared to eugonadal men, and testosterone treatment increases their bone density. The goal of this study was to determine if testosterone treatment of hypogonadal men would also improve their trabecular architecture. We selected ten men, mean age 53 years, who were severely hypogonadal and previously untreated. We treated each man with a testosterone gel for 24 months to maintain his serum testosterone within the normal range. Each subject was assessed by DXA at the spine and hip and by magnetic resonance microimaging (μ MRI) at the distal tibia using a GE Signa 1.5 T MR scanner and a custom-designed phased-array RF surface coil. Each subject was assessed before and at 6, 12, and 24 months of testosterone treatment. The skeletonized binary images were analyzed to yield topological parameters that characterize the trabecular network. Parameters assessed included the ratio of surface voxels (representing plates) to curve voxels (representing rods) and the topological erosion index, a ratio of topological parameters expected to increase upon trabecular deterioration to those expected to decrease. Therefore, the higher the surface/curve ratio and the lower the topological erosion index, the more intact the bone architecture. Statistical analysis was performed using repeated measures analysis of variance. At the end of 24 months of testosterone treatment, the serum testosterone concentration (mean \pm SE) was 468 \pm 73 ng/dL, compared to 88 \pm 16 ng/dL prior to treatment. BMI did not change. After 24 months of testosterone treatment, bone mineral density (BMD) increased significantly, 7.4% at L1-L4 and 3.8% at the total hip. Architectural parameters changed even more; the surface/curve ratio increased 11.2% and the topological erosion index decreased 7.5% (table), consistent with improved trabecular connectivity.

	Pretreatment, mean (SE)	Testosterone Rx, 24 mos, mean (SE)	% Change	P
BMD, L1-L4 (g/cm ²)	0.932 (0.063)	1.000 (0.069)	7.4	0.00 1
μ MRI, surface/curve	6.33 (0.50)	6.96 (0.47)	11.2	0.00 4
μ MRI, topological erosion index	1.32 (0.09)	1.22 (0.08)	-7.5	0.00 4

These results suggest that testosterone improves trabecular architecture and therefore has an anabolic effect on bone

Disclosures: **M. Benito**, None.

29

YOUNG INVESTIGATOR AWARD RECIPIENT

Potential for Diagnosis of Bone Quality by Near IR (NIR) Spectroscopy. **G. Li**^{*}, **A. Huang**^{*}, **N. P. Camacho**^{*}. Hospital for Special Surgery, New York, NY, USA.

There is a pressing clinical need for non-invasive assessments that evaluate bone parameters in addition to density, such as the molecular structure of collagen and apatite. Mid-infrared spectroscopy, a technique based on molecular vibrations, has been increasingly utilized to evaluate bone structure, but is limited by its penetration depth of ~10 microns. In contrast, near-IR (NIR) penetrates to a depth of millimeters, and therefore holds the possibility of non-invasive assessment of bone molecular structure.

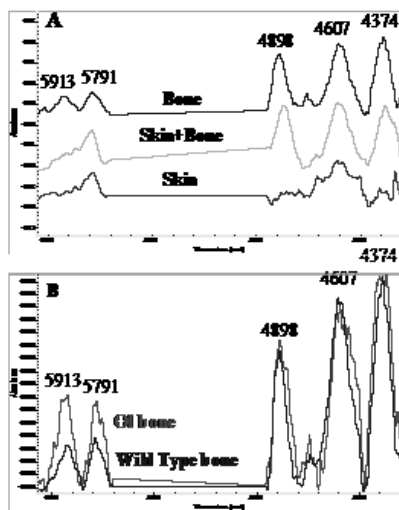


Figure 1. A. Near IR spectra of skin and skin+bone of wild type mouse front palm, and femur bone. B. Near IR spectra of wild type and OI mouse femur bone.

The current study evaluates whether NIR radiation can penetrate through skin into bone, and addresses whether there are differences in the NIR spectra of bone from normal and mutant mice. Femora from 3 +/+ and 3 *oim/oim* mice, a model of type III osteogenesis imperfecta with known mineralization abnormalities (Chipman et al, PNAS 1993), were dissected under IACUC approval. NIR spectra were obtained with a Bruker Vector NIR spectrometer (Bruker Optics, MA) and a reflectance probe (Remspec Corp., MA). NIR spectra were collected in the 4000 - 9000 cm^{-1} range, where absorbances arise from overtone and combination bands of the mid-IR fundamental vibrations of molecular bonds that are present in both the collagen (C-H, C-O, O-H and N-H bonds) and hydroxyapatite (O-H) phases of bone. For the evaluation of the transmission of NIR radiation through skin, NIR data was collected from the underside of the intact forelimb paw, from the paw skin dissected off the bone, and from the bone alone. **Results:** Five NIR bands present in bone, 5913, 5791, 4898, 4607, and 4374 cm^{-1} , were investigated. The bone peaks at 4898 and 4374 cm^{-1} were also obvious in the skin + bone spectra, indicating that NIR radiation did indeed penetrate the mouse skin to sample bone (Fig A). The peak height ratios of 4607/5913 cm^{-1} and 4607/5791 cm^{-1} were significantly different between +/+ and *oim/oim* mice (3.55 ± 0.68 vs 2.29 ± 0.14 , and 2.59 ± 0.48 vs 1.69 ± 0.22 , respectively, t-test, $p < 0.05$), indicating that NIR spectra reflect differences in mineralization parameters in these mice. Although much work is needed to assign specific molecular changes to the NIR absorbances, these preliminary results suggest that it may be possible to non-invasively evaluate bone quality by NIR spectroscopy.

Disclosures: G. Li, None.

30

Non-Destructive Assessment of Microdamage. D. P. Nicoletta, Q. Ni*. Southwest Research Institute, San Antonio, TX, USA.

Quantification of measures of bone quality such as microdamage accumulation and other microstructural characteristics may lead to a more accurate measure of bone strength and therefore fracture risk. It has been shown that age related increases in bone porosity without significant changes in bone mineral density (BMD) result in a decrease in bone strength [1]. Bone fracture toughness is also significantly correlated to changes in porosity, microarchitecture, osteonal morphology, collagen integrity, and microdamage [2], all of which are measures of bone quality. Unfortunately, currently accepted techniques for detection of bone microdamage or other measures of bone quality including microporosity; require serial sectioning and microscopic examination of bone specimens. NMR proton spin-spin (T_2) or spin-lattice (T_1) relaxation time measurements and analytical processing techniques have been used to determine microstructural characteristics including porosity, pore size distribution, and permeability of various types of fluid filled porous materials with characteristic pore sizes ranging from sub-micron to sub-millimeter [3].

The generally accepted microdamage detection procedure is to bulk stain bone *in-vitro* using a dye penetration technique where the dye is allowed to diffuse into the bone material and binds non-specifically to

open bone surfaces. Thus, well-defined microcracks are clearly detectable as regions of concentrated staining. These open surfaces represent small cavities of various shapes (microcracks) where fluid, albeit in minute volumes, is likely to pool relative to the intact bone matrix. We hypothesize that the creation of internal microcracks in cortical bone will result in an effective increase in bone porosity and change in pore size distribution as measured by the NMR spin-spin relaxation (T_2) measurement and its inversion spectrum.

Cortical bone test specimens (4 mm wide by 3 mm thick and 35 mm long) were machined from the diaphysis of human femurs to be used in four point bending fatigue loading to induce microdamage. The use of geometrically well-defined, machined cortical bone specimens allows greater control over the stress and strain applied and measured on each bone specimen. Consequently, the measured damage and NMR spectra can be confidently compared in the context of a known mechanical damage state. Thus, by acquiring an NMR relaxation signal prior to damage, changes in the NMR signal are specifically due to induced microdamage. The use of four point bending allows each specimen to be used for both pre- and post-damage histological characterization. The portion of the specimen that is outside of the four-point bending support pins remains unstressed during bending (the bending moment is zero in this section); this portion of the specimen is used for the pre-damage histological characterization while the gage region of the specimen (the portion of the specimen between the inner loading points) is used for the post-damage histological characterization. Prior to fatigue loading, an initial NMR measurement (pre-damage) using a custom-built 0.5-40 MHz broadband NMR system was performed that represented the undamaged state of the bone. Specimens were fatigue loaded in four point bending until a 20% to 30% drop in specimen stiffness was measured. After cyclic loading, a second NMR measurement was performed on the specimen (post-damage).

In all specimens tested, the NMR relaxation signal is significantly affected by the induced mechanical damage. After fatigue loading of each specimen, the measured increase in NMR determined porosity ranged from 2.1% to 23.6%. In the 0.1 to 10 millisecond relaxation range, there is a shift to longer average relaxation times indicating the creation of new voids or cracks whose volume is on the order of the size of pores in the lacunar-canalicular system. In the 10 to 1000 millisecond relaxation range, a larger shift occurs in which the individual peaks are shifted towards longer average relaxation times again indicating the formation of new internal voids that are about the same volume of Haversian canals or cracks that cause the Haversian canal volume to effectively increase. It is known that the NMR decay signal corresponds to the protons contributed from the all selected regions of pooled fluid within the bone (i.e., intrinsic bone pores plus newly created microcracks). Thus, changes between the pre-damage decay signal and the post-damage decay signal in this range of the decay component are due to the creation of bone microdamage and the subsequent fluid that is pooled within the microcracks, since the intrinsic *in-vitro* specimen porosity attributable to lacunae, canaliculi, or Haversian canals (etc.) has not changed. During this study, it was demonstrated that by using 2 MHz or 27 MHz NMR, similar NMR surface relaxivity constants were obtained, particularly, in the size range of the Haversian canal, which could be used to directly invert T_2 relaxation spectrum to pore size distributions [3]. Thus, in addition to porosity and pore size distributions, the distribution of physical sizes of the population of microcracks can be estimated by this NMR technique and used in conjunction with micromechanical modeling techniques to assess the strength of the bone material.

References

1. McCalden RW, McGeough JA, Barker MB, Court-Brown CM., 1993, *Journal of Bone & Joint Surgery (Am.)*, 75(8): 1193.
2. Yeni, Y.N., C.U. Brown, and T.L. Norman, 1998, *Bone* 22:79-84
3. Ni, Q. Derwin, K. and Wang X., 2004, *Meas. Sci. Technol* 15 58-66.

Disclosures: D.P. Nicoletta, None.

Raman Assessment of Matrix and Mineral. B. R. McCreadie.

University of Michigan, Ann Arbor, MI, USA.

Raman spectroscopy is used to determine the chemical composition of materials. When used to measure the chemical composition of bone, Raman spectroscopy can provide information about both the mineral and organic matrix.

During testing, a laser beam is focused on the specimen surface. A small amount of the light interacts with molecules in the specimen such that the wavelength changes (Raman shift). The Raman shift is dependent on the particular functional unit with which the light interacted. A histogram is plotted showing the magnitude of reflected light at each Raman shift. From this histogram, the chemical composition of the material can be determined. In practice, Raman data is often expressed in terms of ratios. For example, the area of the band (peak) associated with phosphate may be normalized by the area of the band associated with amide I. By scanning the specimen, data from a large number of points may be obtained for each specimen.

Compared to other methods of determining chemical composition, Raman spectroscopy has a high spatial resolution (on the order of microns). "Images" can be constructed to show the spatial distribution of various measures of chemical composition (such as phosphate/amide I ratio). Because this technique depends on light scattered back from the surface, it is able to handle relatively large specimens. Embedded or non-embedded tissue can be used. Little preparation is required, except to create a relatively smooth surface.

Raman spectroscopy has been used to examine a wide range of bone tissue and bone-related diseases and conditions, including bone in aging (1), mechanical deformation of bone tissue (2), microdamage(3), and others(4). Recently, Raman spectroscopy has been used to directly address potential relationships between the chemical composition of bone mineralized extracellular matrix and fracture risk.

One study examined the chemical composition of bone tissue immediately surrounding the fracture site in women with hip fracture, compared to women who died without fracture. The bone tissue was obtained in the same relative location in all individuals. Trends suggested that carbonate/phosphate was higher at the fracture site than at least 2 mm away ($p=0.06$), while the phosphate/amide I was lower ($p=0.09$). There were no significant differences comparing bone tissue at least 2 mm from the fracture site to that obtained from normal individuals, although there was a trend towards higher phosphate/amide I in fractured individuals. The trends seen in this work led us to believe that there is a systemic difference in bone chemical composition between those who fracture and those who do not. We also hypothesized that the fracture site was weaker than surrounding bone due to differences in the chemical composition prior to overt fracture, potentially a result of accelerated remodeling.

In order to address whether differences seen at the fracture site in fracture patients were a cause or a result of the fracture, a small experiment using an animal model was conducted. Five mice received bilateral tibial fractures which were stabilized with an intramedullary pin and tape for two days. Raman spectra were obtained at various distances from the observed fracture site. Differences in phosphate/amide I and carbonate/phosphate ratios between tissue at the fracture site and far from the fracture were not statistically significant and were on the order of 20%, far below that found in human fracture cases. This suggests that the changes seen at the fracture site in hip fracture cases may have existed prior to overt fracture. Changes in matrix and mineral as a function of distance from the fracture site are currently being evaluated.

In order to more fully address whether there are systemic differences in chemical composition between individuals with and without fracture, iliac crest biopsies were obtained from 15 women diagnosed with osteoporotic fracture, and 15 age-matched controls. The results showed that the carbonate/phosphate ratio from cortical bone was higher in fractured women. No differences were seen in other measures of composition in cortical or trabecular bone.

Our current working hypothesis is that there is a systemic difference in bone chemical composition in individuals who fracture and those who do not. There also appears to be some local difference in composition at the fracture site prior to overt fracture, which may be due to microdamage or accelerated remodeling(5), or may simply be normal variation in tissue

composition.

Because there appears to be a systemic difference in the chemical composition of individuals who fracture and those who do not, it may be possible to use Raman spectroscopy as a non- or minimally-invasive screening method to assess fracture risk, either alone or in connection with BMD.

References

- (1) Akkus O. Polyakova-Akkus A. Adar F. Schaffler MB. Aging of microstructural compartments in human compact bone. *Journal of Bone & Mineral Research*. 18(6):1012-9, 2003.
- (2) Carden A. Rajachar RM. Morris MD. Kohn DH. Ultrastructural changes accompanying the mechanical deformation of bone tissue: a Raman imaging study. *Calcified Tissue International*. 72(2):166-75, 2003.
- (3) Timlin JA. Carden A. Morris MD. Rajachar RM. Kohn DH. Raman spectroscopic imaging markers for fatigue-related microdamage in bovine bone. *Analytical Chemistry*. 72(10):2229-36, 2000.
- (4) Carden A. Morris MD. Application of vibrational spectroscopy to the study of mineralized tissues (review). *Journal of Biomedical Optics*. 5(3):259-68, 2000.
- (5) Burr DB. Forwood MR. Fyhrie DP. Martin RB. Schaffler MB. Turner CH. Bone microdamage and skeletal fragility in osteoporotic and stress fractures. *Journal of Bone & Mineral Research*. 12(1):6-15, 1997.

Disclosures: **B.R. McCreadie**, Potential Company 7.

32**FTIR and Backscatter EM Assessment of Matrix and Mineral.** A.

L. Boskey. Starr Chair in Mineralized Tissue Research, Hospital for Special Surgery, New York, NY, USA.

Bone is a composite tissue consisting of a mineral phase (hydroxyapatite) deposited in an oriented fashion on an organic matrix (predominantly collagen). It is our hypothesis that in addition to bone mineral content, size, geometry, connectivity, and the presence of micro-cracks, the strength of bone, and hence its "quality", depends on the distribution of its components within each structural element. Bone mineral and matrix qualitative and quantitative properties vary with tissue site, animal age, and disease state. The spatial variation in mineral content classically was visualized from backscattered electron imaging (BSE) and microradiographs. Recently these techniques have been quantified by computerized calculation of the degree of mineralization of bone (DMB)¹ or the distribution of calcium (Ca_{width}) from quantitative BSE² of bone tissue sections. These quantitative data reveal spatially resolved bone density pixels distribution. DMB and Ca_{width} both correlate with ash weight and with bone mineral density (BMD). BMD is predictive of bone strength, but only partially accounts for bone fragility. Patients with equivalent BMD, microarchitecture, and geometry show different fracture incidences. The DMB is also correlated with the mineral/matrix ratio, a parameter derived from infrared or Raman spectra or microspectroscopy or microspectroscopic images.

Vibrational microscopic imaging reveals the spatial variations of the environment of molecular species in tissue sections.³ No staining is necessary, and based on parameters validated from chemical analyses, insight into the mineral content (mineral/matrix ratio)⁴, the hydroxyapatite crystal size and perfection (crystallinity), the carbonate and acid phosphate substitutions in the hydroxyapatite lattice, the lipid distribution, and the distribution of collagen cross-links can be obtained from a single section.⁵

The images, produced with equivalent color scales can be examined visually to see how parameters vary, and can be evaluated numerically by comparison of pixel images. The data in figure 1, taken from a review in *J Biomed Optics*³, shows trabeculae in two women, one without morphologic or radiographic evidence of osteoporosis (normal) and one who had sustained several fractures (OP). The crystallinity is significantly increased in the osteoporotic case. In studies of human as well as animal models of osteoporosis we have consistently found reduced mineral content (mineral/matrix ratio), increased crystallinity, increased collagen cross-link ratio⁶, increased acid phosphate and decreased carbonate content in comparable bone sites in age- and sex- matched individuals.^{5,6} The distribution of these parameters was also different with the osteoporotic bones having a less Gaussian and sharper distribution of each of these properties. Ca_{width} and DMB distributions similarly are sharper in osteoporotic cases.

Preliminary data validating our hypothesis includes infrared spectroscopic images from patients with equivalent BMD but different fracture histories.

Logistic regression (fracture = 0 or = 1) found the collagen cross-link ratio to be predictive of fracture, with BMD and crystallinity having a weak correlation ($n=20$). Similarly, in mouse bones, crystallinity was directly related to vertebral strength determined by compression testing ($r=0.56$).

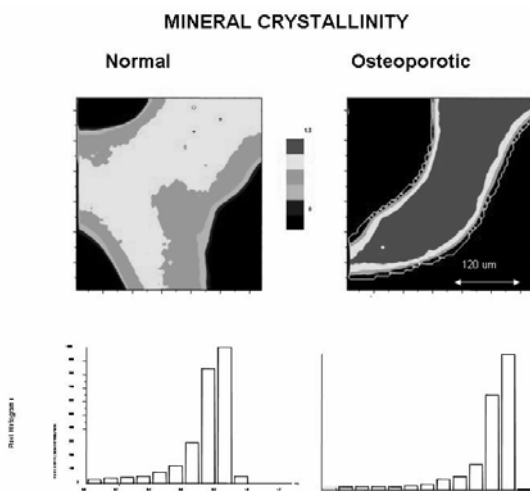
We have also examined the effects of a variety of therapeutic interventions on the spectroscopic parameters of bone quality. Treatment with Nandrolone-decanoate increased the mineral/matrix ratio and decreased the crystallinity of ovariectomized as contrasted to untreated monkeys. PTH treatment broadened the distribution of crystallinity and collagen cross-link ratio in an ovariectomized monkey model as compared with untreated ovariectomized monkeys. Estrogen replacement and Raloxifene therapy broadened the distribution of mineral/matrix ratio and collagen cross link ratio in female patients treated for 2 years with these therapies as contrasted with age-matched placebo treated controls. The effects of other therapies on the vibrational properties of bone are currently under investigation.

These data suggest that when biopsies are available, IR imaging spectroscopy and quantitative backscatter or microradiographic methods can be used to provide insight into the "bone quality". These results are complimentary, but consistently suggest that a broader distribution of mineral and matrix parameters results in less fragile bone.

Support: NIH AR041325

References

1. Follet H, Boivin G, Rumelhart C, Meunier PJ. The degree of mineralization is a determinant of bone strength: a study on human calcanei. *Bone*. 2004;34:783-9.
2. Misof BM, Roschger P, Tesch W, Baldock PA, Valenta A, Messmer P, Eisman JA, Boskey AL, Gardiner EM, Fratzl P, Klaushofer K. Targeted overexpression of vitamin D receptor in osteoblasts increases calcium concentration without affecting structural properties of bone mineral crystals. *Calcif Tissue Int*. 2003;73:251-7.
3. Mendelsohn R, Paschalis EP, Boskey AL. Infrared spectroscopy, microscopy, and microscopic imaging of mineralizing tissues: Spectra-structure correlations from human iliac crest biopsies. *J Biomed Opt*. 4, 14-21, 1999.
4. Faibish D, Gomes A, Boivin G, Binderman I, Boskey A. Infrared imaging of calcified tissue in bone biopsies from adults with osteomalacia. *Bone*. 2005;36:6-12.
5. Boskey A, Mendelsohn R. Infrared Analysis of Bone in Health and Disease, *J. Biomed Opt.* in press, 2005.
6. Paschalis EP, Shane E, Lyritis G, Skarantavos G, Mendelsohn R, Boskey AL. Bone fragility and collagen cross-links. *J Bone Miner Res*. 2004;19:2000-4.



Disclosures: **A.L. Boskey**, None

33

Using Atomic Force Microscopy and Nanoindentation to Assess Bone Material Properties. M. J. Silva. Washington University, St. Louis, MO, USA.

Whole-bone strength depends on bone size, density and tissue properties. Nanoindentation testing, combined with atomic force microscopy (AFM), enables testing of bone tissue properties at the level of the min-

eralized matrix, independent of the effects of size or density.

Background: Nanoindentation is based on a variation of traditional microhardness testing. In a hardness test, a sharp-tipped indenter is pushed into the surface of a specimen and the **hardness** is defined as peak force/indent area. Contemporary nanoindentation testing differs from microhardness testing in two ways. First, the size of the indent is on the order of 1 μm and thus can be placed in a small test area. Second, both force ($\sim 0.5 \mu\text{N}$ resolution) and displacement ($\sim 0.1 \text{ nm}$) are monitored during indentation. Contact stiffness is defined as the slope of the unloading portion of the force-displacement curve and from this the **nanoindentation modulus** of the specimen is estimated. AFM is a technique used in structural biology to assess surface topography of cells, biomolecules and tissues. For non-destructive imaging, a sharp probe contacts the surface at a constant, low-level force ($< 1 \text{ nN}$) while scanning across the specimen surface. By monitoring the vertical motion of the probe, a 3D image of the surface can be constructed. AFM can also be used to determine specimen stiffness, and has been used to determine cell mechanical properties and the micromechanical properties of cartilage. Recently, AFM has been used in combination with nanoindentation of bone; the combined method enables precise placement of the indenter and superb characterization of surface morphology. With AFM the topological features of thin and thick lamellae have been visualized and artifactual surface roughness introduced by uneven material removal with polishing has been described.

Nanoindentation of Bone: Nanoindentation has provided valuable data on the properties of bone at the microstructural level, as it is uniquely suited for testing tissue within individual structures such as trabeculae or cortical lamellae. Because the calculation of nanoindentation modulus requires an assumption of elastic isotropy, there has been concern regarding its accuracy for bone, which is anisotropic. A comparison of nanoindentation and acoustic microscopy values of bone moduli demonstrated that the two methods produced comparable values, providing strong support for the accuracy of nanoindentation⁽¹⁾. Average values for the nanoindentation modulus of wet, human, diaphyseal cortical bone (longitudinal direction) have ranged from 19-23 GPa⁽¹⁻³⁾ (values adjusted to account for wet:dry differences). Moduli of cortical bone tested in the transverse direction are $\sim 30\%$ less than in the longitudinal direction, consistent with relative differences determined by traditional mechanical testing. Comparisons of cortical versus trabecular bone tested in the same direction have demonstrated that trabecular tissue is only $\sim 20\%$ less stiff than cortical tissue. Thus, nanoindentation has helped prove that trabecular tissue does not have inherently different properties than cortical tissue. Nanoindentation testing of human cortical bone from the femoral neck revealed no difference between males and females and, surprisingly, no decrease in modulus or hardness with aging⁽⁴⁾. These data suggest that changes in elastic and hardness properties at the tissue level do not contribute to age-related increases in skeletal fragility. Studies in rats have demonstrated no change in tissue properties following ovariectomy but a decrease in tissue properties following combined ovariectomy and protein deficiency. It should be noted that the data on nanoindentation properties of human bone are still relatively few and there is a need for more comprehensive description of the heterogeneity of cortical and trabecular tissue properties.

Limitations: Nanoindentation testing provides measures of elastic modulus and hardness of bone tissue, properties that do not reflect failure behavior. The limitations of nanoindentation for detecting failure properties are highlighted by results of two rodent studies. In one, nanoindentation detected no differences between osteopetrotic and control rat bone, despite reduced whole-bone strength in the osteopetrotic group. In a second, nanoindentation detected increased modulus and hardness in a murine model of osteoporosis, despite markedly reduced bone strength and toughness determined from bending tests⁽⁵⁾.

Conclusions: Nanoindentation combined with AFM provides unrivaled precision in assessing the modulus and hardness of bone tissue and is uniquely suited for answering questions regarding properties at the microstructural scale. Nonetheless, because failure properties are not assessed, nanoindentation has limitations for assessing bone quality in the context of skeletal fragility.

References

1. Turner CH, Rho J, Takano Y, Tsui TY, Pharr GM 1999 The elastic properties of trabecular and cortical bone tissues are similar: results from two microscopic measurement techniques. *J. Biomech*. 32:437-441.

2. Rho JY, Roy ME, Tsui TY, Pharr GM 1999 Elastic properties of microstructural components of human bone tissue as measured by nanoindentation. *J. Biomed. Mater. Res.* **45**:48-54.
3. Zysset PK, Guo XE, Hoffer CE, Moore KE, Goldstein SA 1999 Elastic modulus and hardness of cortical and trabecular bone lamellae measured by nanoindentation in the human femur. *Journal of Biomechanics.* **32**:1005-12.
4. Hoffer CE, Moore KE, Kozloff K, Zysset PK, Goldstein SA 2000 Age, gender, and bone lamellae elastic moduli. *J Orthop Res* **18**:432-7.
5. Silva MJ, Brodt MD, Fan Z, Rho JY 2004 Nanoindentation and whole-bone bending estimates of material properties in bones from the senescence accelerated mouse SAMP6. *J. Biomech.* **37**:1639-1646.

Disclosures: **M.J. Silva**, None.

34

In Vivo Imaging Techniques for Assessment of Bone Fragility. E. W. Wehrli. University of Pennsylvania, Philadelphia, PA, USA.

Fragility derives from the Latin *fragilis* (breakable), hence bone fragility implies the bone's susceptibility to fracture. What makes the bone susceptible to fracture, however, is not entirely clear. Bone is a composite biomaterial whose mechanical competence hinges on a multitude of parameters that fall into three general categories: (1) the material's overall density, i.e. the mass of bone material per unit bone tissue volume, (2) its macro-, micro- and nanostructural organization, and (3) the material's intrinsic properties determined by its chemical make-up.

The past 30 years have been characterized by unprecedented progress in noninvasive medical diagnostics, leading to an array of imaging technologies, spearheaded by the invention of computed tomography, which makes possible the generation of cross-sectional images from which 3D models of the anatomy of interest can be reconstructed. MRI belongs to the same class of imaging techniques although the underlying physical principles are radically different. Other tomographic techniques such as SPECT and PET make use of radioactive tracers. They all are shown to potentially play a role for the assessment of some property of bone related to skeletal fracture resistance.

Most imaging approaches have focused on #1, an assessment of density. However, bone densitometric techniques, whether of the tomographic or projection type, are not able to measure true density of the bone phase (as defined by mass per unit of bone tissue), rather they measure apparent density, i.e. mass of bone material per unit volume or area of tissue. Nevertheless, the simplest of the densitometric techniques, dual-energy X-ray absorptiometry (DEXA), is currently the mainstay for diagnosis, risk assessment and therapy response monitoring. X-ray computed tomography (CT), provides a great deal more information as it is capable of a volumetric measure of density, thus being able to distinguish between cortical and trabecular bone. This advantage, however, comes at the expense of two orders of magnitude increase in radiation dose (unless practiced at the distal extremities by means of peripheral CT instruments (pQCT) where radiation exposure is very low). CT also provides quantitative insight into the macroarchitecture and geometry of bone, from which indices of strength can be computed by resorting to simple mechanical engineering concepts.

Since most fractures occur at anatomic locations rich in trabecular bone (TB), a particular focus of research during the past 10 years has been the development of methods for noninvasive quantification of TB microarchitecture. Recent advances in MRI and CT now enable visualization and quantitative evaluation of 3D bone architecture in patients. It is shown that with appropriate technology, by correcting for motion and resorting to algorithms suited to process images in the presence of partial volume blurring and noise, detailed architectural information can be gained on scale, topology and anisotropy of the trabecular network. The methodology has further proven its potential for providing direct insight into the bone's mechanical behavior via computational biomechanics. Evidence also exists that μ -MRI-based structural parameters better discriminate patients with osteoporotic fractures from their unfractured peers than does BMD. Other in-vivo structural imaging data indicate that one of the hallmarks of postmenopausal osteoporosis -- the conversion of trabecular plates to rods and their

eventual disruption -- is corroborated, for the first time, noninvasively. Further, MRI has demonstrated its potential to investigate the third, most neglected, dimension of bone quality, the bone's intrinsic material properties, via solid-state imaging techniques (SS-MRI). The feasibility of both P-31 and H-1 SS-MRI has been demonstrated ex vivo, and subsequently in laboratory animals and humans but the methods require technology not currently available commercially to overcome the extremely short T2 relaxation times characteristic of the solid state. Lastly, the extraordinary detection sensitivity of radionuclide scanning opens up new possibilities to study physiologic processes in vivo by means of tracer kinetic approaches. The recognition that in osteoporosis caused by gonadal steroid deficiency, as well as in the second most common metabolic bone disorder, Paget's disease, bone turnover is enhanced, makes this parameter a focus of particular interest. Recently, F-18 dynamic PET has been used to measure the fluoride uptake rate to derive regional dynamic information, not obtainable noninvasively by other means.

In summary, technology now exists for obtaining structural, functional and physiologic information of the skeleton entirely noninvasively. It is likely that many of these procedures currently still in the realm of research, will become part of the routine instrumentarium for diagnosis and treatment follow-up in metabolic bone disease within less than a decade.

References

1. Majumdar S. Magnetic resonance imaging of trabecular bone structure. *Top Magn Reson Imaging* 2002;13(5):323-334.
2. Wehrli FW, Saha PK, Gomberg BR, Song HK. Noninvasive assessment of bone architecture by magnetic resonance micro-imaging-based virtual bone biopsy. *Proc IEEE* 2003;91:1520-1542.
3. Wehrli FW, Gomberg BR, Saha PK, Song HK, Hwang SN, Snyder PJ. Digital topological analysis of in vivo magnetic resonance micro-images of trabecular bone reveals structural implications of osteoporosis. *J Bone Miner Res* 2001;16(8):1520-1531.
4. Wu Y, Chesler DA, Glimcher MJ, Garrido L, Wang J, Jiang HJ, Ackerman JL. Multinuclear solid-state three-dimensional MRI of bone and synthetic calcium phosphates. *Proc Natl Acad Sci U S A* 1999;96(4):1574-1578.
5. Robson PD, Gatehouse PD, He T, Firmin DN, Neubauer S, Bydder GM. Human imaging of phosphorus in cortical and trabecular bone using ultrashort TE pulse sequences. 2003; Toronto, Canada. ISMRM. p 791.
6. Cook GJ, Blake GM, Marsden PK, Cronin B, Fogelman I. Quantification of skeletal kinetic indices in Paget's disease using dynamic 18F-fluoride positron emission tomography. *J Bone Miner Res* 2002;17(5):854-859.

Disclosures: **F.W. Wehrli**, *MicroMRI, Inc.* 2, 4 and Novartis 2.

35

Surrogate Endpoints for Clinical Trials: FDA Perspective. T. E. Kehoe. U.S. Food and Drug Administration, Bethesda, MD, USA.

Bone mass and bone quality are independent determinants of fracture risk. However, bone mineral density is an imperfect surrogate for fracture risk, particularly when used to measure changes in bone mass and risk for fracture following treatment with antiresorptive or anabolic drugs. Until recently, bone quality could only be assessed by bone biopsy. New technological advances, however, will allow for the non-invasive measurement of bone quality, raising the possibility of new and improved surrogates for fracture risk.

Regarding the clinical application of new surrogates for fracture, the first question that must be answered from a regulatory perspective is: in what setting will the surrogate be used? If the intent is to identify patients at high risk of fracture so that therapies can be tailored to suit their needs, then minimal regulatory intervention would be needed. However, if the intent is for the surrogate to replace fracture as the primary endpoint in osteoporosis drug registration trials, the question that must be answered is: why the need for a fracture surrogate when placebo or active-controlled fracture trials in the appropriate patient populations are still viable options?

When we come to a point where placebo or active-controlled fracture

trials are not considered ethical or feasible by a majority of the parties involved, and surrogates for fracture become necessary, some questions that need to be addressed to validate new surrogate include but are not limited to the following:

1. How large should a clinical trial be to validate the surrogate?
2. What sensitivity and specificity, positive and negative predictive value, and other relevant statistics would be required to consider a surrogate valid?
3. What type of fracture should the surrogate be tested against? Morphometric vertebral fractures? Fractures at other skeletal sites? Both?
4. Should the surrogate have equal sensitivity and specificity for mild, moderate and severe vertebral fractures?
5. Should the surrogate show consistent sensitivity and specificity in more than one therapeutic class of drugs (e.g., antiresorptive and anabolic agents)?

Disclosures: T.E. Kehoe, None.

36

The Incorporation of New Surrogates into Clinical Trials. H. Bone. Michigan Bone and Mineral Clinic, Detroit, MI, USA.

Prevention of fractures is the ultimate goal of treatment for osteoporosis. However, fracture risk is the result of the interaction between skeletal strength, other individual characteristics and the environment, and incorporates an important element of chance. The effects of drugs on bone biology and structure can be more directly measured by a number of intermediate endpoints. There is interest in the possible use of such endpoints as surrogates for fracture rates in (phase III) registration trials.

Bone mineral density is closely related to bone strength. It can be measured in animals and humans. It is a predictor of fracture risk, and changes in BMD are correlated with the clinical effects of treatment. BMD has been extensively employed in the evaluation of drugs for osteoporosis. It is the main endpoint for phase II B trials, and for phase III trials for the prevention of osteoporosis. Under limited conditions, BMD can be used as an endpoint for phase III treatment trials in the United States, but not in the EU. Experience with BMD may be informative as we consider the role of newer measures of drug effects.

FDA guidance permits consideration of a well-characterized drug for osteoporosis treatment on the basis of BMD and an interim analysis of fracture data. However, this has had little practical effect, since the European (CPMP, now CHMP) regulatory guidance requires definitive fracture data prior to registration, and because sponsors consider fracture data critical for competitive reasons.

Biochemical markers of bone remodeling provide sensitive and relatively rapid indications of the effects of drugs on bone resorption and formation. Reduction of biochemical markers of bone turnover by "anti-catabolic" agents has been significantly correlated with anti-fracture efficacy, but those markers have so far not been recognized as registration endpoints, in part because they are not structural measurements. Bone remodeling markers are especially useful in earlier-phase studies, characterizing the pharmacology of new drugs, in dose selection, and in monitoring therapy.

A number of new techniques under development give information about bone structure and metabolism that was not previously available in vivo. These techniques include high-resolution QCT and MRI methods, as well as methods for deriving new information from DXA and plain films. Image analysis methods describe changes in bone structure with the goal of estimating the effects of treatment on bone strength, and ultimately on the drug-treatable component of fracture risk. New biochemical markers continue to be developed as well. None of these measurements is currently considered an adequate surrogate for clinical outcomes.

What are the characteristics of tests that should be considered for inclusion in clinical trials? They should be shown in preclinical testing to relate to bone strength and respond favorably to proven and experimental interventions. They should provide information about bone biology or structure that is complementary to previously available information. Such testing has the potential to add information throughout the drug development process. In order to be considered as a possible new surrogate for fracture, a test should perform well as a predictor

not only of fracture but also of the effect of treatment on fracture risk. It should be a practical, reasonably convenient and safe in the clinical trial context, and ideally it should have the potential to eventually be useful in practice. Extensive preclinical and clinical validation would be required before such measures could be used as primary endpoints. (The validation process will be discussed in Dr. Cummings' presentation.) It may be that a composite of such endpoints would be required for optimal information, and that the choice of such endpoints would be influenced by the mechanism of action of the drug under study.

How best can we investigate and validate these endpoints? If sponsors do not incorporate these endpoints into clinical trials, they will not be validated. On the other hand, what incentives do sponsors have to incorporate such endpoints into their trials? One approach to facilitating the evaluation of new measures is to incorporate them into publicly sponsored trials. Developers of the new techniques should be prepared to work collaboratively with NIH and other agencies to make these technologies available in trials in which they can be correlated with clinical outcomes. However, the primary burden for evaluation of these two new techniques almost certainly will fall on the industrial sponsors of therapeutic trials. Such trials will provide regulatory authorities with structured information documented by case report forms. Such information could support the evaluation of both test drugs and the devices or methods themselves.

One intermediate-term approach that may enhance the value to sponsors would be for regulatory authorities to allow meaningful findings from these new techniques (for example, structural analyses of high-resolution images) to be included in the clinical pharmacology sections of the product information. This would allow the information to be officially recognized, without overstating its known significance.

Such data will not be required by regulatory authorities in the foreseeable future, but competitive pressure will probably induce sponsors to incorporate measurements that they expect to respond to their particular investigational agents. It can be expected that for some time, the results of such investigations will be difficult to compare between drugs and across classes. With more extensive validation, it may be possible to give additional weight to such endpoints in registration decisions. However, it will be difficult for physicians, payors and patients to definitively evaluate the role of a new treatment in clinical practice until clinical outcome data are available.

References

1. Committee for Proprietary Medicinal Products: Note for Guidance on Postmenopausal Osteoporosis in Women. <http://www.emea.eu.int/pdfs/human/ewp/055295en.pdf>
2. United States Food and Drug Administration: Guidelines for pre-clinical and clinical evaluation of agents used in the prevention or treatment of postmenopausal osteoporosis. <http://www.fda.gov/cder/guidance/osteo.pdf>
3. Bone HG: Development and Evaluation of New Drugs for Osteoporosis. In: Osteoporosis, 2nd Edition., Marcus R, Kelsey J, Feldman D (eds), Academic Press, San Diego, CA, 2001.

Disclosures: H. Bone, Nordic Bioscience 5.

37

Validating New Surrogate Markers for Fracture. S. R. Cummings. SF Coordinating Center, CPMC Research Institute and U.C.S.F., San Francisco, CA, USA.

A surrogate marker is intended to replace fracture as an outcome for trials. To be a valid surrogate, treatment induced changes in the marker must adequately predict the effect of treatment on fracture risk. A good 'surrogate' accurately and precisely measures changes in a characteristic, such as cortical width, that is in the pathway by which treatment reduces fracture risk. A marker will be a weaker surrogate if treatment also decreases fracture risk by other pathways, such as improving muscle strength.(1)

Validation of a *surrogate marker* produces evidence and confidence that treatment-induced changes in the measurement will accurately and consistently predict the effects of various treatments on risk fractures.(2) This requires several steps:

- 1) Laboratory studies demonstrating that the marker is associated with

biomechanical strength of bone specimens.

2) Human studies findng that treatment changes the marker in the expected direction.

3) Human studies show that the marker predicts fracture risk.

4) Randomized trials with a fracture outcome show that change in the marker (from baseline to follow-up) 'accounts' for a substantial part of the effect of treatment.(1,3)

5) Trials show that changes in the marker account for a substantial part of the effect of several types of treatments on risk of several types of fractures.

Thus, validation requires that a marker be tested in a randomized trial with fracture as an outcome. It must be measured in all participants at baseline and follow-up. Many fracture trials make new measurements of "bone quality" only in a small subset of participants. This can show that the treatment changes the marker in the expected direction but does not validate that the marker is a good surrogate for fracture.

Bone density passed the first 3 steps. But trials with fracture outcomes showed that change in bone density explained little or none of the effect of treatmens on risk of fracture.(4) Bone density and biochemical markers of bone turnover are imperfect surrogates.(4,5) However, before a new measurement can be considered a better surrogate, it must pass the same tests that have been applied to bone density and biochemical markers.

References

1. Fleming TR, DeMets DL. Surrogate endpoints in clinical trials. Are we being misled? *Ann Intern Med* 1996;125:605-13.

2. Prentice RL. Surrogate endpoints in clinical trials: definition and operational criteria. *Stat Med*. 1989;8:431-40.

3. L.S. Freedman, B.I. Graubard and A. Schatzkin , Statistical validation of intermediate endpoints for chronic diseases. *Stat Med* 11 (1992), pp. 167-168.

4. Cummings SR, Karpf D, Harris F, et al. Improvement in spine bone density and reduction in risk of vertebral fracture during treatment with antiresorptive drugs. *Am J Med* 2002;112:281-9

5. Eastell R, Baron I, Hannon RA, et al. Relationship of early changes in bone resorption to the reduction in fracture risk with risedronate. *J Bone Miner Res*. 2003;18:1051-6.

Disclosures: S.R. Cummings, Pfizer, Lilly, Organon, Amgen, Merck, Novartis 2, 5.

38

New Opportunities for Collaborations and Funding. G. E. Lester, J. McGowan. NIAMS, NIH, HHS, Bethesda, MD, USA.

During the past 5 years, NIH has developed several examples of "partnerships" and "collaborations" that facilitate research progress in areas of great interest to both the government and the private sector. Three different examples will be described in this presentation: the public-private partnership of the Osteoarthritis Initiative (OAI); the public-private partnership of the Alzheimer's Disease Neuroimaging Initiative (ADNI); and the Biomedical Informatics Research Network (BIRN).

The OAI is a public-private partnership to develop new resources to stimulate the validation of new biological and structural markers for the progression of osteoarthritis. Currently, new drug development for OA is hindered by the lack of objective and measurable standards for disease progression by which new drugs can be evaluated.

This initiative is funded by the National Institutes of Health (NIH) with additional private funding from several pharmaceutical companies: GlaxoSmithKline, Merck, Novartis Pharmaceuticals Corporation, and Pfizer. The consortium is facilitated by the Foundation for the National Institutes of Health, Inc. and provides approximately 56 million dollars for the 4 clinical centers and 1 coordinating center that are contracted to establish and maintain a natural history database for osteoarthritis including clinical evaluation data and radiological images, and a biospecimen repository over a 7-year period. All data and images collected will be available to researchers worldwide to help quicken the pace of scientific studies and biomarker validation. The Osteoarthritis Initiative (OAI) will follow 5,000 individuals at high risk of developing osteoarthritis or at high risk of progressing to

severe osteoarthritis.

The Alzheimer's Disease Neuroimaging Initiative (ADNI) is a \$60 million, 5-year public-private partnership to test whether serial magnetic resonance imaging (MRI), positron emission tomography (PET), other biological markers, and clinical and neuropsychological assessment can be combined to measure the progression of mild cognitive impairment (MCI) and early Alzheimer's disease (AD). Like the OAI, this initiative is funded through a combination of public money from NIH and corporate and other private participation including Pfizer Inc, Wyeth Research, Eli Lilly and Company, Merck & Co, Inc., Glaxo-SmithKline, AstraZeneca AB, Novartis Pharmaceuticals Corporation, Eisai Global Clinical Development, Elan Corporation, plc, the Institute for the Study of Aging (ISOA), and the Alzheimer's Association and coordinated by the Foundation for NIH. The research is being carried out as a large research grant that supports research at 40-50 sites across the U.S. and Canada. Investigators will recruit approximately 800 adults, ages 55 to 90, to participate in the research: a quarter of the cohort will be cognitively normal older individuals to be followed for 3 years, a quarter of the cohort will be individuals with early AD to be followed for 2 years and one half of the cohort will be individuals with MCI to be followed for 3 years. The project is the most comprehensive effort to date to find neuroimaging and other biomarkers for the cognitive changes associated with MCI and AD.

The Biomedical Informatics Research Network (BIRN) is funded by the National Center for Research Resources (NCRR), a component of the National Institutes of Health (NIH). The University of California San Diego Medical School has received more than \$18.8 million over five years and the Massachusetts General Hospital has been granted nearly \$14 million for three years of support. BIRN is an NIH initiative involving a consortium of 15 universities and 22 research groups that fosters collaborations in biomedical science by utilizing information technology innovations. BIRN's initial three test bed projects focus on brain imaging of human neurological disorders and associated animal models. BIRN's charter is to create an environment encouraging biomedical scientists and clinical researchers to make new discoveries by facilitating sharing, analysis, visualization, and data comparisons across laboratories. A central premise of the BIRN cyberinfrastructure is that the physical location of data and resources should not hamper a research study. Although the initial emphasis is on neuroimaging, the sophisticated hardware and software developed for the BIRN ultimately will benefit the biomedical community at large. The data-sharing tools and infrastructure developed for BIRN will be flexible and extensible, meaning they can be applied to collaborative research in many other scientific fields. The creation of distributed databases, comprising compatible data collected from many different locations, has been a stubborn problem with no clear-cut solution. The challenge lies in translating data from one study into terms that permit direct comparison with the findings from other studies. For instance, brain structure and function often are assessed via magnetic resonance imaging (MRI), but the strength of the magnet varies from one MRI scanner to another, from 1.5 tesla to 3, 5, or even 7 tesla. To address these inconsistencies, the BIRN scientists are developing mathematical algorithms to translate data from scanners of varying strengths into comparable data. Additional aspects of the scan are being standardized, such as the formats for storing all of the experimental conditions and variables, known as the metadata, in the database.

Any of these three examples would be appropriate to bring to bear to address the problem of better surrogates for bone fragility. The application of such models to this area will be discussed.

Disclosures: G.E. Lester; None.

Posters

Novel Assessments of Bone Quality: Non-Invasive

P1

Describing Velocity of Sound in Trabecular Bone via Computer Simulations. R. G. Saade^{*1}, G. M. Tsoukas^{*2}, J. Caminis³.

¹Concordia University, Montreal, PQ, Canada, ²McGill University Hospital Centre, Montreal, PQ, Canada, ³Novartis Pharmaceuticals Corporation, East Hanover, NJ, USA.

A major determinant to fracture is intrinsic bone strength. Material properties of bone, especially density and elasticity, are important surrogates for fracture risk assessment. QUS is a timely method for the evaluation of bone because of its known benefits and its ability to indicate bone strength more effectively than DXA. Albeit the level of understanding of ultrasound interaction with bone is limited. However, the simulation and numerical modeling of ultrasound propagation can help elucidate the interaction and provide insight into bone architecture. The complexity of sound-bone interaction has impeded the development of useful theoretical models. This study explores a simple mathematical model (Sound OS) using a set of partial differential equations which describes the propagation of sound in bone. Sound OS is based primarily on volumetric density and elasticity. It focuses on the propagation of velocity in the porous bone material. The initial purpose of this study was to investigate: (1) the sensitivity of velocity of sound on the density and elasticity of trabecular bone; and (2) the influence of bone porosity on velocity of sound.

Results demonstrated that sound in bone could be simulated and numerically modeled. The model used was capable of reproducing the conditions in the lab.

Sound OS may be a useful tool in studying the interaction between ultrasound and bone architecture. The model could be used to investigate the influence of various bone parameters, such as elasticity, density and porosity, on the propagation of sound in bone so as to further describe parameters of "bone quality/quantity" that may be important in fracture risk modulation.

Disclosures: **J. Caminis**, Novartis Pharmaceuticals Corporation 3.

P2

Sensitivity of Finite Element Analysis of X-ray Images (FEXI) to Anatomical Variations of the Proximal Femur - a Simulation Approach. S. Pisharody^{*1}, R. Phillips^{*1}, J. A. Thorpe^{*2}, C. M. Langton¹.

¹University of Hull, Hull, United Kingdom, ²Hull & East Yorkshire Hospitals, Hull, United Kingdom.

FEXI (Finite Element analysis of X-ray Images) is an osteoporotic fracture prediction technique. Routine two-dimensional clinical radiographic bone images, such as DXA scans, are used to create a 2D plane stress model for finite element analysis. Compressive mechanical loading is simulated to determine the stiffness of the bone. We have investigated the sensitivity of FEXI to variations in trabecular bone density, hip-axis length, hip angle, and head anteversion. A Virtual Anatomy proximal femur was created using the 'vxt' volume graphics library. The resultant bone model was passed through an x-ray simulator to create a 2D image suitable for analysis by FEXI. We found that FEXI-derived stiffness increased linearly with trabecular bone density, decreased non-linearly with hip-axis length, decreased gradually with neck angle, but was insensitive to head anteversion. Multi-parameter sensitivity analysis (MPSA) was performed to determine the relative sensitivity of each parameter on the overall stiffness of the bone. FEXI was most sensitive to hip-axis length (17.4), followed by trabecular bone density (7.9), neck angle (3.4) and head anteversion (0.9).

In conclusion, a simulation approach helps us to understand and analyze the various anatomical parameters that affect the stiffness and hence strength of a bone susceptible to osteoporotic fracture. Clinical validation of the FEXI approach will require extensive analysis of large datasets.

Disclosures: **C.M. Langton**, McCue plc 5.

P3

Bone Mineral and Matrix Density Measurement by Combined

Proton and Phosphorus Solid State MRI. Y. Wu^{*1,2}, J. L. Ackerman^{*2,1}, D. A. Chesler^{*2}, M. I. Hrovat^{*3}, L. Graham^{*1}, Y. Wang^{*1}, M. J. Glimcher¹. ¹Children's Hospital, Boston, MA, USA, ²Massachusetts General Hospital, Charlestown, MA, USA, ³Mirtech, Inc., Brockton, MA, USA.

Noninvasive imaging methods for measuring bone composition (specifically the proportions of mineral and organic matrix) do not exist. Here we demonstrate the use of proton and phosphorus solid state MRI in a combined fashion to quantitatively image the matrix and mineral respectively, which can be used to compute a quantitative image of the degree of bone mineralization (the mass of bone mineral in a unit volume of bone substance).

Conventional MRI detects only fluid constituents of tissues (primarily water and fat). Solid tissue constituents such as bone mineral and the matrix exhibit spin-spin relaxation times far too short to yield detectable MR signals in imaging methods based on spin or gradient echoes. Instead the present technique uses free induction decays (FIDs) rather than echoes to capture signals from all constituents [1,2], while employing a chemically selective suppression technique to eliminate proton signals from tissue water and fat [3].

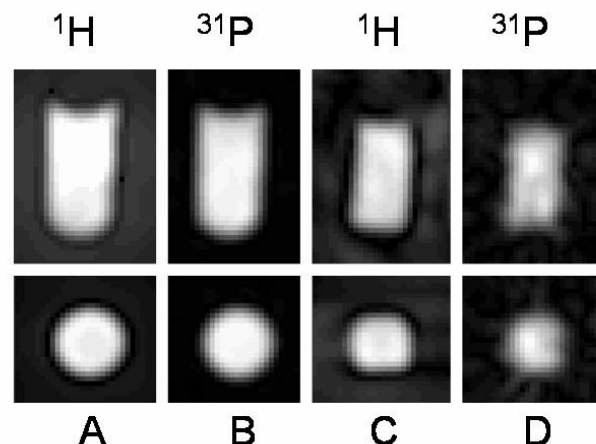
The figure shows on the left corresponding axial and transverse slices of 3D phosphorus and proton projection images of a vial of phosphoric acid (A,B). On the right (C,D) are slices of 3D images of a bovine cortical bone specimen. When appropriately calibrated both proton and phosphorus images accurately reflect the matrix and mineral density respectively.

These data demonstrate that measurements of matched proton and phosphorus solid state MR images are feasible, paving the way toward the quantitative 3D imaging of bone mineralization.

[1] Wu Y, Ackerman JL, Chesler DA, Li J, Neer RM, Wang J, Glimcher MJ. Evaluation of bone mineral density using three dimensional solid state phosphorus-31 NMR projection imaging. *Calcif Tissue Int* 62:512,1998.

[2] Chesler DA, Vevea JM, Boada FE, Reese T, Chang C, Barrère BJ, Liu AM, Thulborn KR. 11th SMRM, Berlin, 1992.

[3] Wu Y, Ackerman JL, Chesler DA, Graham L, Wang Y, Glimcher MJ. Density of organic matrix of native mineralized bone measured by water and fat suppressed proton projection MRI. *Magn Reson Med* 50:59,2003.



Disclosures: **J.L. Ackerman**, SkelScan, Inc. 4.

P4

Bone Mechanical Quality Measured by Ultrasound Critical-angle Reflectometry (UCR). P. P. Antich*, M. A. Lewis*, E. Richer*. UT Southwestern Medical Center at Dallas, Dallas, TX, USA.

We discuss here the use of elastic properties of bone to describe bone quality from a point of view related to an important function of bone, load support.

Ultrasound critical-angle reflectometry (UCR) measures the ultrasound velocity in bone from the amplitude of waves reflected from a selected bone volume. The reflecting elements can be located at the surface of bone, or at depth; in the current device, the depth is limited to 1-2 mm. Cortical and trabecular bone can be measured and distinguished by time of arrival. At a critical angle, the reflected beam experiences an abrupt change determining a velocity either in amplitude (pressure wave velocity) or in phase (shear wave velocity). Bone exhibits a strong directional dependence of velocity, dictated by its intrinsic symmetry. This property allows us to determine the density-normalized (i.e., independent of density) elastic moduli, by taking the squares of the maximum and minimum velocity at a bone site.

In previous studies, the pressure wave velocity has been found to correlate well with the stiffness and breaking strength of cortical and trabecular bone, and the present device concentrates on those measurements. The correlation is strong, but it is local. In particular, properties measured in cortical bone are not necessarily good predictors of properties in trabecular bone and properties measured in bones with different structure do not correlate well with each other (e.g. femoral shaft and neck).

We have built a device to rapidly and effectively measure cortical and trabecular bone ultrasound velocities and their dependence on direction in the clinic. Key features of the new UCR device are: (a) "dual transducer" system with single transmitter and 48 receiver elements, (b) robotic arm to permit accurate positioning and alignment (c) non-allergenic flexible plastic membrane separating the fluid in the transducer head from the skin surface, (d) data acquisition software to extract from the spectra the critical angles for cortical and trabecular bone, and (e) post-processing software to determine the critical angle velocity V at each angle y , and then fit the data to a linear-quadratic formula relating V^2 on the \cos^2 of the angle y , in order to determine two density normalized (to separate mass and velocity effects) elastic moduli.

We observed that while in general UCR properties and density are correlated, such a correlation is not general. Disease conditions, disuse (bedrest) as well as treatment dynamically decouple the two sets. This circumstance establishes a unique role for the UCR measurement, not as indicator of BMD, but as an indicator of a separate property - bone mechanical quality.

Disclosures: P.P. Antich, None.

P5

Bone Strength in Young Women as Measured by a Non-invasive Technique that Analyzes the Response to a Vibratory Stimulus. S. B. Arnaud¹, M. T. C. Liang²*. ¹NASA Ames Research Center, Moffett Field, CA, USA, ²California State Polytechnic University, Pomona, CA, USA.

The purpose of this report is to summarize the progress made in the validation and application of an instrument (MRTA) designed to evaluate the load carrying capacity of the ulna and tibia by determination of EI, estimated from an algorithm that analyzes the response to a vibration (Steele, C.R. J. Biomech Eng., 1988). E is Young's modulus of elasticity, a material property of bone that reflects bone density and matrix and I is the cross-sectional moment of inertia that reflects the distribution of bone about its bending axis and is a reflection of bone geometry. Early measurements in a model of acute disuse in the non-human primate revealed more rapid return of EI in tibias unloaded for 6 months than in mineral content. Biological

validation of the technique in monkeys was carried out by comparison of *in vivo* MRTA measurements with post-mortem tests of the same bones to failure in three point bending ($R^2=0.95$ for $n=12$), (Roberts, J. Biomech. 1995). Current quality control of the test is estimated with an aluminum rod of known EI ($CV=3.8\%$). The ulnas of 10 patients with Type 1 Osteogenesis Imperfecta (OI) provided a biological validation of the technique in humans. Values were 30% lower in OI patients with multiple fractures than in their unaffected relatives with similar bone mineral content (Smith SR et al, JBMR Abst, 1994). After informed consent, we compared values in 16 healthy 22 yr old untrained women (UNT) with 21 world class athletes (WCA) of the same age. The average ($\bar{A} \pm SD$) EI in UNT ulnas was $27 \bar{A} \pm 9 \text{ Nm}^2$ with a range of 10 to 44; whereas the average EI in the WCA ulnas was $41 \bar{A} \pm 17 \text{ Nm}^2$ with a range of 18 to 86 Nm^2 . Mean tibial EI in UNT was $125 \bar{A} \pm 12 \text{ Nm}^2$ (range 80-173) and in WCA $269 \bar{A} \pm 143 \text{ Nm}^2$ (range 108-594). When data are expressed in terms of body weight, or Pcr BW^{-1} , variation in each group remains high (17-40%). This value indicates the number of body weights an individual bone can support: for ulnas, $7.5 \bar{A} \pm 3$ in UNT and $10.5 \bar{A} \pm 3.6$ in WCA and for tibias, $18 \bar{A} \pm 3$ in UNT and $32 \bar{A} \pm 13$ in WCA. Differences in these measures in UNT and WCA were highly significant ($p < 0.01$ or less) in spite of the variation within each group. The validation studies show the importance of architecture in estimates of bone strength. This technique reveals the level of strength present in the ulnas and tibias of young untrained women, its variation and the remarkable degree of strength that is conferred on human bone by athletic training..

Disclosures: S.B. Arnaud, None.

P6

Trabecular Bone Density and Strength Assessment Using Non-Invasive Scanning Confocal Ultrasound Imaging Technology. Y. Qin*, Y. Xia, W. Lin*, E. Mittra*, B. Gruber, C. Rubin. State University of New York at Stony Brook, Stony Brook, NY, USA.

INTRODUCTION: Aging and microgravity induced bone loss is a critical skeleton complication occurred particularly in the weight-supporting skeleton. Bone integrity is dependant on not only the mineral density, e.g., assessed by DEXA, but also the quality of bone which includes the strength and structural parameters. Advances in quantitative ultrasound (QUS) provide a unique method for evaluating both bone strength and density. To improve the accuracy and directly quality measurement, the object of this study is to integrate automatic region of interest (ROI) algorithm in the Scanning Confocal Acoustic Diagnostic (SCAD) system to assess bone qualitative status in the trabecular region.

METHODS: Total of 34 human cadaver calcanei, age from 60 to 97 years old, are tested by SCAD, micro-CT and DEXA, as well as mechanical strength. A new imaging recognition algorithm is developed, integrated in a newly developed SCAD system. The method is designed for the selection of an irregular ROI in the ultrasound attenuation (ATT) images from calcaneus bone. A region growing algorithm automatically searches an initial region in the measured bone quality image until the pixel with the lowest ATT value is found, called seed. The programming evaluates the values of the neighboring eight pixels around the seed, until it reaches to total of 500 pixels. When the ROI is automatically determined, broadband ultrasound attenuation (BUA), and ultrasound velocity (UV) in the real body region are evaluated. The SCAD properties are then correlated to the bone mineral density (BMD), volume fraction, and bone moduli.

RESULTS: Correlations between BMD and ultrasound parameters are significantly improved by using SCAD with the algorithm, yielding correlations between BMD (DEXA) and SCAD parameters as $R^2=0.83$ (BUA), and $R^2=0.65$ (UV). Correlation between bone volume fraction and BUA shows $R^2=0.75$, and shows $R^2=0.54$ (UV). SCAD parameters predict the trabecular bone strength, in which correlation between BUA and elastic modulus is $R^2=0.54$, and correlation between ultimate strength and BUA is $R^2=0.60$.

DISCUSSION: These data have suggested that high resolution bone acoustic images can be generated at particular sites, e.g., calcaneus,

using the SCAD. Data have shown significant correlations between measured ultrasound data and μ CT/DEXA determined bone density/architecture parameters, as well as bone's stiffness, which will ultimately provide a portable, noninvasive device for bone loss assessment in space and on Earth. [Supported by the National Space Biomedical Research Institute (TD00207 & 00405) through NASA Cooperative Agreement NCC 9-58.]

Disclosures: **Y. Qin**, AcousticSCAN, Inc. 4

P7

YOUNG INVESTIGATOR AWARD RECIPIENT

Trabecular Structure Correlates of Vertebral Deformity by Micro-MRI. G. A. Ladinsky*, B. Vasilic*, A. Popescu*, M. Wald*, B. Zemel, P. J. Snyder, L. Loh*, H. Song*, P. K. Saha*, A. Wright*, F. W. Wehrli. University of Pennsylvania, Philadelphia, PA, USA.

There is growing evidence that trabecular bone architecture has a significant role in determining the risk of osteoporotic fracture, but how best to quantify these risk factors has yet to be determined. In this MRI-based virtual bone biopsy (VBB) study, trabecular bone (TB) structural features that might distinguish patients with and without vertebral fractures were evaluated with the distal radius and distal tibia as a measurement site in women >60 years and BMD T scores of -2.5 ± 1.0 . The hypothesis to be tested is that there is a significant component of vertebral fracture risk independent of BMD. Images were acquired at 1.5T and processed to yield bone volume fraction (BVF) maps with a final voxel size of $62 \times 62 \times 103 \mu\text{m}$. Vertebral deformities were assessed from mid-line sagittal MRIs (wedge, biconcavity and compression deformity) and a spinal deformity index (SDI) determined as the weighted sum of the three types of deformity. Digital topological analysis (DTA) was conducted on the skeletonized TB images (in which plates and rods are converted to surfaces and curves) and the voxel type (curve(C), surface(S), junction between fundamental types) determined. DTA voxel densities and TB thickness were determined as described previously and associations examined between these structural measures and SDI using single and multi-parameter regression models. Data are summarized in the Table below. Using multivariate analysis, BVF, erosion index (EI, ratio of parameters expected to increase with osteoclastic resorption divided by those expected to decrease), density of voxels along curve-type trabeculae, and profile-edge voxel density (PE, essentially free ends) strongly correlated with SDI. The strongest correlation was achieved with PE and EI at the distal radius ($r=0.63$, $P<0.0001$). Other notable associations were found for PE, BVF and EI, C pairs. The findings are in agreement with a less connected, more strut-like TB network paralleling increased vertebral deformity load. (Sponsor: RO1 AR49553)

Parameter	r	P	Parameter	r	P
r	radius	radius	r	radius	radius
	(tibia)	(tibia)	Pair	(tibia)	(tibia)
BVF	-0.39 (-0.39)	0.008 (0.007)	PE,EI	0.63 (0.51)	<0.001 (0.002)
S	-0.39 (-0.38)	0.007 (0.01)	PE,BVF	0.51 (0.39)	0.001 (0.03)
EI	0.34 (0.44)	0.02 (0.002)	C, EI	0.58 (0.46)	0.0001 (0.006)

Disclosures: **G.A. Ladinsky**, None.

P8

Assessment of Bone Quality by 3D Analysis of Quantitative Computed Tomography Scans of the Spine and Hip.

K. Engelke^{1,2}, A. A. Mastmeyer^{*2}, C. Fuchs^{*2}, Y. Kang^{*2}, T. Fuerst^{*3}, W. Kalender^{*2}. ¹Synarc, Hamburg, Germany, ²Inst. of Medical Physics, University of Erlangen, Erlangen, Germany, ³Synarc Inc, San Francisco, CA, USA.

Quantitative computed tomography (QCT) is one of the early techniques used for the measurement of bone mineral density. Standard protocols exist for the analysis of single or multiple slices in the spine and the forearm. The advent of spiral CT, the improvement of spatial resolution (0.5 mm isotropically), and the implementation of advanced radiation exposure reduction techniques has sparked renewed interest in QCT. In particular the possibility of rapid (< 1 min) 3D acquisition protocols also offers the possibility to image the most important fracture site, the proximal femur and to retrieve information beyond bone densitometry. However, appropriate analysis algorithms must be developed. In order to exploit the full potential of 3D QCT, we developed semi automated 3D segmentation algorithms for the spine and the proximal femur. The concept of object oriented anatomic coordinate systems was used to define analysis volumes of interests such as head, neck, trochanter and intertrochanteric VOIs in the femur or elliptical and integral mid, inferior, and superior VOIs in the vertebrae of the lumbar spine. In the analysis VOIs standard parameters such as trabecular BMD, BMC, and volume are determined. In addition in particular in the femur cortical indices can be measured: cortical BMD, BMC, volume, and cortical thickness. Finally, further geometrical parameters such as the true 3D length of the neck axis or various polar and cross sectional moments of inertia can be determined. This also applies to the spine. Accuracy of the algorithms can be analyzed using anthropometric phantoms such as the European Spine (ESP) or the European Proximal Femur (EPFP) Phantoms.

In conclusion we developed novel analysis techniques for 3D QCT data of the spine and the proximal femur and are able to measure a large variety of parameters. However, it still needs to be determined which parameters optimize fracture prediction and longitudinal monitoring.

Disclosures: **K. Engelke**, None.

P9

Radiation Dose Estimates in Quantitative Computed Tomography.

T. Fuerst, K. Engelke*, H. K. Genant. Synarc, Inc., San Francisco, CA, USA.

Quantitative computed tomography (QCT) offers several advantages over dual x-ray absorptiometry (DXA) in the assessment of bone mineral density and structure. As such QCT has the potential to provide more information about bone strength, fracture risk and patient response to therapeutic intervention. However one disadvantage of QCT is the larger radiation dose. In this study we estimated radiation dose associated with spine, femur and forearm QCT measurements using a computer program designed for this purpose. Standard QCT acquisition protocols for spiral CT scanners were entered into WinDose 2.1, a CT dose calculation program. The protocols were chosen to provide images with resolution and signal to noise ratio suitable for three dimensional analysis to determine BMD and bone geometry. Specifically, we chose a slice thickness = 1 mm, kVp = 120 and mAs = 100, 170 and 200 for the spine, femur and forearm, respectively. Scan length varied by skeletal site. Anatomical coverage was L1-L2 for the spine, at the proximal femur from the femoral head to 1 cm below the lesser trochanter and at the forearm from the radial styloid to 10 cm proximal. The program calculated the effective dose to a female using ICRP 60 weighting factors. Dose estimation was based on Monte Carlo modeling and the EVA phantom. Actual radiation dose depends on the CT scanner and patient characteristics. Forearm dose estimates were based on a simulated

scan of the distal tibia. The table below shows the calculated QCT effective dose from the WinDose program and comparison doses found in the literature.

Examination	Effective Dose (mSv)
QCT of the spine (L1-L2)	1.3
QCT of the femur	3.6
QCT of the forearm	0.05
DXA of the spine or femur	< 0.01
Spine lateral thoracic and lumbar x-rays	0.6-1.0
Spine AP thoracic and lumbar x-rays	1.1-1.3
Annual background radiation	2.1

Radiation dose for the spine and femur would be larger by approximately two-fold or more in overweight subjects (body mass index approximately greater than 30 kg/m²). Dose reduction algorithms built into modern CT scanners can reduce the radiation dose by 20-30%. These radiation dose estimates include the gonadal dose which might not be appropriate in postmenopausal women. The radiation dose of QCT scans is comparable to the dose for clinical CT examinations of the abdomen and pelvis. QCT offers a valuable tool in the assessment of new osteoporosis treatments but care should be taken to limit radiation dose through available radiation reduction techniques.

Disclosures: T. Fuerst, None.

P10

Structural Dynamics as a Bone Diagnostics: A Preliminary Study.

M. Liebschner*¹, W. Tawackoli*¹, S. Wimalawansa², G. Gunaratne*³, F. Hussain*³, P. Spanos*¹. ¹Rice University, Houston, TX, USA, ²Robert Wood Johnson Medical School, New Brunswick, NJ, USA, ³University of Houston, Houston, TX, USA.

In order to effectively evaluate and monitor the strength and load-carrying capacity of bones in vivo, an objective non-invasive measurement is desirable. The mineral mass of bone, although essential, does not provide a complete measure of bone strength and integrity.

The dynamic response of bone tissue to a mechanically induced vibration provides an indication of the structural integrity and stiffness of the bone. This technique has been extensively used in engineering applications to identify cracks in pressure vessels and engine blocks, as well as to monitor bridges and buildings after earthquakes. We propose to utilize a structural dynamics approach to evaluate varying stages and modalities of bone loss non-invasively. Such tools are critical for determining bone fragility because weakening of load-bearing bones is one of the major concerns of osteoporosis.

In this present human pilot study, we utilized a prototype of our OsteoSonic diagnostic tool on 37 human volunteers. The mean age was 29 years with a range between 19 and 63 years of age (19 female and 18 male volunteers). All subjects signed a consent form before testing. The left and the right forearm were tested at the wrist and the elbow for a total of four measurements per subject. A dynamic mechanical stimulus was induced at either anatomic site of varying frequency for about 20 seconds. The tissue response was measured with an impedance head and recorded.

The dynamic tissue response of the ulna to a mechanical stimulus showed two distinct peaks of acceleration. Following Jurist's protocol, the frequency at which the first peak of maximum acceleration was detected was multiplied with the inner forearm length of the subject. The results showed a trend of this parameter with age, however, the sample size will need to be increased for statistical analysis. For the age-matched normal population, our values were well within one standard deviation reported by Jurist. Therefore, our results suggest that the prototype OsteoSonic can be utilized to obtain comparable data for the dynamic tissue response of the human ulna.

In addition to obtaining values to monitor the progression of bone loss, our device was able to separate bones that previously had fractures. The tissue response of previously fractures forearms to our dynamic vibration was on average 40% lower than the signal measured on the intact bone.

Our preliminary data indicated that our OsteoSonic device is capable of measuring structural properties directly in vivo and may be suitable for mass screening.

Disclosures: M. Liebschner, None.

Novel Assessments of Bone Quality: Invasive

P11

YOUNG INVESTIGATOR AWARD RECIPIENT

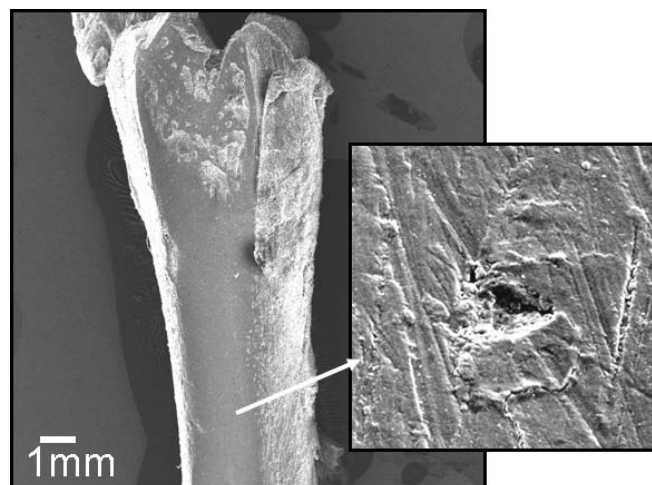
Assessment of Bone Quality at the Sub-micron Scale in Chain Deficiency Osteogenesis Imperfecta. G. E. Lopez Franco¹, D. Stone*¹, A. Huang*², N. Pleshko Camacho², R. Blank¹.

¹University of Wisconsin-Madison, Madison, WI, USA, ²Hospital for Special Surgery, New York, NY, USA.

Bone mineral density is only an imperfect predictor of bone's physiological function. Moreover, bone is a highly organized combination of cells, matrix proteins, proteoglycans, and mineral. Both the composition and the organization of these constituents play vital roles in determining the inherent biomechanical properties of the tissue. Mice harboring the *Col1a2*^{oim} mutation (*oim*) are a well-studied model of osteogenesis imperfecta (OI). This mutation is a frameshift of the gene encoding the $\alpha 2$ chain of type I collagen. To better characterize the tissue-level mechanical consequences of the *oim* mutation, we performed nanoindentation testing in the femur of B6C3FeLe *a/a* mice harboring various *Col1a2* genotypes and C57BL/6J sacrificed at 11 and 17 \pm 1 week of age. We executed nanoindentation using a Triboscope system (Hysitron Inc). Loading, holding and unloading segments described the force profile applied to the sample by using a calibrated Berkovich tip at loads between 3000 and 8000 μ N. Data were analyzed by using the Oliver and Pharr method. Young's modulus and hardness data are summarized in the table below. While $+/+$ compliance values ranged between 1.2 ± 1.9 and 8.2 ± 3.7 nm/mN, *oim/oim* values fell between 16.9 ± 1.5 and 24.7 ± 2.5 nm/mN. Compared to 11 weeks of age and cross orientation, specimens in longitudinal orientation and 17 weeks of age showed the highest Young's Modulus and hardness values for all studied genotypes. Interestingly, a greater hardness and compliance was found in the *oim/oim* compared to the $+/+$ mice. Such findings may be attributed to increased tissue mineralization density, age and genotype-dependence of bone material properties in the model *oim* model. Importantly, not embedding the bone samples allows us to assess mechanical properties without the confounding contribution of the embedding matrix.

Reduced Young's Modulus (Er) and Hardness (H) (GPa)

Orientation	Cross		Longitudinal		Longitudinal	
	Parallel to bone's long axes		Perpendicular to bone's long axes			
Indent						
Weeks	17		17		11	
	Er	H	Er	H	Er	H
B6	19 \pm 4	0.7 \pm 0.2	20.6 \pm 0.8	1 \pm 0.08	N/A	N/A
$+/+$	17 \pm 4	0.6 \pm 0.1	30.6 \pm 0.1	1.4 \pm 0.1	17 \pm 5	0.4 \pm 0.1
<i>oim/+</i>	19 \pm 2	0.5 \pm 0.1	29.0 \pm 1.8	1.4 \pm 0.1	10 \pm 4.7	0.5 \pm 0.1
<i>oim/oim</i>	N/A	N/A	N/A	N/A	10 \pm 3	0.6 \pm 0.1



$A=17464285\text{nm}^2$

Disclosures: **G.E. Lopez Franco**, None.

P12

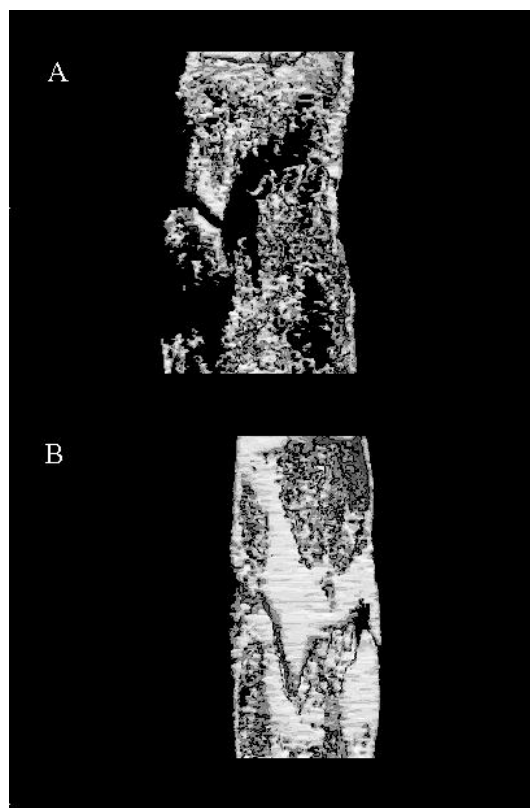
MicroCT as an Improved Method for Measuring Bone Quantity and Quality in a Rabbit Model of Distraction Osteogenesis. R. Hamdy¹, J. Henderson², J. Binette^{*2}, T. Haque^{*1}. ¹Shriners Hospital, McGill University, Montreal, PQ, Canada, ²Centre for Bone and Periodontal Research, McGill University, Montreal, PQ, Canada.

Distraction osteogenesis is a technique used to treat many bone diseases including bone length discrepancies, fractures and non unions. The process involves an osteotomy after which bone ends are distracted using an external fixator and new bone forms within the distracted gap. Due to complications related to prolonged use of the external fixator, ongoing research is aimed at increasing the rate of bone formation to expedite fixator removal. In the following study, we measured and compared the quality of bone formed in rabbits subjected to distraction osteogenesis with and without exogenous BMP7 treatment. Bone regeneration was assessed using histomorphometry, bone mineral densitometry (BMD) and microCT. This is the first report on the use of microCT for analyzing tibial bone repair in distraction osteogenesis.

The right tibia of 46 rabbits was lengthened with a uniplanar fixator. One week after distraction, 75 micrograms of recombinant BMP7 was administered to one group of rabbits while the other received placebo. Rabbits were sacrificed 3, 5 and 7 weeks post surgery and the tibia removed for analyses.

Bone mineral density, assessed on the tibia using a PixiMus densitometer, demonstrated a 100% increase at 5 weeks after BMP7 treatment compared to the placebo. The same bones were scanned on a Skyscan 1072 instrument to attain multiple 2D images. 3D Creator software was used to generate 3D reconstructions of the bone. MicroCT images of the distracted zone at 5 weeks are shown for (a) the placebo and (b) BMP treated samples. Quantitative measurements of bone volume/tissue volume, obtained using CT-Analyser software, corroborated the significant increase in BMD. The same bones were left un-decalcified, embedded in plastic, sectioned and stained with Goldner trichrome to distinguish between mineralized and un-mineralized tissue. Histomorphometric analysis of these sections remained inconclusive.

The results exemplify the difficulties with extrapolating volumetric information on bone formation and architecture from 2D bone area measurements obtained from histomorphometry. The correlation with BMD suggests that computed tomography is a superior method for analyzing the quality and quantity of bone in distraction osteogenesis..



Disclosures: **R. Hamdy**, FRSQ, Shriners 2

P13

Application of a Novel Bone Remodelling Simulator to the Assessment of Bone Quality. C. M. Langton, C. A. Dobson^{*}, R. Phillips^{*}, M. J. Fagan^{*}. University of Hull, Hull, United Kingdom.

We have developed a 3D bone remodelling simulation environment that considers the net effect of osteoblast and osteoclast activity on biopsy and computer-generated cancellous bone samples. The finite element solver predicts the stiffness of the resultant structures, where each voxel is converted directly into a finite element. An integrated histomorphometry tool allows the relationship between structure and mechanical properties to be explored. A graphical interface enables 3D stereoscopic visualization of the bone structures at every stage of an analysis, together with 'fly-throughs' and automatic movie generation. 3D natural tissue bone structures are obtained from μ CT scans, with typical resolutions of 15-25 μm . This data is used directly in the stochastic simulator which is based upon the concept of the basic multi-cellular unit (BMU), where either net resorption or net formation is considered at bone/marrow surfaces. The simulation considers the probability that any surface voxel will be activated into a BMU, and if activated, the length of the resorption cavity or bone deposition. Simulation of anabolic treatment following varying degrees of initial resorption yielded a hysteresis relationship between the stiffness and density of bone, due to the dependence on trabecular perforation.

The simulator also allows the user to specify complex multi-functional non-linear modelling and remodelling rules, based on, for example, local bone age, stress/strain profile and location within a structure. The age of each bone voxel is recorded during simulation so that activity can be biased away from recent remodelling sites. Similarly, values of strain energy density in each voxel can be used to influence activity, facilitating strain-weighted adaptation.

Disclosures: **C.M. Langton**, McCue plc 5.

P14

Can Cortical Width Be Estimated from DXA Data? An In Vitro pQCT Study of the Femoral Neck. J. Reeve¹, P. M. Mayhew*¹, N. Loveridge¹, C. D. Thomas*², J. G. Clement*². ¹University of Cambridge, Cambridge, United Kingdom, ²University of Melbourne, Melbourne, Australia.

Background: The superior femoral neck cortex receives a stress similar to yield stress in a sideways fall (Yoshikawa JBMR, 95). Beyond this stress, bone's toughness might preserve integrity with some impaction. But if the cortex becomes locally elastically unstable, displacement should abort the beneficial effect of toughness. Local elastic stability (σ) in a cortical sector curved in the plane of cross section depends on the product of sector curvature ($1/R$) and thickness (t). In recent work (Lancet, in press), many older female femoral necks scanned ex vivo by pQCT had thin lateral cortices and σ s close to the yield stress. To investigate elastic stability in vivo, we explored the utility of surrogate measures for estimating t from DXA.

Methods: We scanned with pQCT (Scanco Densiscan) and DXA 77 male and female femurs age range 20-95, all cases of sudden death. From pQCT we selected the cross sectional images of the "narrow neck" region where the ratio of lateral-medial to anterior-posterior widths was 1.4. Cortices were segmented into 1/16ths and their widths measured using the histological referents of Crabtree et al (2001) and adjusting for the partial volume effect. Resolution was 0.275 mm. Next, 2-D density maps were converted into density histograms across the section to simulate those generated by routine hip DXA. From the real DXA density 'profiles' analysed by Beck's HSA software (pixels twice the length) the centre of gravity (centroid), neck width, lateral distance (centroid to lateral sub-periosteum), cross sectional area (CSA) and BMD (g.cm⁻²) were calculated.

Results: mass, density and distance measurements from the DXA scans predicted lateral cortical width poorly, with the best predictor being BMD ($P=0.048$ for model). Using the simulated high resolution DXA scans from pQCT improved predictive ability little. However, the sum of densities in those pixels located between 1.9 and 4.4mm medial to the lateral margin predicted cortical width, (mean 1.13 mm, RMS error 0.15; $R^2=0.42$ $P<0.0001$ age and sex adjusted). No variant of the full width at half maximum (FWHM) approach was useful. For medial thickness, the FWHM approach suggested by Hangartner's result (JBMR 1998), was modified so 95 not 50% maximum was the threshold endocortically to allow for the effects of trabeculae. The mean width of 3.6mm was then predicted with a RMS error 0.49mm; $R^2=0.45$ $P<0.0001$.

Conclusions: Cortical widths of the femoral neck may be estimable with fair precision from DXA scan data. This should prove valuable in the clinical investigation of cortical thickness as a key determinant of the elastic stability of the proximal femur in a fall.

Disclosures: J. Reeve, None.

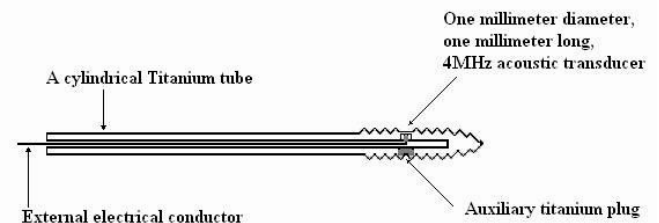
P15

Implantable Miniaturized Ultrasonic Transducers for Measuring Bone Resorption and Remodeling. J. L. Katz¹, D. Hazony*².

¹University of Missouri-Kansas City, Kansas City, MO, USA, ²Case Western Reserve University, Cleveland, OH, USA.

A set of implantable titanium miniaturized ultrasonic transducers (MUT) has been designed and developed for both in vitro and in vivo measurements of bone resorption and remodeling. The MUTs in the first system have a cavity at one end and the ultrasonic transducer at the other end of a titanium orthopaedic screw. Calibration of speed of sound, attenuation and density in the cavity are done in solutions of graded concentrations of collagen powder in distilled water. In vitro measurements of bone formation in the cavity can then be performed in cell culture experiments. The same MUTs can be used in animal model studies of bone resorption and remodeling in osteoporosis. The MUTs in the second system have been designed and developed for inclusion in orthopaedic screws that are used in external fixators for

fracture repair and distraction osteogenesis. In this system the ultrasonic transducers are incorporated in the front portion of the screws located so that they are enclosed within the cortical bone. The 1mm diameter transducer is mounted from the inside of the tubing through the auxiliary titanium plug. The acoustic beam is normal to the tubing in a controlled direction. Only titanium is exposed to the body. The electrical ground is made with the titanium tubing. The external electrical drive is provided through the inside of the tubing. In vivo experiments with this system is planned using an animal model. Planned for both sets of animal experiments is a patented system developed by one of us, Patent #5,143,069 (1992) "Diagnostic Method of Monitoring Skeletal Defect By In Vivo Acoustic Measurement of Mechanical Strength Using Correlation and Spectral Analysis (S. J. Kwon and J. L. Katz) that will be used in external noninvasive measurements of the acoustic parameters simultaneously with the measurements made with the implanted screws. This will allow correlation between the two sets of measurements so that the noninvasive measurements can be used in humans to follow potential changes in bone quality.



Disclosures: J.L. Katz, MedSonics Co. (Start-up Company) 1.

P16

Bone Elastic Modulus Assessment via Atomic Force Microscopy of Bone Marrow Stromal Cell Transplants. M. H. Mankani¹, M. Balooch*¹, S. Marshall*¹, P. Gehron Robey², G. W. Marshall*¹.

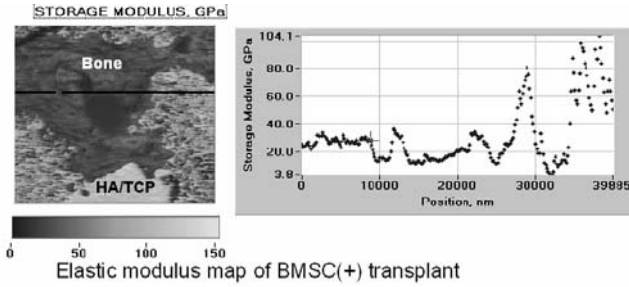
¹UCSF, San Francisco, CA, USA, ²National Institute of Dental and Craniofacial Research, NIH, Bethesda, MD, USA.

The long-term purpose of our research is to determine how osteoprogenitor cells from the bone marrow, bone marrow stromal cells (BMSCs), mediate the structural bone changes in post-menopausal osteoporosis. We have begun by examining the mechanical properties of new bone formed by transplants of cultured normal BMSCs placed in a normal recipient. We hypothesized that engineered bone formed by transplanted, autologous cultured BMSCs has an elastic modulus comparable to endogenous bone and to new bone formed by osteoconduction in the same recipient. Local mechanical properties can be determined using atomic force microscopy (AFM)-based nano-indentation, both in discrete mode to obtain hardness and elastic modulus on a micro-scale and in force modulation mode to map the elastic modulus on a nano-scale.

An adolescent male mongrel dog underwent bone marrow harvest, isolation of BMSCs in tissue culture, and expansion of the cells via sequential passaging, as earlier described (Mankani, et al; Radiology; 2004). BMSCs were combined with hydroxyapatite/tricalcium phosphate (HA/TCP) to form experimental BMSC(+) transplants. We also created control BMSC(-) transplants containing HA/TCP but no BMSCs. The dog underwent creation of bilateral critical-sized calvarial defects; one side received a BMSC(+) transplant and the other a BMSC(-) transplant. Transplants were recovered eighteen months following transplantation and evaluated by histology and AFM-based nano-indentation.

By histology, the BMSC(+) transplant had formed abundant lamellar cortico-cancellous bone throughout the transplant. The BMSC(-) transplant had minimal new bone which was localized to areas adjacent to the normal calvarium, presumably secondary to osteoconduction. By AFM, elastic modulus of bone in the BMSC(+) transplant (22.9 GPa, SD 2.20) and normal calvarium (22.6 GPa, SD 1.95) were significantly higher ($p<0.01$ and $p<0.05$, respectively) than

the bone in the BMSC(-) transplant (18.8 GPa, SD 0.45), via ANOVA (see figure).



BMSC transplants produce new bone with elastic modulus comparable to adjacent pre-existing normal bone, and significantly higher than bone created through osteoconduction. A comparable transplantation study in an animal model of osteoporosis is now underway.

Disclosures: **M.H. Mankani**, None.

P17

Bone Microstructure and Elasticity Assessed by High Resolution Scanning Acoustic Microscopy. **K. Raum**^{*1}, **F. Chandelier**^{*2}, **I. Leguerney**^{*2}, **M. Talmani**^{*2}, **A. Saied**^{*2}, **F. Peyrin**^{*3}, **R. Cleveland**^{*4}, **P. Laugier**^{*2}. ¹Martin Luther University of Halle-Wittenberg, Halle, Germany, ²University Paris VI - CNRS, Paris, France, ³ESRF, Grenoble, France, ⁴Boston University, Boston, MA, USA.

This study aimed at i) validating scanning acoustic microscopy (SAM) for the assessment of cortical bone microstructure using reference data obtained with synchrotron radiation μ CT (SR- μ CT), ii) deriving the anisotropic stiffness coefficient c_{33} at the tissue level. Ten human specimens of cortical bone (radius) were explored using 200 MHz SAM and SR- μ CT with a spatial resolution of 8 and 10 μ m respectively. Site-matched regions were analyzed on both the acoustic impedance (Z) and degree of mineralization of bone (DMB) images. Structural parameters, including diameter and number of haversian canals per cortical area (Ca.Dm, N.Ca/Ar) and porosity Po were assessed with both methods using a custom developed image fusion and analysis software. A model was used to relate the DMB to mass density and calculate local stiffness c_{33} from the combination of Z and DMB. A strong correlation was found for microstructural properties derived from both techniques (Table 1)

	SR- μ CT	SAM	R ²	RMSE
N.Ca (mm ⁻¹)	10.4 \pm 4.8	10.8 \pm 5.3	0.97	5.6
Ca.Dm (μ m)	54.3 \pm 9.3	54.9 \pm 9.5	0.72	5.2
Po (%)	5.7 \pm 2.4	6.5 \pm 2.3	0.91	0.92

The derived stiffness c_{33} (35.9 \pm 12.8 GPa) was highly correlated to the square of Z (R²=0.99, p<10⁻⁴) while the correlation coefficient of a power fit between DMB and c_{33} was only moderate (R² = 0.31, p < 0.0001). This indicates that measurements of DMB are unlikely to predict accurately bone elasticity. Factors such as collagen cross linking, orientation, mineral cluster size which will not affect density measurements could influence both acoustic and elastic properties. Our findings suggest that SAM fulfills the requirement for simultaneous evaluation of cortical bone microstructure and elastic properties at the tissue level.

Disclosures: **P. Laugier**, None.

P18

Staining Techniques for μ CT of Microdamage in Bone. **R. K. Roeder**^{*}, **H. Leng**^{*}, **X. Wang**^{*}, **G. L. Niebur**. University of Notre Dame, Notre Dame, IN, USA.

The role of microdamage in bone quality is not well understood, in part due to our limited capabilities for measuring microdamage. The use of fluorescent labels under UV or light microscopy, in addition to being invasive and destructive, assumes that measurements made on a finite number of two-dimensional sections are representative of the entire sample. Three-dimensional imaging techniques are required in order to measure the inhomogeneity and anisotropy of microdamage relative to local variations in mechanical loading, bone mineral density, architecture or fracture sites. Therefore, the objective of this work was to develop staining techniques suitable for micro-computed tomography (μ CT) of microdamage in bone using radio-opaque contrast agents.

Damaged bovine cortical and trabecular bone specimens were stained using calcein and either lead sulfide (PbS) or barium sulfate (BaSO₄), and imaged using UV light microscopy and μ CT (Scanco μ CT 80), respectively. Cortical bone beams were loaded in four-point bending fatigue, sectioned at the midspan, and each specimen half was stained with calcein and PbS, respectively. Similar damage patterns were observed in the paired specimens, validating the new technique. The amount of PbS stain, measured from the ratio of integrated peak intensities in the image histogram, was significantly greater (p<0.001) for damaged specimens versus the undamaged control. Notched cortical bone beams were also loaded in four-point bending fatigue and stained with BaSO₄. In damaged specimens, μ CT images showed distinct regions of bright voxels ahead of the notch. Damage accumulation was evident with increased loading cycles (Fig. 1). Trabecular bone cylinders were loaded in axial compression and stained using either calcein or BaSO₄. The median peak intensity in the μ CT image histogram was significantly greater (p<0.001) in damaged specimens versus the undamaged control. In summary, we conclude that both BaSO₄ and PbS are suitable contrast agents to detect the presence, and to a limited extent the morphology, of microdamage in both cortical and trabecular bone using μ CT.

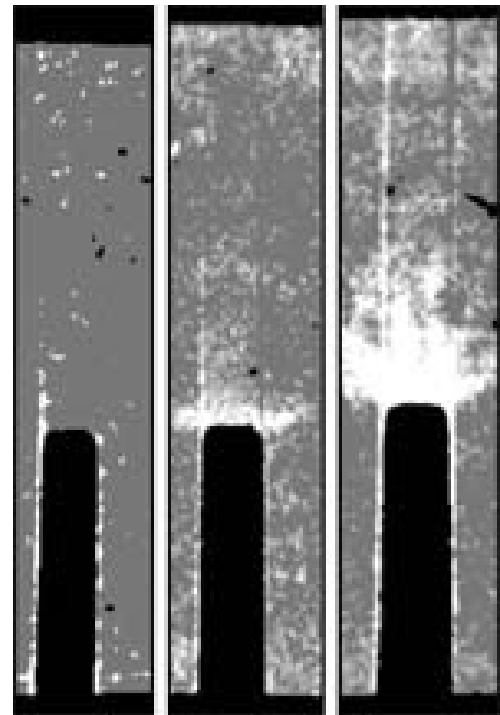


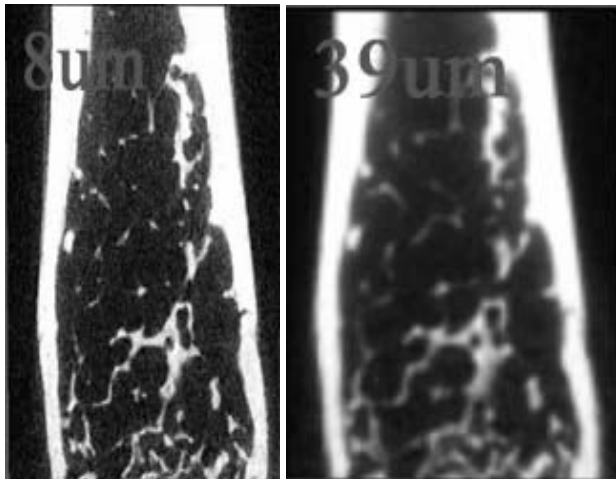
Figure 1. μ CT images of BaSO₄ stained bovine cortical bone showing an unloaded control (left) and damage accumulation ahead of a notch loaded to <50,000 (center) and >500,000 cycles (right). The field height is \approx 4 mm.

Disclosures: **R.K. Roeder**, None.

P19

The Effect of MicroCT Image Voxel Size on Trabecular Bone Characterization in Mice. E. M. Johnson*, V. Kundra*, D. D. Cody. M.D. Anderson Cancer Center, Houston, TX, USA.

To evaluate how voxel size affects trabecular bone characterization in mice, this study examined multiple voxel-size reconstructions for *ex-vivo* μ CT imaging. Nine left mouse femurs, the control side of tumor bearing mice from a different study, were scanned on a GE Healthcare MicroCT Scanner (GE Healthcare, London, ON) with a detector element size of 0.008 mm. The scanner was operated at 80 kVp, 80 μ A, and required 120 minutes to complete each scan. The reconstruction software allows binning of signal data acquired for each detector element to produce reconstructions of each femur at isotropic voxel sizes of 8, 16, 24, 31, and 39 μ m. An identical volume of interest (VOI) was examined for the five reconstructed data sets of each of the nine femurs that included secondary spongiosa but excluded cortical bone and the growth plate (average VOI: 1.0 x 1.0 x 0.7 mm³). The bone volume percentage (BV%), trabecular thickness (TbTh, μ m) and bone mineral density (BMD, mg/cc) of the femur specimens was estimated using software provided by the scanner manufacturer. It should be noted that the file size increases exponentially as voxels that make up the image set become smaller. At voxel sizes of 16 μ m and below, files may become so large that some computers and/or software will be unable to accommodate them. Large files also require additional overhead in the form of transfer time, archiving, and restoring. This study suggests the assessment of TbTh was compromised with voxel sizes as small as 16 μ m and improves with decreasing voxel size. The study found that BV% and BMD did not change with voxel size, and that the range of the voxel sizes used in this study could be considered appropriate for use in assessing these parameters.



Results (Voxel Size n=9)

Voxel Size (μ m)	BV%	TbTh (μ m)	BMD (mg/cc)	Femur Size (MB)
8	18	16	269	897
16	15	38	271	114
24	15	45	269	34
31	15	50	267	14
39	15	55	267	7

Disclosures: E.M. Johnson, None.

P20

YOUNG INVESTIGATOR AWARD RECIPIENT

The Effects of Changing Loading Mode on Initiation and Propagation of Microcracks in Trabecular Bone. G. L. Niebur, X. Wang*. University of Notre Dame, Notre Dame, IN, USA.

Propagation of microcracks may be one mechanism by which microdamage contributes to age-related fracture risk. The goal of this study was to investigate the initiation and propagation of microcracks

in trabecular bone due to changing loading modes.

Twenty-eight on-axis trabecular bone specimens were prepared from 20 bovine tibiae. Fourteen specimens were subjected to on-axis compression to 2% strain followed by torsional loading to a maximum shear strain of 4%. The remaining specimens were subjected to torsional loading followed by on-axis compression to the same strain levels. Microdamage was labeled by xylenol orange and calcein stains to differentiate formation and propagation in each loading mode. Microdamage was quantified under UV epifluorescent microscopy at 100X magnification. Morphology was measured using micro-CT, and correlations of microdamage formation to architecture were studied.

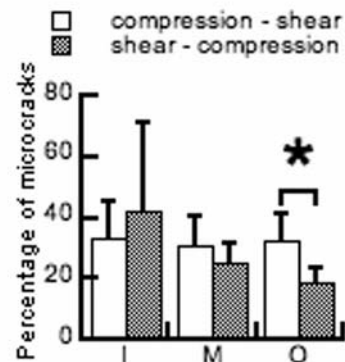


Figure 1: Percentage of existing microcracks that propagated during the second loading within the (I) inner, inter(M)ediate and (O)uter 1/3 of the specimen radius.

order, but the crack surface density was higher for specimens that were first loaded in torsion.

Microcracks in trabecular bone propagate when the loading mode changes. The propagating microcracks were, on average, longer than those due to a single load, which could have a detrimental effect on fracture toughness. Both initiation and propagation of microcracks increased with changes in architecture that are consistent with osteoporosis. As such, microdamage may play a greater role in fracture susceptibility of osteoporotic trabecular bone.

Disclosures: G.L. Niebur, None.

Fracture Risk Assessment in the Clinical Setting

P21

Agreement Between Bone Mass Measured by Computed Tomography in Lumbar Spine, Femoral Neck, Trochanter and Femoral Condyles in Patients with Proximal Femoral Fractures. A. Høiseth¹, G. Singh^{*2}, K. Stromsoe^{*3}. ¹Sentrum Rtg., Oslo, Norway, ²Aker University Hospital., Oslo, Norway, ³Aker University Hospital, Oslo, Norway.

Are there, in the elderly, confounding factors, such as bone and joint degenerations, making measurement of bone mass and geometry invaluable as fracture risk factors.

In 20 patients with proximal femoral fractures, aged 65-87, CT slices were obtained centrally in vertebrae L1 to L4, 5 contiguous slices in the trochanter, 9 in the condyles and 5 at right angle to the long axis of the femoral neck in the non-fractured femur. By defining cancellous bone as having CT values between 70 and 200 and cortical bone as CT values above 200, mean density and area of cancellous and cortical bone was measured, mass values were derived by multiplying density with area. In trochanter, neck and in the vertebrae separate mass values were derived for cortical and cancellous bone. Agreements were expressed as simple correlation coefficients.

There were strong agreements between all mass values in contiguous slices in the femur ($r > 0.9$). Inconsistent agreements between bone mass in the lumbar vertebrae ($r = 0.2 - 0.7$) and vertebral bone mass was hardly associated with femoral bone mass. The cancellous bone mass in the neck was poorly correlated with all other femoral mass parameters ($r \sim 0.4$), the bone mass in the femoral condyles had a fair association with trochanteric parameters ($r \sim 0.7$) poor with neck parameters ($r \sim 0.4 - 0.5$), while the cortical and total bone mass in the neck was highly associated with cancellous, cortical and total bone mass in the trochanter ($r \sim 0.8 - 0.9$). Bone mass variation in the femoral neck was mainly determined by the cortical bone mass variation. Weight was a strong determinant of femoral bone mass ($r \sim 0.6$), but with very inconsistent associations with vertebral mass. High age is an important risk factor for fractures independent of bone mass as measured by DXA. If the former is a dominant risk factor, little may be achieved by antiresorptive intervention. Particularly in the elderly, little attention has, however, been given to cortical and cancellous structure and mass. In the elderly, however, degenerations may interfere with fracture risk assessment. This preliminary study indicates very inconsistent measurements between vertebrae. In the femur, however, there were consistent associations between measures and with weight, indicating little effect from confounding factors; femoral parameters will be further assessed as fracture risk factors in the elderly population, vertebral parameters may not be useful.

Disclosures: **A. Hoeseth**, None.

P22

Discrimination of BMD-matched Recent Hip Fracture Subjects by FEXI (Finite Element Analysis of X-ray Images). **C. M. Langton**¹, **J. A. Thorpe**^{*2}, **S. Pisharody**^{*2}, **D. K. Langton**^{*2}, **S. A. Steel**², **S. Das**^{*2}. ¹University of Hull, Hull, United Kingdom, ²Hull & East Yorkshire Hospitals, Hull, United Kingdom.

The preferred method of assessing the risk of a fragility fracture is currently a measure of bone quantity, as bone mineral density (BMD) by dual energy X-ray absorptiometry (DXA). However, other bone quality factors contribute to the overall risk of fracture, including anatomical geometry and the spatial distribution of bone.

FEXI analysis of routine two-dimensional clinical radiographic images, such as DXA scans, involves the simulation of a mechanical compression test by 2D plane-stress finite element analysis, and provides a measure of whole bone stiffness ($N\ mm^{-1}$). A novel feature is that the grey level of each image pixel is converted into a corresponding value of Young's modulus in the finite element model.

We have investigated the ability of FEXI of the proximal femur to discriminate between 15 female subjects who had recently suffered a non-traumatic hip fracture (DXA scan performed within 1 week of subject being chair-mobile) and 15 age, sex, and total hip BMD-matched control subjects (no previous fracture, non-steroidal). Paired-sample T-test analysis was performed, the fracture cohort being significantly heavier, contrary to expectation, and exhibiting higher stiffness of the proximal femur.

This pilot study suggests that FEXI has the potential to provide a measure of bone quality that may predict fracture risk independent of BMD. Facilitated by semi-automated segmentation of the proximal femur from a hip DXA image and a batch processor that enables multiple scans to be analysed concurrently, FEXI may be readily implemented into clinical trials.

Paired-sample T-test Analysis

Parameter	Fracture	Control	p-value
Age (years)	79.1 \pm 5.0	78.5 \pm 2.0	0.691
Weight (Kg)	60.4 \pm 8.8	55.2 \pm 7.8	0.045
Total Hip BMD ($g\ cm^{-2}$)	0.700 \pm 0.119	0.701 \pm 0.118	0.801
FEXI ($N\ mm^{-1}$)	25.7 \pm 2.0	24.7 \pm 1.6	0.051

Disclosures: **C.M. Langton**, McCue plc 5.

P23

Vitamin K and Fracture Risk: An Effect on Bone Width Not BMD? **S. Kaptoge**¹, **N. Dalzell**^{*1}, **A. Welch**^{*1}, **M. J. Shearer**², **K. T. Khaw**^{*1}, **J. Reeve**¹. ¹University of Cambridge, Cambridge, United Kingdom, ²Vitamin K Research & Diagnostic Units, St Thomas Hospital, London, United Kingdom.

Most studies on nutrition and bone health have studied bone mineral density (BMD) as a surrogate endpoint for fractures, but bone geometry is also an important BMD independent determinant of fracture risk. For the same bone mass, wider bones have greater bending resistance as measured by the section modulus (Z). No studies have so far assessed effect of nutrition on bone geometry variables.

We analysed data from 670 women aged 67-79y (mean=72, SD=3) at recruitment into the longitudinal population based EPIC-Norfolk study to assess effects of dietary nutrients on subperiosteal diameter (PD) and Z. Up to 4 hip DXA scans were performed within 8 years of follow up: 2 scans (n=472; 2.9y), 3 scans (350; 5.5y) and 4 scans (79; 7.4y). Hip structural analysis software was used to derive structural parameters from the DXA scans at the narrow neck (NN), intertrochanter (IT) and shaft (S) regions. Nutrient intakes were estimated as the mean intake from up to three 7-day diet diaries completed at baseline (n=670), 1.5 years (383) and 3 years (296). A linear mixed model was used to assess effects of dietary nutrients on PD and Z adjusted for anthropometry and physical activity.

Both PD and Z increased with age: PD NN [0.020 cm/yr 95% CI (0.018, 0.023)]; IT [0.015 (0.012, 0.017)]; S [0.006 (0.004, 0.008)]; Z all regions [0.015 cm^3/yr (0.013, 0.018)]; and were positively associated with weight, height and lifetime physical activity (all $P < 0.059$). Higher intake of vitamin K was independently associated with having larger PD [$\beta = 0.033$ (0.011, 0.054) cm per 100ug/d difference $P = 0.003$], an effect that did not significantly differ by region ($P = 0.141$ for interaction). Higher potassium and carotene intakes significantly modified the effect of aging on Z, increasing the rates of Z increase by 0.003 cm^3/yr per 1 SD increase ($P < 0.029$). Alcohol intake was positively associated with Z ($P = 0.028$). There was no significant effect of vitamin K on BMD. In a subset of 277 women who had biochemical measurements, the vitamin K effect on PD was independent of effects of sex hormone binding globulin and creatinine which increased rates of PD expansion with aging ($P < 0.025$).

The results indicated significant effects of dietary nutrients on bone width and section modulus. Their statistical significance was in part attributable to improved precision in measurement of both outcome variables and dietary nutrient intakes from repeated measurements of these rather imprecise indices. The effect of vitamin K on bone width was consistent with evidence from previous studies associating higher vitamin K intake with lower risk of hip fracture.

Disclosures: **S. Kaptoge**, None.

P24

Cortical PQCT Measures Are Associated with Fractures in Hemodialysis Patients. **S. A. Jamal**¹, **C. Gordon**^{*2}, **D. C. Bauer**³.

¹University of Toronto, Toronto, ON, Canada, ²Hamilton Health Sciences Centre, Hamilton, ON, Canada, ³University of California, San Francisco, CA, USA.

Fractures are common in hemodialysis (HD) patients yet DXA measurements at the hip and spine are not associated with fractures in this group. One potential explanation is that HD patients have a selective decrease in volumetric cortical bone density, not identified by standard DXA testing. We used peripheral quantitative computed tomography (pQCT) of the distal radius to examine associations between volumetric cortical and trabecular densities and fracture in 36 men and 16 women, 50 years and older, who had been on HD for at least one year. We inquired about low trauma fractures since starting HD and confirmed all self reported fractures by review of radiology reports. Prevalent vertebral fractures were identified by morphometry. pQCT measurements were taken of the non-dominant radius using the

Stratec XCT 2000. At 4% of the ulna length we assessed volumetric trabecular density (mg/cm^3), and at 20% of the ulna length we assessed volumetric cortical density (mg/cm^3), total area (mm^2), cortical area (mm^2), and cortical thickness (mm). We used logistic regression analyses to examine the relationship between fracture (prevalent vertebral and /or self-reported non-spine) and each of the pQCT measures described above. Results are adjusted for age, weight and gender and reported as Odds Ratios (OR) per standard deviation decrease in the independent variable. The mean (\pm SD) age was 65.9 ± 8.9 years, the mean weight was 72.9 ± 15.2 kg and most (35 of 52 subjects) were Caucasian. The mean PTH was 33.8 pmol/L ($12.6 - 57.2$). Of the 52 subjects 27 subjects had either a prevalent vertebral fracture or low trauma fracture since starting dialysis. The mean trabecular density was 159.7 ± 60.6 cm^3 , cortical density 1119.7 ± 72.9 cm^3 , total area 320.1 ± 121.3 mm^2 , cortical area 66.4 ± 22.8 mm^2 and cortical thickness 1.8 ± 0.6 mm. There was no association between fractures and trabecular density (OR = 1.2; 95% Confidence Interval (CI): 0.43 to 1.7) or total area (OR = 1.1; 95% CI: 0.49 to 1.7). A decrease in cortical density was associated with an increased odds of fracture (OR = 15.7; 95% CI: 2.9 to 83.9), as was a decrease in cortical area (OR = 3.0; 95% CI: 1.3 to 7.2), and a decrease in cortical thickness (OR = 3.3; 95% CI: 1.4 to 7.8). Serum PTH was inversely correlated ($r = 0.6$) with cortical density but was not associated with fractures. Cortical, but not trabecular parameters are associated with fractures in HD patients. These findings may explain the lack of association between fracture and DXA measured at the hip and spine. Further studies are needed to determine the relationship between PTH and other determinants of cortical bone density and fracture in HD patients.

Disclosures: **S.A. Jamal**, None.

P25

Femur Strength Index and Hip Axis Length Predict Hip Fracture Independent of Bone Density. **K. G. Faulkner¹, W. K. Wacker^{*1}, C. Simonelli², P. K. Burke³, S. Ragi⁴, L. Del Rio⁵.** ¹GE Healthcare, Madison, WI, USA, ²HealthEast Clinics, Woodbury, MN, USA, ³Osteoporosis Diagnostic and Treatment Center, Richmond, VA, USA, ⁴Centro de Diagnóstico e Pesquisa da Osteoporose do Espírito Santo, Vitoria, Brazil, ⁵CETIR Centre Médic, Densitometria Ósea, Barcelona, Spain.

Hip fracture risk depends on femur BMD as well as subject age, height, weight, and bone structure. Structural parameters such as hip axis length (HAL), cross sectional moment of inertia (CSMI) and cross sectional area (CSA) can be measured with newer DXA systems. Femur Strength Index (FSI) combines BMD, structure (CSMI, CSA), age, height and weight to estimate the ability of a hip to withstand a fall on the greater trochanter. We compared neck BMD with FSI, HAL, CSMI and CSA for assessing hip fracture risk.

DXA scans were obtained in 2506 women, 365 with prior hip fracture and 2141 controls using Lunar Prodigy (GE Healthcare) at 4 centers. The non-fractured hip was measured in fracture subjects. All scans were acquired and analyzed at the centers; BMD, HAL, CSMI and CSA were determined by the Lunar Hip Strength Analysis program. FSI is the ratio of a subject's estimated femoral strength (based on age, BMD and bone structure) and the expected force of a fall on the greater trochanter (based on height and weight). Larger FSI values indicate greater femoral strength, corresponding to lower fracture risk. Neck BMD, structure and FSI values were compared between fracture and control groups using unpaired t-tests; logistic regression models were used to calculate odds ratios for hip fracture.

Age-adjusted BMD was significantly lower and HAL significantly longer in fracture subjects vs. controls. After adjustment for BMD and HAL, CSMI and CSA were not significantly different between groups. After adjustment for T-score and HAL, FSI was significantly lower in the fracture group, consistent with a reduced capacity to withstand a fall. Odds ratios were BMD 2.0, HAL 1.3, and FSI 1.5 per SD change in each measurement. ROC analysis showed a regression model combining FSI, HAL and T-score was significantly better at predicting

fracture than T-score alone (AUC=0.744 vs. 0.706, $p < 0.001$).

We conclude that Femur Strength Index and HAL are significant predictors of hip fracture, even after adjustment for BMD. Predictive power for fracture was significantly improved by combining T-score, Femur Strength Index, and Hip Axis Length.

	Age	Height	Weight	Neck BMD	HAL	CSMI	CSA	FSI
	t	t	t			I		
Fracture	71 yrs	156 cm	63.0 kg	0.722 cm^2 *	g/103 mm^2 *	8186	109 mm^2	1.34 *
Control	66 yrs	156 cm	64.0 kg	0.812 cm^2	g/101 mm	8302	120 mm^2	1.56

*Significantly different than controls ($p < 0.0001$)

Disclosures: **K.G. Faulkner**, None.

P26

Plasma Estradiol Predicts Bone Structure and Strength at the Macroscopic Level 5 years Later and Fracture Risk over 5 Years. **R. L. Prince¹, A. Devine¹, S. S. Dhaliwal², I. M. Dick¹.**

¹University of Western Australia, Perth, Australia, ²Curtin University, Perth, Australia.

We and others have previously demonstrated that estrogen status is a predictor of DXA BMD and future fracture. Peripheral Quantitative Computerized Tomography (pQCT) measures bone volume, mass and density and its distribution in the bone cross section, which allows discrimination of cortical and trabecular components and the calculation of the stress strain index (SSI), a measure of bone strength. The aim of this study was to assess the relationship of estrogen status to bone structure as measured by pQCT five years later and incident fracture risk over five years.

pQCT measurements of the distal tibia and radius at the 4% site were made using a Stratec XCT 2000 pQCT on 1150 women mean age (SD) 80 ± 2.6 at the conclusion of a five year double blind placebo controlled study of the effect of calcium supplementation on fracture outcome. Total estradiol, using a super sensitive assay, and serum SHBG were measured at baseline and the ratio of these, the free estradiol index (FEI), calculated. Radiologically verified fractures, excluding phalanges, nose and face, occurred in 195 subjects (17%). All analyses were undertaken in SPSS (version 11.2) using linear and logistic regression after adjustment for calcium therapy status, age and BMI.

FEI was positively associated with distal radius and tibia total, trabecular and cortical density and SSI in bending in the x and y direction and polar (torsional) SSI. For example at the distal radius the β coefficients were 0.22, $p < 0.001$; 0.18, $p < 0.001$; 0.16, $p < 0.001$; 0.16, $p < 0.001$; 0.19, $p < 0.001$ and 0.19, $p < 0.001$ respectively.

Logistic regression indicated that high FEI was associated with a reduced five year fracture incidence (RR per SD increase 0.68, 95% CI 0.52-0.87). When any distal radius or tibia density or SSI value was added to the analysis both FEI and the measure of structure or strength were both predictors of incident fracture. For example fracture risk was dependent on both FEI (0.75, 0.58-0.97) and radius total density (0.67, 0.55-0.82) or FEI (0.74, 0.58-0.95) and polar SSI (0.68, 0.56-0.84).

This study confirms estrogen status in elderly women as an important determinant of distal radial and tibial macroscopic structure and strength. It also demonstrates that the relationship between fracture risk and FEI is not completely accounted for by an effect of estrogen on bone structure or strength, raising the possibility that estrogen modifies non bone related factors such as falls risk or by effects on micro-architecture or the molecular structure of bone.

Disclosures: **R.L. Prince**, None.

P27

YOUNG INVESTIGATOR AWARD RECIPIENT

Collagen Age-profiling by Measurement of Isomerised and Non-isomerised C-telopeptides of Type II Collagen; A Potential Biochemical Index of Bone Quality. D. J. Leeming¹, D. Kasper¹, I. Byrjalsen¹, C. Christiansen². ¹Nordic Bioscience A/S, Herlev, Denmark, ²Centre for Clinical & Basic Research, Ballerup, Denmark.

CTX-I is a degradation product of collagen type I, which is generated during osteoclastic bone resorption. Newly synthesized bone matrix contains the α -form of CTX, but with aging the motif spontaneously isomerizes to the β -form. The α/β ratio has been reported to be high in trabecular bone and low in cortical bone, and it has been suggested to carry some potentials as an index of bone quality. The purpose of the study was to assess how two different anti-resorptive treatments, i.e. HRT and bisphosphonate, influence the α/β ratio in healthy postmenopausal women.

The native α -CTX, and the age-related isomerized β -CTX were measured in fasting, second void morning urine. Subjects were healthy postmenopausal women participating in randomized, placebo-controlled, double-blind clinical trials. Duration of anti-resorptive therapies was 24 months.

The α/β ratio showed significant ($p < 0.0001$) increases of 1.41% per menopausal year, and it was found that the index was independent of the rate of bone resorption as assessed by urinary β -CTX ($r = 0.03$; $p = 0.50$).

The anti-resorptive therapies had different effects on the index of the α/β ratio depending on the mechanisms of action and administration route. Thus, the time-averaged mean relative change from baseline at the end of the 2-year study period was -47% for bisphosphonates ($p < 0.0001$ vs placebo), -7% for HRT (NS vs placebo), and +1% for placebo.

The fact that the ratio is independent of the rate of bone resorption suggests that the α/β -ratio could provide qualitative information on skeletal status. The different changes in the α/β -ratio evoked by the various anti-resorptive therapies likely reflect relative treatment effects on the trabecular and cortical compartments with potential implications for vertebral and non-vertebral fracture prediction.

Disclosures: **D.J. Leeming**, Nordic Bioscience Diagnostics 3.

P28

Bone Quality in Premenopausal Women with Idiopathic Osteoporosis. J. Fleischer¹, M. Donovan¹, H. Zhou², D. McMahon¹, D. Dempster^{1,2}, R. Müller³, E. Shane¹. ¹Columbia University, New York, NY, USA, ²Helen Hayes Hospital, West Haverstraw, NY, USA, ³ETH and University Zürich, Zürich, Switzerland.

Most young women with osteoporosis (OP) have an identifiable cause. Others have an idiopathic form for which no cause can be found. To characterize bone cell activity and bone quality in IOP, 9 otherwise healthy premenopausal women, who presented with OP and fragility fractures, underwent tetracycline-labeled transiliac bone biopsy. Secondary causes of OP were excluded. Compared to age and sex matched controls ($n = 18$), significant differences in cancellous bone turnover were identified. Although osteoid thickness and surface did not differ, parameters that reflect bone formation were significantly lower in IOP patients, wall width by 12% ($p < .01$), mineral apposition rate by 18% ($p < .01$), mineralizing surface by 42% ($p \leq .02$), bone formation rate by 52% ($p < .01$) and activation frequency by 54% ($p = .07$). Conversely, bone resorption variables were increased, including a markedly longer resorption period ($p = .02$) and increased eroded surface ($p = .05$). Despite abnormalities in bone turnover, structural parameters assessed by 2-dimensional (2D) histomorphometry, such as cancellous bone volume (BV/TV) and trabecular width (Tb.Wi), did not differ, although there was a trend toward lower trabecular number (Tb.N; $1.7 \pm .07$ vs $1.9 \pm .05$; \pm SEM; $p = .12$) and increased trabecular separation (Tb.Sp; 429 ± 20 vs 388 ± 17 μ m; $p = .16$) in women with IOP. To further investigate microarchitecture, biopsies were analyzed by micro-CT. Consistent

with the 2D results, BV/TV and bone surface/bone volume (BS/BV) did not differ significantly between groups ($p = .61$ and $p = .47$, respectively), but bone surface/total volume (BS/TV; $3.74 \pm .19$ vs $4.34 \pm .13$; $p = .02$) was significantly lower in IOP subjects. Trabecular thickness (Tb.Th; 226 ± 19 vs 194 ± 10 μ m; $p = .16$) tended to be higher and Tb.N tended to be lower ($1.6 \pm .07$ vs $2.3 \pm .49$; $p = .18$) in IOP subjects. Tb.Sp was significantly higher (551 ± 27 vs 464 ± 30 μ m; $p = .04$). Moreover, there was significantly greater ($p < .05$) intra-individual variability in Tb.Th and Tb.Sp in IOP subjects than controls. In summary, women with IOP have evidence of increased bone resorption and decreased bone formation compared to controls. Microarchitectural changes were less pronounced, although with more sensitive micro-CT analysis, significant increases in Tb.Sp, decreases in BS/TV, and evidence of structural heterogeneity were detected. The micro-CT data suggest abnormal bone remodeling in premenopausal women with IOP is associated with loss of whole trabecular elements, rather than thinning of individual trabeculae, changes that may ultimately lead to abnormal bone quality and increased fragility.

Disclosures: **J. Fleischer**, None.

P29

Does Hip Geometry Explain the Adverse Effect of Aging on Hip Fracture Risk? S. Kaptoge¹, N. Dalzell^{1*}, K. T. Khaw^{1*}, T. J. Beck², N. Loveridge¹, J. Reeve¹. ¹University of Cambridge, Cambridge, United Kingdom, ²Johns Hopkins University, Baltimore, MD, USA.

Bones made wider by subperiosteal bone formation and endosteal remodelling may become stiffer, but their structural stability can be compromised if the bone's cortices become too thin. We previously found that subperiosteal and endosteal bone expansion was faster in women than men aged >65 years and was accompanied by medial shifting of the centre of mass in three hip structure regions. We have now evaluated whether part of the effect of aging on hip fracture risk, was attributable to increasing hip asymmetry.

Hip structural analysis (HSA) applied to DXA scans was used to derive structural measurements at the narrow neck (NN) intertrochanter (IT) and shaft (S) regions for 778 women in the EPIC-Norfolk population-based prospective cohort study. The distance of a cross section's centre of mass from the supero-lateral cortical margin (lateral distance, in cm) was measured with good precision (NN, coefficient of variation 2.6%). During 8 years of follow up, 21 women suffered incident hip fracture and 4 of these took bisphosphonates. Cox regression was used to assess the predictive effect of age and independent contributions of lateral distance and other structural variables. The coefficient for age was compared in different models.

Aging increased risk of hip fracture RR = 1.26 95% CI (1.08, 1.47) per 1 year. Including lateral distance as an additional predictor reduced this effect to 1.23 (1.06, 1.44) at NN region, 1.25 (1.07, 1.45) at IT region and 1.24 (1.06, 1.45) at S region. These were reductions of between 4-8% in log hazard ratio for age. Inclusion of other hip structural variables reduced the effect of aging similarly. Geometric variables that had significant effects on hip fracture risk independent of age and medication use in all 3 HSA regions were: cross-sectional area (CSA), average cortical thickness (avgcort), average cortical buckling ratio (avgcortbr) and BMD (calculated as CSA/width). The relative risk (RR) estimates per 1 SD decrease (increase for avgcortbr) ranged from 1.76-3.04 depending on variable and region (all $P < 0.020$). Geometric variables that had region specific age and medication independent effects were: subperiosteal diameter (IT), endosteal diameter (IT & S), section modulus (IT), and lateral distance (IT) with RR estimates in the range of 1.70-2.11 per 1SD adverse change (all $P < 0.030$). When adjusted for CSA, lateral distance [NN 1.57 (1.03, 2.39) & IT 1.75 (1.20, 2.54)] and width [IT 1.95 (1.32, 2.88) & S 1.48 (1.01, 2.18)] were significantly associated with hip fracture risk. This provides insight into why BMD successfully predicts hip fracture; but the independent effect of age to predict fractures was largely unexplained.

Disclosures: **S. Kaptoge**, None.

Effects of Treatment on Bone Quality: Clinical Studies

P30

Site-Specific Variations in Therapeutic Effects of Salmon Calcitonin-Nasal Spray (CT-NS) on Bone Quality (BQUAL): Trabecular Microarchitecture (TMA), and Bone Quantity (BQUANT): BMD; Results from the Quest Study. C. H. Chesnut III, MD, FACP¹, S. Majumdar², D. Newitt², A. Shields¹, M. Olson^{*3}, M. Azria³, L. Mindeholm³. ¹University of Washington, Seattle, WA, USA, ²U Cal San Francisco, San Francisco, CA, USA, ³Novartis Pharma, Basle, Switzerland.

Reduction in osteoporotic (OP) fracture risk in response to certain anti-resorptive therapies may be due less to effects on BQUANT-BMD than on BQUAL-TMA. To explore this hypothesis the 2 yr QUEST study in 91 postmenopausal (PM) OP women assessed the effects of CT-NS+calcium (Ca) vs. placebo (P)+Ca on BMD(DXA) and TMA (high resolution MRI) at multiple skeletal sites.

Although no significant change through 2 yrs was noted in BMD(spine/hip/distal radius) in CT-NS or P groups, regardless of the change in BMD a consistent and significant improvement or preservation in TMA through 2 yrs was noted in the CT-NS group at distal radius and hip (T2*), with consistent and significant deterioration noted in these parameters in the P group (example, at distal radius +2.0% app BV/TV, +1.7% app trab #, -2.3% app trab spacing in CT-NS, compared to -9.1%, -6.9%, +12.9% in P; changes significant within and between groups, $p < 0.001-0.05$).

As well, in the Ca only P group significant deterioration was noted in parameters of TMA at distal radius and hip, even in women gaining or showing no change in BMD at spine, hip, or distal radius (example: in women in the P group gaining or showing no change in BMD at the total hip, a significant ($p < 0.005$) deleterious +10.0% increase for the MRI-T2* measurement at the lower trochanteric site).

These results suggest 1) a beneficial effect of the anti-resorptive therapy CT-NS on TMA regardless of its effect on BMD, 2) a potential loss in TMA in PM-OP women receiving only calcium even when BMD is stable or increasing, and 3) a possible independent effect of anti-resorptive therapies on BQUANT-BMD and BQUAL-TMA.

Supported by a grant from Novartis Pharma

Disclosures: **C.H. Chesnut III, MD, FACP**, Novartis Pharma 2, 5.

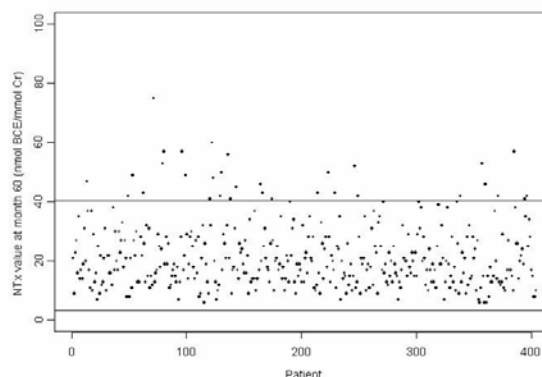
P31

Bone Turnover with Long-term Alendronate Use: Evidence From the FIT Long-term Extension (FLEX) Study. D. C. Bauer¹, M. C. Hochberg², A. Schwartz¹, A. Chattopadhyay^{*3}, A. Lombardi³, A. C. Santora³. ¹UCSF, San Francisco, CA, USA, ²University of Maryland, Baltimore, MD, USA, ³Merck Research Laboratories, Rahway, NJ, USA.

Prompt and substantial reductions in bone turnover follow initiation of treatment with alendronate in postmenopausal women with osteoporosis. We evaluated the effects of long-term use of alendronate on biochemical markers of bone turnover. Women who had received alendronate (5 mg/day for 2 years then 10 mg/day) during the Fracture Intervention Trial (FIT) were eligible for screening and re-randomization into the FLEX Trial (n=1099), where they received alendronate 5 mg/day, 10 mg/day, or placebo for an additional 5 years for a total of up to 10 years of alendronate use. Urinary cross-linked N-telopeptide of type I collagen (NTx)(Osteomark, Ostex International) and serum bone specific alkaline phosphatase (bone ALP)(Ostase, Hybritech) were measured during FLEX at 12 and 60 months. Among the 402 women who continued to take alendronate (>70% compliance), the median NTx value at the end of FLEX (60 month) was 19.0 nmol BCE/mmol, and 92% fell within the premenopausal range (between 3.4 and 40.2 nmol BCE/mmol Cr, based upon the

premenopausal mean \pm 2SD in the OFELY study). No subject had 60-month NTx levels that were below the lower normal limit of the premenopausal range (Figure). Results were similar with bone ALP. These data confirm the stable, long-term maintenance of NTx and bone ALP at premenopausal levels during up to 10 years of treatment with alendronate.

FLEX: NTx values at month 60 for ALN treated patients



Disclosures: **D.C. Bauer**, Merck 2.

P32

Ratio of Low to High Mineralized Bone and Bone Remodelling: Comparison between Osteoporotic Women Treated with Risedronate and Healthy Pre-menopausal Women. B. Borah¹, E. L. Ritman^{*2}, T. E. Dufresne^{*1}, S. M. Jorgensen^{*2}, S. Liu^{*1}, R. J. Phipps¹, R. T. Turner³. ¹Procter & Gamble Pharmaceuticals, Mason, OH, USA, ²Mayo Clinic College of Medicine, Rochester, MN, USA, ³Department of Exercise and Medicine, Oregon State University, Corvallis, OR, USA.

Changes in mineralization can influence bone strength. The purpose of the study was to compare bone mineralization in iliac crest biopsies from post-menopausal women with osteoporosis, treated with risedronate or placebo. Of particular interest was to estimate the distribution and relative proportions of low and high mineralized bone which influence bone quality, and compare to healthy normal pre-menopausal women. Micro-CT with x-ray radiation from a Synchrotron source was used to generate high-resolution (4 microns) 3-D images with sufficient gray level contrast to delineate low and high mineralized bone fractions. We determined the average degree of mineralization, and the ratio of low to high mineralized bone by volume (BMR-V, bone mineralization ratio-volume) and by surface area (BMR-S, bone mineralization ratio-surface) in paired biopsies taken at baseline and after three years treatment with risedronate (n=11) or placebo (n=8). We further analyzed biopsies (n=7) taken from the same patients who were on treatment for two additional years and compare with healthy normal pre-menopausal women (n=7). Risedronate significantly increased the average mineralization, reduced BMR-V (-70.1%) and BMR-S (-54.1%) respectively from baseline at year 3 and were consistent with a significant reduction from baseline of histomorphometric turnover indices assessed by mineralizing surface, MS/BS (-72.8%) and activation frequency, Ac.f. (-60.4%). Comparing pair-wise changes from baseline, risedronate significantly reduced the low mineralized bone fraction in comparison to placebo. For all patients in the risedronate group, BMR-V and BMR-S showed significant correlation to MS/BS (R^2 : 0.83 and 0.92 respectively). After 5 years of treatment, risedronate maintained BMR-V, BMR-S and the average degree of mineralization at the 3 year level which is consistent with sustained reductions of biochemical markers of bone between year 3 and 5. Importantly, risedronate increased the average mineralization and reduced BMR-V and BMR-S to levels determined in healthy normal pre-menopausal women, suggesting that long-term risedronate treatment reduced turnover in osteoporotic women to a healthy level and may provide an appropriate balance of low and high mineralized bone to optimize fracture reduction.

Disclosures: **B. Borah**, Procter & Gamble Pharmaceuticals 3.

P33

Bone Histomorphometric Findings After 10 Years Alendronate Treatment of Postmenopausal Women. R. Recker¹, K. Ensrud², S. Diem^{*2}, E. Cheng^{*2}, S. Bare^{*1}, P. Masarachia^{*3}, P. Roschger⁴, P. Fratzl^{*5}, K. Klaushofer⁴, A. Lombardi⁶, D. Kimmel³. ¹Creighton University, Omaha, NE, USA, ²University of Minnesota, Minneapolis, MN, USA, ³Merck & Co, Inc, West Point, PA, USA, ⁴Ludwig Boltzmann Institute, Vienna, Austria, ⁵Max Planck Institute, Potsdam, Germany, ⁶Merck Research Laboratories, Rahway, NJ, USA.

FLEX (FIT Long-term EXtension) was a 5-year randomized, placebo (PBO)-controlled trial, designed to assess the efficacy and safety of long-term treatment with alendronate (ALN). 1099 postmenopausal women who had received 3-6 years treatment with ALN (5 mg/d during the first two years and 10 mg/d thereafter) in the Fracture Intervention Trial (FIT), were randomized to placebo (ALN/PBO) (N=437), ALN* 5 mg/d (N=329) or 10 mg/d (ALN/ALN) (N=333). Transilial bone biopsies were obtained from 31 women following dual fluorochrome labeling. Trabecular bone turnover, quantity, microarchitecture and mineralization were assessed. Twenty-nine specimens were suitable for quantitative back-scatter electron microscopy (qBEI; MCC and CAW), eighteen for histomorphometry (2D) and fourteen for micro-computed tomography (3D). Since there were no differences between the 5mg/d and 10mg/d ALN groups, the two groups were pooled. Results are shown in the table.

Abbrv	Mean (S.D.)	ALN/PBO (N=14)	ALN/ALN (N=15)
MCC	Mean Calcium Concentration (%)	22.1 (0.58)	22.4 (0.54)
CAW	Calcium Width	3.57 (0.38)	3.48 (0.45)
	2D Endpoints	(N=9)	(N=9)
BV/TV	Bone Volume (%)	18.3 (5.2)	19.5 (6.2)
OV/BV	Osteoid Volume (%)	1.1 (0.4)	0.9 (0.7)
Tb.N	Trabecular Number (#/mm)	1.3 (0.2)	1.3 (0.2)
Tb.Th	Trabecular Thickness (µm)	142 (27)	148 (35)
OS/BS	Osteoid Surface (%)	11.6 (4.7)	9.9 (6.3)
O.Th	Osteoid Thickness (µm)	4.8 (0.4)	5.1 (0.7)
MAR	Mineral Apposition Rate (µm/d)	0.6 (0.1)	0.5 (0.1)
MS/BS	Mineralizing Surface (%)	3.0 (3.4)	1.4 (1.6)
	3D Endpoints	(N=6)	(N=8)
BVF	Bone Volume Fraction (%)	16.5 (4.9)	16.6 (6.0)
BSD	Bone Surface Density mm ² /mm ³	1.0 (0.4)	1.2 (0.5)
Tb.N	Trabecular Number (#/mm)	1.3 (0.2)	1.4 (0.3)
Tb.Th	Trabecular Thickness (µm)	130 (20)	121 (26)

In this study, all patients were initially treated with ALN for ~5 years, followed by an additional five years of PBO or ALN. All patients in both ALN/PBO and ALN/ALN groups displayed double fluorochrome label in trabecular bone. The cortical and trabecular bone tissue of both groups appeared normal, lacking qualitative abnormalities such as woven bone, osteitis fibrosa, defective mineralization, and non-lamellar bone. There were no differences between the groups for any quantitative endpoint. These data, from a limited sampling, suggest that iliac trabecular bone tissue remains normal following use of ALN 5 or 10 mg/d for 5-10 years.

*Manufactured by Merck & Co., Inc, 5 Station, NJ

Disclosures: **R. Recker**, Merck & Co, Inc 2, C.

P34

Application of a Three Dimensional Skeleton Graph Analysis to Patients Treated by Alendronate or Placebo on Micro-computed Tomography Images. C. L. Benhamou¹, A. Basillais^{*1}, G. Aufort^{*2}, G. Chappard^{*1}, R. Jennane^{*2}, P. Masarachia^{*3}, D. Kimmel³. ¹Inserm U 658 Hopital Porte Madeleine, Orleans, France, ²Lesi, Polytech Orleans, Orleans, France, ³Merck Research Laboratories, West Point, PA, USA.

It has been shown that after 2 or 3 years of alendronate* treatment, trabecular microarchitecture was better than after placebo on morphological parameters¹, for instance on TbTh, TbN and BV/TV. 3D Skeleton Graph Analysis offers an access to topological parameters, and has been previously applied to trabecular bone. The objective was to assess another kind of parameter in this series of specimens: nodes count of the trabecular network and connectivity, derived from the Euler number.

Bone biopsies were obtained from 88 osteoporotic women, including 60 placebo and 28 after alendronate. The bone biopsies were scanned by micro-computed tomography (GEMS-EVS) with a 20 µm voxel size. The image threshold was chosen to separate bone from background after analysis of the grey level histograms of the whole sections in a standardized way. Then the binarized volumes were analyzed to assess both morphological and topological parameters. T tests were used for the comparison between alendronate and placebo groups.

The 3D analysis of trabecular bone showed that all the morphological parameters were significantly greater in alendronate group. The nodes count was significantly higher in the alendronate than in the placebo group. The connectivity and the degree of anisotropy (DA) were not statistically different between groups.

Parameter	Placebo Mean ± SD	Alendronate Mean ± SD	p-value
Age (years)	66.1 ± 7.6	66.2 ± 6.7	NS
BV/TV (%)	15.4 ± 6.8	18.9 ± 6.2	0.01
TbTh (µm)	194 ± 50	212 ± 42	0.05
TbN (mm ⁻¹)	0.78 ± 0.23	0.89 ± 0.21	0.02
TbSp (µm)	741 ± 110	676 ± 102	0.005
DA	2.11 ± 0.61	2.04 ± 0.54	0.30
Nodes count (mm ⁻³)	5.37 ± 2.67	6.55 ± 2.38	0.01
Connectivity (mm ⁻³)	-3.74 ± 1.53	-4.17 ± 2.36	0.31

This study has shown that after 3 years of alendronate, the microarchitecture was better than after placebo not only on morphological parameters, but also on the nodes count, while anisotropy was not changed.

*Manufactured by Merck & Co., Inc., Whitehouse Station, NJ, USA

1. Recker R et al, Trabecular bone microarchitecture after alendronate treatment of osteoporotic women. Curr Med Res Opin 2005;21:185-194.

Disclosures: **C.L. Benhamou**, Merck & Co, Inc 2.

P35

The Role of BMD and Bone Turnover in Skeletal Assessment. P. Miller¹, R. Wasnich^{*2}, S. Bonnick³. ¹Colorado Center for Bone Research, Lakewood, CO, USA, ²Radiant Research - Honolulu, Honolulu, HI, USA, ³Clinical Research Center of North Texas, Denton, TX, USA.

The recent Surgeon General's report¹ states that measures of bone mineral density (BMD) and biochemical markers of bone turnover are adequate and appropriate surrogates for fracture efficacy in clinical trials of osteoporosis drugs. The usefulness of these measures has been disputed. For example, some reports have claimed that BMD changes "explain" only a large proportion (as high as 80%) of fracture risk reductions observed during anti-resorptive therapy, while others have reported very low proportions. This "proportion of variance" analysis

has limited clinical utility, and can be misleading: as shown in the table, even when a combination of measurement sites is used, depending on the follow-up interval and how BMD is analyzed, the same set of data can yield widely varying proportions².

Percent of Vertebral Fracture Risk Reduction "Explained" by BMD (95% CI) Using BMD Measured at Multiple Sites

Duration of Follow-up	With or Without Baseline of each BMD site	Vertebral Fracture Arm		Clinical Fracture Arm	
		BMD Actual Value	BMD % Change From Baseline	BMD Actual Value	BMD % Change From Baseline
One Year	W	46.3% (23.0%, 89.1%)	45.2% (22.5%, 87.1%)	14.6% (-, 23.1%, 68.4%)	16.3% (-21.0%, 71.5%)
	W/O	19.2% (9.3%, 37.1%)	36.4% (16.8%, 71.3%)	19.8% (8.9%, 54.6%)	8.7% (-28.1%, 55.0%)
End of Study (3-4 years)	W	80.1% (45.9%, 145.5%)	82.5% (48.6%, 147.4%)	64.1% (23.6%, 171.4%)	61.2% (20.3%, 167.7%)
	W/O	35.0% (20.9%, 62.8%)	78.8% (47.1%, 140.3%)	44.3% (23.7%, 115.7%)	66.6% (25.7%, 178.9%)

BMD has been shown to have a strong, continuous association with fracture risk. A similar association has been shown for biochemical markers of bone turnover in relation to both vertebral and non-vertebral fractures³, such that greater reductions in turnover are associated with greater reductions in the risk of fracture.

Although neither BMD nor turnover "explains" all of bone strength or fracture risk, non-invasive routine measurement of other properties of bone is not possible at present, and large, well-designed trials have validated the importance of these measures. BMD and turnover remain cornerstones of diagnosis and management of osteoporosis.

1. U.S. Department of Health and Human Services. Bone Health and Osteoporosis: A Report of the Surgeon General. Rockville, MD: U. S. Department of Health and Human Services, Office of the Surgeon General; 2004.

2. Shih J, et al. Proportion of fracture risk reduction explained by BMD changes using Freedman analysis depends on choice of predictors (abstract). Osteoporos Int 2002;13:S38-S39.2. Bauer DC, et al. Change in bone turnover and hip, non-spine and vertebral fracture in alendronate-treated women: the Fracture Intervention Trial. J Bone Miner Res 2004;19:1250-58.

Disclosures: **P. Miller**, Merck & Co, Inc 2, 5, 8.

P36

Bisphosphonate (BP)-Induced Osteosclerosis with Pathologic Fractures in a Breast Cancer Patient. **M. Castro**^{*1}, **D. Novack**², **M. P. Whyte**².

¹Glens Falls Hospital, Glens Falls, NY, USA,

²Washington University School of Medicine, St. Louis, MO, USA.

During the last 8 yrs, the bisphosphonates (BP) pamidronate (PAM) and zoledronate (ZOL) have gained widespread use to diminish the risk of skeletal events due to metastatic cancer. Because such patients usually die from their metastatic disease within a year or two, long term follow up of extended BP use has not been reported. We describe a 62-year-old woman with breast cancer who received intravenous BP therapy monthly for 7 yrs prior to recognition of an acquired osteopathy featuring marked osteosclerosis and recurrent fractures. She presented in '93 with a Stage II, premenopausal, ER (+), HER2 (+), poorly differentiated, invasive, ductal breast cancer. Despite adjuvant chemotherapy and tamoxifen, she suffered an osteoblastic

skeletal relapse in '95. During the next 4 yrs, she received aromatase inhibitors and a variety of cytotoxic drugs prior to developing progressive disease in the bone and liver in '97. Then, commercial availability of trastuzumab led to a prompt and durable clinical remission. Because of persistent osteoblastic changes on x-rays, monthly PAM was also instituted in '97 (90 mg/m² x 39 doses) and changed to ZOL in '01 (4 mg/m² x 43 doses). Subsequently, she suffered a non-displaced "chalk stick" fracture of the left femur in winter '03, a displaced fracture of a metatarsal in summer '04, and a displaced right femur fracture in '04. Recent metastatic survey and FDG-PET scan had disclosed no areas of hypermetabolism; MRI of the liver revealed no recurrent metastases; bone

x-rays showed persistent osteoblastic changes ascribed to her prior active metastases; and serum tumor proteins CA27.29 and CEA remained normal (formerly elevated during active metastatic disease). Metabolism consultation noted serial increase in bone mineral density (BMD). In '99, '01, and '04, BMD T-scores in her spine were +6.6, +8.0, and +12.0 and hip 'not done', +6.3, and +8.4, respectively. Her 24 hr urine calcium and serum CK-BB and alkaline phosphatase levels were normal. Despite high bone mass, hydroxyproline and deoxypyridinole levels in urine were low-normal and suppressed, respectively. During surgery for the fractured right femur, a drill bit bent, necessitating screw placement in a different location. Histologic examination of bone fragments disclosed no cancer, but was insufficient to assess bone morphology. Conclusion: Osteoclast toxicity causing marked osteosclerosis and fractures has not been reported among cancer patients receiving BP's. While the risk-benefit ratio of high dose BPs for short durations seems favorable, protracted BP therapy may cause an osteopathy that heightens fracture risk due to bone brittleness.

Disclosures: **M.P. Whyte**, None.

Effects of Treatment of Bone Quality: Pre-Clinical Studies

P37

Increased Bone Mass Is Highly Correlated With Increased Bone Strength in Cynomolgus Monkeys Treated With AMG 162, a Fully Human RANKL Antibody. **J. E. Atkinson**¹, **P. Cranmer**^{*1}, **T. Saunders**^{*1}, **M. Niehaus**^{*2}, **S. Y. Smith**³, **A. Varela**^{*3}, **M. S. Ominsky**¹, **M. E. Cosenza**^{*1}, **P. J. Kostenuik**¹. ¹Amgen Inc., Thousand Oaks, CA, USA, ²Covance Laboratories GmbH, Munster, Germany, ³CTBR, Montreal, PQ, Canada.

AMG 162 is a fully human monoclonal antibody that binds with high affinity and specificity to RANK Ligand (RANKL) and thereby inhibits osteoclast formation, activation, and survival. In rodents, RANKL inhibitors consistently improve bone mass and strength. AMG 162 rapidly increases BMD in humans, but the effects of RANKL inhibition on bone strength have not been previously described in a remodeling species. We therefore examined bone mass and bone strength in male cynomolgus monkeys (4-5 years old) that were treated with AMG 162 (50 mg/kg/month, SC) or placebo (n = 8/group). Animals were sacrificed at month 6 (3/group) or month 12 (3/group) of treatment. Recovery animals (2/group) were sacrificed 3 months after the end of treatment (month 15). Right femurs and lumbar vertebrae (L3 & L4) were analyzed by pQCT and by DXA for bone mineral content (BMC) and geometric parameters. Biomechanical parameters were determined by destructive mechanical testing in three-point bending (femur) or compression (L3 & L4). One year of AMG 162 treatment resulted in significantly greater pQCT-derived cortical area (26%) and cortical BMC (30%) at the femoral midshaft (p<0.01 vs placebo). Greater bone mass in AMG 162-treated animals was accompanied by a 40% increase in femur bending load (p<0.01 vs placebo). To compare the relationship

between bone mass and strength, data for different timepoints were merged. Regression analysis of maximum load vs pQCT-derived cortical BMC demonstrated strong, positive linear relationships for both groups: AMG 162, $r^2 = 0.85$; placebo, $r^2 = 0.95$ ($p < 0.002$). Similar relationships between maximum load and pQCT-derived cortical area were observed: AMG 162, $r^2 = 0.85$; placebo, $r^2 = 0.97$ ($p < 0.002$).

At the lumbar spine, AMG 162-treated monkeys had significantly greater BMC by DXA (45%), and greater maximum compressive load (101%), apparent strength (97%), and toughness (78%) ($p < 0.05$ vs placebo at 12 months). As in the femur, strong, positive linear relationships were observed between maximum load and BMC: AMG 162, $r^2 = 0.53$; placebo, $r^2 = 0.52$ ($p < 0.002$).

These results demonstrate that AMG 162 increases trabecular and cortical BMC and also improves cortical bone geometry in cynomolgus monkeys. These changes are strongly correlated with increases in bone strength. This relationship suggests that RANKL inhibition results in improvements in bone quantity and quality in primates. AMG 162 may therefore provide a safe and effective treatment for reducing fractures.

Disclosures: J.E. Atkinson, Amgen Inc. 1, 3.

P38

Continuous Suppression of RANKL Increases Bone Mineral Density and Bone Strength in Transgenic Rats That Overexpress a Secreted Osteoprotegerin Transgene. T. J. Corbin^{*1}, P. Kostenuik¹, M. S. Ominsky¹, X. Li¹, S. Morony¹, K. Warmington¹, Z. Geng¹, M. Grisanti¹, H. Tan¹, V. Shen^{*2}, B. Bolon^{*1}, J. McCabe^{*1}. ¹Amgen, Thousand Oaks, CA, USA, ²Skeletech Inc., Bothell, WA, USA.

RANK ligand (RANKL) and its receptor RANK are critical for the formation, activation, and survival of osteoclasts. RANKL is implicated in bone loss conditions such as postmenopausal osteoporosis, bone metastasis, and rheumatoid arthritis. Osteoprotegerin (OPG), an endogenous protein that binds and neutralizes RANKL, was originally identified based on increased bone mass in mice that over-expressed a soluble OPG transgene (OPG-Tg). While OPG-Tg mice have been valuable for examining the effects of continuous RANKL inhibition on bone, rats are the preferred species for many animal models of bone disease (including ovariectomy, adjuvant-induced arthritis, and fracture repair). We therefore generated OPG-Tg rats that over-express a soluble rat OPG transgene driven by a liver-specific (ApoE) promoter. A high bone mass phenotype was confirmed in these rats by analyzing serum and BMD (by DXA) in female OPG-Tg rats ($n=10$) and age-matched wild-type (WT) controls ($n=6$) at 16, 20, 24 and 28 weeks of age. Serum TRAP-5b, an osteoclast-specific marker of bone resorption, was 80-90% lower in OPG-Tg rats at all ages compared to age-matched WT controls ($p < 0.01$). OPG-Tg rats had significantly ($p < 0.01$) greater BMD in the lumbar vertebrae (LV) at all ages (22-30% greater than WT). Histomorphometry revealed a 32% increase in bone volume in the LV of 28-week-old OPG-Tg rats compared to age-matched WT rats ($p < 0.01$). Osteoclast number (% trabecular perimeter) was reduced by 98% in the LV of OPG-Tg rats ($p < 0.01$ vs. WT), while osteoblast number (% trabecular perimeter) was reduced by a non-significant 47% in OPG-Tg vs. WT rats ($p=0.11$). The continuous life-long suppression of bone resorption in these rats might be expected to have deleterious effects on bone quality. We assessed bone quality by performing destructive mechanical testing of the 5th LV (L5) of 28-week-old OPG-Tg and WT rats. Compression testing of L5 revealed a 2-fold increase in max load and a 2.6-fold increase in stiffness in OPG-Tg rats compared to WT controls ($p < 0.01$). These data show that over-expression of soluble OPG in rats results in a high bone mass phenotype that is associated with profound and continuous suppression of bone resorption. Increased BMD in OPG-Tg rats is associated with substantial improvements in bone strength, which suggests that the persistent suppression of RANKL results in improved bone quality. These data suggest that RANKL inhibition may be a safe and effective approach for improving bone strength.

Disclosures: T.J. Corbin, None.

P39

Biomechanical and Structural Differences in the Skeletal Efficacy of PTH or Alendronate in Two Year Old Rats. Y. Ma, A. Schmidt^{*}, R. Cain^{*}, Q. Zeng^{*}, J. Oskins^{*}, S. Iturria^{*}, H. Bryant, M. Sato. Lilly Research Labs, Indianapolis, IN, USA.

Ovariectomized (Ovx) or intact rats at about 19 months of age were treated with hPTH (1-38) (10 (Ovx only), 30 $\mu\text{g/kg/d}$ sc) or alendronate (ABP 28 $\mu\text{g/kg}$ twice weekly s.c) for 4 months. Ovx rats were severely osteopenic, having been ovariectomized at 6 months of age and allowed to lose bone for 13 months before initiating treatment. Therefore, skeletal efficacy of PTH or ABP were evaluated in femora and vertebrae of severely osteopenic and senile intact rats, during the last 4 months of life. In Ovx rats, PTH dose dependently increased midshaft strength (20% and 34%), femoral neck strength (25% and 23%) and vertebral strength (135%, 182%) over Ovx vehicle controls. Strength parameters were restored by PTH to the level of age-matched Sham controls. In intact animals, PTH 30 $\mu\text{g/kg}$ increased midshaft strength by 15%, femoral neck strength by 14%, and vertebral strength by 60% over intact controls. For both intact and Ovx rats, PTH strength benefits resulted from significant increases in midshaft BMD (11 to 21%), midshaft BMC (10 to 22%), vertebral BMD (23 to 42%), vertebral BMC (22 to 42%), trabecular area (199% to 394%), trabecular thickness (39% to 134%), BFR/BS (57% to 314%), cortical area (7% to 16%), cortical thickness (11% to 21%), and periosteal bone formation rate (330% to 370%). In Ovx rats, ABP had no effect on midshaft strength or femoral neck strength, but increased vertebral strength by 48% relative to Ovx controls. ABP vertebral effects may be partially explained by a 16% increase in vertebral BMD, and 16% increase in vertebral BMC relative to Ovx controls. In intact rats, ABP had no significant effect on midshaft strength, femoral neck strength, or vertebral strength. However, ABP did increase vertebral BMD by 7%, but had no effect on vertebral BMC or femoral midshaft BMD in intact animals. ABP increased trabecular area (55%) in intact but not Ovx rats, while ABP had no effects on cortical area or cortical thickness. In both Ovx and intact animals, ABP markedly reduced bone formation activity, BFR/BS by -75% and -79%, respectively. Regression analyses showed that PTH and ABP have generally positive, but not identical, relationships between bone strength and bone mass or structure. The data taken together showed that PTH was superior to ABP in increasing bone mass, improving the spatial architecture, and enhancing strength of axial and appendicular sites in severely osteopenic and senile intact rats, even towards the end of their normal lifespan.

Disclosures: M. Sato, Eli Lilly & Co. 1, 3.

P40

AMG 162, a Fully Human Anti-RANKL MAb, Reduces Bone Resorption and Increases BMD in Mice That Express Chimeric (Human/Mouse) RANKL. P. J. Kostenuik, K. Warmington, M. Grisanti^{*}, S. Morony, Z. Geng, H. Tan, C. Christensen^{*}, R. Elliott^{*}, H. Nguyen^{*}, L. Martin^{*}, J. Viray^{*}, J. McCabe^{*}. Amgen, Inc., Thousand Oaks, CA, USA.

Introduction: RANKL plays a critical physiological and pathological role in osteoclast formation, activation and survival. OPG (osteoprotegerin) is the natural inhibitor of RANKL, and recombinant human OPG (huOPG-Fc) has been used as an effective antiresorptive agent in numerous animal models of bone disease. AMG 162, a fully human monoclonal antibody, is a new RANKL inhibitor that increases BMD in postmenopausal women. However, AMG 162 does not recognize native rat or murine RANKL. To facilitate the preclinical investigation of AMG 162, we genetically engineered mice to express a chimeric form of RANKL that is bound and neutralized by AMG 162. We then compared the pharmacodynamic response of these mutant (huRANKL) mice to AMG 162 and to huOPG-Fc, a cross-species RANKL inhibitor.

Methods: Knockin technology was used to replace the 5th exon of the murine RANKL gene with a hybrid exon containing a human coding

region and a murine non-coding region. Mice that are homozygous for this mutation are referred to as huRANKL mice. Heterozygote (hu/muRANKL) mice expressed one native RANKL allele and one chimeric allele. 6-8 week old male and female huRANKL mice, hu/muRANKL mice, or normal mice were treated twice per week with PBS, or AMG 162, or huOPG-Fc (5 mg/kg, SC). Radiographs were taken weekly, and mice were sacrificed after three weeks of treatment. Serum was collected at necropsy for biochemical markers of bone remodeling, and tibiae were harvested for BMD analysis (pQCT) and histomorphometry.

Results: AMG 162 caused rapid suppression of bone resorption in huRANKL mice, as evidenced by an early (1 week) increase in the radiodensity of long bone metaphyses. In huRANKL mice, both AMG 162 and huOPG-Fc caused similarly dramatic reductions in serum TRAP-5b (an osteoclast-specific resorption marker) and reduced osteoclast surfaces. These changes were associated with dramatic increases in bone volume and BMD at the proximal tibia. Heterozygous (hu/muRANKL) mice demonstrated an intermediate pharmacologic response to AMG 162. AMG 162 had no pharmacologic effects in normal mice, while huOPG-Fc had the expected (and similar) antiresorptive effects in both normal and huRANKL mice.

Conclusion: AMG 162, the first fully human RANKL monoclonal antibody, rapidly and effectively suppresses bone resorption in mice that express a mutant "humanized" form of RANKL. These mutant mice have no gross phenotype or abnormalities, apart from their unique ability to respond to AMG 162. These huRANKL mice therefore represent a useful preclinical model for studying the pharmacology of AMG 162.

Disclosures: **P.J. Kostenuik**, Amgen Inc. 1, 3.

P41

The RANKL Inhibitor OPG Increases Bone Mass and Improves Cortical Geometry in Male Monkeys. **M. S. Ominsky¹, P. J. Kostenuik¹, P. Cranmer^{*1}, S. Y. Smith², J. E. Atkinson^{*1}.**

¹Amgen, Inc., Thousand Oaks, CA, USA, ²CTBR, Senneville, PQ, Canada.

RANKL is the primary physiological and pathological mediator of osteoclast differentiation, activation, and survival. RANKL inhibition leads to rapid, profound, and sustained suppression of bone resorption and increased bone mineral density (BMD). While BMD is an important component of bone strength, the geometric distribution of bone mass is an important co-factor, especially in long bones subjected to bending forces. An optimal osteoporosis therapy should increase periosteal dimensions, reduce endosteal dimensions, and improve BMD. However, these ideal therapeutic responses have not been previously described at the same skeletal site in a remodeling species. We used OPG-Fc to examine the effects of RANKL inhibition on cortical geometry and BMD in 2-3 year old intact male cynomolgus monkeys. OPG-Fc was injected once weekly for 6 months at 15 mg/kg (n = 5 by SC injection; n = 3 by IV injection: data combined), while control animals (n = 5) received PBS (SC). Distal radii and proximal tibiae were analyzed by pQCT at baseline and at month 6. OPG-Fc significantly increased cortical volumetric BMD (vBMD) in the midshaft of both the radius (8%) and tibia (10%) compared to placebo-treated controls (p<0.05). OPG treatment significantly improved cortical geometry and trabecular BMD at the proximal tibia and distal radius metaphyses (Table 1). Increased cortical thickness was mediated by increased periosteal circumference and/or reduced endosteal circumference at both sites, and these changes led to large increases in cross-sectional moments of inertia (CSMI). CSMI is an important component of bone strength, and the product of CSMI and cortical vBMD can be used to calculate a bone strength index (BSI). BSI values in OPG-treated animals were significantly improved at both sites, which may be associated with improvements in bone strength. The ability of OPG to increase both the size and mineral density of cortical bone suggests that RANKL inhibition maintains bone formation despite significant suppression of bone resorption.

Table 1: % Difference Between OPG- and Placebo-treated Monkeys at 6 Months

pQCT Parameter	Proximal Tibia	Distal Radius
Cortical Thickness [mm]	+77**	+302**
Cortical vBMC [mg]	+119**	+332**
Periosteal Circumference [mm]	+14*	+21**
Endosteal Circumference [mm]	+3	-41**
CSMI [mm ⁴]	+135*	+220**
Bone Strength Index [mg-mm]	+166**	+278**
Trabecular vBMD [mg/cm ⁴]	+75**	+215**

Disclosures: **M.S. Ominsky**, Amgen, Inc. 1, 3.

P42

Both hPTH(1-34) and Risedronate Prevent Loss of Bone Trabecular Structure and Both Whole Bone and Localized Bone Strength in a Mouse Model of Glucocorticoid-Induced

Osteoporosis. **W. Yao¹, G. Balooch^{*2}, M. Balooch^{*1}, N. E. Lane¹.**

¹University of California at Davis, Sacramento, CA, USA, ²University of California at San Francisco, San Francisco, CA, USA.

Glucocorticoid (GC) therapy results in significant bone loss and fractures that frequently occur at higher BMD levels than those in postmenopausal women. **Objectives:** The purpose of this study was to assess if concurrent treatment of mice with GC and risedronate (RIS) or hPTH (1-34) (PTH) would maintain bone structure and mechanical properties (whole bone and localized) compared to GC treatment alone. **Methods:** Four groups of mice were randomized to placebo (PL), GC (1.4mg slow release pellet x 21days), GC + RIS (5µg/kg, sc, 5x/wk) and GC + hPTH(1-34) (40µg/kg, sc, 5x/wk) and treated for 21 days. After sacrifice, the 5th LVB were processed for bone histomorphometry and Elastic Modulus Mapping (EMM) was performed using Scanning Probe Microscopy-based technique. Compression tests were performed on the 4th lumbar vertebrae (LVB) and 3-pt bending tests were performed on the right tibia. **Results:** Compared to the PL treated mice, total TBV, TbTh. and TbN were lowered by 54%, 42%, 9% (p<0.05), respectively, in the GC-treated animals. These changes were accompanied by an increase in Oc.S and a decrease in MAR, bone formation rate and an increase of apoptotic osteocytes (p<0.05). Both RIS and PTH prevented bone loss with GC treatment. RIS prevented the elevated bone resorption and number of apoptotic osteocytes while PTH prevented the decreased in bone formation induced by GC administration. EMM in GC-treated mice revealed extensive heterogeneity in local mechanical properties, with areas of reduced EM at both the trabeculae surface and around the osteocyte lacunae of up to 40% (14.0±1.9 GPA) as compared to PL (23.8±3.1). This heterogeneity in EM was not seen at either the trabecular surface or around the osteocyte lacunae in GC+PTH (25.7±5.2) and GC+RIS (25.3±4.2) groups. Preliminary vertebral bone compression testing revealed that, the LVB4 of mice treated with GC+PTH and GC+RIS had a 65%-83% increase in strength (p<0.01), 55-59% increase in compression modulus (p<0.01), respectively, compared to GC-treated mice. 3-pt bending of GC-treated tibia revealed reduced stiffness (10.1%) and energy to failure (24.3%) compared to PL (p<0.05), while GC+PTH and GC+RIS treated mice had an increase in energy to failure (21-22%) compared to PL. **Conclusions:** These results indicate that PTH and RIS treatments in the presence of GC-treated mice prevent the deterioration of both localized and whole bone material properties through preventing the GC induced changes in bone cell activity which then maintains cortical and trabecular bone mass and structure.

Disclosures: **N.E. Lane**, None.

P43

Correlation Between Pamidronate Concentration in Bone and Biomechanical Properties of Rat Femora in Osteoporotic Fracture Model. K. Yang*. Yonsei University, Seoul, Republic of Korea.

Purpose: We investigated the correlation between mechanical properties of the rat femora and pamidronate concentrations in bone after long-term administration of pamidronate in rat osteoporosis model. **Material & Method:** We performed bilateral ovariectomy in twenty-five 3-month-old female Sprague-Dawley rats. Three months after ovariectomy, disodium pamidronate (0.5mg/kg) was injected every month for 6 months. After the six-month administration periods, the left femoral shaft was fractured using the closed fracture technique. Five weeks after fracture, rats were euthanized and the mechanical properties of the femora and bone mineral density of the right femoral head were measured. Pamidronate concentration in bone was checked by high-performance liquid chromatography. **Results:** Twenty-three rats survived and were completed the analysis. The higher the concentration of the pamidronate in bone, the lower the biomechanical parameters including load to failure, stiffness, stress, and Young's modulus and bone mineral density of the femoral head (Table). The concentration of the pamidronate in bone was not correlated with the strength of callus (load to failure and stress). **Discussion:** Pamidronate suppresses osteoclast mediated normal and abnormal bone remodeling. The weakening of bone due to accumulated microstructural damage and deficient repair processes are suspected after long-term administration of high dose pamidronate. It may also cause weakening of the weight bearing bone if higher load is applied to the limb. Left femora were fractured to load more weight on the right femora. We confirmed that the strength of the femora weakened according to the bone concentration of the pamidronate. We should keep the dosage of the pamidronate as low as possible in cases such as osteogenesis imperfecta, Paget's disease, and osteoporosis which need long-term administration of the pamidronate. The long-term administration of the pamidronate didn't suppress the fracture healing process in this model.

Linear Regression between Pamidronate Concentration in Bone and Biomechanical Parameters

dependant variables	linear regression	p-values
load to failure (N)	-0.474 X + 136.1	0.015
stiffness (N/mm)	-0.059 X + 88.9	0.027
stress (N/mm ²)	-0.133 X + 83.3	0.039
Young's Modulus	-0.003 X + 76.2	0.032
BMD (mg/cm ²)	-0.981 X + 287.6	0.005

Disclosures: **K. Yang**, None.

P44

RANKL Has Detrimental Effects on Cortical and Trabecular Bone Volume, Mineralization and Bone Strength In Mice. Y. Y. Yuan*¹, A. G. Lau*¹, P. J. Kostenuik², S. Morony², S. Adamu², F. Asuncion², T. A. Bateman¹. ¹Bioengineering Department, Clemson University, Clemson, SC, USA, ²Metabolic Disorders, Amgen Inc., Thousand Oaks, CA, USA.

RANKL is an essential mediator of osteoclast formation, activation and survival. Preclinical studies have shown that RANKL inhibition significantly improves bone density and strength at both cortical and trabecular sites. RANKL inhibitors have also been shown to improve cortical geometry in rodents and primates. Cortical structural and material properties are important determinants of bone strength. We hypothesized that the direct injection of RANKL will cause detrimental effects on bone geometry and density and therefore degrade strength.

Ten-week-old C57BL/6J female mice (n=12/group) were injected twice daily (SC) with murine recombinant RANKL (0.4 or 2 mg/kg/day) or vehicle (VEH) for 10 days. Mice treated with high-dose RANKL exhibited significant weight loss (11% vs. VEH, p<0.001) and hypercalcemia. Low dose RANKL did not cause significant

hypercalcemia or weight loss. Bone turnover was greatly accelerated by RANKL, as evidenced by 3-4-fold increases in serum alkaline phosphatase in mice treated with low- and high-dose RANKL, respectively (p<0.001 vs. VEH at day 10).

Both doses of RANKL caused substantial catabolism of both cortical and trabecular bone. Dry and ash weights were used to determine the % mineral content (%Min) of the femoral diaphysis (purely cortical bone) and the proximal femoral metaphysis (mixed cortical and trabecular bone). Both doses of RANKL caused significant reductions in %Min at both sites (p<0.05 vs. VEH). MicroCT analysis of the proximal tibial metaphysis revealed a profound loss of trabecular bone in RANKL-treated mice. Trabecular bone density was reduced by 85% with both doses of RANKL (p<0.001 vs. VEH).

Cortical bone geometry and strength were also negatively influenced by RANKL. MicroCT analysis of an 8 mm section of the femoral diaphysis showed that both doses of RANKL significantly reduced cortical bone volume (10-13% vs VEH, p<0.001). Biomechanical testing confirmed that RANKL directly reduces bone strength. Three-point bending of the femoral diaphysis showed that both doses of RANKL caused significant reductions in maximum bending load (19-25% lower than VEH, p<0.001).

These data demonstrate for the first time that RANKL administration has direct catabolic effects on both trabecular and cortical bone. These catabolic effects included reductions in bone volume, mineral density, and a significant decrease in bone strength. Inhibition of RANKL is therefore a logical and potential approach for improving cortical and trabecular bone mass and strength.

Disclosures: **Y.Y. Yuan**, Amgen Inc. 2.

P45

In Contrast to Clinical Results, Combining PTH with a Bisphosphonate Has a Synergistic Effect on Trabecular Bone in Ovariectomized Rats. R. J. Arends*, H. N. Chan*, T. M. C. van de Klundert*, A. G. H. Ederveen. NV Organon, Oss, The Netherlands.

Osteoporosis can be therapeutically approached in two different ways: by use of anti-resorptive agents or by use of anabolic agents. Nowadays, anti-resorptive agents like bisphosphonates, estrogens and SERMs are widely used to prevent menopause related bone loss. However, these treatments are only limited in preventing bone loss and do not restore the lost bone. Daily administration of parathyroid hormone (PTH), however, has been found to possess this anabolic quality and is therefore a promising agent to treat osteoporosis. But stopping PTH treatment results in a rapid loss of newly gained bone. Preclinical studies have been described in literature to address the hypothesis that there may be an advantage in using PTH in combination with anti-resorptive agents. The results published so far are inconclusive, partially due to the large variety of different experimental set-ups used.

In the present study, we evaluated the effect of PTH (16.5 µg/kg.d.sc), ethinyl estradiol (EE, 2 µg/kg.d.sc) and bisphosphonate (BP, 200 µg/kg.d.sc) on the bone mass and bone strength of ovariectomized female rats (OVX). Sixty-four three-month-old female Wistar rats were ovariectomized and randomized in 8 groups (n=8). The animals were left untreated for two weeks to await development of moderate osteopenia. The sham-operated and the control OVX animals were treated with vehicle starting two weeks after surgery, while other groups (all OVX) received EE, a high dose BP, PTH or a combination of PTH plus either EE or a high dose BP. All animals were sacrificed after 6 weeks of treatment. Both femurs were collected for bone mineral density measurement by pQCT and biomechanical testing by use of an indentation test, three-point bending test and cantilever bending test. In addition, the fourth lumbar vertebral body (L4) was dissected for a compression test.

Our study demonstrated that treatments with either BP or PTH alone, or combined treatment of PTH with EE or BP significantly restored the ovariectomy-induced bone mass and bone strength loss in rats. Moreover, combined treatment of PTH with BP strongly augmented

the effect of PTH alone.

In conclusion, these preclinical in vivo data suggest that a bisphosphonate and PTH may act synergistically on bone mass and bone strength in rats thereby improving bone quality. This, however, is in contrast to a recent clinical study that failed to demonstrate any additive effect of the combined treatment of both agents in women. The fact that the above described results in rats are not in line with human data warrants carefulness in extrapolating these data to clinical outcome. Further animal studies to evaluate this discrepancy are ongoing.

Disclosures: **A.G.H. Ederveen**, *NV Organon* 3.

P46

Bone Quality Is Maintained with Continuous and Intermittent Administration of Ibandronate. **F. Bauss**¹, **D. W. Dempster**².

¹Roche Diagnostics GmbH, Penzberg, Germany, ²Helen Hayes Hospital, Columbia University, West Haverstraw, NY, USA.

Background. Improved bone strength is an essential prerequisite for long-term clinical use of bisphosphonates and is influenced by several factors, including bone mineral density (BMD), bone microarchitecture, and defect repair. Ibandronate (IBAN), is a potent, nitrogen-containing bisphosphonate in clinical development for oral and intravenous (i.v.) administration with extended dosing intervals. Preclinical studies demonstrate that treatment with IBAN increases bone strength and reverses bone loss in animal models of osteoporosis.¹

Objective. To review preclinical evidence supporting the maintenance or improvement of bone quality with daily and intermittent IBAN.

Methods. Bone quality was explored in a range of animal models of osteoporosis and in intact animals through analyses of BMD, biomechanical properties, bone architecture and bone repair.

Results. In ovariectomized (OVX) rats, 1 year treatment with daily (0.2-25ug/kg/day) and intermittent (25 and 125 ug/kg every 25 days) IBAN dose-dependently increased BMD ($p \leq 0.0001$), trabecular bone volume ($p < 0.05$) and bone strength ($p < 0.01$) compared with OVX controls.³ Increases in BMD were positively correlated with bone strength ($p \leq 0.0001$). Increased trabecular separation, was prevented by all doses of IBAN. In adult OVX monkeys, BMD was significantly increased ($p < 0.05$ versus OVX controls) after 16 months of treatment with a clinically relevant intermittent IBAN regimen (up to 150ug/kg i.v. at 30-day intervals).⁴ Bone mass, microarchitecture and strength were dose-dependently preserved at all clinically relevant sites. Multiple regression analyses of bone mass and structural variables resulted in a prediction up to 88% of ultimate load.⁵ In adult beagle dogs, treatment with continuous IBAN (1ug/kg/day) and two intermittent regimens (3ug/kg/day for 1 week, 2-week drug-free interval, and 6ug/kg/day in a 1 week on/6 week off regimen) for 9 months did not adversely affect bone defect repair.⁶ Importantly, newly-formed bone closely resembled primary cortical bone formed during fracture repair.

Conclusions. Bone quality, assessed by bone mass, architecture, strength and repair is maintained or improved with daily and intermittent IBAN. Normal bone histomorphometry in women with postmenopausal osteoporosis receiving daily and intermittent IBAN support this conclusion.⁷

References:

1. Bauss F, et al. *Osteoporos Int* 2004;15:423-33.
2. Bauss F, et al. *J Rheumatol* 2002;29:2200-8.
3. Smith SY, et al. *Bone* 2003;32:45-55.
4. Müller R et al., *J Bone Miner Res* 2004;19: 1787-96
5. Bauss F, et al. *J Pharm Tox Methods* 2004;50:25-34.
6. Recker RR, et al. *Osteoporos Int* 2004;15:231-7.

Disclosures: **D.W. Dempster**, *Merck, Sanofi-Aventis, Novartis, Eli Lilly, NPS Pharmaceuticals, GlaxoSmithKline, Roche Laboratories, Proctor and Gamble* 5, 8.

P47

Conditional Knock-Out of the BMP4 Gene in Osteoblasts Using the 3.6 Col1a1-Cre Model Results in Osteopenia and Selective Reduced Cortical Thickness and Mineral Content. **S. E. Harris**¹,

D. Guo², **W. Yang**¹, **J. Zhang**³, **H. Anderson**⁴, **M. A. Harris**¹, **B. Kream**⁵, **A. Lichtler**⁵, **B. Hogan**^{*6}, **H. Kulesa**^{*7}, **J. Q. Feng**⁸. ¹U. Texas Health Sci Ctr San Antonio, San Antonio, TX, USA, ²U. of Missouri at Kansas City, Kansas City, MO, USA, ³U. Missouri at Kansas City, Kansas City, MO, USA, ⁴Kansas University Medical School, Kansas City, KS, USA, ⁵U of Connecticut Medical Center, Farmington, CT, USA, ⁶Duke University, Durham, NC, USA, ⁷Vanderbilt University, Nashville, TN, USA, ⁸U Missouri at Kansas City, Kansas City, MO, USA.

Bone Morphogenetic Protein 4(BMP4) is a member of family of growth factors that control a vast number of developmental processes. BMP4 is highly expressed in osteoblasts, osteocytes and odontoblasts in vivo postnatally. The knock-out of BMP4 results in embryonic lethality between 7.5 and 9.5dpc. Therefore, we deleted BMP4 in collagen type I expression domains using 3.6Col1a1-Cre line, which deletes BMP4 in early osteoblasts, mature odontoblasts, tendon, and other collagen type I expression domains. Conditional knock-out of BMP4 (BMP4 cKO) using the 3.6 Col1a1 results in some embryonic lethality between 13.5 and 18 dpc, due to reduced bone development and defects in heart function. However, most BMP4 conditional knock-out mice survive, with a few dying of hydronephrosis by 20-30 days. The animals that survive past 1-2 month have normal kidney function, as assayed by BUN and calcium and phosphate content in serum. We have now analyzed a set of 9 month old animals that still exhibit osteopenia, reduce BMD, with selective loss of cortical bone(Figure). The animals are of normal size and weight and the length of the long bones is normal but with pronounced cortical thinning with reduced second moment of inertia, Imin, as determined by uCT. Using a new acid-etch SEM procedure, we found that the mineral in the BMP4 cKO is more easily dissolved by the acid treatment, resulting in a large number of small pores in the bone structure. The decreased mineral content is supported by decrease in BMD in legs and arms(n=3) and decreased mineral content by alizarin red staining. In conclusion BMP4 is required postnatally, up to at least 9 months for proper cortical bone formation and mineral quantity and quality. All animal procedures were approved by the animal care and oversight committees.



Disclosures: **S.E. Harris**, *None*.

Genetic Determinants of Bone Quality

P48

YOUNG INVESTIGATOR AWARD RECIPIENT

Genetic Variability in Bone Brittleness Is Established Early in

Life. C. Price*, K. J. Jepsen. Mount Sinai School of Medicine, New York, NY, USA.

It is generally accepted that osteoporotic fracture risk is influenced by genetic factors. Whereas substantial research has been conducted toward understanding the genetic factors contributing to bone mass and morphology, very little is understood about the genetics of bone quality. We and others have demonstrated that whole bone mechanical properties, particularly those related to brittleness, vary significantly among inbred mouse strains [1,2]. This provided evidence that genetic background is a strong determinant of tissue fragility. However, the manner in which genetic background influences bone brittleness remains largely unknown.

To better understand how genetic variability in bone quality arises during growth, we quantified femoral morphology and composition throughout life for three inbred strains. Left femurs from female A/J (A), C57B/6J (B6), and C3H/HeJ (C3H) mice were examined at 14, 28, 56, 112, 182, and 365 days of age for ash content analysis. Ash content was determined using standard methods [1]. Ash content was examined because this trait is positively correlated with bone stiffness and negatively correlated with bone ductility [3] (Currey).

Each strain showed a non-linear increase in ash content between 14 and 112 days of age. Little change in ash was observed beyond 112 days. Significant differences in ash content were observed among the strains at all ages ($p < 0.05$ ANOVA). From the earliest time point (14 days of age), B6 mice showed the smallest ash values compared to A and C3H, which were similar. This suggested that B6 femurs were constructed of tissue of lower material stiffness, but greater ductility, throughout life, and that differences in material quality among the strains might be observed prior to 14 days of age. Thus genetic factors influencing material quality appear to be established early in life. Morphological analyses suggested that the lower ash content was associated with a more structurally efficient growth pattern in B6 mice. A/J and C3H strains showed a less structurally efficient growth and both showed similarly large ash content values. This study indicated that genetic variation in bone quality is established early in life and that bone quality may be coupled with morphology based on genetically controlled growth patterns. Therefore, understanding how and when material quality is established among inbred mouse strains may provide new insight into how genetic factors influence fracture risk.

1. Jepsen, JBMR 2001, 16(10); 2. Li, Funct Integr Genomics 2002 1(6); 3. Currey, J Biomech 2004, 37

Disclosures: C. Price, None.

P49

YOUNG INVESTIGATOR AWARD RECIPIENT

Identification of Mouse Chromosomes Influencing Bone

Brittleness. H. Courtland¹, J. Ryan^{*1}, A. Hill^{*2}, E. Lander^{*3}, J. Nadeau^{*2}, K. Jepsen¹. ¹Mount Sinai School of Medicine, New York, NY, USA, ²Case Western Reserve University, Cleveland, OH, USA, ³The Broad Institute of MIT and Harvard University, Cambridge, MA, USA.

Although fracture susceptibility is significantly correlated with genetic factors [1], the manner in which interacting genes lead to structurally and mechanically diverse bone tissues is not well understood. Previous research using inbred mice demonstrated that A/J (A) femurs are significantly more brittle (decreased ductility) than C57BL/6J (B6) femurs [2]. Since genetic variation in brittleness did

not vary with bone morphology, but with a compositional (bone quality) trait, ash content [3], the possibility exists that both parameters can be mapped to chromosomes within the mouse genome. To better understand how genetic variation in brittleness arises, we conducted a phenotypic analysis of B6-i^A Chromosome Substitution Strains (CSSs). Each CSS is inbred and identical to the B6 host except that chromosome (i) is replaced with the corresponding intact chromosome from the A donor. A total of 19 (17 autosomes, X, Y) CSSs were characterized in this study. Femurs from 14-16 week old (young adult) A, B6 and B6-i^A mice ($n=2-25$ per group) were harvested for analysis of ash content and post yield deflection (PYD) under 4-point bending.

Our data confirmed that femurs of B6 and A mice exhibited ductile (large PYD) and brittle (small PYD) phenotypes, respectively. In comparison to the host and donor strains, some B6-i^A femurs (e.g., 1, 4), exhibited PYD values identical to B6 (ductile) while others exhibited intermediate PYD values (e.g., 9, 10, 11). Strains significantly different from B6 (male B6-(13 and 18)^A and female B6-(8, 12, 16, 18, and X)^A (ANOVA, $p < 0.05$) indicated that one or more genes on donated chromosomes were responsible for a brittle phenotype. The lack of overlap between male/female CSSs with a brittle phenotype suggests sex differences in the genetic regulation of brittleness or a sex-dependent regulation of unsubstituted genes. Although mean ash content was not statistically associated with specific chromosomes, it was inversely related to PYD and explained 42% of total PYD variability across CSSs (Pearson, $p < 0.05$).

This study demonstrates that bone brittleness in young adult mice is strongly dependent on genetic background as B6 mice were able to gain a brittle phenotype by the substitution of individual A chromosomes. Although an increase in ash content likely causes a brittle phenotype in some CSSs (16, 18), in CSSs where ash content did not differ from the B6 background (8, 12), a brittle phenotype must arise through additional bone quality traits.

1. Fox Ost Int 1998 2. Jepsen JBMR 2001 3. Jepsen Mouse Gen. 2003 4. Nadeau Nat Gen 2000 5. Martin Nat Gen 1999.

Disclosures: H. Courtland, None.

P50

Using Inbred Mouse Strains to Identify Models for Determining Genetic Regulation of Bone Strength. L. Donahue. The Jackson

Laboratory, Bar Harbor, ME, USA.

The measurement most often used to predict bone strength is bone mineral density measured by x-ray absorptiometry. Yet other bone traits, including size, shape, architecture and material properties, as well as muscle mass, are important qualitative contributors to bone strength and should be considered when predicting fracture risk. Coupled with this expanded interest in characterizing bone and muscle, is an intense search for genetic determinants of fracture based on these recognized indices of bone strength. Interpretation of these studies is complicated by heterogeneity in human populations and by environmental differences, indicating that genetic regulation of bone strength is complex and that animal models are critical to progress in this field. The purpose of this work was to determine which muscle and bone phenotypes best predict femoral bone strength in inbred strains of mice and to discover models appropriate for further genetic analyses of factors that contribute to bone strength.

We collected skeletal geometry, muscle mass, volumetric BMD (vBMD), and bone strength data from female mice of 9 genetically diverse inbred strains of mice. pQCT (SA Plus, Stratec) was used to measure vBMD, periosteal perimeter (Ps.pm), and muscle area at the mid diaphysis; digital calipers were used to measure femur length and medio-lateral diameter (M/L) at mid diaphysis; peak load, stiffness, and energy to break (EB) were measured by three point bending (MTS). EB is often used as a measure of the toughness of bone, or the amount of energy required to cause bone to fracture.

We found that peak load and stiffness were both predicted by femur length ($p=.002;.001$), M/L diameter ($p=.009;.029$), muscle area ($p=.001;.011$), and vBMD ($p=.006;.002$). EB was predicted by Ps.pm ($p=.044$), M/L ($p=.037$), and muscle area ($p=.009$), but was

independent of vBMD. A strategy to genetically decompose the EB phenotype could be based on crosses between a low EB (low bone size/muscle area) strain and a high EB (plus high bone size/muscle area) strain. Such a combination is present in SWR/J and FVB/NJ, or in 129/SvImJ crossed to C57BL/6J. The F2 generation progeny from either cross would provide mice that could be used to analyze the genetic regulation of EB.

These data show that bone geometry, density and muscle mass are important determinants of femoral strength, and illustrate that bone strength is a complex trait with genetic regulation. We propose a genetic model using inbred strains of mice to discover the genetic regulation bone geometry, muscle mass, and BMD, allowing determination of their relative contributions to overall bone strength.

Disclosures: **L. Donahue**, None.

P51

Identifying Genetic Loci for Bone Quality Parameters in Murine Inbred Strains. **G. H. van Lenthe**¹, **T. Kohler***¹, **R. Voide***¹, **L. R. Donahue**², **R. Müller**¹. ¹ETH and University Zurich, Zurich, Switzerland, ²The Jackson Laboratory, Bar Harbor, ME, USA.

Bone quality is often used as a term to lump all unknown parameters that contribute to bone strength. However, with advancing technologies, many of these previously non-measurable parameters can now be quantified. Here we will refer to those aspects of bone quality directly related to bone strength, and describe how we can use this in genetic studies of murine bone function.

Micro-computed tomography (μ CT) provides an ideal imaging tool to non-invasively assess the detailed three-dimensional (3D) structure and architecture of bone. μ CT-based finite-element (μ FE) analysis can then be applied to calculate bone strength directly from structure. We postulate that this μ FE-based strength measure is the parameter par excellence to quantify structural bone quality, because it provides a functional assessment of a complex 3D architecture, it is non-invasive and non-destructive, and it can be expressed with only one scalar value. μ FE analysis is especially valuable in small animal bones where experimental testing becomes very difficult and is often associated with large experimental errors.

We applied μ FE analysis to femora of two murine growth-hormone deficient inbred strains (B6-*lit/lit* and C3.B6-*lit/lit*). They were μ CT-scanned using a 20 μ m resolution, automatically aligned, and femoral neck strength was calculated; μ CT-based morphometric parameters were determined to further describe bone structure and architecture.

The CV for bone strength ranged from 5 to 12%, which is markedly lower than found for experimental testing. Male femora were 7% stronger than female ones. More intriguing was that strength was 17% higher for the B6-*lit/lit* mice, whereas their bone volume was 18% lower; this emphasizes the great importance of a proper 3D arrangement of bone to achieve adequate strength. Neck cross-sectional area was well correlated ($R^2=0.66$) with femoral cross-sectional area indicating overall genetic control of bone architecture.

To further investigate the genetics of femoral neck strength, an F2 population of 2,000 mice was produced. We have started analyzing their femora and L5-vertebra, to assess specific genetic influence on cortical and trabecular bone, and to determine the associated genetic loci.

We conclude that μ FE-derived bone strength is an ideal method for bone quality assessment; it is precise and allows high-throughput characterization enabling identification of genetic loci directly for bone strength rather than via surrogate measures. Nevertheless, surrogate measures of bone architecture like size, shape, mass, etc., might prove helpful to provide insight into which structural qualities contribute most to bone strength.

Disclosures: **G.H. van Lenthe**, None.

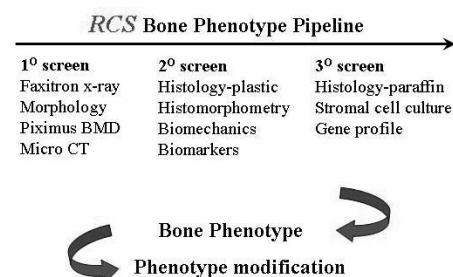
P52

Comprehensive Skeletal Phenotyping to Assess Bone Quality in Genetically Defined Mice. **J. E. Henderson**¹, **J. S. Binette***¹, **A. Li***¹, **W. Li***¹, **A. Fortin***², **E. Skamene***³. ¹Medicine, Centre for Bone and Periodontal Research, McGill University, Montreal, PQ, Canada, ²Emerillon Therapeutics, Montreal, PQ, Canada, ³Medicine and Human Genetics, McGill University, Montreal, PQ, Canada.

Recombinant congenic strains (RCS) of mice derived from inbred A/J (A) and C57BL/6J (B) strains were used as a discovery platform to identify genes that confer susceptibility or resistance to osteoporosis. Inbred RCS mice carry approximately 12.5% of the donor genome in 87.5% of the background genome, allowing for a more focused approach to the search for candidate genes. A high throughput, cost-effective phenotyping tool that was modeled on clinical principles was used to screen adult mice for variations in bone quality (Fig 1).

A complete primary screen was performed on 165 mice from the 2 parental strains and from 14 RCS. BMD was significantly lower in the femur and vertebra of A compared with B mice. This was corroborated by micro CT and histomorphometric analyses that showed lower BV/TV in the A mice. Trabecular bone architecture was compromised in A strain mice, as shown by an increase in the structure model index (SMI) that compares plate-like to rod-like structures. Strain A mice also showed reduced osteoblast and osteoclast activity, reduced calcein labeling in situ and a 50% reduction in circulating c-telopeptide (CTX). Only one of 14 RCS reliably demonstrated pheno-deviance in trabecular bone. Consistent with the A phenotype, BcA84 mice showed decreased BMD and BV/TV, increased SMI and decreased bone apposition and turnover. Since BcA84 has only 12.28% of the A genome introgressed within the B background it represents an excellent source for segregation and linkage studies aimed at identification of pertinent gene(s). Another BcA strain showed a similar phenotype by micro CT, but it was not supported by the highly variable BMD data.

We conclude that 1) RCS mice represent a valid discovery platform to identify genes that influence bone quality; 2) comprehensive skeletal phenotyping can be used as a rapid and reliable tool to identify relevant bone phenotypes; 3) BMD is less reliable than quantitative CT for initial identification of bone pheno-deviants; 4) quantitative CT correlates with histomorphometric and biochemical indices of bone turnover; 5) trabecular and cortical bone are regulated by different genetic mechanisms.



The Centre for Bone and Periodontal Research



Disclosures: **J.E. Henderson**, None

P53

Assessment of Bone Structure and Elasticity in C3H and BL6 Mice Using High Resolution Scanning Acoustic Microscopy. T. Hofmann^{*1}, K. Raum^{*1}, I. Leguerney^{*2}, A. Saied^{*2}, F. Peyrin^{*3}, L. Vico⁴, P. Laugier². ¹Martin Luther University of Halle-Wittenberg, Halle, Germany, ²University Paris VI - CNRS, Paris, France, ³ESRF, Grenoble, France, ⁴INSERM, Saint-Etienne, France.

Purpose: to investigate the potential of scanning acoustic microscopy (SAM) for bone phenotyping. Femur taken from 5 BL6 and 5 C3H mice were explored using 200 MHz SAM and SR-μCT (spatial resolution of 8 and 10 μm respectively). Site-matched regions were analyzed on both the acoustic impedance (Z) and degree of mineralization of bone (DMB) images. Bone diameter *B.Dm*, cortical width *Ct.Wi*, and cancellous diameter *Cn.Dm* were evaluated within a 1-mm region of the mid-diaphysis. Tissue elasticity *c₁₁* was extracted from the combination of acoustic impedance (Z) and DMB images. The parameters were evaluated in small site-matched regions manually selected within the epiphysis, the cortical and trabecular regions of the cortex. Both imaging methods showed the same morphological features with significantly higher *Ct.Wi* in the C3H strain. DMB was not correlated with *c₁₁* ($R^2 = 0.13$), but a second order polynomial regression between Z and *c₁₁* was highly significant ($R^2 = 0.995$, $p < 0.0001$). All tissue properties were lower in the B6 mice than in the C3H mice (Table I). However, the difference of DMB was much less pronounced than the differences of *c₁₁* and was not significant ($p < 0.05$) in the epiphysis. Significant differences are marked with an asterisk (unpaired t-test, $p < 0.05$).

Table I

	DMB [g/cm ³]		Z [Mrayl]		<i>c₁₁</i> [GPa]	
	B6	C3H	B6	C3H	B6	C3H
epiphysis	1.22 ± 0.02	1.23 ± 0.01	6.7 ± 0.5	7.4 ± 0.3*	22.7 ± 3.7	28.1 ± 2.5*
	1.28 ± 0.03	1.33 ± 0.01*	6.5 ± 0.3	7.8 ± 0.3*	21.7 ± 2.4	30.1 ± 2.6*
cortical						
trabecula	1.13 ± 0.03	1.27 ± 0.02*	5.8 ± 0.5	6.9 ± 0.3*	17.3 ± 2.7	23.8 ± 1.9*
r						

These findings indicate that SAM might suited to reveal differences in tissue properties that are not displayed on μCT images.

Disclosures: **P. Laugier**, None.

P54

Bone Quality of Mouse Tibiae Measured by Nanoindentation and Three-point Bending and Their QTL Mapping. Y. Jiao^{*1}, Z. Fan^{*2}, H. Chiu^{*3}, F. Jiao^{*1}, E. C. Eckstein^{*3}, J. Rho^{*3}, W. G. Beamer⁴, W. Gu¹. ¹University of Tennessee Health Sciences Center, Memphis, TN, USA, ²Marquette University, Marquette, WI, USA, ³University of Memphis, Memphis, TN, USA, ⁴The Jackson Laboratory, Bar Harbor, ME, USA.

It has speculated that regulate bone quality measured by nanoindentation technology represents a novel approach in our understanding of molecular mechanisms that control bone matrix properties. In this study, we measured bone quality of mouse tibiae by nanoindentation and three-point bending. We then mapped and compared their quantitative trait loci (QTLs).

Materials and Methods: 1) Mouse tibiae for age testing were from C57BL/6J and C3H/HeJ and for QTL mapping were from a F2 population derived from C57BL/6J and C3H/HeJ. Those tibiae were from the same population used for the analysis of QTLs of bone mineral density. 2) For nanoindentation measurement, a Triboindenter (Hysitron, Inc. Minneapolis, MN) was used to conduct all indentation tests. The Oliver-Pharr method was used to determine the elastic modulus. 3) The bone strength of the same set of bones was tested for three-point bending using ISO 4049, with the support width adjustable to accommodate specimen sizes outside the scope of ISO 4049. 4) Genome scan was

performed in The Jackson Laboratory using microsatellite markers. 5) QTL mapping was conducted using Map Manager QTX software.

Results and Discussion: 1) Mice at 4, 8, 16, 32, and 40 weeks were used for the nanoindentation tests. The data at 16 weeks of age shows a moderated variation compared with older ages within a strain; 2) Analysis of data of nanoindentation obtained from first set of 364 tibiae at age of 16 weeks revealed four QTLs for hardness (Chr. 9, 12, 13, and 16) and three for stiffness (two on Chr. 12 and one on Chr. 16). Using 683 out of a 1000 total F2 population, the QTLs on Chr. 12 and 13 were confirmed;

3) Analysis of data of three-point bending of the same 364 tibiae detected four QTLs of Elastic Modulus (Chr. 2, 11, 15, and 19) and 11 QTLs of Maximum Loading (hardness). Using the animals from second set of the population (a total of 485 progeny), QTLs on Chr. 4, 5, 6, 13, 15, 16, 17, and 18 were confirmed; 4) Most of the QTLs from three-point bending have been mapped on to the same locations of bone mineral density. The QTL on Chr. 4 (60% influence) has the most impact on the bone strength measured by three-point bending. The QTL on Chr. 12 (12%) has the most influence on nanoindentation property. Our study suggests that nanoindentation has a great potential as a novel approach to improve our understanding of molecular mechanisms that control the matrix properties of bone.

Disclosures: **Y. Jiao**, None.

P55

Genetic Loci Influencing Age-Related Declines in Bone Quality. D. H. Lang, N. A. Sharkey, G. P. Vogler^{*}, D. J. Vandenberg^{*}, D. A. Blizard^{*}, J. T. Stout^{*}, G. E. McClearn^{*}. Pennsylvania State University, University Park, PA, USA.

This study was designed to increase our understanding of the genetic architecture responsible for age-related declines in bone quality. While peak bone mass has been shown to predict fracture risk, insight into the mechanisms that influence both bone acquisition and the rate of bone loss could provide a means for preventing increased fracture risk in aged individuals.

The primary aim of this work was to identify quantitative trait loci (QTL) for age related differences in bone quality between young (200 day) and old (800 day) C57BL/6J X DBA/2 (BXD) recombinant inbred (RI) mouse strains.

Skeletal measures were assessed in BXD RI strains at both 200 and 800 days of age. Strain means were used in QTL analyses to search for chromosomal regions influencing skeletal phenotypes at 200 and 800 days of age. Additionally, the differences in RI strain means between 800 and 200 day skeletal phenotypes were used to search for chromosomal regions influencing change in bone quality as a function of age.

Three-point bending tests were used to assess the mechanical integrity of femora and tibiae and shear tests were performed on the femoral neck. Separate sex-specific QTL analyses were performed using QTL Cartographer. LOD scores of 3.3 or greater were considered significant while scores between 1.9 and 3.3 were suggestive.

Of primary interest are the QTLs for phenotypes reflecting decrements in bone quality as a function of age. Therefore the QTL results from the sex-specific interval mapping analyses summarized in Table 1 only include those traits displaying age-related strain differences and with LOD scores of 3.3 or greater in one of the three analyses described previously (cM corresponds to peak centimorgan position of the maximum LOD score or logarithm of the odds that linkage between a marker and a trait did not occur by chance).

The most interesting results are those on chromosomes 2, 3, 4, 5, and 9 where significant QTLs were identified for age-related differences, but were not identified in the specific 200 and 800 day analyses. The identification of QTLs for skeletal phenotypes at a distinct point in time does not necessarily indicate that the QTL is influencing age-related changes in bone quality. QTLs influencing a change in bone integrity as a function of age may be fundamentally more important in relation to osteoporosis and fracture risk in old age.

Table 1: QTL interval mapping results. *A - data adjusted for animal size, U - unadjusted, B -Both

Chr.	Phenotypic Trait	*	Sex	200 Day		800-200		800 Day	
				RI	Strain	RI	Strain	RI	Strain
				Means	Differenc	es	es	Means	es
				cM	LOD	cM	LOD	cM	LOD
2	Fem. Neck Ult. Load	A	M			23	3.3		
2	Femur Neck Ult. Load	U	M			27	4.6	51	2.3
3	Femur Head Diameter	B	M			34	3.7		
4	Femur Head Diameter	A	F			19	3.3		
4	Tibia Shaft Yield Disp.	A	F	59	1.9	58	4.2	36	1.6
5	Femur Shaft Stiffness	A	F			13	3.7		
9	Tibia % Water	A	M			13	3.3		
9	Femur Shaft Yield Disp.	A	M			26	3.3		
10	Femur Neck Ult. Work	A	F			2	3.0	2	4.0
11	Femur Shaft Ult. Work	U	F	26	2.4	26	3.4	26	2.2
12	Femur Epiph. Width	A	M			46	3.3	46	3.2
16	Femur Shaft Ult. Load	A	F	12	1.5	19	2.0	18	3.3
16	Femur Shaft Stiffness	B	F			16	4.1	16	3.8
16	Tibia Length	U	F			19	3.3		
16	Femur Shaft Ult. Work	B	F			21	4.0	21	4.1
18	Tibia Shaft Stiffness	U	M			49	2.1	49	3.3
20	Femur Shaft Ult. Disp.	U	F			27	2.1	30	3.5

Disclosures: **D.H. Lang**, None.

Effects of Bone Morphology/Geometry on Bone Quality

P56

Reduced Loading Due to Spinal Cord Injury During Growth Results in "Skinny" Bones: A Case Study. **L. M. Giangregorio¹, N. McCartney²**. ¹Toronto Rehabilitation Institute, Toronto, ON, Canada, ²McMaster University, Hamilton, ON, Canada.

The present study evaluated the influence of reduced loading during growth on bone and muscle at the tibia by comparing bone density, bone geometry and muscle cross-sectional area (CSA) in a male who sustained spinal cord injury (SCI) at birth (from here called SCI-B) to that of two matched controls without SCI, and also to four individuals with spinal cord injuries of similar level and injury completeness but sustained at age 15 or greater. All subjects with SCI were at least 3 years post-injury and had experienced motor incomplete lesions at the cervical level. Computed tomography was used to measure volumetric bone density, bone geometry (maximum, minimum and polar area moments of inertia - I_{max} , I_{min} , I_{pol}) and muscle CSA at the tibia (66% of tibia length, measured proximally from the distal end). The absence of weight bearing loading during growth had a dramatic impact on muscle area. Lower leg muscle CSA of SCI-B was only 62.6%±5.9% of values of non-SCI controls, and 71.6%±12.4% of values in other males with SCI. There was a striking impact of SCI at birth on bone geometry. In SCI-B, bone CSA was roughly half (52%±3.9%) that of non-SCI controls, and 71.6%±15.6% of the values obtained in other males with SCI. The area moment of inertia variables (I_{max} , I_{min} , and I_{pol}) in SCI-B ranged from 21% to 30% of control values, or 70-79% lower than controls. Further, the moment of inertia variables in SCI-B ranged from 25% to 67% of the values obtained in other males with SCI, indicating that suffering SCI in the early stages of life has a remarkable impact on bone shape. Interestingly, tibia bone density did not appear to be affected in SCI-B when compared to non-SCI controls, as the average difference in bone density was -1.2±0.70 percent. Among the other males with SCI, bone density was 4%-19%

lower than in SCI-B. Muscle atrophy and bone loss are a commonly reported consequence of SCI. This case reveals that important changes in bone geometry occur after SCI, and that mechanical loading during growth plays a vital role in the development of bone size and shape.

Disclosures: **L.M. Giangregorio**, None.

P57

YOUNG INVESTIGATOR AWARD RECIPIENT

Bone Quality Is Related to Bone Morphology in Young Adult Male Tibiae. **S. M. Tommasini¹, M. Munyoki², P. Nasser², M. B. Schaffler², K. J. Jepsen²**. ¹CUNY Graduate School, New York, NY, USA, ²Mt Sinai School of Medicine, New York, NY, USA.

The reasons why individuals with more slender bones for their body size are at increased risk of stress fracture are not fully understood.¹ Based on studies using inbred mice, slender bones had higher mineral content suggesting that bone morphology and quality might be biologically coupled during growth to satisfy mechanical demands.² However, the increased mineral had the adverse effect of being associated with increased bone brittleness and poor tissue damageability under fatigue loading. To determine whether the human skeleton shows a similar relationship between bone quality and morphology as the mouse skeleton, we conducted a biomechanical and compositional evaluation of the tibiae of young adult males.

Tibiae from 17 male donors (age 17-46 yrs) were measured for bone geometry [length, cortical area, AP and ML width, moments of inertia (I_{AP} , I_{ML} , J)]. Slenderness was defined as the inverse ratio of the section modulus [$J/(\text{width}^2)$] to tibia length and body weight.³ The diaphyses were cut into rectangular beams and tested in 4-point bending for monotonic properties [modulus, strength, work, post-yield strain (PYε)] and tissue damageability.⁴ Ash content was determined using standard methods.² Partial correlation coefficients were determined between each morphological and compositional parameter and each tissue level mechanical property while taking age into consideration.

The data indicated that not all bone is made the same way. Significant correlations ($p < 0.05$) were observed between AP width and two mechanical properties related to tissue brittleness (PYε, work) indicating that the tissue of individuals with narrow tibiae was less ductile. Further, there was a significant correlation between tissue damageability and tibia slenderness consistent with the mouse model suggesting that slender bones accumulate more cracks under equivalent loading conditions. However, unlike the mouse model, age-corrected ash content did not correlate with any mechanical or geometric parameter and therefore, was not a strong explanatory variable of the variation in tissue fragility.

Current non-invasive methods that assess bone quality (BMC, ultrasound) provide measures of bone stiffness, but cannot provide measures of ductility and damageability, which may be important for the response of bone under extreme loading conditions (military training, falls). If the relationship between quality (ductility, damageability) and morphology (slenderness) holds over a wider range of bones, then morphology may be a useful predictor of bone quality and bone fragility.

¹Beck, Bone 2000, 27; ²Jepsen, JBMR 2001, 16; ³Selker, J Biomech 1989, 22; ⁴Jepsen, J Biomech 1997, 30.

Disclosures: **S.M. Tommasini**, None.

P58

Development of the Parameterized Unit Cell Models for

Evaluation of Human Cancellous Bone Stiffness and Strength. **J. Kim*, P. Faghri*, J. Z. Ilich**. University of Connecticut, Storrs, CT, USA.

Mechanical properties and strength of bones depend not only on bone mineral density (BMD) or bone volume fraction (BV/TV) but also on trabecular micro-architecture. Our objective was to develop a simplified, generalized numerical scheme that can be used as a clinical

tool to predict age-related changes in stiffness and strength of human cancellous bone.

Attempts to take into account trabecular micro-architecture have been made using micro-finite elements and homogenization techniques. The former have advantage in describing realistic trabecular architecture, but are valid only for a particular bone, and location, and do not provide direct information on age-related changes in mechanical properties caused by changes in structural parameters such as trabecular thickness and number. Homogenization techniques assume trabecular bone to be a structure of either repeated unit cells or representative volume elements, and are capable of providing parameterized longitudinal data on mechanical properties considering age-related changes in trabecular morphology.

We propose here a simplified three-dimensional (3D) unit cell approach to investigate the effects of trabecular thinning and resorption on Young's modulus, compressive and tensile strengths, using an asymmetric principal strain failure criterion. The 3D unit cells will be modeled using twenty-node brick elements. From the existing measured data on BMD over time (every 6 months over 3 years) in postmenopausal women, trabecular thinning will be simulated using a level-1 unit cell and trabecular resorption using a level-2 unit cell with random strut removal. Trabecular thicknesses will be parameterized based on BV/TV. The horizontal and vertical struts in level-2 unit cell will be randomly removed according to BV/TV. Special-purpose 3D structured mesh generator will be used for detailed meshing.

Existing areal BMD (g/cm^2) measurements will be reassessed for the portion of trabecular bone. For 3D analysis, a volumetric BMD (g/cm^3) will be approximated as follows: for a cylinder: $\text{vBMD} = \text{BMD} \times (4/\pi W)$ where W is a diameter; and for a cube $\text{vBMD} = \text{BMD} \times (A_p)^{0.5}$ where A_p is a projected area. BV/TV is then obtained by $\text{BV}/\text{TV} = \text{vBMD}/\rho_s$ where ρ_s is the density of an individual trabecula, and will be an input to the numerical analysis.

The novelty of this model consists of incorporating bone loss such as trabecular thinning and resorption into a generic, parameterized 3D unit cell model in the finite element method to quantify compressive and tensile strengths of cancellous bone. The model will enable evaluation of bone stiffness, strength, and fracture risk for postmenopausal women, which take into account trabecular thinning and resorption with age.

Disclosures: J.Z. Ilich, None.

P59

Contributions of Cortical and Trabecular Architecture to

Biomechanical Properties of Human Vertebrae. J. P. Roux^{*1}, Z. Merabet^{*1}, M. E. Arlot¹, F. Duboeuf^{*1}, P. D. Delmas¹, M. L. Bouxsein². ¹INSERM Research unit 403, Claude Bernard University, Lyon, France, ²Orthopedic Biomechanics Laboratory, Beth Israel Deaconess Medical Center and Harvard Medical School, Boston, MA, USA.

Vertebral fractures are common in elderly persons, yet the mechanisms of injury underlying these fractures remain obscure. Whereas there is clear evidence for a strong influence of the quantity of bone (i.e., bone mass or BMD) on the mechanical behavior of vertebrae, there are less data addressing the relative influence of cortical and trabecular microarchitecture. Thus, the aim of this study was to determine the relative contributions of bone mass, trabecular microarchitecture and cortical thickness to the mechanical behavior of human lumbar vertebrae. We obtained 19 L3 vertebrae (10 men and 9 women, aged 26-93 yrs), and assessed BMD (g/cm^2) of the vertebral body by lateral DXA; vBMD (g/cm^3 , as BMC / directly measured vertebral body volume); 3D trabecular microarchitecture (BV/TV, trabecular thickness, degree of anisotropy, and structure model index) and thickness of the anterior cortex by μCT (35 μm voxel size, Skyscan). Then, compressive stiffness and failure load were measured, and apparent modulus and ultimate strength computed using the minimal cross-sectional area of the vertebral body. Bivariate regression analysis showed that BMD was strongly correlated to compressive stiffness ($r=0.86$) and failure load ($r=0.82$). Except for

trabecular number, all trabecular parameters ($r = 0.50-0.76$, $p=0.03-0.0002$) and anterior cortex thickness ($r = 0.58-0.65$, $p=0.01-0.003$) were also strongly correlated with mechanical behavior. The quantity of bone (ie; BV/TV, BMD or BMC) explained 42 to 74% of variability in mechanical properties. Trabecular architectural features were strongly correlated with BMD and BV/TV ($r = 0.58$ to 0.95), and thus did not improve prediction of mechanical properties over that provided by BMD. Conversely, anterior cortical thickness was not correlated with trabecular architecture and weakly with BMD ($r = 0.52$). Accordingly, the combination of BMD or BV/TV with anterior cortical thickness significantly improved the prediction of mechanical properties, with the combination explaining 58 to 80% of variability in mechanical properties. Our data imply that measurements of cortical thickness may enhance predictions of vertebral fragility, and that therapies which improve both vertebral cortical as well as trabecular bone properties may provide a greater reduction in fracture risk.

Disclosures: J.P. Roux, None.

P60

Age-related Changes Reduce Cortical Stability in the Femoral Neck: Cause of Exponentially Increasing Hip Fracture Risk? J.

Reeve¹, P. Mayhew^{*1}, C. D. Thomas^{*2}, J. G. Clement^{*2}, N. Loveridge¹, T. J. Beck³, W. Bonfield^{*1}, C. J. Burgoyne^{*1}.

¹University of Cambridge, Cambridge, United Kingdom, ²University of Melbourne, Melbourne, Australia, ³Johns Hopkins University, Baltimore, MD, USA.

Background: Hip fracture risk rises 100-1000 fold over 6 decades of age. Loss of resistance to bending is not a major feature of normal ageing of the femoral neck. Another cause of fragility is local buckling or elastic instability. We wondered if this increases markedly with ageing since it might trigger hip fracture in a sideways fall. Bones adapt to their local experience of mechanical loading. The suggestion that bi-pedality permits thinning of the under-loaded supero-lateral femoral neck cortex arises from the failure of walking to transmit much mechanical load to this region.

Methods: We measured with computed tomography the distribution of bone in the mid-femoral neck of 77 proximal femurs from cases of sudden death aged 20-95. We then calculated the critical stress, from the geometric properties and density of the cortical zone most highly loaded in a sideways fall, as a threshold for elastic instability.

Findings: With normal ageing, this thin cortical zone in the upper femoral neck got markedly thinner (Fig), with in women a 2 to 3-fold fall in critical stress and rather less in men. This compromised the capacity of the femur to absorb energy in a sideways fall, independently of osteoporosis. Patients with hip fracture had further reduced stability.

Interpretation: As we age, hip fragility increases because under-loading of the supero-lateral cortex leads to atrophic thinning. Because walking does not load sufficiently the upper femoral neck, the fragile zones in healthy bones may need strengthening, eg with more well-targeted exercise.

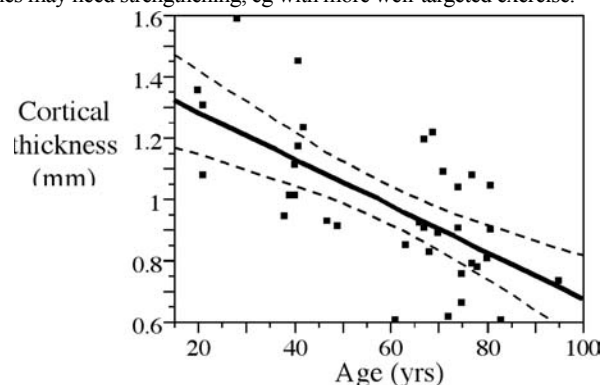


FIG: Thickness of the posterior part of the supero-lateral cortex plotted against age for 35 women. Regression +95% CI

Disclosures: J. Reeve, None.

P61

Severity of Vertebral Fracture Reflects Deterioration of

Trabecular Bone Microarchitecture. G. P. Dalsky¹, J. San Martin¹, P. Chen^{*1}, H. K. Genant², Y. Jiang³, P. D. Delmas⁴, E. F. Eriksen⁵. ¹Eli Lilly and Company, Indianapolis, IN, USA, ²University of California; Synarc, San Francisco, CA, USA, ³University of California, San Francisco, CA, USA, ⁴Claude Bernard University, Lyon, France, ⁵Novartis Pharma AG, Basel Switzerland. (Dr. Eriksen was employed by Eli Lilly and Company at the time of data analysis.)

This study describes the relationship at baseline between the severity of vertebral fractures, defined by qualitative features and vertebral height reductions using visual semiquantitative (SQ) analysis of radiographs and trabecular microarchitecture analyses of iliac crest biopsy samples in a subset of patients from the teriparatide Fracture Prevention Trial (Neer et al, N Engl J Med 2001). Bone structure indices measured by 2D histomorphometry and 3D microCT in 74 and 51 patients, respectively, are shown for each baseline fracture SQ severity grade, classified by vertebral height loss. There were significant correlations observed among the 2D and 3D measurement groups ($r = -0.64$, $p < 0.01$ and $r = -0.82$, $p < 0.01$, respectively); a multivariate ANOVA was performed for each set of measurements. A subject's maximum SQ grade is a strong predictor of the bone microarchitecture quality. An increase in vertebral fracture severity is characterized by a reduction in trabecular bone volume, impaired trabecular connectivity, and a transformation of trabeculae from plate-like to more rod-like morphology (2D, $P=0.009$; 3D, $P=0.07$, Wilks' Lambda multivariate test, table, mean \pm SD). These results demonstrate that a deterioration of bone structure, with low trabecular bone volume, is a continuous and progressive process. Microarchitectural deterioration is exponential when bone volume falls below a critical value of $\sim 15\%$ (Parkinson & Fazzalari, J Bone Miner Res 2003). In conclusion, this correlation between baseline SQ vertebral fracture severity and histological features of bone quality deterioration explains the accelerated cascade of risk observed in patients with severe fracture.

Bone quality and vertebral height loss

	SQ0 (<20%)	SQ1 (20- 25%)	SQ2 (25- 40%)	SQ3 (>40%)
2D Trabecular bone volume	0.25 \pm 0.09 (n=6)	0.17 \pm 0.07 (n=23)	0.14 \pm 0.06 (n=35)	0.12 \pm 0.05 (n=10)
2D Marrow star volume	16.1 \pm 24.0 (n=6)	22.0 \pm 30.9 (n=22)	35.0 \pm 36.1 (n=31)	41.8 \pm 33.6 (n=9)
3D Trabecular BV/TV	0.16 \pm 0.05 (n=4)	0.14 \pm 0.07 (n=19)	0.13 \pm 0.05 (n=19)	0.08 \pm 0.03 (n=9)
3D Structure model index	1.41 \pm 0.33 (n=4)	1.79 \pm 0.55 (n=19)	1.96 \pm 0.46 (n=19)	2.12 \pm 0.49 (n=9)

Disclosures: **G.P. Dalsky**, Eli Lilly and Company 3.

P62

Bone Quality and Vertebral Fracture: A Matter of Scale. J. H. Kinney^{*1}, J. S. Stolk^{*1}, R. K. Nalla^{*2}, R. O. Ritchie^{*2}.

¹Lawrence Livermore National Laboratory, Livermore, CA, USA, ²Lawrence Berkeley National Laboratory, Berkeley, CA, USA.

Bone mineral density is not a reliable indicator of fracture risk, as there is overlap in fracture frequency between normal and osteoporotic populations. Also, the rate of bone turnover appears to be a predictor of risk independent of bone mass. These observations support a possibility that age-related changes in the quality of the hard tissue contribute to fracture risk in the aged.

Many variables can affect fracture risk, including changes in hard tissue strength, toughness, and architecture. Assessing the importance of each variable is a matter of scale. For any material, there is a critical slenderness ratio λ_c that depends only on the yield strain. For long bones ($\lambda \ll \lambda_c$) yield stress and fracture toughness are important mechanical properties. However, for structures rich in trabecular bone, like vertebrae, $\lambda \sim \lambda_c$, there is a competition between tissue failure (governed by stress) and loss of structural stability (mediated by inelastic buckling); trabecular architecture determines which failure

mode dominates.

We present evidence that the increased risk of vertebral fracture results from a change in failure mechanism; in young bone, vertebral fracture is governed by the strength of the hard tissue (bone quality) whereas in osteoporotic bone, fracture is mediated by the stability of the trabecular lattice (architecture). The transition in mode of fracture depends on the relationship of the slenderness ratios of the individual trabecular members to λ_c . A thoracic vertebra (T10) from a 30yr female with normal bone mass and a lumbar vertebra (L1) from a 63yr male with low bone mass (osteopenic) were imaged in their entirety with synchrotron radiation tomography on beam-line 8.3.2 at the Advanced Light Source (ALS, Berkeley, CA). Cubes of bone (4mm on edge) were removed from the images and meshed for finite-element analysis. A fully dynamic, geometric nonlinear implicit finite-element simulation was performed using parallel linear algebra. A J_2 plasticity constitutive model, with material constants appropriate for trabecular bone, was used to simulate the load response of the trabecular lattice. Results were analyzed within the context of stability theory.

Simulations and analysis determined that the mechanism by which fracture is initiated was different in the two cases; tissue strength controlled fracture in the normal bone, whereas inelastic stability mediated fracture in the osteopenic bone. In addition, fracture in the osteopenic vertebra was sensitive to the rate of bone turnover. The results suggest that anti-resorptive agents reduce risk of vertebral fracture both by preserving stable trabecular bone architecture and by reducing bone turnover.

Disclosures: **J.H. Kinney**, None.

P63

Effects of Long-term Tennis Playing on Bone Gross Geometry at the Distal Radius: a Quantitative Magnetic Resonance Imaging Study. G. Ducher^{*1,2}, S. Mème^{*3}, C. Magni^{*4}, J. Viala^{*4}, C. Chappard², D. Courteix¹, C. Benhamou^{1,2}.

¹ATOSEP, Orleans, France, ²Inserm U658, Orléans, France, ³CBM UPR 4301, Orleans, France, ⁴Hospital of Orléans, Orleans, France.

The purpose of this study was to characterize the geometric changes of the dominant radius in response to long-term tennis playing using magnetic resonance imaging (MRI).

Twenty competitive tennis players (10 men and 10 women, age: 23.1 ± 4.7 years, with 14.3 ± 3.4 years of practice), were recruited. Axial slices were obtained on both distal radii with a spin-echo sequence (TR: 645 ms, TE: 20 ms, pixel size: $195 \times 195 \mu\text{m}$, slice thickness: 2 mm) using a 1.5 T MR device. Six contiguous slices were analysed, covering 1.2 cm of the distal radius, starting 1.8 cm far from the articular surface between the radius and the lunatum. The total bone area, cortical area, endocortical area and muscle area were manually defined on each slice. Volumetric measurements were calculated as the summed products of measured areas and slice thickness over the region of interest. Bone mineral content (BMC) was derived from the DXA scan of the distal radius in order to match the region of interest scanned by MRI. Volumetric bone mineral density (BMD) was calculated as the quotient of DXA-derived BMC on the MRI-derived total bone volume. The comparison between the dominant and nondominant radius was performed by a parametric paired t-test.

Significant relative side-to-side differences ($p < 0.0001$) were found in muscle volume (+9.7%), BMC (+13.5%), total bone volume (+10.3%) and endocortical volume (+20.6%) but not in cortical volume (+2.6%, ns). The asymmetry in total bone volume explained 75% of the variance of the BMC asymmetry ($p < 0.0001$). Volumetric BMD was slightly higher on the dominant side (+3.3%, $p < 0.05$). On both sides, muscle volume was related to all bone parameters, except volumetric BMD ($r = 0.48-0.83$, $p < 0.05-0.0001$). The asymmetry in muscle volume did not correlate with any of the asymmetries in bone parameters. BMC was still greater on the dominant side after adjusting for muscle volume, whereas the side-to-side differences in bone geometric parameters disappeared.

This study indicates that the greater BMC induced by long-term tennis playing at the dominant distal radius is mainly due to increased bone

size, improving mechanical strength. Cortical volume is not significantly increased, except in the one-handed backhand players. The muscular volume and strength appeared to play a role in the bone response to loading. However, muscle and bone asymmetries were not correlated, suggesting that other stimuli, directly applied to the radius, may also stimulate bone mineral accrual.

Disclosures: C. Benhamou, None.

P64

Regional Trabecular Morphology by Micro-CT Is Correlated with Failure of Thoracic Vertebrae Under a Posteroanterior Load. M. M. Sran¹, S. K. Boyd², D. M. L. Cooper^{*2}, K. M. Khan¹, R. F. Zernicke^{*2}, T. R. Oxland^{*1}. ¹UBC, Vancouver, BC, Canada, ²UofC, Calgary, AB, Canada.

Manual therapy techniques such as spinal mobilization are commonly used in the treatment of back pain. These techniques are also used in individuals with osteoporosis. (1) Under a posteroanterior (PA) load (to mimic PA spinal mobilization), thoracic cadaver specimens fail at the base or middle of the spinous process, rather than in the vertebral body. (2) Traditional predictors of skeletal failure, lateral or AP DXA or geometry of the spinous process or vertebral body, do not predict PA failure load. This may be due to BMD being an integrated measure of the entire vertebra. Thus the objective of this study was to measure trabecular bone morphology, including bone volume ratio (BV/TV), trabecular number (Tb.N), thickness (Tb.Th) and separation (Tb.Sp) using μ CT in four regions of thoracic vertebrae and to correlate those measures with PA failure load at the adjacent vertebra. We measured failure load and failure site in 11 T5-8 cadaveric spine segments (mean age 77 yr) when a PA load was applied at the spinous process of T6 using a servohydraulic material testing machine (Instron 8874, Canton, MA), simulating a commonly used spinal mobilization technique. The T7 vertebra was dissected and sectioned to produce regional samples of the spinous process, the central lamina, and a central vertebral body core (8 mm diameter). Each sample was scanned with μ CT (Skyscan 1072, Aartselaar, Belgium, 15 μ m nominal isotropic resolution). We segmented and analysed four trabecular regions (spinous process base, spinous process middle, central lamina, and vertebral body centrum). BV/TV at the base or middle of the T7 spinous process (fracture sites), mean Tb.N and mean Tb.Th at the base were strongly correlated with PA failure load of T6 (BV/TV base: $r=0.74$, $p=0.01$; BV/TV middle: $r=0.73$, $p=0.01$; Tb.N base: $r=0.64$, $p=0.03$; Tb.Th base: $r=0.65$, $p=0.03$). Tb.Th of the central lamina was significantly greater than Tb.Th of the spinous process base ($p=0.002$). BV/TV of the base and middle regions of the spinous process were correlated with failure at those sites, and differences in trabecular thickness at the base (compared with the lamina) may have influenced the site of fracture.

References:

1. Sran & Khan, Manual Therapy 2005
2. Sran et al., Spine 2004

Disclosures: M.M. Sran, None.

P65

A Mathematical Model to Identify Mechanical Factors Leading to a Fracture. S. J. Wimalawansa¹, G. Gunaratna², M. Liebschner^{*3}. ¹Robert Wood Johnson Medical School, New Brunswick, NJ, USA, ²Department of Physics, University of Houston, Houston, TX, USA, ³Department of Bioengineering, Rice University, Houston, TX, USA.

Anti-osteoporotic agents are expensive and may have significant adverse effects. Therefore, it is helpful to reliably identify subjects requiring therapy. Bone density, which is currently the principal means of detecting osteoporosis, is known to only partially account for bone strength. The levels of connectivity and anisotropy of the trabecular bone play a significant role in determining the strength of bones.

Reliability of diagnostic tools can only be enhanced by properly accounting for consequences of these structural aspects.

We have validated a mathematical model of bone to determine the leading causes of fractures and bone degradation [1] and, consequently characteristic represent a fracture load. The model representing trabecular bone consists of a disordered cubic network of struts and nodes [2]. We determined that the removal of trabecular elements had a larger detrimental effect on fracture load than any other factors. We concluded that reductions in load carrying ability are caused by destruction of pathways along which stress can be transmitted [3]. The remaining stress pathways have to meander between these fractures. We demonstrated that availability of stress pathways and not the density of bone that mainly determines reductions in fracture load.

To test the validity of Equation, we used computations on digitized images of trabecular bones. At high driving frequencies, only trabecular elements on the edge are excited; it is predicted that the fracture load and Γ are related [4]. For small values of Γ (i.e., weak bones), the relationship is independent of the original bone. This supports the contention that Γ can be used as a diagnostic for fracture load. We also have tested the validity of Equation using previously published data on the fracture load of human vertebrae (age 15-90 years), which confirms the expression. The computations on mathematical models and those constructed from digitized images helped us to understand that (1) longer micro-fractures (connectivity) determine the level of bone weakness, and (2) vibrational analysis can be used to determine this. The prototype we developed is capable of determine the use of vibration (linear response functions) to identify the location of large fractures and to estimate reductions in bone strength.

References

- (1) G. H. Gunaratne et al, Phys. Rev. Lett, 88, 068101, 2002
- (2) M. J. Silva and L. J. Gibson, Int. J. Mech. Sci., 39, 549-563, 1997
- (3) J. Espinoza-Ortiz, et al, Phys. Rev. B, 66, 144203, 2002
- (4) G. H. Gunaratne, Phys. Rev. E, 66, 061904, 2002

Disclosures: S.J. Wimalawansa, None.

P66

Withdrawn

P67

Patterns of Intracortical Bone Loss Reveal Changes in Bone Quality. D. Casagrande¹, J. Williams^{*2}, J. Bird^{*2}, M. Cordova^{*2}, R. Ghillani^{*2}, D. Laudier^{*2}, C. Terranova^{*3}, R. Levy^{*2}, K. Jepsen². ¹AECOM, Bronx, NY, USA, ²MSSM, New York, NY, USA, ³CUNY, New York, NY, USA.

Osteoporosis is a disease of chronic bone loss, leading to increased fracture risk. Although common practice determines bone quality in terms of BMD, BMD does not accurately predict fracture risk. BMD measurements are limited because they do not reflect bone loss at the biological level nor the effects of biomechanical stresses on bone loss. To gain a better understanding of bone quality and fragility, we analyzed bone loss for cadaveric radial and femoral cross sections. Cadaveric radii (24 female, 23 male; age 43-100) and femurs (12 females, 5 males; age 62-96) were sectioned at sites 30% and 50% of their length, respectively. For each diaphyseal cross section, bone loss was quantified by measuring pore size (area) and the distance of the pore from the periosteum. This analysis was performed separately for each anatomical quadrant.

The data indicated that bone loss, in both the radius and femur, progresses from the endosteum toward the periosteum with the inner (endosteal) 1/3 of the cortex having significantly greater pore sizes than the outer (periosteal) 1/3. This is consistent with prior work indicating that bone loss occurs not by eroding the endosteal surface but by the expansion and coalescence of resorption cavities within the inner 1/3 of cortex. Bone loss within the radial cortex appeared to be punctuated, with loss occurring subendosteally, then progressing to the midregion, and later to the subperiosteal region. Within the femoral cortex, bone loss was more uniform and its progression was less

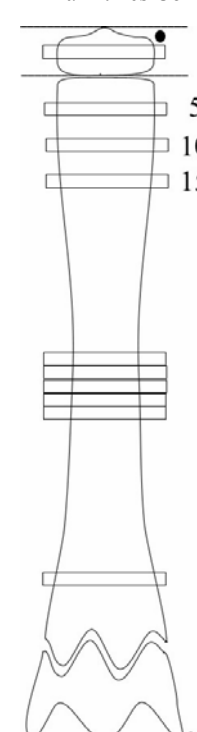
punctuated. Pore size in the midregion did not significantly differ from the outer or inner regions. Among the radial cross sections, the ulna side appeared to have more total pore area than the other quadrants. Among femoral cross sections, the medial side appeared to have the least total pore area compared to other quadrants. Based on mechanical principles, these patterns of bone loss will have profound effects on bone quality. Resorption within the inner 1/3 of the cortex will have a more deleterious effect on bone strength compared to resorption on the endosteal surface. The increase in subendosteal porosity may effectively lead to a rapid decrease in cortical thickness. The more uniform loss of bone in the femoral cortex may preserve cortical thickness and explain why osteoporotic hip fractures occur more than a decade later than osteoporotic distal radius fractures. Biomechanical stresses imposed on the radius and femur, due to their relationship with associated structures, may lead to different loading environments within their cortices and explain the variation in bone loss patterns between the quadrants of each cortex.

Disclosures: D. Casagrande, None.

P68

Peripheral Quantitative Computerised Tomography of the Tibia in Young Pigs. E. C. Firth*, C. Rogers*, M. Kruger*, D. O'Brien*, A. Darragh*. Massey University, Palmerston North, New Zealand.

The purpose was to define a suitable method for determining volumetric bone density (BMD_v) of the tibia in young pigs, to avoid problems associated with the relative changes in bone size, mineral content and mineral density in the growing animal when using DXA imaging. All procedures were approved by the Massey University Animal Ethics Committee, Palmerston North, New Zealand.



Ten pigs were housed indoors in pens, fed on full cream milk with added vitamins and minerals according to National Research Council requirements, and were euthanised at age 6 weeks (live weight of 13.85±0.6 kg). After coxo-femoral disarticulation, the tibia was scanned using peripheral quantitative computerised tomography, (XCT2000, Stratec Medical, Germany; slice thickness 2mm, voxel size 0.4mm, CV of repeated scanning procedure less than 1.2% for any parameter) at sites related to the externally measured bone length, and shown in the figure (dot = length measurement sites, - - - = limits of proximal epiphysis, rectangles = CT slices). In the epiphysis and metaphyses, trabecular BMD_v (45% of the core area of the bone), and cortical-subcortical BMD_v (outer 55%) and total BMD_v were determined using an outer contour threshold of 200mg/cm³; in the diaphyseal slices, 280mg/cm³ was used (the low threshold was chosen because of the low density of new bone in the young animal). Differences between sites were determined by ANOVA (p<0.05).

Trabecular BMD_v in the proximal epiphysis was 219.5± 6.8 mg/cm³. Trabecular BMD_v of the proximal metaphysis decreased from 5mm (230.7±12.8mg/cm³) to 15mm (173.1±12.4mg/cm³) distal to the proximal physis, but total density increased (5mm 290.8±10.6mg/cm³, 15mm 337.7±10.4mg/cm³), due to the greater cortical-subcortical BMD_v of the bone further from the physis. The variance was least at the 10mm site. There was no significant difference between the 5 contiguous diaphyseal sites in area, mineral content, or density, which latter was 709± 6.7mg/cm³.

We conclude that in young pigs, bone size and density be determined from one mid-diaphyseal site, and trabecular BMD_v at 10mm from the proximal and distal physes. The technique is simple, and allows the separation and relative change in the size and density of trabecular and

cortical fractions to be assessed as they respond to nutritional, hormonal, pharmacological or exercise interventions.

Disclosures: E.C. Firth, None.

P69

Texture Analysis of Calcaneum Image for Micro-architecture Description with Morphological Tools. S. Sevestre-Ghalila*¹, A. Ricordeau*², N. Mellouli*², A. Benazza-Benyahia*³, C. Chappard*⁴, C. L. Benhamou*⁴. ¹Ecole Supérieure de la Statistique et de l'Analyse de l'Information, Tunis, Tunisia, ²IUT de Montreuil, Université Paris 8, Montreuil, France, ³Ecole Supérieure des Télécommunications, Tunis, Tunisia, ⁴CHR d'Orléans, Orléans, France.

In this paper, we propose a method for extracting morphological close to classical 3D-morphological bone parameters enabling the description of the trabecular microarchitecture from radiological images of the calcaneus.

Radiographic film is used for the formation of each image; the region of interest is 2.7 cm X 2.7 cm. This area only includes trabecular bone in the posterior part of the calcaneus and has a reproducible location [1].

A number of 31 images of Osteoporotic Patients (OP) with vertebral fractures and (or) with other kind of fractures and 39 images of Control Patients (CP) matched for age, are considered.

Related to the approach of [2], our first step consists in extracting the grey-scale skeleton of the microstructures contained in the underlying images[3]. The principal arches of the skeleton network are longitudinal in the region of interest and originating in the subtalar joint, they correspond to the compression trabeculae. As noted in [4], osteoporosis tends to alterate the trabeculae that are the least required during the body motion (transversal direction on the image).

We extract 2-D parameters closed to 3D-parameters with respect to its mean such as the trabeculae thickness and trabeculae spacing. Therefore we compute two mean measures which we call by "Inter-projected distance" and "Intra-projected distance" respectively related to trabeculae thickness and trabeculae spacing. To distinguish the transversal and longitudinal properties, we compute these means for each class of oriented segment. From number of pixels of the 2 previous classes we obtain 18 micro-architecture descriptors.

The evaluation dispersion of each feature for CP and for OP class show that OP has a larger variation than CP ands are significantly different (9 features with p<0.01 for Wilcoxon test)

Then we show the complementarity of the morphological features with respected to the bone density (BMD) and Age by applying the principal components analysis (PCA).

To classify OP and CP, logistic regression models were applied. The best models well classify 78% patients with 90.1 in the CP class and a very good fit with a small p-value (<0.001).

References:

- [1] C.L. Benhamou et al. J. Bone Mineral Res, vol. 9, 1994.
- [2] Gereats, Ph Thesis, Netherland.
- [3] S. Chen, F.Y. Shih, IEEE Trans. on Image Proc, vol 5, (10), 1996.
- [4] P. Banerji and S.G. Kabra J. British Editorial Soc. of Bone and joint Surgery, 65-B, (2), 1983.

Disclosures: S. Sevestre-Ghalila, None.

Effects of Bone Mineral and Matrix on Bone Quality

P70

YOUNG INVESTIGATOR AWARD RECIPIENT
Highly Mineralized Locations in Bone: Source of Strength or

Weakness? O. Akkus*, J. Yerramshetty*. University of Toledo, Toledo, OH, USA.

Moderately mineralized younger bone has lower stiffness, lower strength but greater deformability, and thus, greater fracture resistance. Conversely, highly mineralized older bone has brittle characteristics such that it is stiffer and stronger while it has compromised resistance to fracture. Recently we demonstrated that microcracks selectively initiate in highly mineralized locations of bone. It is believed that highly mineralized tissue absorbs strain energy input in the form of cracks whereas the younger tissue and lamellar interfaces contain crack growth. Therefore, an increase in the amount, size and/or proximity of highly mineralized loci pose the risk of catastrophic failure in the event of a mechanical challenge. The current study investigated age-related changes in the spatial distribution of highly mineralized loci in cortical bone. Spatial maps of mineralization were constructed using Raman microscopic scans over a macroscopic area (~5x2 mm). An array of 11x30 measurement points was taken from matched locations of 4 donors (38, 52, 66 and 85 years-old) at the mid femoral diaphyses. Based on our previous observations of mineralization scores in the vicinity of microcracks, measurement points with a mineralization value greater than 12 was assigned as a highly mineralized location and their positions were mapped (Fig 1). Contiguous pixels were grouped as one cluster and the number of pixels within a cluster was counted to obtain the size of each cluster. It was observed that the volume fraction of highly mineralized locations increased with age (Fig 2, left). The area covered by individual clusters also increased with age (Fig 2, right). These results suggest contiguous brittle planes as a novel measure of bone quality and mechanical tests will investigate whether this measure is a correlate of fracture susceptibility.

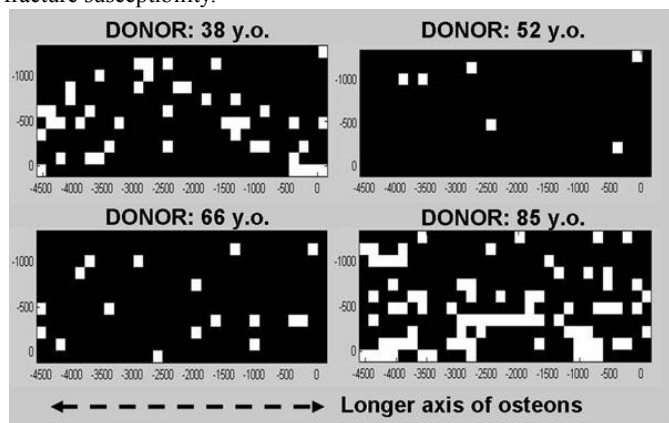


Fig 1. Maps of highly mineralized locations (white pixels, each pixel is 0.15x0.175=0.025 mm²)

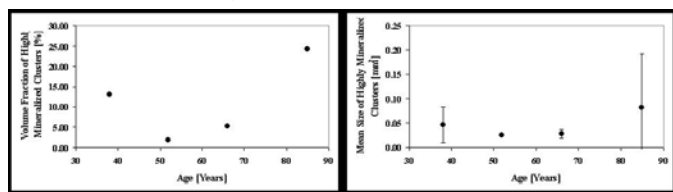


Fig 2. Variation of volume fraction of highly mineralized loci (left) and mean areas of highly mineralized clusters (right) between donors.

Disclosures: O. Akkus, None.

P71

Establishing Chemical and Mechanical Matrix Properties During Intramembrous Bone Formation. S. Judex¹, B. Busa^{*1}, Y. Qin¹,

L. Miller². ¹State University of New York, Stony Brook, NY, USA, ²Brookhaven National Laboratories, Upton, NY, USA.

A large variety of physiologic, pathologic, and pharmacologic stimuli may alter bone's (re)modeling activity and change the ratio of new bone to older bone. As the quality and mechanical integrity of a bone represents a composite of its heterogeneous properties, the quality of the newly formed bone during (re)modeling may significantly influence its overall quality. Here, we measured changes in chemical and mechanical properties of the matrix during rapid bone modeling and hypothesized that these measures of quality assessed in newly formed bone tissue would require several weeks to approach the levels of older bone. Rapidly growing 7wk old Sprague-Dawley female rats (n=8) were injected with six fluorochrome labels over a time span of 3wk and sacrificed. Chemical and mechanical properties of the tibial middiaphysis were measured in seven 100 x 20 µm regions distributed between the endocortical and periosteal surface by in-situ infrared micro-spectroscopy and nano-indentation. The age of these regions was determined by the spatial location of the fluorochrome labels. To compare matrix properties in these actively growing rats to fully established tissue properties of adult rats, the middiaphyseal tibia of 4m old rats (n=4) was subjected to similar assays.

None of the chemical properties analyzed, including the ratios of phosphate/protein, carbonate/protein, Type A/Type B carbonate, and the degree of collagen cross-linking, differed significantly between 2-6d, 10-14d, and 8-22d old bone, even though aging caused an increasing, but not significant, trend in all properties. Compared to the much older intracortical regions, only the phosphate to protein ratio of the 2-6d old bone was significantly smaller (~20%). Similarly, chemical properties found intracortically in 11wk old rats were not significantly different from those of adult 4mo old rats, except for the carbonate/protein ratio which was 20% smaller. The small differences in chemical properties between spatial locations, representing bone of different ages, did not cause significant differences in their elastic moduli.

Data from this study indicate that bone has the ability to rapidly establish its mechanical and chemical tissue properties even during a phase in which the skeleton experiences rapid growth. If these data can be extrapolated to human haversian bone, they also suggest that the increase in bone fragility with heightened remodeling activity is not a result of the compromised quality of the newly formed bone tissue.

Disclosures: S. Judex, None.

P72

Requirement of Osteoclasts for the Formation of Normal Bone Structure During Development. X. Dai^{*}, E. R. Stanley^{*}. Albert Einstein College of Medicine, Bronx, NY, USA.

Osteoclast deficiency leads to defective bone resorption and osteopetrosis with increased trabecular bone volume and high bone density. Targeted disruption of the colony stimulating factor-1 receptor (CSF-1R) gene in mice resulted in an impaired osteoclastogenesis and absence of mature osteoclasts. On an outbred genetic background, ~40% of *Csf1r*^{-/-} mice survived to adulthood exhibiting the typical osteopetrotic phenotype, while on the FVB/NJ background, all *Csf1r*^{-/-} mice died before 1 month of age and 40% of them possessed spontaneous fractures in long bones suggesting a biomechanical weakness of these bones. The long bones of 2-wk old *Csf1r*^{-/-} mice possessed increased bone density and trabecular bone volumes, an expanded epiphyseal chondrocyte region and a poorly formed cortex with disorganized collagen fibrils and a severely disturbed matrix structure with an irregular distribution of cellular components. These abnormalities of bone structure and quality provide a plausible explanation for the long bone weakness in developing *Csf1r*^{-/-} mice. In addition, the mineralization of bone matrix at secondary sites of ossification in these mice was significantly reduced.

Osteoblasts deposit bone matrix, give rise to osteocytes and are considered to be responsible for the formation and maintenance of structural integrity of the bones. In *Csf1r*^{-/-} mice, individual osteoblasts were found to have preserved their typical ultrastructure and matrix-depositing activity. However, the layered organization of osteoblast

clusters on the bone-forming surface and the direction of their matrix deposition toward the bone surface have been lost, resulting in their abnormal entrapment by matrix. We have shown that (1) purified osteoblasts do not express CSF-1R, (2) the bone defects in *Csf1r*^{-/-} embryos develop later than the development of osteoclasts in normal embryos, and (3) transplanted *Csf1r*^{-/-} femoral anlagen develop normally in the presence of wildtype osteoclasts. Thus this abnormal behavior of osteoblasts is due to lack of regulation by osteoclasts. We conclude that the osteoclast plays an important role in regulating osteoblastic bone formation during development.

Disclosures: **X. Dai**, None.

P73

Heterogeneity Index of Mineralization Is an Important Intrinsic Determinant of the Quality of Bone. **G. Boivin**, **P. J. Meunier**.

INSERM Unité 403, University Claude Bernard Lyon1, 69372 Lyon Cedex 08, France.

Bone quality determinants include the mean degree of mineralization of bone (DMB) mainly measured by quantitative microradiography (1-4) and by back-scattering (3). Mean DMB and intra-individual Heterogeneity Index of the distribution of DMB (mean full width at half-maximum of the individual DMB curve) are parameters known to vary with secondary mineralization of basic structure units. The intra-individual Heterogeneity Index depends on the rate of remodeling, a high turnover leading to a great heterogeneity of DMB and conversely a low turnover leading to a decreased heterogeneity. From the individual data, a mean Inter-individual Heterogeneity Index (Inter HI) can be calculated. In control women, divided into pre- and post-menopausal groups, the mean DMB is not different between the two groups while Inter HI is significantly higher ($p=0.038$) in pre- than in post-menopausal group, and reflects a significant homogenization of DMB with age ($p<0.01$).

Antiresorptive agents cause a decrease of the remodeling rate. In osteoporotic women treated for 2-3 yrs with alendronate (10mg/day), mean DMB is significantly increased (5) with a shift of DMB values towards highest values. In parallel, and specially after 3 yrs, the Inter HI is decreased concomitantly to the shift of DMB. If such a high DMB combined with a low Inter HI was maintained after long-term treatments, the mechanical properties of bone tissue could be changed. When less potent antiresorptive agents as raloxifene (6) and estrogen (7) are used, mean DMB is increased but the shift of DMB is not accompanied by significant changes in Inter HI except after high doses of estrogen. Conversely, in case of accelerated remodeling activity, for example in 11 patients with primary hyperparathyroidism, mean DMB is decreased with a shift of the distribution of DMB towards the lowest values but Inter HI does not change. In patients treated with teriparatide during 6 and 18 months (8) mean DMB is decreased but Inter HI is increased as expected after a short prolongation of bone formation activity. Beside DMB, this new approach leads to consider also Inter HI as a determinant of bone quality. It remains to evaluate the properties of bone at the tissue (microhardness) and crystal (infrared spectroscopy) levels, and to compare them with the quality of the mineralization evaluated as DMB and Inter HI.

References

1. Boivin & Meunier 2002 CTI 70:503-511
2. Boivin & Meunier 2003a OI 14 suppl 3:19-24
3. Boivin & Meunier 2003b OI 14 Suppl 5:22-28
4. Follet et al. 2004 Bone 34:783-789
5. Boivin et al. Bone 2000, 27:687-94
6. Boivin et al. 2003 JCEM, 88:4199-205
7. Boivin et al. 2005 Bone in press
8. Arlot et al. 2005 JBMR in press

Disclosures: **G. Boivin**, None.

P74

Long-Term Strontium Ranelate Administration in Monkeys Preserves Characteristics of Bone Mineral Crystals and Degree of Mineralization of Bone. **D. Farlay**^{*1,2}, **G. Boivin**^{1,2}, **G. Panczer**^{*3}, **A. Lalande**^{*4}, **P. J. Meunier**¹.

¹INSERM Unité 403, University Claude Bernard Lyon1, 69372 Lyon Cedex 08, France, ²Centre Technologique des Microstructures, University Claude Bernard Lyon1, France, ³CNRS UMR 5620, University Claude Bernard Lyon1, Villeurbanne, France, ⁴Institut de Recherches Internationales Servier, Courbevoie, France.

Strontium ranelate which simultaneously increases bone formation and decreases bone resorption, prevents of bone loss and increases bone mass and bone strength in ovariectomized and intact rats (1-3). Strontium ranelate has also demonstrated its antifracture efficacy in the treatment of post-menopausal osteoporosis (4). The present study investigated the interactions of strontium (Sr) with bone mineral in monkeys after long-term strontium ranelate treatment and after a period of treatment withdrawal.

Iliac bones were obtained from control monkeys, from animals after a 52-week strontium ranelate administration period (200, 500, 1250 mg/kg/day PO) and in parallel-treated groups (same 3 doses), 10 weeks following final strontium ranelate administration ($n=3-7$ per group). Sr uptake and distribution in bone mineral were quantified by X-ray microanalysis (5), changes at the crystal level by X-ray diffraction (5), the degree of mineralization of bone (DMB) and the inter-individual Heterogeneity Index (Inter HI) by quantitative microradiography (6-8).

After strontium ranelate administration, a dose-dependent Sr uptake occurred into cortical and cancellous bone, with higher content ($\times 1.6$) in new than in old bone. Ten weeks after treatment withdrawal, this Sr uptake decreased by 50% and this occurring almost exclusively in new bone. At the end of strontium ranelate treatment as after a withdrawal period, there was a preservation of both crystal characteristics (suggesting that Sr was only weakly linked to crystals by ionic substitution) and of parameters reflecting the mineralization of bone at tissue level (DMB and Inter HI). In monkeys, long-term strontium ranelate administration results in a dose-dependent bone strontium uptake (mainly into newly formed bone) which preserves the degree of mineralization of bone and the bone mineral at the crystal level. These observations demonstrate the absence of any deleterious effect of long-term strontium ranelate treatment on bone mineralization, a major determinant of bone quality.

References

1. Marie et al. 1993 JBMR 8:607-15
2. Marie et al. 2001 CTI 69:121-9
3. Ammann et al. 2004 JBMR 19:2012-20
4. Meunier et al. 2004 NEJM 350:459-68
5. Boivin et al. 1996 JBMR 11:1302-11
6. Boivin and Meunier 2002 CTI 70:503-11
7. Boivin and Meunier 2003a OI 14 suppl 3:19-24
8. Boivin and Meunier 2003b OI 14 Suppl 5:22-28

Disclosures: **D. Farlay**, Servier 2.

P75

A Study on the Relationship Between Skeletal Fragility and Bone Mineral Quality in Ovariectomized and Dietary Induced

Metabolic Acidosis Sheep Model. **P. A. West**^{*1}, **J. M. MacLeay**^{*2}, **D. Wheeler**^{*2}, **A. L. Boskey**¹. ¹Hospital for Special Surgery, New York, NY, USA, ²Colorado State University, Ft. Collins, CO, USA.

Introduction: Osteoporosis research could benefit from the development of a practical large animal model. The aim of the current study was to examine the effects of ovine ovariectomy and dietary induced metabolic acidosis on bone fragility and mineral quality using a compression test and FT-IR Imaging Spectroscopy (FT-IRIS) respectively.

Methods: 24 skeletally mature Rambouillet-Columbia cross ewes

were assigned to 4 groups of 6. Group 1 (ND) = normal diet, Group 2 (OVX) = normal diet + ovariectomized, Group 3 (MA) = MA diet without OVX and Group 4 (OVX/MA) = MA diet + ovariectomized. L3, L4, L5 and L7 vertebral body were removed post mortem after 180 days.

Compression Test: The L3 and L5 vertebrae were tested in compression as whole vertebral bodies whereas the L7 vertebra was tested as cancellous cubes. Maximum stress and modulus were calculated from the load/displacement data obtained at a rate of 100 Hz during testing.

FT-IRIS: Cancellous bone from the L4 vertebrae was embedded in PMMA, cut into 2 μm thick sections and imaged in transmission mode. 1030/1020 cm^{-1} ratios (bone quality) were calculated from the images (3 per animal) and averaged.

Statistics: Statistical significance was determined by one-way ANOVA.

Results: Biomechanical Testing: For L3 and L5 vertebrae the combination of OVX and MA significantly reduced the maximum compression strength ($p < 0.05$) over ND and OVX whereas MA alone did not induce a significant reduction. A significant effect of MA diet was noted in the cancellous bone cubes (L7) with both MA and OVX/MA significantly lower than ND and OVX treatments ($p < 0.05$). No differences were noted between treatment groups for compressive modulus for whole vertebral body or vertebral body cancellous bone ($p > 0.05$).

FT-IRIS: 1030/1020 cm^{-1} intensity ratio comparisons between the four groups revealed differences in the bone quality. The OVX/MA group significantly increased ($p < 0.05$) and the MA group increased, compared to ND and OVX.

Discussion: Compression tests of whole body vertebral specimens and cancellous bone cubes indicate significantly increased skeletal fragility with the MA diet ($p < 0.05$). Similarly, IR imaging analysis revealed increased 1030/1020 cm^{-1} intensity values with the MA diet; the OVX/MA group resulted in a significant increase. These results agree with previous studies that relate weaker osteoporotic bone to higher 1030/1020 cm^{-1} intensity ratios due to decreased bone formation and increased resorption of smaller bone crystals. This study indicates that in a sheep model MA diet can rapidly induce changes in bone similar to those seen in human osteoporosis.

Disclosures: P.A. West, None.

P76

TGF- β Regulation of the Mechanical Properties and Composition of Bone Matrix. G. Balooch^{*1}, M. Balooch^{*1}, R. K. Nalla^{*2}, S. Schilling^{*3}, E. Filvaroff^{*4}, G. W. Marshall^{*1}, E. H. Filvaroff^{*4}, S. J. Marshall^{*1}, R. O. Ritchie^{*2}, R. Derynck^{*1}, T. N. Alliston¹.

¹University of California San Francisco, San Francisco, CA, USA,

²University of California - Berkeley, Berkeley, CA, USA, ³Duke

University, Durham, NC, USA, ⁴Genentech, South San Francisco, CA, USA.

The ability of bone to resist fracture is determined by bone mass and architecture and the quality of bone matrix. Extensive study has implicated estrogen, parathyroid hormone, TGF- β and other cytokines in the control of bone mass and architecture and its deregulation in metabolic bone diseases such as osteoporosis. Although less is known about the mechanical properties and composition of bone matrix, their importance is clinically apparent, as in osteopetrosis and osteogenesis imperfecta. The factors that regulate the mechanical properties and composition of bone matrix are largely unknown. In this study, we utilize a novel combination of high-resolution approaches, including atomic-force microscopy with nanoindentation, X-ray tomography, and Raman micro-spectroscopy to investigate TGF- β regulation of bone matrix properties, independently of its effects on bone mass and architecture. Properties were evaluated in genetically engineered mice with differing levels of TGF- β signaling, ranging from 16-fold (D4 mice) and 2.5 fold (D5 mice) over-expression of TGF- β in bone, to decreased TGF- β signaling due to osteoblast expression of a dominant negative TGF- β receptor (DNT β RII mice) or targeted deletion of the

Smad3 gene (Smad3^{+/-} and ^{-/-} mice). Bone matrix mechanical properties, such as elastic modulus, correlated with the level of TGF- β signaling. Bone matrix from mice with elevated TGF- β signaling (D4, D5) had up to 23% reduced elastic modulus and hardness relative to wild-type littermates ($p < 0.05$). However, mice in which TGF- β signaling was impaired (DNT β RII, Smad3 ^{+/-}, and Smad3 ^{-/-}) had up to 54% increased elastic modulus and hardness ($p < 0.05$). Though no phenotype had previously been described for Smad3 ^{+/-} mice, the elastic modulus of these bones was as elevated as in Smad3 ^{-/-} bones. Histomorphometric, X-ray, and XTM analyses showed that Smad3 ^{+/-} bone also possessed increased trabecular bone volume, cortical thickness and bone mineral concentration relative to wild type mice, with a phenotype much like that of DNT β RII mice. Furthermore, both DNT β RII and Smad3^{+/-} mice exhibited increased resistance to fracture in three point bending assays. Therefore, partial reduction of TGF- β signaling is sufficient to increase several functionally relevant parameters of bone quality. Our results are among the first to show that bone matrix mechanical properties are controlled by growth factor or cytokine signaling.

Disclosures: T.N. Alliston, None.

P77

YOUNG INVESTIGATOR AWARD RECIPIENT

Collagen and Mineral Content and Organization Relate to Bone Nanomechanical Properties. E. Donnelly^{*1}, R. M. Williams^{*1}, C. Xiao^{*2}, R. Mendelsohn^{*2}, S. P. Baker^{*1}, A. L. Boskey^{3,4}, M. C. H. van der Meulen^{1,3}. ¹Cornell University, Ithaca, NY, USA, ²Rutgers University-Newark, Newark, NJ, USA, ³Hospital for Special Surgery, New York, NY, USA, ⁴Weill Medical College of Cornell University, New York, NY, USA.

Skeletal function depends critically on bone structural integrity, which is governed by tissue apparent density, microarchitecture, and "quality." Although changes in tissue composition accompany reductions in bone apparent density in diseases such as osteoporosis, relatively little is known about the material properties of bone tissue or how perturbations in tissue composition affect the local mechanical properties. Mechanical characterization of bone at the microstructural level can provide additional insight into the origins of skeletal fragility seen in osteoporosis. Cancellous tissue is characterized by a layered microstructure with variable proportions of collagen and mineral. The lamellar material is substantially stiffer than the interlamellar material at the nanomechanical level. However, the microstructural origin of the observed differences in mechanical properties of these structures has not been investigated. The purpose of this study was to relate the nanomechanical properties of lamellar bone to the collagen and mineral content of the tissue. Nanoindentation was used to assess the indentation modulus of lamellar and interlamellar tissue in normal human vertebral cancellous bone. Second harmonic generation microscopy and Raman microscopy were used to examine collagen and mineral, respectively, at the same location in the tissue. The stiff lamellae corresponded to areas of highly ordered, collagen-rich material with a relatively high mineral:matrix ratio, while the compliant interlamellar regions corresponded to areas of unoriented or collagen-poor material with a lower mineral:matrix ratio. The lamellar bone tissue was ~30% stiffer, contained ~50% more oriented collagen, and had 60-100% greater mineral:matrix ratio than the interlamellar tissue. These observed differences in the mechanical properties and composition and organization of lamellar and interlamellar tissue are consistent with previous scanning electron microscopy studies showing greater mineral and collagen content and organization in lamellar bone tissue. Future studies will examine the effects of metabolic status and disease on these quality measures.

Disclosures: E. Donnelly, None.

P78**Withdrawn****P79**

Osteogenesis and Osseointegration of Rabbit Tibial Bone with Fibrin Glue Coated and Uncoated Bioactive Calcium Phosphate Ceramics. A. Srinivasan¹, V. Harikrishna^{*2}, U. PR^{*2}, A. John^{*2}.

¹Ohio State University, College of Dentistry, Columbus, OH, USA,

²Sree Chitra Tirunal Institute for Medical Sciences and Technology, Biomedical Technology Wing, Trivandrum, Kerala, India.

The objective of this study was to evaluate the osteogenic potential of fibrin glue (FG) coated bioactive calcium phosphate ceramics in rabbit tibia bone. A 2 mm defect was made in the right and left tibia bone of adult male New Zealand white rabbits. These defects were filled with indigenously synthesized 300 - 350 µm size ceramic granules, uncoated and 5 mg FG coated porous Hydroxyapatite (HA), non-porous Bioactive Glass System-Apatite Wollastonite type (BGS-AW) and Calcium Phosphate Calcium Silicate System (HABGS), and sacrificed after 3 and 6 months. The rabbits were maintained as per the regulations of CPCSEA. Radiographic and angiographic techniques were employed to study the healing and vascularization of the defect with implant. Bone labeling was performed by intramuscular injection of oxytetracycline and alizarin complexone at 4 weeks intervals to study the bone mineralization rate. SEM and Energy Dispersive X-ray Analysis (EDS) was performed to study the bone-implant interface and the distribution of calcium and phosphate in the interface. XRD and FTIR of the bone implant interface was carried out to understand the material degradation and bone mineral quality at the interface. Quantitative histomorphometric analysis was done to quantify the percentage of new bone formation. X-rays and SEM revealed FG coated HA, BGS, HABGS and uncoated implants well integrated with the host bone and vascularized by 3 months. Bone apposition rate was high for the FG coated HA, BGS and HABGS granules than for the uncoated granules. Osteogenesis was by osteoconduction for uncoated granules and FG coated granules showed bimodal mineralization pattern where the bone formation was by osteoconduction and osteoinduction mode. Histologically, FG coated and uncoated ceramic granules showed good healing response with mature woven bone at 3 months and lamellar bone at 6 months without any inflammation or soft tissue formation surrounding the implant. Quantitative histomorphometric analysis showed more bone formation in BGS and HABGS than HA at 3 and 6 months. EDS revealed the calcium phosphate ratio was different at the implant bone interface for uncoated HA (1.74), BGS (1.51) and HABGS (1.60) after 6 months. XRD of the bone implant interface revealed the presence of amorphous apatite peaks for HA, BGS and HABGS, and typical AW and whitlockite peaks for BGS and HABGS after 6 months of post implantation. We conclude that bone mineralization pattern and osseointegration was different with the three different granules with and without FG.

Disclosures: **A. Srinivasan**, None.

P80

A Fracture Resisting Molecular Interaction in Trabecular Bone: Sacrificial Bonds and Hidden Length Dissipate Energy as Mineralized Fibrils Separate. G. E. Fantner^{*}, T. Hassenkam^{*}, J. H. Kindt^{*}, J. C. Weaver^{*}, H. Birkedal^{*}, L. Pechenik^{*}, L. S. Golde^{*}, M. M. Finch^{*}, P. J. Thurner^{*}, G. Schitter^{*}, G. D. Stucky^{*}, D. E. Morse^{*}, P. K. Hansma^{*}. University of California, Santa Barbara, Santa Barbara, CA, USA.

Properties of the organic matrix of bone as well as its function in the microstructure have been shown to be important contributors to the remarkable mechanical properties of bone. A molecular energy dissipation mechanism in the form of sacrificial-bonds and hidden-length was previously found in bone constituent molecules of which the efficiency increased with the presence of Ca²⁺ ions in the experimental solution. Here we present evidence for how this sacrificial-bond hidden-length mechanism contributes to the mechanical properties of the bone composite. From investigations into the nanoscale arrangement of the bone constituents (by Atomic Force Microscopy and high resolution Scanning Electron Microscopy) in combination with pico-Newton adhesion force measurements between mineralized collagen fibrils, based on single molecule force spectroscopy, we find evidence that a non fibrillar organic matrix is present between mineralized collagen fibrils which acts as a “glue” holding the fibrils together. We propose that this “glue” resists the separation of mineralized collagen fibrils which results in an energy dissipation mechanism that protects the bone in daily exercise, even below the strains where microcracks occur. Like in the case of the sacrificial bonds in single molecules, the effectiveness of this “glue” increases with the presence of Ca²⁺ ions. By targeting the Ca²⁺ dependency of “glue” effectiveness, we were able to show that this molecular scale strengthening mechanism increases the fracture toughness of the macroscopic bone material.

Possible molecules that are involved in this sacrificial-bond mechanism (sacrificial molecules) are non fibrillar collagens, glycoproteins and other bone associated polymers (osteopontin, osteonectin, bone sialoprotein). We investigate the possible sacrificial-bond function of these bone constituents by single molecule force spectroscopy and adhesion measurements to hydroxyapatite crystals. With this knowledge, we hope to better understand the molecular processes involved in bone fracture which might lead to new ways to assess bone quality and give new ideas for fracture prevention.

Disclosures: **G.E. Fantner**, None.

AUTHOR INDEX

Ackerman, J. L.	P3	Corbin, T. J.	P38	Haque, T.	P12	Liu, S.	P32
Adamu, S.	P44	Cordova, M.	P67	Harikrishna, V.	P79	Liu, Y.	15
Akkus, O.	P70	Cosenza, M. E.	P37	Harris, M. A.	P47	Liu, Y.	15
Alliston, T. N.	P76	Courteix, D.	P63	Harris, S. E.	P47	Loh, L.	P7
Anderson, H.	P47	Courtland, H.	P49	Hassenkam, T.	P80	Lombardi, A.	P31, P33
Antich, P. P.	P4	Cranmer, P.	P37, P41	Hazon, D.	P15	Long, J.	15
Arends, R. J.	P45	Cucchiara, A.	28	Henderson, J.	P12	Lopez Franco, G. E.	P11
Arlot, M. E.	P59	Dai, X.	P72	Henderson, J. E.	P52	Loveridge, N.	P14, P29, P60
Arnaud, S. B.	P5	Dalsky, G. P.	P61	Hill, A.	P49	Ma, Y.	P39
Asuncion, F.	P44	Dalzell, N.	P23, P29	Hochberg, M. C.	P31	MacLeay, J. M.	P75
Atkinson, J. E.	P37, P41	Darragh, A.	P68	Hoeiseth, A.	P21	Magni, C.	P63
Aufort, G.	P34	Das, S.	P22	Hofmann, T.	P53	Majumdar, S.	P30
Azria, M.	P30	Davies, K.	15	Hogan, B.	P47	Mankani, M. H.	P16
Baker, S. P.	P77	Del Rio, L.	P25	Hrovat, M. I.	P3	Marshall, G. W.	P16, P76
Balooch, G.	P42, P76	Delmas, P. D.	17, P59, P61	Huang, A.	29, P11	Marshall, S.	P16, P76
Balooch, M.	P16, P42, P76	Dempster, D.	P28, P46	Hussain, F.	P10	Martin, L.	P40
Bare, S.	P33	Deng, H.	15	Ilich, J. Z.	P58	Masarachia, P.	P33, P34
Basillais, A.	P34	Derynck, R.	P76	Iturria, S.	P39	Mastmeyer, A.	P8
Bateman, T. A.	P44	Devine, A.	P26	Jamal, S. A.	P24	Mayhew, P.	P60
Bauer, D. C.	P24, P31	Dhaliwal, S. S.	P26	Jennane, R.	P34	Mayhew, P. M.	P14
Bauss, F.	P46	Dick, I. M.	P26	Jepsen, K.	P48, P49, P57, P67	McCabe, J.	P38, P40
Beamer, W. G.	P54	Diem, S.	P33	Jiang, Y.	P61	McCartney, N.	P56
Beck, T. J.	P29, P60	Dobson, C. A.	P13	Jiao, F.	P54	McClearn, G. E.	P55
Benazza-Benyahia, A.	P69	Donahue, L.	P50	Jiao, Y.	P54	McMahon, D.	P28
Benhamou, C.	P63	Donahue, L. Rae	P51	John, A.	P79	Mellouli, N.	P69
Benhamou, C. L.	P34	Donnelly, E.	P77	Johnson, E. M.	P19	Même, S.	P63
Benhamou, C. Laurent	P69	Donovan, M.	P28	Jorgensen, S. M.	P32	Mendelsohn, R.	P77
Benito, M.	28	Duboeuf, F.	P59	Judex, S.	P71	Merabet, Z.	P59
Binette, J.	P12, P52	Ducher, G.	P63	Kalender, W.	P8	Meunier, P. J.	P73, P74
Bird, J.	P67	Dufresne, T. E.	P32	Kang, Y.	P8	Miller, L.	P71
Birkedal, H.	P80	Dvornyk, V.	15	Kaptoge, S.	P23, P29	Miller, P.	P35
Blank, R.	P11	Eckstein, E. C.	P54	Kasper, D.	P27	Mindeholm, L.	P30
Blizard, D. A.	P55	Ederveen, A. G. H.	P45	Katz, J. L.	P15	Mittra, E.	P6
Boivin, G.	P73, P74	Elliott, R.	P40	Khan, K. M.	P64	Morony, S.	P38, P40, P44
Bolon, B.	P38	Engelke, K.	P8, P9	Khaw, K. T.	P23, P29	Morse, D. E.	P80
Bonfield, W.	P60	Ensrud, K.	P33	Kim, J.	P58	Müller, R.	P28, P51
Bonnick, S.	P35	Eriksen, E. F.	P61	Kimmel, D.	P33, P34	Munoz, F.	17
Borah, B.	P32	Fagan, M. J.	P13	Kindt, J. H.	P80	Munyoki, M.	P57
Boskey, A. L.	27, P75, P77	Faghri, P.	P58	Kinney, J. H.	16, P62	Myers, E. R.	27
Boutroy, S.	17	Faibish, D.	27	Klaushofer, K.	P33	Nadeau, J.	P49
Bouxsein, M. L.	17, P59	Fan, Z.	P54	Kohler, T.	P51	Nalla, R. K.	16, P62, P76
Boyd, S. K.	P64	Fantner, G. E.	P80	Kostenuik, P.	P387, P38, P40,	Nasser, P.	P57
Bryant, H.	P39	Farlay, D.	P74	P41, P44		Newitt, D.	P30
Bunker, B.	28	Faulkner, K. G.	P25	Kream, B.	P47	Nguyen, H.	P40
Burgoyne, C. J.	P60	Feng, J. Q.	P47	Kruger, M.	P68	Niebur, G. L.	P18, P20
Burke, P. K.	P25	Filvaroff, E.	P76, P76	Kulessa, H.	P47	Niehaus, M.	P37
Busa, B.	P71	Finch, M. M.	P80	Kundra, V.	P19	Novack, D.	P36
Byrjalsen, I.	P27	Firth, E. C.	P68	Ladinsky, G. A.	P7	O'Brien, D.	P68
Cain, R.	P39	Fleischer, J.	P28	Lalande, A.	P74	Olson, M.	P30
Camacho, N. P.	29	Fortin, A.	P52	Lander, E.	P49	Ominsky, M. S.	P37, P38, P41
Caminis, J.	P1	Fratzl, P.	P33	Lane, N. E.	P42	Oskins, J.	P39
Casagrande, D.	P67	Fuchs, C.	P8	Lang, D. H.	P55	Oxland, T. R.	P64
Castro, M.	P36	Fuerst, T.	P8, P9	Langton, C. M.	P13, P2, P22	Panczer, G.	P74
Chan, H. N.	P45	Gehron Robey, P.	P16	Langton, D. K.	P22	Pechenik, L.	P80
Chandelier, F.	P17	Genant, H. K.	P9, P61	Lau, A. G.	P44	Peyrin, F.	P17, P53
Chappard, C.	P63, P69	Geng, Z.	P38, P40	Laudier, D.	P67	Phillips, R.	P13, P2
Chappard, G.	P34	Ghillani, R.	P67	Laugier, P.	P17, P53	Phipps, R. J.	P32
Chattopadhyay, A.	P31	Giangregorio, L. M.	P56	Leeming, D. J.	P27	Pisharody, S.	P2, P22
Chen, P.	P61	Glimcher, M. J.	P3	Legueme, I.	P17, P53	Pleshko Camacho, N.	P11
Cheng, E.	P33	Golde, L. S.	P80	Leng, H.	P18	Popescu, A.	P7
Chesler, D. A.	P3	Gomberg, B.	28	Levy, R.	P67	Pr, U.	P79
Chesnut III, MD, FACP, C. H.	P30	Gordon, C.	P24	Lewis, M. A.	P4	Price, C.	P48
Chiu, H.	P54	Graham, L.	P3	Li, A.	P52	Prince, R. L.	P26
Christensen, C.	P40	Grisanti, M.	P38, P40	Li, G.	29	Qin, Y.	P6, P71
Christiansen, C.	P27	Gruber, B.	P6	Li, W.	P52	Ragi, S.	P25
Clement, J. G.	P14, P60	Gu, W.	P54	Li, X.	P38	Raum, K.	P17, P53
Cleveland, R.	P17	Gunaratna, G.	P65	Liang, M. T. C.	P5	Recker, R.	P33
Cody, D. D.	P19	Gunaratne, G.	P10	Lichtler, A.	P47	Recker, R. R.	15, 27
Conway, T.	15	Guo, D.	P47	Lieschner, M.	P10, P65	Reeve, J.	P14, P23, P29, P60
Cooper, D. M. L.	P64	Hamdy, R.	P12	Lin, W.	P6	Rho, J.	P54
		Hansma, P. K.	P80	Liu, P.	15	Richer, E.	P4

Ricordeau, A.	P69	Wasnich, R.	P35
Ritchie, R. O.	16, P62, P76	Weaver, J. C.	P80
Ritman, E. L.	P32	Wehrli, F. W.	28, P7
Rocha-Sanchez, S.	15	Welch, A.	P23
Roeder, R. K.	P18	West, P. A.	P75
Rogers, C.	P68	Wheeler, D.	P75
Roschger, P.	P33	Whyte, M. P.	P36
Roux, J. Paul	P59	Williams, J.	P67
Rubin, C.	P6	Williams, R. M.	P77
Ryan, J.	P49	Wimalawansa, S.	P10, P65
Saade, R. George	P1	Wright, A.	28, P7
Saha, P. K..	P7	Wu, Y.	P3
Saied, A.	P17, P53	Xia, Y.	P6
San Martin, J.	P61	Xiao, C.	P77
Santora, A. C.	P31	Xiao, P.	15
Sato, M.	P39	Xiong, D.	15
Saunders, T.	P37	Yang, K.	P43
Schaffler, M. B.	P57	Yang, W.	P47
Schilling, S.	P76	Yao, W.	P42
Schitter, G.	P80	Yerramshetty, J.	P70
Schmidt, A.	P39	Yuan, Y. Y.	P44
Schwartz, A.	P31	Zemel, B.	28, P7
Sevestre-Ghalila, S.	P69	Zeng, Q.	P39
Shane, E.	P28	Zernicke, R. F..	P64
Sharkey, N. A..	P55	Zhang, J.	P47
Shearer, M. J.	P23	Zhang, Y.	15
Shen, H.	15	Zhao, L.	15
Shen, V.	P38	Zhou, H.	P28
Shields, A.	P30		
Simonelli, C.	P25		
Singh, G.	P21		
Skamene, E.	P52		
Smith, S. Y.	P37, P41		
Snyder, P. J.	28, P7		
Song, H.	P7		
Spanos, P.	P10		
Sran, M. M.	P64		
Srinivasan, A.	P79		
Stanley, E. R..	P72		
Steel, S. A.	P22		
Stölken, J. S.	16, P62		
Stone, D.	P11		
Stout, J. T..	P55		
Stromsoe, K.	P21		
Stucky, G. D.	P80		
Talmant, M.	P17		
Tan, H.	P38, P40		
Tawackoli, W.	P10		
Terranova, C.	P67		
Thomas, C. David.	P14, P60		
Thorpe, J. A.	P2, P22		
Thurner, P. J.	P80		
Tommasini, S. M.	P57		
Tsoukas, G. M.	P1		
Turner, R. T.	P32		
van de Klundert, T. M. C.	P45		
van der Meulen, M. C. H.	P77		
van Lenthe, G. H.	P51		
Vandenbergh, D. J..	P55		
Varela, A.	P37		
Vasilic, B.	28, P7		
Viala, J.	P63		
Vico, L.	P53		
Viray, J.	P40		
Vogler, G. P..	P55		
Voide, R.	P51		
Wacker, W. K.	P25		
Wald, M.	28, P7		
Wang, X.	P18, P20		
Wang, Y.	P3		
Warmington, K.	P38, P40		